Influence of land use, climate and topography on the fire regime in the Eastern Savannas of Colombia

Thesis submitted for the degree of

Doctor of Philosophy

at the University of Leicester

by

Milton Hernan Romero Ruiz

Department of Geography

University of Leicester

May, 2011

Abstract

Influence of land use, climate and topography on the fire regime in the Eastern Savannas of Colombia

Milton Hernan Romero Ruiz

Changes in natural vegetation as a result of land use and fire are an important factor that contributes to loss of biodiversity and climatic change. More than 30% of the global land surface shows frequent burning particularly in the tropics. Even though natural savannas in Colombia are experiencing high impact due to land use, there has not been a systematic quantification of the change rate of land use/cover or fire occurrence. The Eastern Colombian Savannas represent around 6% of the savannas in South America. This study identifies the land use/cover change (LUCC) patterns between three periods (1987-1988, 2000-2001 and 2006-2007) using Landsat and CBERS satellite images. The area burned between 2000-2009 using a novel regional algorithm tailored for MODIS data is quantified and validated. Results show that for the year 2000, 22% of the savanna ecosystems had been transformed, with flooded and high savannas being most affected. The annual rate of change from natural to non-natural between 1987-2007 was -0.85%. The fire assessment showed that on average 2.75 +/- 0.5 million ha of the savannas burn each year, being highly variable as 3.4 million ha burned in 2002-2003 which was 1.9 million ha less than in 2005-2006. However, it was shown that during 2000-2009, 39% of the savannas never burned. Fires predominate in the high plain savannas, with lowest occurrence along the Andean foothills, in forested areas and croplands. Based on predictive models implementing statistical methods, it was shown that in the occurrence of fires, the climate variables are important but only predict a 44%. The best predictive model with an accuracy of 78% includes variables such as climate, land use/cover, land form and topography. This study presents the first complete map at regional scale for almost two decades of LUCC and a decade of fire activity in Colombian savannas.

Dedication

To my Parents, brothers and friends

To my people in Llanos region in Colombia

To Suzette Flantua and Sonia Sua

Acknowledgements

I would like to express my gratitude to the many people who have supported me throughout my PhD experience. I am deeply grateful to my Supervisor, Dr. Kevin Tansey for the direction and patience, and particularly for providing expert guidance throughout my research. I am also indebted to Dr. Juan Carlos Berrio, Co-Supervisor, for his constructive feedback on my thesis and his knowledge and assistance in fieldwork, and of course for his valuable friendship and support throughout my stay in Leicester. My appreciation also goes to Javier Medina, Federico Cardona, Cici Alexander and Agata Hoscilo, PhD colleagues for their constant support and who have given me strength and enthusiasm to complete my research. Also everyone of the staff of Department of Geography of Leicester University for their continuous support and help.

I am particularly thankful to Suzette Flantua for her continuous writing English help and for the constant discussion about my research. To Sonia Sua who helped me in the discussion and analysis of land cover maps: Nestor Bernal for their accessory in the statistics analysis; Pilar Angulo, Adriana Sarmiento and Carolina Santos for her comments on the thesis: Natalia Gonzalez for her help

with climate data analysis and Gildardo Tovar for his help in the thesis design. I am very thankful to Professor Andres Etter who pressured me to write some of the results of this thesis. Last, many thanks to all my family, friends and colleagues who have supported me throughout the highs and lows.

I am thankful to the “Instituto de Investigaciones en Recursos Biológicos Alexander von Humboldt”: in particularly to Dolors Armenteras who always encouraged me to undertake this research and the Humboldt UNISIG group for permitting discussion with them. Also MODIS, Landsat and CBERS program teams, The Nature Conservancy (TNC), Instituto de Hidrología, Meteorología y Estudios Ambientales de Colombia (IDEAM), Instituto Geográfico Agustín Codazzi (IGAC), Instituto Amazónico de Investigaciones Científicas (SINCHI), Sistema Integrado de Monitoreo de Cultivos Ilícitos (SIMCI), for providing me the data collection for this research which would have never accomplished without it.

Finally, the thesis was supported by the Programme Alban, the European Union Programme of High Level Scholarships for Latin America, scholarship No. (E06D100666CO) and Foundation for Future of Colombia COLFUTURO.

Contents

List of Figures

List of Tables

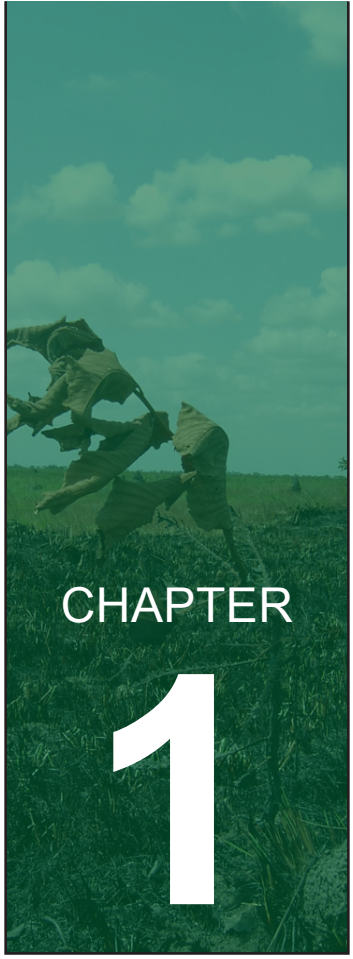

Overview of Manacacias river near to Puerto Gaitan (Meta, Colombia)

CHAPTER 1

Introduction

At a global scale, distribution, function and maintenance of the major ecosystems are determined by climatic factors such as temperature and precipitation (Bond *et al.* 2004). Changes in these climate conditions due to land degradation, fires and human population growth can affect ecosystems over time. In fact, these transformations cause not only land degradation but also have considerable ecological consequences like notable alteration in vegetation dominance from herbaceous to woody plant species, loss of biodiversity and species composition, ecosystem dysfunction, risk of flood or drought, soil erosion, modification of soil properties and agrochemical pollution (Pielke *et al.* 2002; Foley *et al.* 2005).

Moreover, the distribution of several ecosystems is determined by the presence of fire (Bond *et al.* 2004). Grasslands, Mediterranean shrub lands and savannas depend on the fire regime for their preservation (Goldammer 1993). Even though fires are natural processes in these ecosystems, fire regimes have been changing over the past two decades causing a high impact in terms of

ecological, economical and social aspect (Bowman *et al.* 2009). Today, fire is a worldwide phenomenon that affects all vegetated ecosystems.

Only in the last two decades, and thanks to advances in remote sensing, scientists have begun to quantify systematically land cover changes and fires with the aim to explain the impact of these factors on the global warming. These studies show that savanna ecosystems play the most important role in terms of fire dynamics worldwide. Historically savannas have been extensively managed by humans for different production purposes, influencing ecological processes such as fire frequency and biomass accumulation, and consequently altering the carbon cycle (Grace *et al.* 2006). Savanna vegetation plays a role in the global carbon cycle given their below-ground storage capacity, seasonal burning, regrowth and tree-grass dynamics. Savanna fires are a major source of CO_2 release to the atmosphere (Mouillot *et al.* 2006), and fires associated with tropical grazing systems are thought to have been contributing to more than 40% of globally burned phytomass (Hall and Scurlock 1991).

1.1. Savanna ecosystems

Tropical grasslands savannas are a continuous grass-dominated ecosystem of variable extent with shrubs and isolated trees, which can be found over a wide range of rainfall, temperature and soil conditions (Beard 1955; Solbrig *et al.* 1996). This formation is found widespread all over the world covering around 15 million km^2 to 24 million km^2 dominating half of the African continent (12 million km^2). Savannas are also found all throughout South Asia (2.5 million km^2) and Australia (1.9 million km^2). South America encloses the world's second largest area of moist savannas, containing an unique assemblage and diversity of plants and animals (Furley 1999). Figure 1.1 shows the distribution of the savanna ecosystems in the north of South America. These savanna ecosystems occupy 2.69 million km^2, of which 76% is found in the 'Cerrado' area of Brazil, 11% in the Colombian-

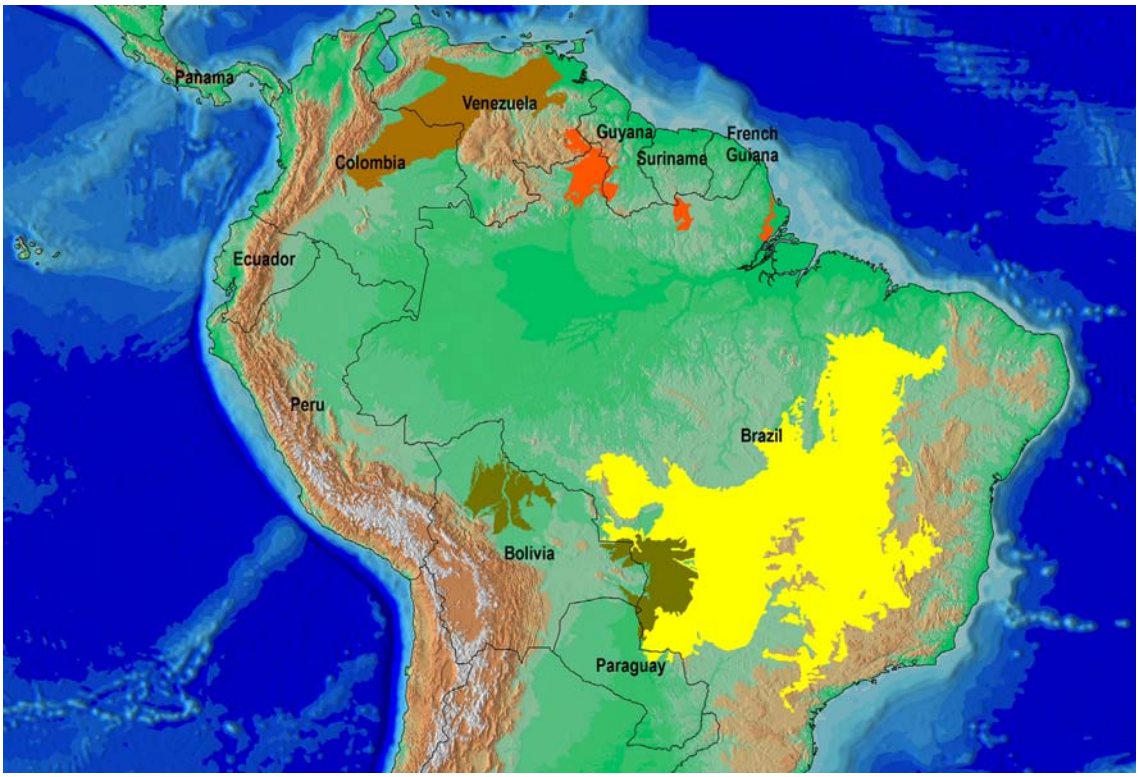

Figure 1.1. *Savanna ecosystem distribution in the North of South America. In yellow: Brazilian savannas 'Cerrado'; Brown: Colombian-Venezuelan 'Llanos'; yellow-green: Bolivian-Paraguay 'Chaco'; Orange: 'Guyana Shield' (Olson et al. 2001).*

Venezuelan 'Llanos', 5% in Bolivian-Paraguay 'Chaco' area and 1.5% in Guyana Shield (Sarmiento 1990).

Savannas are associated with the tropical wet and dry climate type where mean annual precipitation is between 400 - 2500 mm, with a marked seasonal water availability and the majority of rainfall being confined to one season of the year. The annual temperature is higher than 26°C (Solbrig *et al.* 1996; Huber *et al.* 2006). The duration of the dry season can vary from three to nine months, with a mode of five to seven months. The savanna soils are nutrient-poor, fragile, have low fertility, and high calcium, magnesium and aluminium content (Farinas 2008). These conditions are reflected in low agricultural productivity and the poor nutritional quality of natural pastures.

Sarmiento (1984) developed a typology of savannas integrating the hydrological seasonality (wet and dry annual sequence) and geomorphological conditions that determine soil water availability. This resulted in the categorization

of three main savanna types according to their different soil moisture availability and ecological functions:

i. **Seasonal savannas (SS)**: These savannas show two hydrological seasons; the first between four to six months, when the soil water content is low and the second one when the soil water availability is favourable. These savannas are characterised by a continuous C_4 grass vegetation cover with trees and scrub;

ii. **Hyper-seasonal savannas (HS)**: This type of savanna presents four different hydrological conditions: First, a period of two or three months without soil water available; a second period which lasts one or two months with moderate soil water available followed by a third period with six or seven months with a soil water excess and a fourth period lasting just one month with a similar soil water content to the second period. These savannas present a continuous grass cover, but with a larger proportion of C_3 than C_4 type species;

iii. **Semi-seasonal savannas (SeS)**: This type of savanna represents the most extreme condition of soil water excess and is characterised by approximately nine months with water excess and only two or three months with favourable soil water availability. These savannas have almost only mono-specific communities dominated by C_3 grasses. The Eastern Colombian Savanna (ECS) are characterized as 'hydrologic' savannas, with extreme seasonal fluctuation in the water table level (Pennington *et al.* 2006).

Although savannas of Africa and South America have the same origin and they share many structural and functional similarities, these ecosystems differ in ecological terms, flora and fauna as well as in land use and human population pressure (McNaughton *et al.* 1993). These differences are specified by McNaughton *et al.* (1993), Solbrig *et al.* (1996) and Fariñas (2008) as:

i. Local edaphic limitations result in variations in the regional patterns, particularly due to low fertility and flooding;

ii. In South America the leaf-harvesting ants are much more important herbivores than large mammals which is the case in Africa;

iii. South American precipitation oscillates between 800 and 2200 mm; in contrast to the African precipitation that ranges from 400 to 1000 mm;

iv. Almost one fifth of the world's population lives in the African savannas; South American savannas have a low population density and even some areas without inhabitants;

v. Rice, soya, sorghum, peanut, palm oil and pine plantation, extensive ranching and petroleum exploitation are the most important economic driving forces in South America, while sorghum, rice, millet, cocoa, coffee and traditional uses are in Africa;

vi. South American savannas are threatened by advances of the agricultural frontier, the petroleum expansion, introduced African grasses and extensive ranching. In Africa, savannas endure substantial population growth rates and extended dry periods.

Savannas are increasingly recognised as having global importance as centres of fauna and flora diversity and speciation. They are characterised by the coexistence of herbaceous vegetation and significant areas of forest usually in riparian environments (Scanland 2002; Veneklaas *et al.* 2005). Although they appear uniform, savannas have a rich diversity in terms of tree, scrub and herbaceous plants (Furley 1999). The relative abundance of these elements typify important aspects of this formation such as fauna habitats, biomass formation, nutrient cycling and combustion features for fire (Scanland 2002).

1.2. Land use/cover change and degradation in savannas

Since nomadic pastoralism times, savannas have been used to produce goods and services for humans by cutting and burning vegetation, fishing, hunting and harvesting. However, due to increasing population densities, patterns of resource use are changing rapidly as establishment of intensive agriculture, cattle ranching and infrastructure constructions are expanding (Chacón 2007). Currently, countries are focusing on intensifying agricultural production through establishment of large scale industrial agricultural and infrastructure projects, mainly encouraged by the economic internationalization (Correa *et al.* 2006).

The ecological impacts of these transformations lead to land degradation. This is a process of loss of the capacity of soil to sustain life, which is furthermore the result of factors associated with climatic changes, increasing anthropogenic pressures by population growth and land activities (Critchley *et al.* 1992). During the last five decades, human beings have been responsible for major land cover changes in a quick and extensive way (MA 2005). Studies estimate that during the last 300 years the area of cropland has increased globally from 300 - 400 million ha in 1700 to 1500 - 1800 million ha in 1990, which implies a 4.5 - 5 times increase in three centuries and a 50% net increase just in the twentieth century (Lambin *et al.* 2003). Similarly, the area under pasture increased from around 500 million ha in 1700 to 3100 million ha in 1990 (Goldewijk and Ramankutty 2003). These studies show a decrease from 5000 - 6200 million ha in 1700 to 4300 - 5300 million ha in 1990 of forest and 3200 million ha in 1700 to 1800 - 2700 million ha in 1990 of savannas, steppes and grasslands (Goldewijk and Ramankutty 2003).

Nowadays, land cover change is considered one of the principal factors influencing global change (Foley *et al.* 2005). Changes in land use also determine the vulnerability of places and people to economic or sociopolitical perturbations.

1.3. Fire in savanna ecosystems

Fire is both a natural and non-natural component of numerous ecosystems of the Earth (Bush *et al.* 2008). Fire activity is defined as a phenomenon that occurs when enough heat is applied to a vegetable fuel, that produces combustion. The term 'fire regime' describes when and how often an area is burned, as well as the frequency, severity, size and patchiness of fires. Fire regimes can have different impacts on fuels, fodder and biodiversity by changing the composition of plant species and by altering habitats (William *et al.* 2009). Globally, over 390 million ha of burned area was detected between 2000 and 2007, of which 80% occurred in woodlands and scrublands, and 17% in grasslands and croplands (Tansey *et al.* 2008). Thirty-eight percent of the fires occur in the southern hemisphere particularly in the tropical belt between 20°N-30°S (Dwyer and Pereira 2000; Tansey *et al.* 2008). Figure 1.2 shows the fire global activity between 2000 and 2007. Most of the fires are associated with savanna vegetation present in Africa, Australia and South America (Andreae 1992).

Fires are regarded as a seasonal event of which the highest peaks are associated with the dry period. Worldwide, there are two peaks of fire activity: one in July-August and a second in December-January (Dwyer and Pereira 2000). In southern South America most of the fires start in June showing a peak between August and mid-October. In Northern South America, specifically in Colombia and Venezuela, fires occur in the dry season between the end of November and early April, reaching a peak in February (Dwyer and Pereira 2000).

Fires produce elevated emissions of gases, however, there is uncertainty on the quantities and types of particles that are emitted (Crutzen and Andreae 1990). Figure 1.3 shows how global CO_2 emissions have increased during the last four decades related to income (Gross Domestic Product), energy and population.

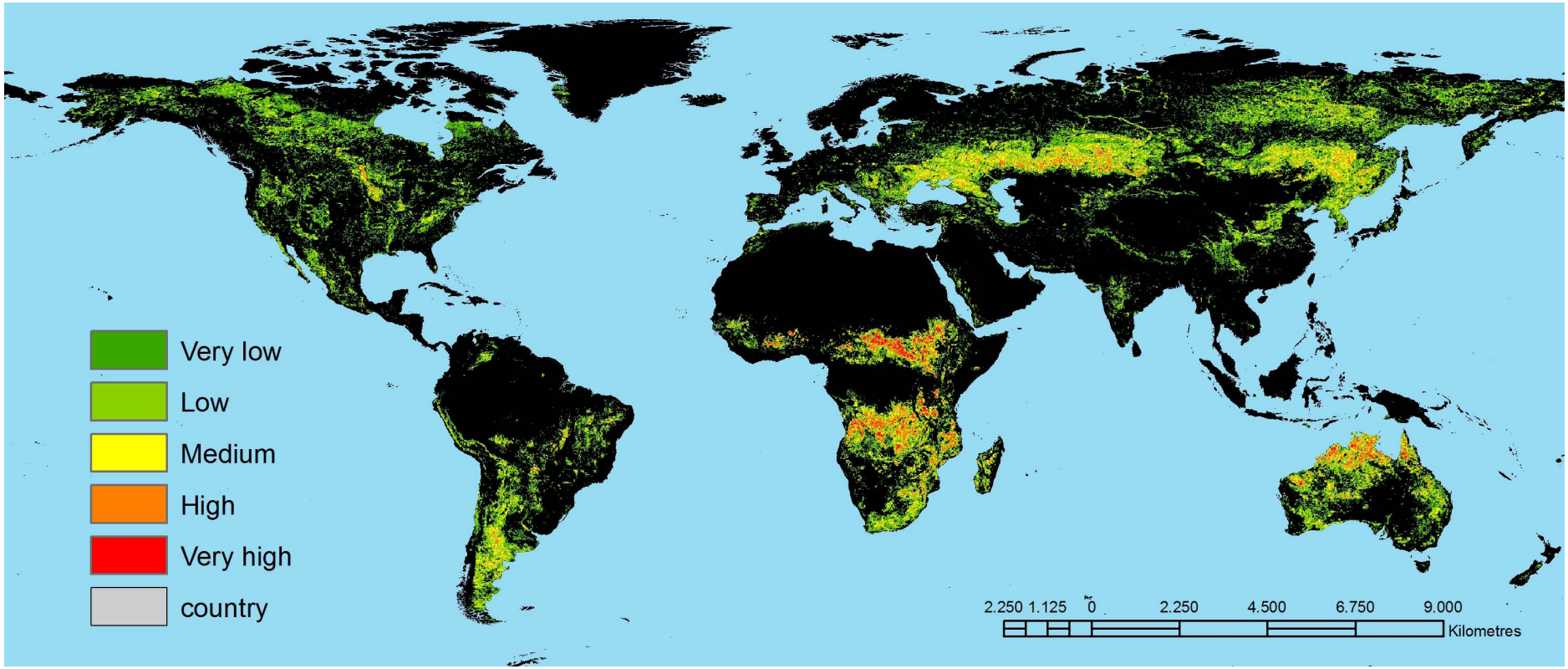

Figure 1.2. *The occurrence of global fire activity 2000-2007. Colour shows the frequency of fire occurrence during the seven year period (Tansey et al. 2008).*

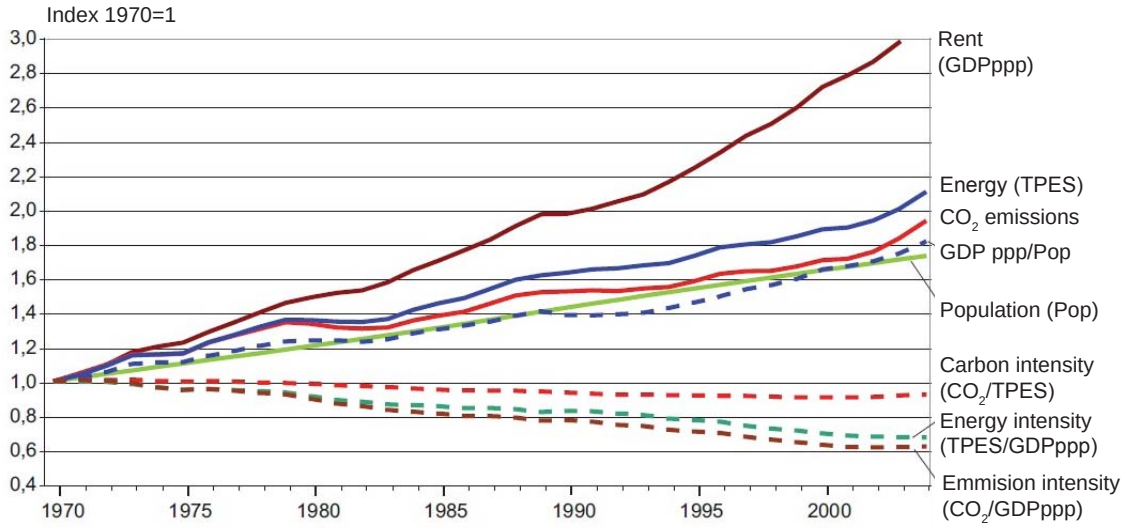

Figure 1.3. *Index of indicators for relative global development during the period 1970-2004: Gross Domestic Product measured in ppp (GDPppp), Total Primary Energy Supply (TPES), CO_2 emissions (from fossil fuel burning, gas flaring and cement manufacturing) and Population (Pop). In addition, in dotted lines, the figure shows Income per capita (GDPppp/Pop), Energy Intensity (TPES/GDPppp), Carbon Intensity of energy supply (CO_2/TPES) and Emission Intensity of the economic production process (CO_2/GDPppp) (IPCC 2007).*

CO_2 emissions from fires are estimated to have increased from 30 to 50% mainly in the tropical areas and this trend is thought to continue into the future (Mouillot *et al.* 2006). At present, fires in savannas ecosystems are stated to be the most important source of CO_2 release to the atmosphere, contributing to more than 40% of globally burned biomass (Mouillot *et al.* 2006).

1.4. Fire regime dynamic

Defining the ecological factors that affect the fire regime and how the intensity of these factors can be modified by human activity, are of the most important questions to be answered to improve understanding of the role of fire in the formation of savannas.

A detailed conceptual framework of fire occurrence in ECS can be built and it is shown in Figure 1.4. Fire events can be divided in two principal types: natural and non-natural (Levine 1992; Mbon *et al.* 2004). Natural events can be caused by thunderbolts or vegetation decomposition while non-natural fires are related to

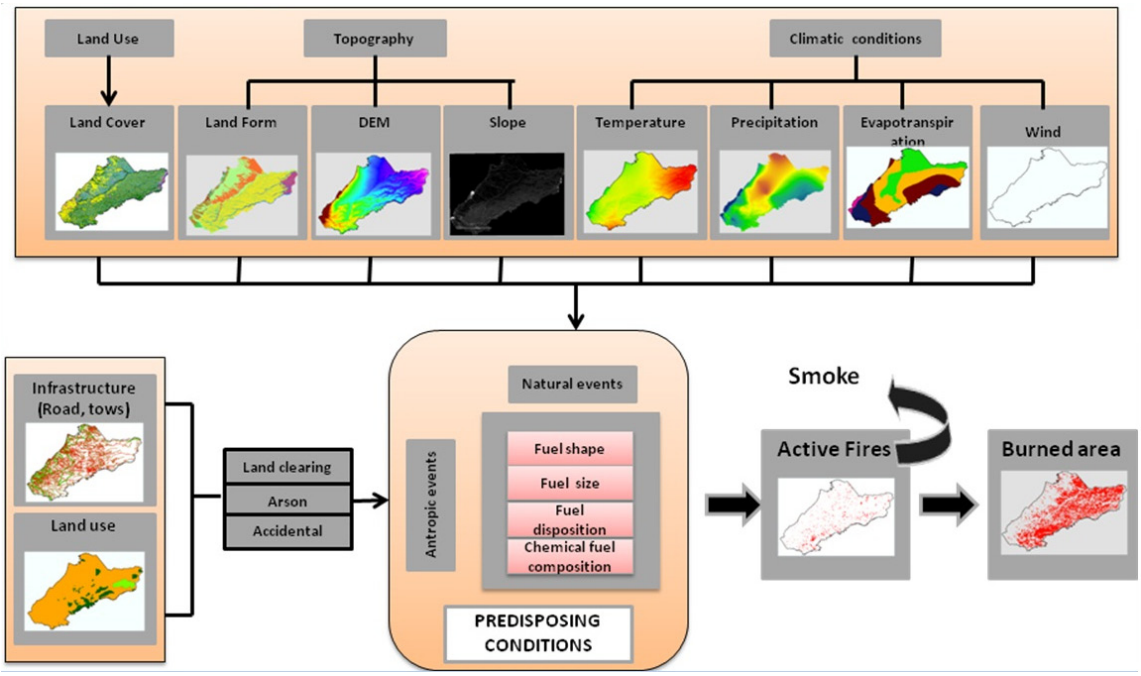

Figure 1.4. *Conceptual framework of fire occurrence. Adapted from Stolle et al. 2003.*

agriculture and infrastructure expansion, land clearing, by accident or arson. The combination of predisposing conditions increases the possibility of fire occurrence. Climatic factors like low precipitation, high temperatures, high evaporation and wind velocity facilitate a fire event. In addition topographic aspects like slope, LFor, soils and land cover conditions define the shape and area of a fire. Land cover also provides the necessary fuel for fires. The vegetation structure, life form (tree, scrub and grasses), combustion material (decomposition material, litter and woody elements) and chemical composition are the most important aspects that facilitate the ignition. Many authors discuss the spatial association between fires and these aspects (Dwyer and Pereira 2000; Eva and Lambin 2000; Roy 2003).

After ignition begins, the first step is the incipient phase, where the fuel begins to latch, around 20% of oxygen is available in the area and flames can reach temperatures of 637 °C. Next phase is the free combustion where more fuel material are involucrated, greater amount of smoke is produced, oxygen is reduced and the upper temperature reaches 700 °C. After that, the latent phase advances, which is the most dangerous phase; temperatures, smoke and combustion gases are above 700 °C. The final phase sets off where the fire

is extinguished due to the total combustion of fuel. As charcoal materials are deposited at the burned area and in the near surroundings, burned scars appear in the landscape.

Some authors like Finney (1998) and Stolle *et al.* (2003) discuss how climate conditions influence fire occurrence. For example, Finney (1998) shows that the solar radiation, humidity and winds are some of the principal climate factors that influence the generation and propagation of vegetation fires. Solar radiation intensity is greatest when the sun's rays fall perpendicular to the surface and this perpendicularity varies according to the season (Chuvieco *et al.* 2001). Moreover, Finney (1998) also discusses the influence of the relative humidity in the duration and severity of fires and the availability of fuel for ignition and combustion. Depending on humidity or dryness regime, the vegetation can become more or less resistant to the fire occurrence. So, if a humidity regime is low then the vegetation water content is low; the probability of ignition increases. In consequence lower humidity increases the likelihood of a fire event. With respect to the amount of fuel, the dry severity periods generates vegetation loss and death by water deficit, leading to greater availability of easily ignited fuel which is more likely to be affected by fires.

Chuvieco *et al.* (2001) shows that the water content of dead material fluctuates widely in response to changes in relative humidity of the area, precipitation and solar radiation. On the other hands with increasing temperature, relative humidity decreases, so that the moisture content of these fuels is maximum at early morning and early afternoon the least. Similarly, the moisture content of litter depends on the weather conditions, sun exposure and the soil moisture content. More air and desiccation, causes less soil moisture and drier leaf litter, which increases their flammability and combustibility and that of standing dead fuels (Zárate 2004). Finally, according to Rothermel (1991), the wind affects the generation and spread of fire due to the fluctuation of its speed and direction. Generally, the higher the wind speed the greater will be the intensity and speed of propagation. The inclination and elongation of the flame generated by the wind

favour the transmission of heat due to the decrease of the distance between the flame and fuel production. Another aspect that makes the wind one of the most important factors is based on the provision of increased amounts of oxygen to the fire reaction making it more efficient, drying out the vegetation and serving as a transport mechanism of sparks into unaffected areas.

1.5. Fire regime and landscape management

Fire regimes are also the product of people. People are an important source of ignition and they can manipulate fire regimes, by prescribing fire or by suppressing it (Williams *et al*. 2009). The fire has been recognized as an indicator of anthropogenic activity to help identify critical areas of deforestation and changes in land use (Malingreau and Gregoire 1996). The use of fire by humans has produced positive and negative effects on the environment and on the well-being and quality of human life (Hough 1993; Mbon *et al*. 2000). Man has used fire to develop roads, establish cultural areas, eliminate grass and other types of nondesirable vegetation, to eliminate culture wastes, extract natural resources, for hunting activities, land use management and to develop methods to prevent natural disasters (Mbon *et al*. 2000).

Eva and Lambin (2000) show that in the African savannas the fire regime differs as a result of the different land use management systems. Barbosa and Fearnside (2005b) found that most fires in the savannas of northern Brazil were started by humans, but that the spread of fire is independent of human presence. Romero-Ruiz *et al*. (2009) found that the overall proportion of unexpected and large fires in uninhabited areas like National Parks can be explained by the periodic movement of indigenous people living in reserves, moving around for their subsistence and using fire for hunting activities and cleaning of pests. In other contexts, such as the ecosystems of the Amazon basin, indigenous reserves and national parks are shown to be inhibiting factors on deforestation rates associated with burning activities, as four (Indigenous territories) to nine (national parks)

times higher deforestation rates are found outside their boundaries (Nepstad *et al*. 2006).

The effect of the ecological determinants associated with the fire regime of the savannas are being modified by human activities, especially through the transformation of the ecosystem into agroecosystems where the natural characteristics of the savannas are completely replaced, such as for intensive agriculture. Due to the low palatability and forage quality of the native grasses and woody plants in savannas a constant burning is necessary to obtain fresh new growth of grasses for maintaining the cattle. Coutinho (1990) found in the Brazilian savannas an increased burning frequency associated with the more intensive management of native pastures for cattle grazing. The study of Mistry and Beraldi, 2005 on the effect of cattle ranching on the fire regime found that the introduction of exotic grasses on fertile soils increases the fire regime in frequency. However, Bilbao and Medina (1990) showed for the Venezuelan savannas that the incorporation of exotic species has led to the reduction of fires attributable to the low fertility of soils. Introduced species require more nutrients and suppression of fires in areas of low fertility (Huntley and Walker 1982, Sarmiento 1984). Moreover it has been reported that these species inhibit the regeneration of trees and shrubs, affect the persistence of native species and pose a threat to biodiversity as the regional fauna depend on them for survival (Hoffman and Haridas 2008).

1.6. Study rationale

Despite their considerable geographical range and their importance within the landscapes of the Americas, tropical savannas have received limited attention in comparison to the well known and protected ecosystems such as the Amazon and Andes forests (Furley 1999). After the ‘Cerrado’ ecosystem, the ‘Llanos’ ecosystem constitutes the second largest area of savanna system in South America (Sarmiento 1984). Currently, these savannas are one of the

tropical areas that are most threatened in terms of land degradation and loss of biodiversity. In a study by San José and Montes (2001) an annual loss of 2.3% of the savanna ecosystem in Venezuela was reported between 1980 and 1990 due to agricultural activities. Studies in the Colombian savannas are of high importance because:

i. The Eastern Colombian Savannas (ECS) have over 55% of the wetlands of Colombia, forming part of the important hydrological system of the Orinoquian Basin;

ii. The ECS have a high biodiversity in terms of fish and migratory birds. They form an important corridor for many species of mammals and reptiles that migrate between the Amazon, Guyana and Andes regions;

iii. Currently only 5% of this savanna ecosystem is under National Park status;

iv. Nowadays, the ECS are considered one of the most important areas of development in Colombia. Programs for the establishment of large extents of palm oil plantations, rice, sorghum, sugar cane cultures and expansion of petroleum exploitation with subsequent increase of infrastructure and population growth are being implemented since 2000. As such, new threats are expanding from inside the ecosystem itself;

v. A study of the fire dynamics in the ECS shows that this region shows the most dynamic fire activity in Colombia: Sixty-eight percent of the fires that occurred in Colombia between 2000 and 2007 were found in this ecosystem (Tansey *et al.* 2008).

Authors like Sarmiento (1984), Huber *et al.* (2006), Pennington *et al.* (2006) have shown that changes in land use along with the regime of fires are two of the mainly factors that determining the presence of savannas. In the case of the

ECS, these processes have been similarly dominant in defining the ecosystem dynamic. Land use change humans is related to the presence of human who have replaced the natural vegetation by introduction of exotic grasses, infrastructure development and agricultural frontier expansion mainly rice cultures, palm oil plantations and currently sorghum and sugar cane cultures. Fire activity during the dry season is the second dominant factor in shaping the landscape of the savannas. Until now, in Colombia no systematic quantification of land use/cover change (LUCC) and fires has been done for this ecosystem.

To understand the LUCC and fire dynamics that have occurred and are occurring in the ECS, it is necessary to study the fire regime and its relationship with climatic, land use/cover (LUC) and other environmental factors. To understand the LUCC and fire activity that have occurred and are occurring in the ECS, it is necessary to study to fire regime and its relationship with climatic, land use/cover (LUC) and other environmental factors. For this purpose it was decided to use remote sensing data that allow obtaining information of great extensions of areas in real time during various decades and at different scales. Furthermore in the case of the ECS, the remote sensing data is practically the only source of information as hardly any quantifiable historical information exists on land use/cover and fire activity at a regional scale and which has been furthermore acquired in a systematical way. The results of the study contribute substantially to the formation of a conceptual and technical baseline for the establishment of a monitoring system in the ECS. This system would allow a precise and continuous mapping of land cover transformations and burned area which are crucial for political decisions on the sustainable use of these savannas.

1.7. Objectives

This study aims to quantify the frequency, area and severity of fires in the ECS using remote sensing techniques. The relationship between fire patterns

and environmental conditions, namely LUC, climate, land form and topography is evaluated. The following objectives are stated:

i. To identify the spatial patterns of regional land use/cover changes (LUCC) in the Eastern Colombian Savannas during the last three decades (1980-2007) based on satellite imagery analysis and fieldwork.

ii. To develop a regional algorithm to extract burned scars and determine the burned area, frequency and severity, based on a spatial-temporal model over a period of 10 year (2000-2009);

iii. To analyse and discuss the role of land use/cover, climate and topography on the fire regime using spatial and statistical methods;

iv. To discuss the impact of land use/cover change and fire regime in savannas on a regional and global scale.

1.8. Outline of the thesis

The thesis is divided into seven chapters; the following section presents a brief summary of the structure of the thesis and its content.

Chapter one provides an overview of the savanna ecosystem in a global context, describing the problems associated with land degradation and fire activity which is essential to understand the savanna dynamics. In addition, this first chapter describes the importance of this research study and its objectives.

A literature review is presented in chapter two. The main concepts of remote sensing detection, with a brief description of basic physical principles and

different methodologies used for land use/cover maps and burned scar detection are embodied.

An overview of the geographical localization, biotic, abiotic and socioeconomic characteristics is described in chapter three, to provide a better understanding of the ECS heterogeneity. Finally, this chapter introduces the use of China-Brazil Earth Resources Satellite (CBERS), Landsat and Moderate Resolution Imaging Spectroradiometer (MODIS) satellite images that constitute the principal data source for developing this research.

Chapter four develops the first objective of this investigation. Firstly, a detailed description of land use/cover mapping methodology is presented. Next, a Markov chain mathematical model is explained with the purpose of identifying the main types of changes. Finally, a brief discussion and summary of the results are given at the end of the chapter.

Chapter five discusses the fire regime as an answer to objective two. First of all, a detailed description of the methodology used for the detection of fire scars is explained. Then the products of the preprocessing, processing, regional algorithm, validation steps are presented and a comparison of the fire products. The main results, discussion and summary close the chapter.

Chapter six is focused on the LUC, climate, topography, fire integration and the application of spatial and statistical modelling to determine the relation between these variables to be able to answer objective three. First the methodology to integrate these variables is explained followed by the main results, discussion and summary.

Chapter seven summarize the results in relation to the stated objectives of this study and gives a general discussion about the role of LUC and fire regime in the savanna ecosystem viewed from the perspective of savanna dynamics and finally some recommendations on future work.

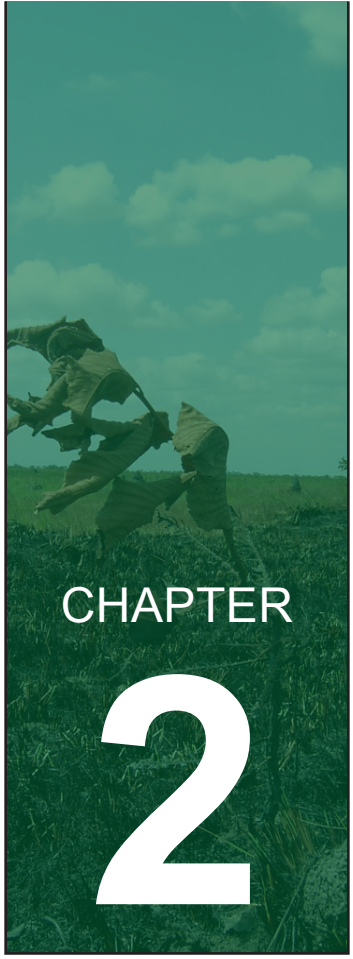

*Palm oil (*Elaeis guianensis*) plantation in Villanueva (Casanare, Colombia).*

CHAPTER **2**

Observing savanna ecosystems

Scientists always have been interested in understanding the global functioning of the Earth system with the intention of reaching an increased comprehension of and capacity to predict its behaviour. Ecological processes, climatic change and environmental degradation, among many aspects, determine the land use relationship between natural and social environments. This allows advances in remote sensing technologies to be made that can give scientific communities and international policy makers recommendations on improved land use and management of the Earth (Dwyer and Pereira 2000). During the last few decades knowledge regarding the change in land use/cover has advanced considerably. This not only serves in the conservation and management of the natural resources but it is also an indicator of the present state of the ecosystems (Dedios 2007).

2.1. Land cover change and fire regime approach

Land cover change is the most important variable of global change affecting ecological systems (Menault *et al*. 1993), as it plays an essential role in regional, social and economic development and global environmental changes. It contributes significantly to Earth – atmosphere interactions and biodiversity loss is a major factor in sustainable development and human responses to global change, and is important in integrated modelling and assessment of environmental issues in general (Xiuwan, 2002). Furthermore regional and local land use changes driven by the growing demands of the world population are also considered prime factors contributing to the observed global climate change trends (Foley *et al*. 2005; Pielke *et al*. 2002). Concerns about land-use/cover changes emerged in the research agenda on global environmental change several decades ago with the realization that land surface processes influence climate. In the mid 1970s, studies focused on defining how land-cover change modifies surface albedo and thus surface-atmosphere interaction, which have an impact on regional climate (1–3). In the early 1980s it was recognized that Land management practices are a major factor controlling the amounts of carbon within the terrestrial pool by influencing vegetation and soil characteristics (Grace *et al*. 2006; Ramankutty *et al*. 2007). Looking at a much broader range of impacts of land-use/cover change, of primary concern are impacts on biotic diversity worldwide, soil degradation, and the ability of biological systems to support human needs (Mbon *et al*. 2000). Land-use/cover changes also determine, in part, the vulnerability of places and people to climatic, economic, or sociopolitical perturbations (Mbon *et al*. 2000). When aggregated globally, land-use/cover changes significantly affect essential aspects of Earth system functioning.

The global study by Goldewijk and Ramankutty (2003) estimated that around half of the land clearing during the past three centuries has taken place in the savanna biome. Grace *et al*. (2006) estimated that worldwide savannas are being transformed at an average rate of more than 1% per year, but reliable

data on savanna transformation rates are still not available. Grace *et al*. (2006) point to important comprehension gaps in the knowledge and uncertainty about the ecological consequences of the transformation processes resulting from increasing land use changes in savanna ecosystems, with several contradictory views and unresolved aspects about their role in the global climate change. An important aspect of such knowledge gaps concerns the intra and interregional biophysical and land use variability that makes extrapolations difficult. Historically, savanna ecosystems have been extensively managed worldwide by humans for different production purposes, driving ecological processes such as fire frequency and biomass accumulation and consequently affecting the carbon cycle (Barbosa and Fearnside, 2005; Grace *et al*. 2006; Hoffmann *et al*. 2002), given their belowground storage capacity, seasonal burning, regrowth and tree-grass dynamics. Nowadays savannas are becoming increasingly important in the world food supply, especially in Latin America, and they are, therefore, prone to increasing human impacts (Ayarza *et al*. 2007; Brannstrom *et al*. 2008).

Additionally fires, whether natural or anthropogenic, also have pronounced climate forcing effects. Savanna fires are a major source of CO_2 release to the atmosphere (Mouillot *et al*. 2006), and fires associated with tropical grazing systems are thought to have been contributing to >40% of globally burned phytomass (Hall & Scurlock, 1991). Emissions from fires have increased over the last 100 years, from 30% to 50% mainly in the tropical areas (Mouillot *et al*. 2006). Furthermore, the emitted products from fires in savannas, other than CO_2, can remain in the atmosphere for a long period (Crutzen *et al*. 1979; Galanter *et al*. 2000), thus exacerbating the greenhouse effect (Carmona-Moreno *et al*. 2005).

Van der Werf *et al*. (2003) estimates carbon emissions from fires in the tropics to represent 9% of the net primary productivity (NPP) (4 PgCyr_1), of which 25% is consumed by tropical savanna fires. However, the spatiotemporal variability of carbon emissions from fire and other sources (such as cattle) in savannas is high due to the local and regional biophysical and land use heterogeneity (Wassmann and Vlek, 2004). Emissions from fires, for instance, vary significantly due to local

and regional differences in ecosystem type, biomass, and combustion efficiency (Van der Werf *et al*. 2003; Romero-Ruiz *et al*. 2010).

Satellite sensors provide the only means to study and understand the global distribution and timing of fire (Roy *et al*. 2010). In addition to type and cause, the prevailing characteristics of fire in a region are of great interest to scientists and ecosystem managers. The frequency, seasonality, severity, fuel consumption and spread patterns of fires that prevail are referred to as the fire regime (Bond and Keeley, 2005: Gill, 1975). How fire regimes will change as human population, their land use practices, and the climate changes is unclear. Climate and land use/cover changes are likely to affect fire regimes directly, through changes in the ways fire is used, and, indirectly, by modifying the environmental conditions and the amount of fuel available for fire (Frost, 1999, Archibald *et al*. 2009). Of the different variables defining a fire regime, only the frequency and seasonality of fire can be derived in a demonstrably reliable manner from satellite date, usually as summary statistics of burned area or active fire counts, with results depending on the scale of the analysis and on the completeness and reliability of the satellite time series (Giglio *et al*. 2006; Boschetti and Roy, 2008).

A number of research works have been carried out by using various methodologies and algorithms to derive land use/cover change and fire regime information from different sets of remotely sensed data (Lambin *et al*. 2003). However, the complex heterogeneity of savannas makes it difficult to develop a general method for all applications in different savanna regions in the world. Fine resolution, spatially explicit data on land-use/cover changes are required to define the impact of landscape fragmentation on biodiversity, composition, structure and functionality of ecosystems. Understanding of the causes of land-use change has moved from simplistic representations of two or three driving forces to a much more profound understanding that involves situation-specific interactions among a large number of factors at different spatial and temporal scales.

In conclusion, remote sensing techniques have become a fast and cost efficient method for studying large regions and enable careful decision-making (Cihlar 2000). Furthermore, remote sensing is extremely useful for areas where the accessibility is complicated, mainly due to lack or poor quality of roads. The use of remote sensing allows obtaining a rapid and precise inventory of land cover through time. By quantifying and predicting the changes in land cover at a high resolution and a regional scale, it provides the necessary data to improve our understanding of the impacts on changes in biodiversity, landscape degradation and at a global scale climate change as well as human interaction with the environment (Lambin *et al*. 2003).

2.2. Observations using remote sensing methods

Remote sensing techniques have become key essential tools to understand main changes and disturbances on the Earth's surface (Ehlers *et al.* 1990; Weng 2001; Palacios-Sanchez *et al.* 2006). Thanks to their capacity to obtain data of great extensions of areas in real time, during long periods of time and at different scales, remote sensing techniques have taken a high-priority role in understanding, monitoring and predicting the geographic phenomena of the Earth, as well as comprehending the human influences and the environmental changes that are occurring. Implemented since the beginning of the 20th century, when the first aircraft took pictures of the Earth, these tools offer a valuable source of data to monitor land cover efficiently, effectively and at low cost (Mas 1999). In the last five decades, significant advances have been made in space science, remote sensing platforms and sensors, which have improved the capability of constantly taking images of the Earth through space and time.

2.2.1. Physical principles

The basic principle of remote sensing is to analyse and interpret the electromagnetic radiations reflected by any object on Earth, without being in direct contact with the same (Mather 2005). Each object on the earth's surface and atmosphere reflects, absorbs, transmits and/or emits electromagnetic energy in different proportions according to the internal components of the feature. The electromagnetic energy moves at the speed of the light in the form of waves or particles. Through the electromagnetic spectrum the energy is defined by the wavelength and (sub-) divided in fringes that represent regions with particular characteristics of their own, in terms of physical processes of energy detection (Figure 2.1).

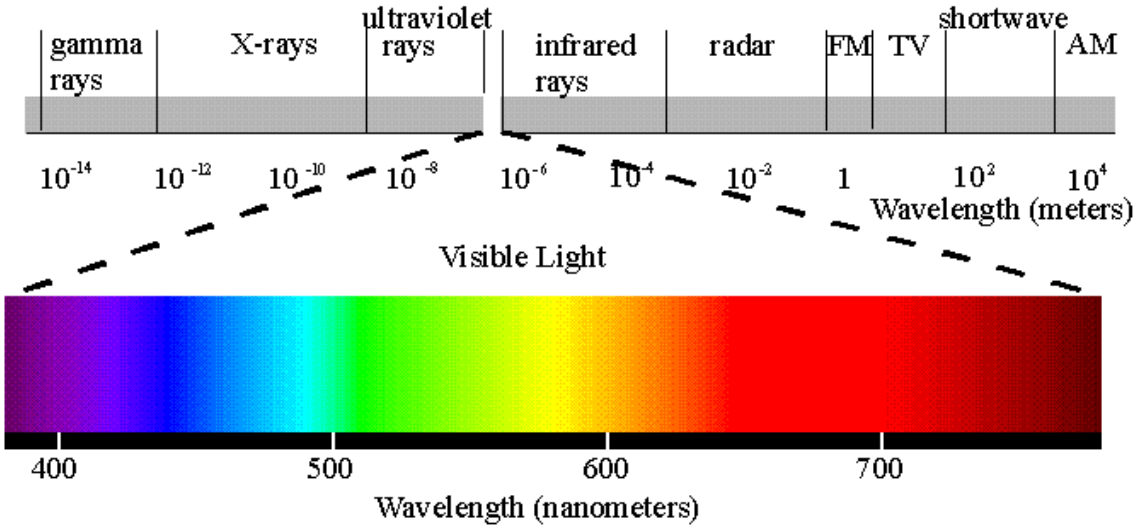

Figure 2.1. *Electromagnetic spectrum. This spectrum is classified by wavelength into radio, microwave, infrared, the visible region, ultraviolet, X-rays and gamma rays according the physical processes of energy detection (http://www.optics.arizona.edu/Nofziger/UNVR195a/Class12/EMspectrum1.gif).*

The interaction between solar radiation, atmosphere and terrestrial surface depend on the wave length of the radiation and the internal characteristics of the objects. Outside of the Earth system no loss of radiation exists, only attenuation of this energy. At the moment that the solar radiation enters the atmosphere, part of it is reflected or dispersed by the atmospheric particles, while another crosses the atmosphere and reaches the Earth's surface on reaching the terrestrial surface the energy can behave in three different ways: **i.** Reflect: part of the

radiation is returned to space; ii. Absorb: part of it passes to increase the energy of the object and; iii. Transmit: part of it is transmitted to the soil or other objects. The fraction of the energy that is reflected is denominated 'reflectivity' or 'albedo' (ρ); the absorbed fraction is denominated 'absorptivity' (ά) and the transmitted fraction is denominated 'transmitivity' (τ). The sum of ρ and τ and ά is equal to 1.

Each material reflects the incident radiation in different ways allowing it to be distinguished from other materials/objects. This reflectivity is subordinated to the atmospheric conditions, the slope and orientation of the landscape and the geometry of the point of view. In case of surface features, two types exist, those that reflect the radiation directly with an angle similar to the incident angle (specular surfaces like water bodies) and those that reflect the radiation towards all directions (Lambertian surfaces, the majority of land objects). The remote sensing techniques take the reflective values for classifying objects, while the quantification of the absorbance allows the determination of the characteristics of a vegetation cover (Sabins 1997).

2.2.2. Spectral behaviour of surface elements

In order to conduct any remote sensing interpretation, it is necessary to understand the principal biophysical properties of the objects on the Earth before beginning the study with remote sensing data (Lea 2005). Each surface of the Earth presents different characteristics in terms of reflectivity.

Spectral characteristics of different Earth surface materials, allow distinguishing these materials with remote sensing techniques. The blue band (0.45-0.52 µm) is useful for separating clouds, but not useful for water, vegetation and soil types as these surfaces have similar reflectance values. The red band (0.63-0.69 µm) and the near infrared band (0.75-0.90 µm) allow separating soil and vegetation.

In the case of clear water, the absorption is high and the reflectivity is low; the electromagnetic spectrum shows a small spike in the green region and decreases as the wavelength increases. Hence, clear water appears dark-bluish. Depending on the cloudiness of the atmosphere and the depth of the water column, the reflectivity changes, allowing distinguishing different types of water (Lillesand and Kiefer, 1994). For instance turbid water increases the reflectance in the red end of the spectrum, due to some sediment suspension. Hence turbid water appears brownish (Figure 2.2).

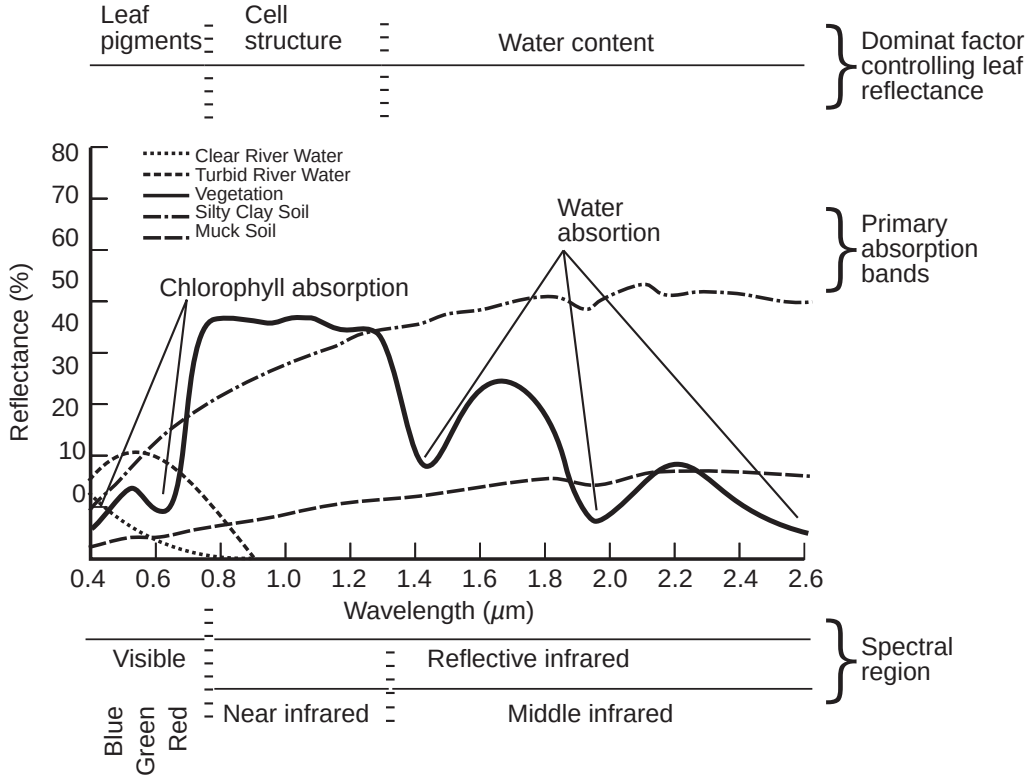

Figure 2.2. *Spectral reflectance curves of different Earth's elements.*

For the soil the transmittance is low to null and practically all energy is absorbed or is reflected. Features such as the moisture content, particle size distribution, iron oxide content, soil mineralogy, soil structure and organic matter determine the spectral characteristics. For example, in sandy soils the reflectivity is usually higher than in loamy soils due to the greater quantity of organic matter that presents a lower reflectivity. The typical spectral reflectance curve increases with wavelength in the visible portion of the spectrum and then stays relatively constant

in the near and short infrared, with some local dips due to water absorption at 1.4 and 1.9 μm and due to clay absorption at 1.4 and 2.2 μm (Lillesand and Kiefer, 1994).

For clouds, the reflectance is high and the absorption is low in the visible bands. The reflectance diminishes in the near infrared, and finally in the middle infrared the absorption is high and the reflectance is low (Figure 2.2).

For vegetation, the abundance, composition and conditions are the basic properties that determine the spectral quantity and quality of solar reflectance radiation arriving to satellite sensors (Rogan *et al.* 2002). Figure 2.2 shows the spectral behaviour of vigorous vegetation. In this type of vegetation, a low reflectivity is detected in the visible bands due to the absorbing effect of the pigments in their leaves that capture the radiation around the 0.445 μm ($x10^{-6}$) wavelength. A second absorption occurs near to 0.645 μm due to presence of chlorophyll pigments. Between these two portions of the spectrum, a band centred on 0.55 μm is less absorbent, showing a maximum relative reflectivity between visible bands. Near infrared shows high reflectivity, mainly due to the internal cellular structure of the leaves. This is reduced progressively towards the mid-infrared, reaching 1.45 μm where the effect of absorbing water causes a drastic reduction of the reflectivity. The absorption occurs at the 1.92 μm and 2.7 μm (Mather 2005). As a plant senescence the level of reflectance in the near infrared decreases, but is not being affected significantly in the visible bands.

2.2.3. Remote sensing of land cover change

Through time, approximations for mapping LUC have improved, mainly depending on the spatial, temporal and spectral resolution of the sensor and needs of the user (Weng 2002). The methods developed to classify LUC go from low to high complexity (Civco 1993) and are grouped in three main categories (Table 2.1).

Table 2.1. Low to high level methods developed to classify LUC using remote sensing techniques.

	Low-Level	Medium-Level	High-Level
Method	Different vegetation Index [4] Supervised and unsupervised classification	Object-oriented analysis [5]	Artificial neural network [6] Automata Cellular Analysis [7] Decision trees [8]
Principles	Part of the spectral response of the different objects measured in the different spectral regions that the remote sensor work [1]	Take into account the spectral properties of the objects and associate them to the spatial properties such as texture, context and shape. [2]	Take into account the spectral, spatial and temporal properties of the objects and incorporate the human knowledge [3]
Advantages	• Objective and quantitative criteria are employed; • Statistically-based algorithms are used; • Independently of human image analysts; • Consistency and reproducibility. • Use of secondary information possible.	• Incorporation of spectral attributes such as tone. • Incorporation of spatial attributes such as shape, size, shadow, pattern, texture. • Interpreted areas of similar properties not pixels.	• Incorporation of spectral attributes such as tone; • Incorporation of spatial attributes such as shape, size, shadow, pattern, texture; • Interpreted areas of similar properties not pixels; • Human image analysts perform these tasks rather intuitively.
Disadvantages	• High scene-dependence; • Produces fragmented areas or salt and pepper-like patterns; • Generally procedures are established by inflexible computer algorithms; • Based only on spectral properties for a single-date; • Spatial attributes are not considered (Shape, texture and patterns).		• Rules and decisions depend on the human image analysts; • Complex.

1. Civco 1993, Chuvieco *et al.* 2004, Mbon *et al.* 2004; 2. Civco 1993, Willhauck 2000, Bauer and Steinnocker 2001, Blaschke and Strobl 2001; 3. Civco 1993; 4. Chuvieco *et al.* 2004; 5. Kartikeyan *et al.* 1998; 6. Civco 1993; 7. Li *et al.* 2001; 8. Hansen *et al.* 2002.

Furthermore, to do an analysis of changes of land use, two principal methods have been used, that take into account the alterations in abundance, condition and compositions of the elements within the remote sensor data on different spatial and temporal scales (Stow 1995; Rogan *et al.* 2002). These techniques are:

i. **Pre-classification enhancement**: This is based on mathematical combinations that enhance the spectral characteristics within each band. All band enhancements are compared at different periods in time to obtain the changes in pixels of the determined area (Muchoney and Haack 1994; Mas 1999). Differential vegetation indices and principal components are methods that work according to the described methodology (Chavez and Kwarteng 1989; Rogan *et al.* 2003). This technique has the advantage that it is systematic; however, the images must be within the same phenological period (Coppin *et al.* 2004).

ii. **Post-classification analysis**: This method compares two independent classifications of different periods, in order to obtain changes in composition of elements inside the area of interest. High geometrical accuracy is required for the generated classification (Sigh 1989; Mas 1999). This technique has the advantage that it allows the use of images from different phenological periods but has the disadvantage that it does not detect subtle changes (Stow *et al.* 1990; Rogan *et al.* 2003).

Independent of the specific aim of the classification method, four general steps are required to extract the satellite data information (Cihlar 2000). Depending on the spatial, spectral and temporal characteristics of the sensor, options in decision-taking are available during four steps of the process. The steps are as followed:

i. **Data acquisition**: The first step in all classifications is the acquisition of the satellite images. High resolution data with spatial resolution between 1 and 30 m are generated in periods of two or three weeks (Landsat and ASTER, every 16 days; CBERS every 26 days). Moderate and coarse resolution data with spatial resolution of 250,

500, 1000 m is generated in periods of one or two days (MODIS, AVHRR, SPOT-VEGETATION);

ii. **Preprocessing**: This step is divided in three components: geometric corrections, composition and radiometric correction. With high resolution data only geometric and radiometric corrections are needed. The low frequency of acquisition does not allow an image composition, as only individual adjacent scenes of different periods are used in order to eliminate clouds. With moderate and coarse resolution data, all the preprocessing steps are implemented. To eliminate atmospheric noise, bidirectional effects, clouds and shadows, a composition is made of several days from which new image products are generated (Emery *et al.* 1989; Nishihama *et al.* 1997). The correction process is an essential research procedure that makes the data spectrally comparable and extracts enhanced information (Jensen 2000). This process eliminates discrepancies in scene illumination and viewing geometry, identifies atmospheric scattering or absorption and estimates spectral reflectance at a superficial level (Mather 2005). The ancillary information such as aerosol and water vapour provides the basic information to identify gases, aerosols and thin clouds such as cirrus;

iii. **Classification**: Different techniques from satellite image classification have been developed, depending on the spectral and spatial attributes of the image. While in high resolution data the spatial and spectral attributes are important for classification, in moderate and coarse resolution only the spectral attribute is relevant. Generally, techniques of classification include two types of approaches, which make different assumptions on the basis of the researcher's knowledge of the image scene to be classified. Supervised classification is one of the techniques that allow the classification of a scene according to

the priori knowledge of land cover types to be mapped. Unsupervised classification is the other technique in which a priori information is not necessary. Unsupervised classification methods works with predefined parameters of the spectral properties and with a statistical process that determines the different elements inside of the image scene (Cihlar 2000; Jensen 2000);

iv. **Product generation**: All classifications require verification of the accuracy and precision of the product. The classification product derived by the high resolution data is generally corroborated with fieldwork, aerial photography and airborne video (Magnussen 1997). In contrast, classifications of moderate and coarse resolution images are corroborated with high resolution data and in some cases with fieldwork and aerial photography.

In order to classify LUC, numerous vegetation indices have been developed. These algorithms have been developed relating the spectral data and biophysical characteristics of the vegetation such as the leaf area, biomass, water content, chlorophyll and other biophysical characteristics. The Normalized Difference Vegetation Index (NDVI) was the first one to be developed and is the base for the development of later algorithms (Table 2.2).

These approaches have been the base for the classification of LUC with Landsat. They have been proven and evaluated from a world-wide to regional level. Studies were done by Vogelmann and Rock (1988) and Eva and Lambin (1998) among others.

2.2.4. Observation of fire activity

Satellite technology has become the principle tool to obtain temporal and spatial data that allows the detection of processes occurring at the Earth's surface

Table 2.2. Different indices developed to detect LUCC.

Acronym	Index
NDVI	$(\rho_{NIR} - \rho_R)/(\rho_{NIR} + \rho_R)$
RVI	ρ_{NIR} / ρ_{RED}
TVI	$\sqrt{(\rho_{NIR} - \rho_{RED}) / \rho_{NIR} + \rho_{RED})} + 0.5$
CTVI	$((\rho\ NDVI + 0.5)) / ABS(NDVI + 0.5) * \sqrt{ABS(NDVI + 0.5)}$
NDII	$\rho_{IRC} - \rho_{SWIR} / \rho_{IRC} + \rho_{SWIR}$
MSI	$\rho_{SWIR} - \rho_{IRC} / \rho_{SWIR} + \rho_{IRC}$
NDVI53	$\rho_{SWIR} - \rho_R / \rho_{SWIR} + \rho_R$
NDVI47	$\rho_{NIR} - \rho_{FIR} / \rho_{NIR} + \rho_{FIR}$
MSAVI	$[(2 * \rho_{IR} + 1) + (2 * \rho_{IR} + 1)^2 - 8 * (\rho_{IR} + \rho_R)]^{1/2} / \rho_R$
N37I	$\rho_R - \rho_{SWIR} / \rho_R + \rho_{SWIR}$
NDWI	$\rho_{NIR} - \rho_{SWIR} / \rho_{NIR} + \rho_{SWIR}$
TTVI	$\sqrt{(ABS(\rho_{NIR} - \rho_{RED} / \rho_{NIR} + \rho_{RED})} + 0.5$
NDVI75	$\rho_{SWIR} - \rho_{MIR} / \rho_{SWIR} + \rho_{MIR}$
NDVI51	$\rho_{SWIR} - \rho_B / \rho_{SWIR} + \rho_B$
NDVI152	$\rho_{SWIR} - \rho_G / \rho_{SWIR} + \rho_G$
EVI	$G * (\rho_{IR} - \rho_R) / (\rho_{IR} + C1 + \rho_R - C2 * \rho_B + 1)$
MNDWI	$\rho_G - \rho_{MIR} / \rho_G + \rho_{MIR}$
TSA **VI**	$a(\rho_{NIR} - a * \rho_{RED}) / \rho_{RED} + a * \rho_{NIR} - a * b$

ρ: Surface reflectance; NDVI: Normalized Difference Vegetation Index; NDII: Normalized Difference Infrared Index; SAVI: Soil Adjusted Vegetation Index; MSAVI: Modified Soil Adjusted Vegetation Index; EVI; Enhanced Vegetation Index; MSI; Moisture Stress Index; NDWI: Normalized Difference Water Index; RVI: Radio Vegetation Index; NRVI: Normalized Ratio Vegetation Index; TTVI: Thiam's Transformed Vegetation Index; CTVI: Corrected Transformed Vegetation Index.

such as vegetation fires (Kendall *et al.* 1997; Dwyer and Pereira 2000). For fires, two methods are used: the detection of active fires and the detection of burned area. Active fire detection is based on the amount of emission or instantaneous radioactive power that is produced by area in flames which can be detected by the satellite (Koufman *et al.* 1998; Dwyer and Pereira 2000; Stropianna *et al.* 2000; Giglio and Justice 2003; Wooster and Zhang 2004; Laris 2005). The detection of fire scars is based on the multispectral characteristics that are present in burned areas within a satellite image (Van Wagtendonk *et al.* 2004; Laris 2005). For their implementation, algorithms that work according to the characteristics of the sensors have been designed, such as with AVHRR NOAA (Eva and Flasse 1996; Koffi *et al.* 1996; Barbosa *et al.* 1999), ATSR (Eva and Lambin 1998), SAR (Kasischke 1996), MODIS (Koufman *et al.* 1998), and VEGETATION SPOT 4 sensors (Gregoire *et al.* 2003; Tansey *et al.* 2004a).

Low resolution sensors only capture information at a resolution of one kilometre and larger. Consequently, they present difficulties in the identification of areas where burn scars are small which leads to both the overestimation and underestimation of the burned area (Eva and Lambin 1998; Maggi and Stroppiana 2002; Russell-Smith *et al.* 2003; Boschetti *et al.* 2004; Fraser *et al.* 2004; Hoelzmann *et al.* 2004; Laris 2005; Silva and Pereira 2005; Wang *et al.* 2006). Algorithms based on data obtained by low resolution satellite images are being applied at global scales (Malingreau *et al.* 1990; Meneaut *et al.* 1992; Russell-Smith *et al.* 1997; Bucini and Lambin 2002; Laris 2002; Bowman *et al.* 2003; Boschetti *et al.* 2004). Problems due to low resolution have been described by a number of authors (Moody and Woodcock 1996; Eva and Lambin 1998; Maggi and Stroppiana 2002) and are summarised below:

i. Fire characteristics depend on the type of the vegetation, season (dry/wet) and geographic zones that are affected. The detection thresholds that have been developed assume that all the fires have the same spatial-temporal characteristics producing unique thresholds for their

identification (Laris 2005; Wang *et al.* 2006; Lobada and Csiszar 2007). These algorithms were not designed for local scale studies;

ii. The number of active fires and burned area can be over -or under- estimated (Li *et al.* 2001). Algorithms confuse highly reflective surfaces such as water, clouds, hot surfaces and suffer from sun glint (Dwyer and Pereira 2000; Csiszar *et al.* 2006; Wang *et al.* 2006; Lobada and Csiszar 2007);

iii. The duration of an active fire is generally very short, and as a consequence it may not be detected by orbiting sensors if the temporal resolution is low (Laris 2005);

iv. Fire size and burned area can be very small (< 10 ha) and may not be detected by low resolution sensors such as NOAA AVHRR, AATSR or SPOT VEGETATION with spatial resolutions in the order of 1 km^2 (Laris 2005);

v. The time of the satellite overpass may limit the detection of active fires. Fire activity is generally lower in the morning than in the afternoon. Most sensors pass during the morning, resulting in an incomplete picture of fire activity (Eva and Lambin 1998; Lobada and Csiszar 2007);

vi. The presence of atmospheric noise and clouds restricts the accurate detection of fire and burned areas in some regions (Laris 2005).

As has been pointed out, one of the problems with algorithms is the determination of burned area from a reflectance threshold. This threshold is taken directly from the satellite image and it is related to its temporal and spatial resolution. Low resolution may cause the signal from the ground to be a mixture of the different land covers found at sub-pixel level. Therefore a pixel that contains a fire scar along with other land cover types will exhibit a decrease in the reflectance

value below the detection threshold (Razafimpanilo *et al.* 1995; Laris 2005). Studies have shown that detection decreases with burned area size (Barbosa *et al.* 1999; Maggi and Stroppiana 2002; Yates and Russell-Smith 2002; Boschetti *et al.* 2004). Moreover, in savanna areas the vegetation cover dries during the fire season which in turn decrease reflectance, possibly leading to confusion in the detection algorithms (Laris 2005).

At present, algorithms implemented at a local scale are being developed using moderate and high resolution satellite images. These algorithms allow the correction of some of the errors previously mentioned by taking into account vegetation type characteristics (Barbosa *et al.* 1999; Pereira 1999; Roy *et al.* 1999). Examples of local scale algorithms for the detection of burned area are presented by Eva and Lambin (1998), Arino *et al.* (2001), Li *et al.* (2001), Pereira (2003), Roy and Landmann (2005) while information on active fires can be found in Wang *et al.* (2006), Xie *et al.* (2007). Local scale studies have been presented for southeastern Asia (Jones 1997), Africa (Arino and Melinotte 1995), Brazil (Miranda *et al.* 1994) and Europe (Chuvieco and Martin 1994; Boles and Verbyla 2000). These algorithms are being used to relate aspects of landscape with spectral indices in an attempt to quantify fire intensity (Bannanari *et al.* 1995). The frequency, severity and area of a fire will depend on the meteorological conditions at the time of the fire, the type and structure of the landscape, land use and land cover, biomass, species heterogeneity, distribution and age, and combustion rates (Levine 1992; Shvidenko and Nilsson 2000; Bachmann and Allgoewer 2001; Li *et al.* 2001; Lobada and Csiszar 2007). Temperature, relative humidity and combustion rate are highly correlated with fire severity (USDA 1995; van Wagner 1997; Flenningan *et al.* 2005). Spectral contrast between burned and non-burned areas are the result of direct charcoal deposition and the removal of the vegetation that cause a superficial heating of the soils, leading to a low albedo and evapotranspiration suppression (Robinson 1991; Laris 2005). The burned areas show contrasts with other covers in the visible and the infrared spectrum (near, medium and thermal) (Franca *et al.* 1995; Eva and Lambin 1998). The distinction of burned and non-burned areas is a function of the initial vegetation

reflectance values (Roy and Landmann 2005). For example, cover types with high values of reflectance in the infrared such as forest areas, exhibit greater changes in reflectance magnitude after a fire. In general, areas with burned scars surrounded by wooded vegetation are more difficult to detect compared to areas surrounded by dry grasses (Eva and Lambin 1998).

Furthermore studies in burned areas have advanced through the handling and use of spectral indices (Chuvieco *et al.* 2004). These indices employ the properties of reflectance of the soils after an event of fire i.e. charcoal and ashes deposition, removal and alteration of the structure of the vegetation (Smith *et al.* 2007). The spectral indices are obtained by the combination of data collected in different spectral regions (Chuvieco *et al.* 2004; Mbon *et al.* 2004; Lozano *et al.* 2005). With high (Landsat, Ikonos) and medium resolution images (MODIS), indices for the detection of burned areas have been developed (Table 2.3)

All these indices use the decrease of observed reflectance value to detect burned areas. Indices like the Normalized Difference Vegetation Index (NDVI), Soil Adjusted Vegetation Index (SAVI), Burned Area Index (BAI), Normalized Difference Water Index (NDWI) and Normalize Burn Radio (NBR) have been examined to improve the detection of burned area (Kasischke and Frech 1995; Fernández *et al.* 1997; Chuvieco and Martin 2002; Key and Benson 2006; Phua *et al.* 2007). In savanna areas the use of vegetation indices is very useful because of the general absence of vigorous vegetation. Several have been applied and validated with MODIS images in South Africa (Smith *et al.* 2007). Indices like BAI, NDVI, VI3 and GEM have been shown to present commission or omission problems in the detection of burned areas (Eva and Lambin 1998; Pereira 1999; Chuvieco and Martin 2002). However many of these indices have not been applied to the savanna ecosystem (Smith *et al.* 2007).

Table 2.3. Different indices developed to detect fires.

Acronym	Index
NDVI	$(\rho_{NIR} - \rho_R) / (\rho_{NIR} + \rho_R)$
GEMI	$n(1-0.25n) - (\rho_r - 0.125) / (1 - \rho_r)$
BAI	$[(G_r - \rho_r) + (G_{NIR} - \rho_{NIR})^2]^{-1}$
SAVI	$(\rho_{NIR} - \rho_R)(1+L) / (\rho_{NIR} + \rho_R + L)$
MIRBI	$10\rho_{SWIR} - 9.8\rho_{LNIR} + 2.0$
NBR	$(\rho_{NIR} - \rho_{SWIR}) / (\rho_{NIR} + \rho_{SWIR})$
CSI	ρ_{NIR} / ρ_{SWIR}
VI6T	$(\rho_{NIR} - S_{TIR}) / (\rho_{NIR} + S_{TIR})$
NBRT	$[\rho_{NIR} - (\rho_{SWIR} S_{TIR})] / [\rho_{NIR} + (\rho_{SWIR} S_{TIR})]$
CSIT	$\rho_{NIR} / (\rho_{SWIR} S_{TIR})$
NDVIT	$(\rho_{NIR} - \rho_R S_{TIR}) / (\rho_{NIR} + \rho_R S_{TIR})$
SAVIT	$(\rho_{NIR} - \rho_R S_{TIR})(1+L) / (\rho_{NIR} + \rho_R S_{TIR} + L)$

BAI: Burned Area Index; **CSI**: Char Soil Index; **GEMI**: Global Environmental Monitoring Index; **MIRBI**: Mid-InfraRed Bi-spectral Index; **NBR**: Normalized Burn Radio; **NDVI**: Normalized Difference Vegetation Index; **SAVI**: Soil Adjusted Vegetation Index; **VI6T**: Vegetation Index Number 6 Thermal; **NBRT**: Normalized Burn Ratio-Thermal; **CSIT**: Char Soil Index-Thermal; **NDVIT**: Normalized Difference Vegetation Index-Thermal; **SAVIT**: Soil Adjusted Vegetation Index-Thermal.

2.3. Summary

In summary, land-use/cover changes emerged in the research agenda on global environmental change several decades ago with the realization that land surface processes influence climate. These changes significantly affect essential aspects of Earth system functioning. Nowadays savannas are becoming increasingly important in the world food supply, especially in Latin America, and they are, therefore, prone to increasing human impacts. Additionally fires, whether natural or anthropogenic, also have pronounced climate forcing effects. A number of research works have been carried out by using various methodologies and algorithms to derive land use/cover change and fire regime information from different sets of remotely sensed data. However, the complex

heterogeneity of savannas makes it difficult to develop a general method for all applications in different savanna regions in the world. Fine resolution, spatially explicit data on land-use/cover changes are required to define the impact of landscape fragmentation on biodiversity, composition, structure and functionality of ecosystems.

Algorithms for the detection of active fires and burned area have allowed monitoring and management of fires at regional scales and have assisted in determining potential thresholds that are related to type of fuel, combustion rate and climatic conditions of each region. It has been possible to reduce omission and commission errors and to apply thresholds associated with regional vegetation characteristics and to use vegetation indices.

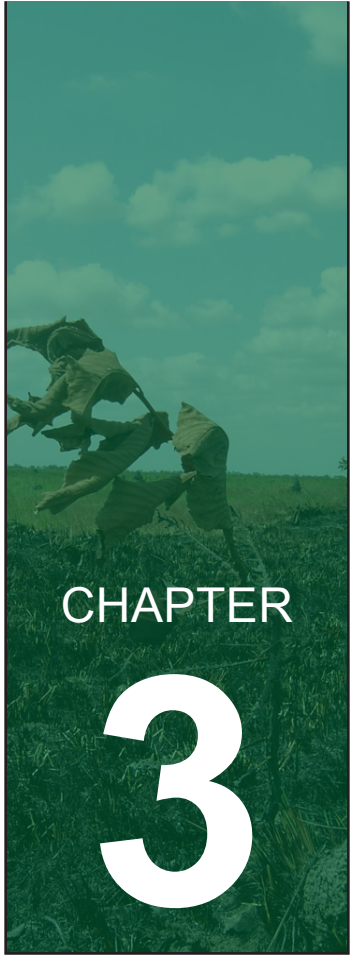

Meander of Meta river near to Cumaral town (Meta, Villavicencio)

CHAPTER 3

Study area and data

In this chapter a description is given for the Eastern Colombian Savannas (ECS) and the data used for analysis which include satellite images, environmental and topographic maps.

3.1. Study area

The ECS are part of the Colombian-Venezuelan “Llanos” region. Sixty-five percent of these savannas are located in Venezuela, where as 35% is found in Colombia (Romero *et al.* 2004). The ECS lies between 2.5° to 7° N and 74° to 67° W, with an altitudinal range of 200 and 1,200 masl, located 110 km east of Bogota. The major towns are Villavicencio, Yopal, Arauca and Puerto Carreño (Figure 3.1). The ECS cover an area of 17 million ha (15.4% of the Colombian territory) and are located in the states of Arauca, Casanare, Vichada and Meta within the extreme northeast part of the Orinoquian Basin. The northern boundary is marked by the Arauca river and crosses in a southeast direction towards the Meta river, while the Orinoco river forms part of the eastern boundary of the ECS.

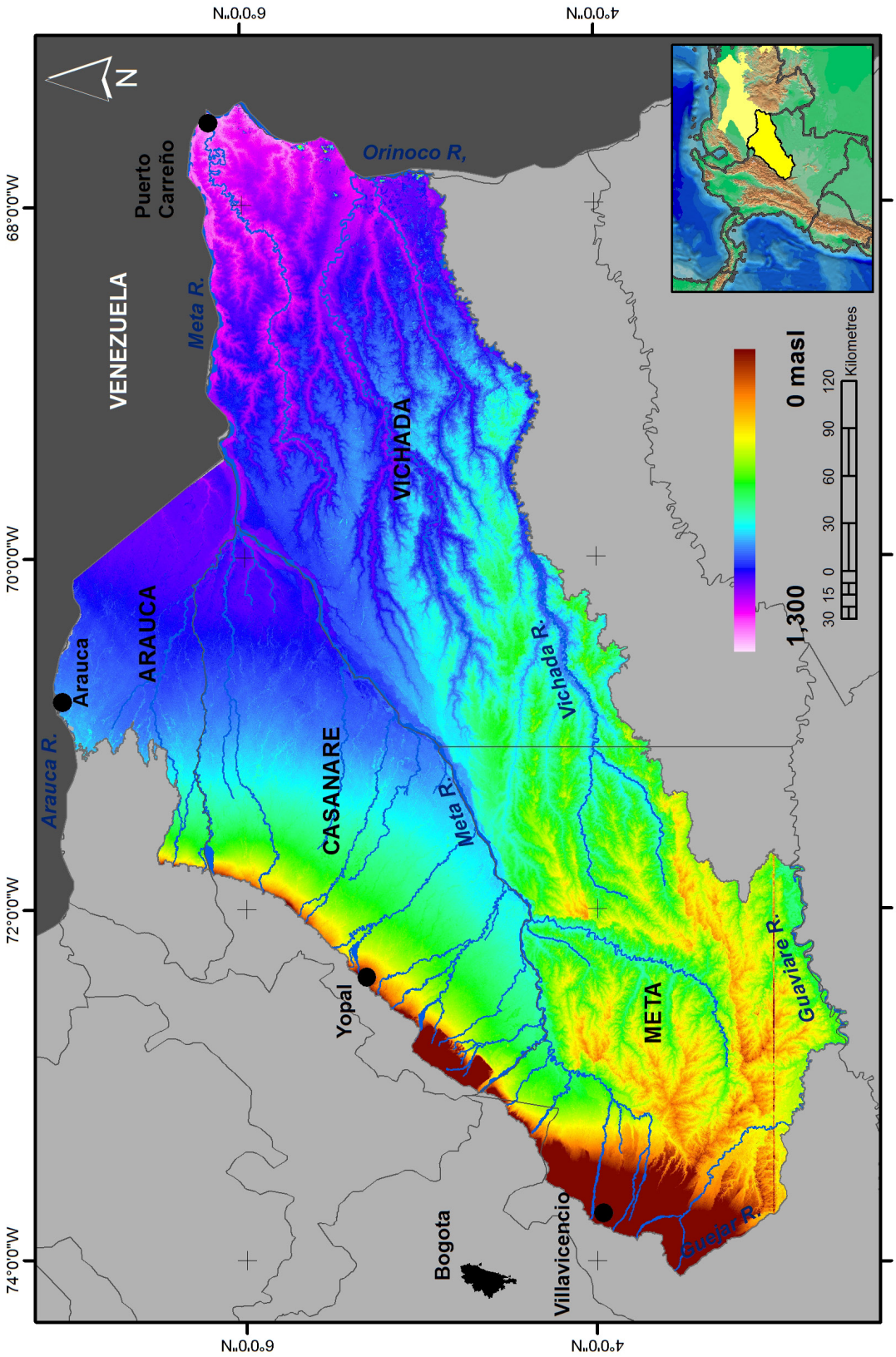

Figure 3.1. *Geographical location of the ECS, in a northeast area in Colombia.*

The eastern limit follows the Middle Orinoco river in an extension of 270 km from Puerto Carreno up to the Vichada river bordered by into the Orinoco river. The southern and western boundaries are the ecosystem transition zone between Amazonian tropical rain forest in Vichada, Guaviare and Guejar rivers (south) and Andean tropical rain forest, 1,300 masl (west).

The ECS comprises mainly of flat and concave land-forms with some isolated table-mountains, cliffs and hills. Nineteen percentage of the region is semi-undulated with slopes between 1 and 3 %, located mainly in the southern part of the region between Meta and Vichada rivers while the slopes reach a 5% inclination between the Yucao and Manacacias rivers. Only 4% of the area presents rough and steep slopes located in some outcrops rocks around Orinoco river in the eastern area and foothill region located at west with slopes between 11 and 30%.

3.1.1. Climate

A total of 34 climate stations are located within the ECS which acquired information about rainfall, temperature and evapotranspiration between 1938 and 2007 (appendix 1). However, these data are not distributed uniformly throughout the study area. For this reason the climate dataset of WorldClim was used to obtain precipitation and temperature maps and 17 bioclimatic maps. This set of global climate layers with a spatial resolution of a square kilometre, provided the data to generate the necessary maps through interpolation of average monthly climate data from global weather stations from the period from 1950 to 2000. WorldClim data implemented the thin-plane smoothing spline algorithm implemented in ANUSPLIN (Hutchinson 1995), using latitude, longitude and elevation.

In general, the climate of this region is considered typical tropical wet and dry climate which is classified as wet seasonal tropical (Aw Köppen Climate Systems) with a single dry season between November and April and a single rainy season between May and October (Rangel *et al.* 1995). Seasonality is driven by the

Inter-Tropical Convergence Zone (ITCZ), a term used to describe the alternation of the north-east moist trade winds coming from the Atlantic Ocean. During the dry season these winds discharge their humidity along the coastal area, cross the llanos and arrive at the eastern slopes of the Andes mountain range in north-east direction (Huber *et al.* 2006). This creates a precipitation gradient (1500-4500 mm) along a northeast to southwest transect and an absence of rainfall during the dry season (WWF 1978), see Figure 3.2.

The mean annual temperature fluctuates between 27 and 30°C in the dry months (end November - Middle April) and 23-26°C in the rainy season which corresponds to the tropical lowlands regime (Armenteras *et al.* 2005). The relative humidity is around 60 to 90%, with the exception of the Puerto Carreño region where values vary between 50 and 80%.

3.1.2. Geology

The geological history of the ECS dates back to the Archean-Proterozoic period ca. 2500 millions of years ago (Ma), where a proto-continent was formed from the deposition of fine sediments from the ocean. At the beginning of the Proterozoic about 1700 Ma. and through processes of metamorphism, volcanism and tectonism, these deposits turned into migmatites with granitoid components, that eventually formed the Guiana Shield. The ECS lays on the 'Migmatic Complex of Mitu' formation, which is part of the western most area of Guiana Shield. At present day the ECS are restricted to the Orinoco river boundaries and the westernmost granitic upwelling areas in Vichada department (IGAC 1999).

During the Cretaceous period, the Precambrian base (Guiana Shield) was covered by sediments of fluvial-lacustrine origin. These deposits came from the Andes mountains, which began to emerge in the Lower Cretaceous (140 to 100 Ma). Large amounts of sediments were deposited in the eastern plains filling the Guiana Shield depressions and forming extensive flat areas. In the Upper Cretaceous (100 to 25 Ma), the marine sedimentation was accentuated on the

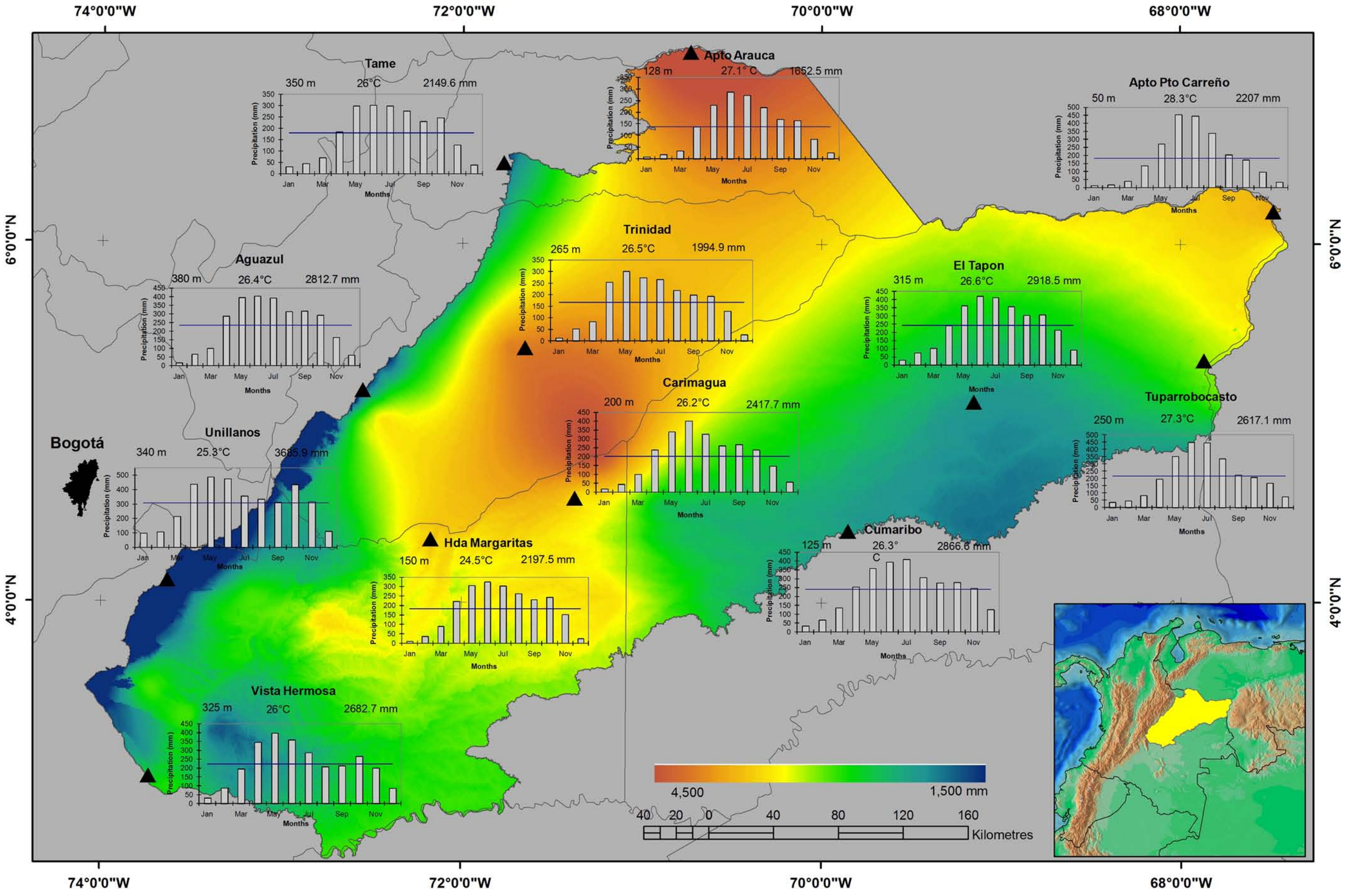

Figure 3.2. *Map of annual precipitation in the ECS. Map precipitation interpolation was generated with Worldclim data (www.worldclim.com) and climatic graphs of monthly rainfall and temperature average acquired from IDEAM between 1938 and 2007.*

western area of Andean mountains, while in the eastern area sandy sediments came from the Guiana Shield, forming higher elevations (IGAC 1999). During the Miocene epoch (25 to 12 Ma), the area was covered by superficial bodies of water and new transgressions occurred, depositing sediments and forming the currently observed flat areas (IGAC 1999; Rippstein *et al.* 2001).

During the Pliocene the Guayana shield was compressed by the oceanic tectonic plate. This event formed a fold causing uprisal of the Eastern Cordillera (Andes formation ridge) and the Orinocense foothills. Later during the Plio-Pleistocene period, the last Andes uplifting event occurred and enormous amounts of sediments were transported and deposited in the eastern plains. Finally, glaciations during the late Quaternary period and profuse precipitation caused the opening of deep channels, accumulating sediments at the base and flat plains; forming the present day topography, geomorphology and hydrological network. Additionally, activity of numerous parallel faults in the eastern Andean region led to lifting and folding of the high plain, and collapse of the alluvial area (IGAC 1999; Correa *et al.* 2006).

3.1.3. Physiography and geomorphology

According to Sarmiento (1984) and IGAC (1999), the ECS present four major physiographic regions, 9 sub-provinces and 18 land-forms (Figure 3.3). The main characteristics are shown below:

i. **High Plains (HP)**: Refers to the extensive Tertiary flat plateau that reaches an altitude between 100 and 300 masl. This physiographic formation is located between the Meta, Metica, Vichada and Orinoco rivers, covering 65% of the area. They were formed during the Late Pliocene and are characterised by the presence of tertiary sediments with various incision levels of the early Pleistocene age (IGAC 1999). Two sub-provinces conform this physiographic province:

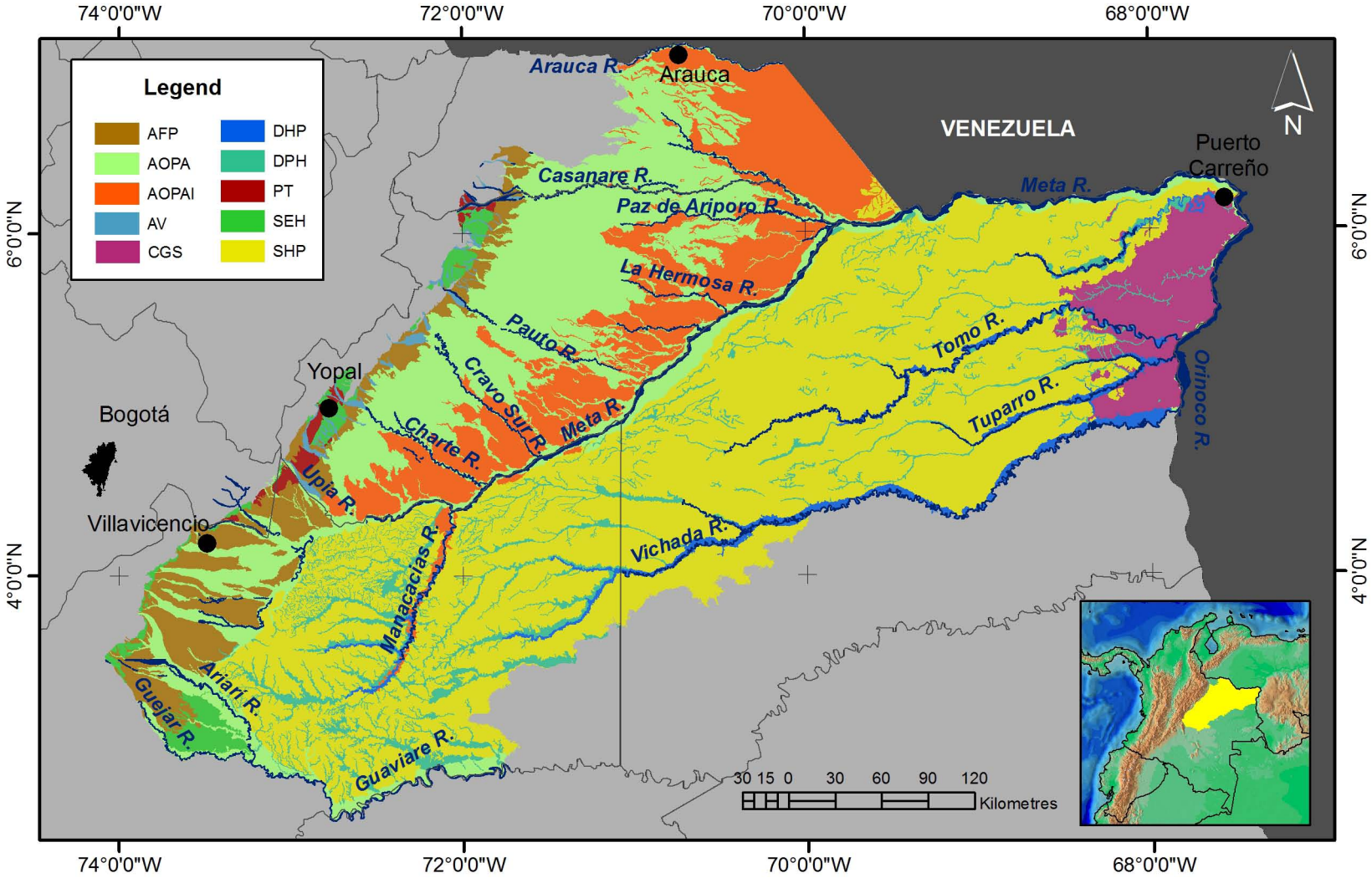

Figure 3.3. *Eastern Colombian Land Form (physiographic) sub-provinces.* ***DHP****: Depositional High Plains;* ***SHP****: Structural High Plains;* ***GKS****: Guiana Kraton Shield;* ***SHE****: Structural and Erosional Hills;* ***AFP****: Alluvial and Fluvial Piedmont;* ***TP****: Tectonic Piedmont;* ***AOPA****: Alluvial Overflow Plain of Andean rivers;* ***AOPAI****: Alluvial Overflow Plain with Aeolian Influence);* ***AV****: Alluvial Valley.*

i.1. **Structural High Plains (SHP)**: Correspond to the plateau sector, that has experienced denudation processes by erosion that formed the actual flat to undulate relieve (Romero *et al.* 2004);

i.2. **Depositional High Plains (DHP)**: Correspond to areas that originate from erosive and landslide processes that occurred in the structural high plains, generating material deposition (Romero. *et al.* 2004).

ii. **Guiana Kraton Shield (GKS)**: This is an old and stable residual relief of Precambrian period and a product of the erosion of the mountain chains that survived the merging and splitting of continents. This province is composed by the sandy foothills (Table-mountains, cliffs, hills and mounds) and plains west of the Orinoco river, between Puerto Carreño and Vichada river;

iii. **Piedmont or foothills (P)**: This is a landscape formed at the foot of the Andes mountains as a product of one or more successive mud flow events from steep mountains to lowlands areas (Villota 1992). Foothills was formed in the late Quaternary and is located along the western part of the Orinoco basin, between Arauca and Ariari - Guejar rivers. Four sub-provinces conform this physiographic province:

iii.1. **Tectonic Piedmont (TP)**: Corresponds to a new and unstable area formed between the Late Pliocene to Early Pleistocene (IGAC 1999).

iii.2. **Alluvial and Fluvial Piedmont (AFP)**: A series of alluvial and fluvial plain fans slightly tilted as a result of overflowing of the major rivers (Meta, Arauca, Casanare) that descend from the Andes to the Orinoco plains.

iii.3. S**tructural and Erosional Hills (SEH)**: A series of ridges, hills and slopes in low altitude hills that are formed at the bottom of the Andes mountains. This formation is located near Ariari and Guejar rivers and in the headwaters of Charter and Upia rivers.

iii.4. **Alluvial Valley (AV)**: Flat surfaces that dissect the alluvial fans of the tectonic piedmont, forming linear valleys delineated by abrupt slopes. They are common in the headwaters of the Arauca, Casanare, Pauto, Cravo Sur, Charte and Upia rivers.

iv. **Alluvial Overflow Plains (AOP)**: Refers to flat to concave low plane areas, permanent or occasionally flooded. They are formed by Andean and Orinoquian fluvial sediments and aeolian sedimentation processes. They can be found at elevations from 30 to 80 masl. Two sub-provinces conform this physiographic province:

iv.1. **Alluvial Overflow Plains of the Andean rivers (AOPA)**: Correspond to very low plains formed by the overflow of large rivers and abandoned meanders of rivers that originate from the Eastern Andes mountains, such as Ariari, Guaviare, Meta, Upia, Arauca and Casanare rivers. Rivers flow varies widely according to the season. In humid season, rivers regularly overflow while during dry period floods do not occur.

iv.2. **Alluvial Overflow Plains with Aeolian Influence (AOPAI)**: Correspond to the south and southeast forms the plains of overflow, located in the Arauca and Casanare departments. These areas are flat, concave and serve as a “trap” for sediments carried by the wind.

3.1.4. Soils

The main soil types in each landform and sub-province are shown in Table 3.1. Soils were developed from Tertiary sedimentary rocks (sandstones, limestones and mudstones) and Quaternary alluvial and colluvial sediments (Malagon 2003). The ECS show predominantly coarse to fine textured soils (sandy loam to clay loam). Sandy loam consists of more than 90% quartz while the clay loam is dominated by kaolinite. Soils are black to dark brown near the surface and strong brown, dark reddish or yellowish at higher depths. They show a moderate to fast infiltration rate, due to the high stoniness and proximity to the Precambrian base close. These soils are strongly acidic, with low fertility and cation exchange capacity; low to medium level of organic carbon and phosphorus, poor in magnesium, calcium and potassium and high content of aluminium. In general, these soils are chemically poor as a product of a long climatic and geological history (Malagon 2003). The dominant taxa are Entisols (Troporthent, Ustorthent), Ultisols (Paleudult, Kandiudult) and Inceptisoles (Dystropept) (IGAC 1979; IGAC 1983a; Cochrane *et al.* 1985; IGAC 1999; Malagon 2003).

3.1.5. Flora

As previously mentioned, this region is predominantly covered by extensive grassland areas, frequently interrupted by forests, wetlands, swampland and scrub patches (Sarmiento 1984). Grassland areas are characterized by the presence of monocotiledonea species, especially members of the Poaceae, Cyperaceae and Xyridaceae families and some dicotiledonean species of Leguminosae, Apocynaceae and Melastomataceae families. In contrast, in forest and scrub formations, the dicotiledonea species are the most important elements (such as Apocynaceae, Burceraceae, Leguminosae, Clusiaceae, Chrysobalanaceae and Melastomataceae). Finally, wetlands and swamplands are characterized by the presence of aquatic plants families such as Pontederiaceae, Commelinaceae, Cyperaceae, Polygonaceae. Romero *et al.* (2009) reported 2692 plant species which corresponds to 6.57% of the total plant diversity of Colombia.

Table 3.1. Topography, slope, texture, drainage and depth characteristics of soils in different land-forms in ECS (Malagón 2003).

ABB	Landform	Topography	Slope (%)	Texture	Drainage	Depth
GCS	Table-mountains, cliffs, hills and mound	Rough and steep	> 50	Sandy loam to clay loam	Good	Very superficial to superficial
DHP	Valleys	Flat and concave	< 3	Sandy loam to silty loam	Poor to swampy	Very superficial to superficial
	Glacis	Undulate and flats	< 7	Clay loam	Good to poor	Superficial to moderately deep
	Dunes and Medans	Slightly undulating	< 5	Sandy loam	Good to excessive (tops) poor (bottom)	Deep to very deep
SHP	Flat plains	Convex to flat	< 7	Sandy loam to silty loam	Good	Deep
	Rolling plains	flat to rolling and medium sloping in hillsides	10 - 25	Clay to clay loam		Moderately deep to deep
	High hill or "Serranias"	Undulates a semi-rolling: short and highly inclined slopes	20 - 50	Clay loam		
AOPA	High terraces	Inclined to undulates	< 5	Sandy loam to clay	Good	Moderately deep
	Low terraces			Clay to clay loam	Imperfect to poor	Superficial to moderately deep
	Overflow plains	Flats	< 2	Clay to silty loam to silty		
AOPAI	Low terraces	Flats to concavo		Sandy loam to sandy and silty loam to clay loam	Imperfect to poor	
	Flooding levels	Flat		Sandy loam to silty loam	Poor	
	Dunes and medans	Inclined to undulate	< 5	Sandy	Good to excessive (tops) Poor (bottom)	Deep to very deep
TP	Terrace fans	Inclined to undulate	7 - 12	Sandy loam to clay loam	Good	Superficial to moderately deep
	Smalls tables or plateaus	Inclined to strongly inclined	7 - 25	Sandy loam	Excessive drained	Superficial to moderately deep
AFP	Alluvial and fluvial fans	slightly inclined to flats	< 7	Clay loam	Good to moderate	Deep to moderately deep
SEH	Ridges, hills and slopes	Rough	20 - 60		Moderate to rapid	Superficial to moderately deep

Three main vegetation types can be found associated with physiographic formations:

i. **High savannas**: Correspond to the more extended and continuous grass vegetation formation in the region. There are located to the south of the Meta river and west of Manacacias river over depositional and structural high plains. Physiognomically, these savannas are characterized by a large and continuous grass area disrupted by narrow strips of forest networks associated with rivers and creeks commonly called gallery forests (Veneklaas *et al.* 2005). These savannas are dominated by open grasslands, reaching heights of 1 to 1.5 m and are rich in Juncaceae, Xyridaceae and Cyperaceae elements. A gallery forest network is characterized by semi-dense to dense forest, associated with palms and scrub elements. Trees reach heights between 10 and 20 m and normally three different strata can be differentiated. Most represented families are: Leguiminosae, Arececaceae, Rubiaceae, Chrysobalanaceae, Euphorbiaceae, Melastomataceae and Myrtaceae.

ii. **Flooded savannas**: This formation, the second most extended formation in the region, is located to the northwest of the Meta river over dunes and alluvial overflow plains of the Andean rivers. This vegetation formation is characterized by an ample mosaic of seasonally flooded grasslands with sporadic patches of trees and scrub that grow in shallow depressions and some wetlands and swamplands (FAO 1966; Blydenstein 1967; Armenteras *et al.* 2005). The main feature of flooded grasslands is the open grass cover up to 2 m height, with reduced scrub elements and dominance of monocotyledonous species (specially members of Poaceae and Cyperaceae). Tree and scrub patches commonly called “Matas de Monte” are characterized by semi-dense to dense forest with heights

between 20 to 25 m Species of members of Palmaceae, Cecropiaceae, Moraseae, Burseraceae and Euphorbiaceae among others constitute this formation (IGAC 1999). Wetlands and swamplands formations, which are formed by permanent or seasonal water deposition, are composed by aquatic plants elements such as *Eleocharis interstincta, E. jasksiana, Websteria confervoides,* among others (Diaz 1999).

iii. **Sandy savannas**: This formation is located in the most western part of the region, which is constituted by the physiographic formation of the Guiana kraton shield. Physiognomically, these savannas are low and open, with poor presence of species. Some species are: *Mesosetum loliiforme, Licania Wurdackii, Acosmium nitens.*

Table 3.2 shows a summary of the characteristics of the different savanna vegetation types in the ECS.

Table 3.2. Overview table of the characteristics of savanna vegetation types in the ECS (Etter 1985, 1998a)

Savanna type	Physiognomy	Dominant species
High savannas	Dense tussock grassland with scattered trees	*Trachypogon ligularis,T vestitus, Andropogon bicornis, Curatella americana, Panicum spp. Leptocoryphium lanatum*
Flooded savannas	Dense tussock grasslands	*Andropogon bicornis, Axonopus purpusii, Leptocoryphyium lanatum, Trachipogon spp.*
Sandy Savannas	Open grassland with scattered tress	*Bulbostylis spp., paspalum carinatum, Curatella americana, Byrsonima crassifolia, Paspalum spp.*

3.1.6. Fauna

The ECS play an important ecological role as they form a bridge between different floral and faunal elements that potentially migrate between Amazonas, Guiana and Andes regions. As a consequence of their limited geographical distribution a number of exclusive species are present and ecosystems with

different floristic composition, species dominance or community structure are found. The ECS contain nearly 9% of the total diversity of Colombia in terms of plants and animals.

In terms of fauna, Maldonado-Ocampo and Usma (2006) assert that for fishes the Orinoquian region is the second richest area in Colombia with 658 species, just after the Amazonas region. This number corresponds to 46% of the Colombian fish diversity. Fifty-six species (8.5%) are endemic and 10 species are threatened to some degree. In terms of amphibians, Chavez and Santamaria (2006) report 57 species, which corresponds to 1% of the Colombian biodiversity. Regarding reptiles, 119 species are reported, which corresponds to 23% of the Colombian reptile diversity. Twelve species are threatened to some degree. With respect to birds, 783 species have been reported, which corresponds to 42% of Colombian bird diversity (McNish 2007). Thirteen percent correspond to migratory species and 8 species are endemic. In terms of mammals, 167 species have been reported, which corresponds to 35% of Colombian biodiversity. Nine species are under some degree of threat.

3.1.7. Land use

Figure 3.4 shows the land use processes in the ECS. Since pre-hispanic times local ethnic groups survived on the savannas by cutting and burning the vegetation, fishing, hunting and harvesting (Romero 1993; Sanchez 2005). In the 1960s, farmers from the mountainous zone arrived and implemented extensive cattle ranching and converted savannas into large croplands areas. They applied pasturing on native species and occasionally burned large areas of grasslands to eliminate lignified material, which introduced nutrients into the soils for grass regeneration. Since the 1980s, there has been an increase in the direct use of the land by the establishment of agricultural ecosystems. This change incorporates the introduction of fertilizers due to the high physical and chemical limitations of this ecosystem and the climatic seasonality that reduces the possibilities of crop production (Lopez *et al.* 2005).

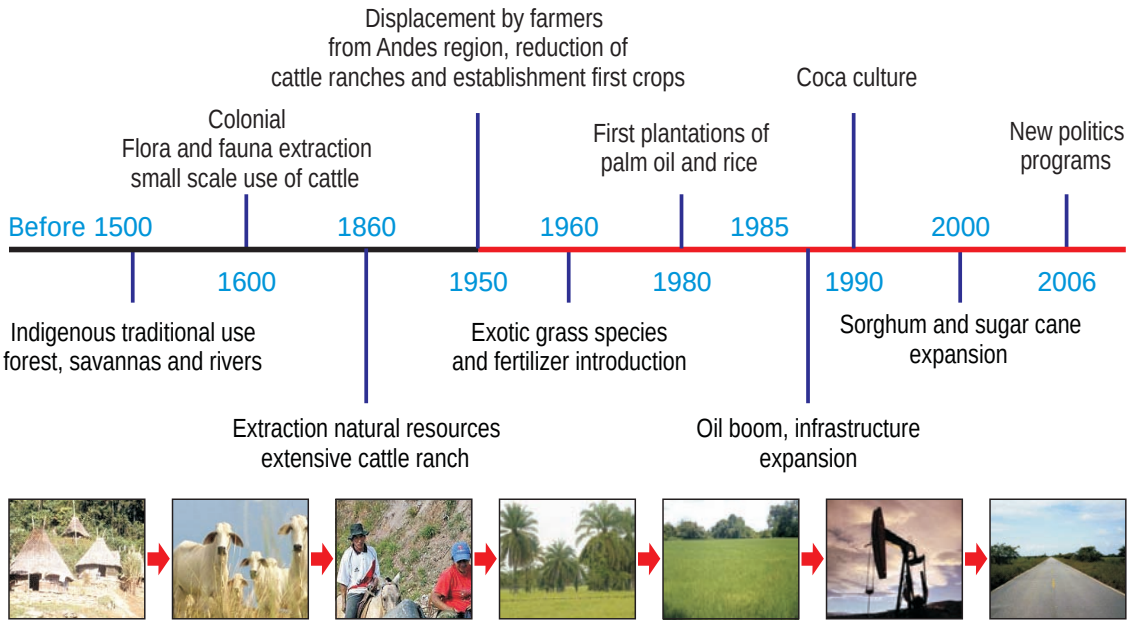

Figure 3.4. *Historical time line of land use for ECS since pre-historical time when indigenous people used savanna in traditional way up to recent years when the ECS started to present new developed perspectives.*

Exotic grasses have been introduced with the implementation of cattle ranching and extensive pasturing. In present days, other factors besides farming are causing problems such as an expansion of mono-specific African palm and rice plantations, the development of road infrastructure, oil production, sorghum and sugar cane and coca culture and the perspective of economic internationalization (Baptiste 2006). Moreover there have been many regional conflicts associated to land use and management since the promotion of large scale development projects in the area and associated population growth rate increase.

According to the population censuses (DANE - 1951, 1964, 1973, 1985, 1993; http://www.dane.gov.co) the population of “Llanos Orientales” region has increased from 66,000 people in 1951 to 624,741 people in 1995 (Rudas 2003). This represents a population density increase from 0.21 habitants per ha in 1951 to 2.01 in 1995, of which approximately 70% live in the foothill area. The census of 2005 showed a sharp increase in the population to 1,712,454 habitants, representing 4.5% of the Colombian population. Land tenure in the region includes privately owned ranches (>80% of area), as well as indigenous reserves formally established in the 1990s with a total area of 1 340 000 ha, and the protected area ‘El Tuparro National Park’ of 548 000 ha created in 1973 (Fig. 3.5).

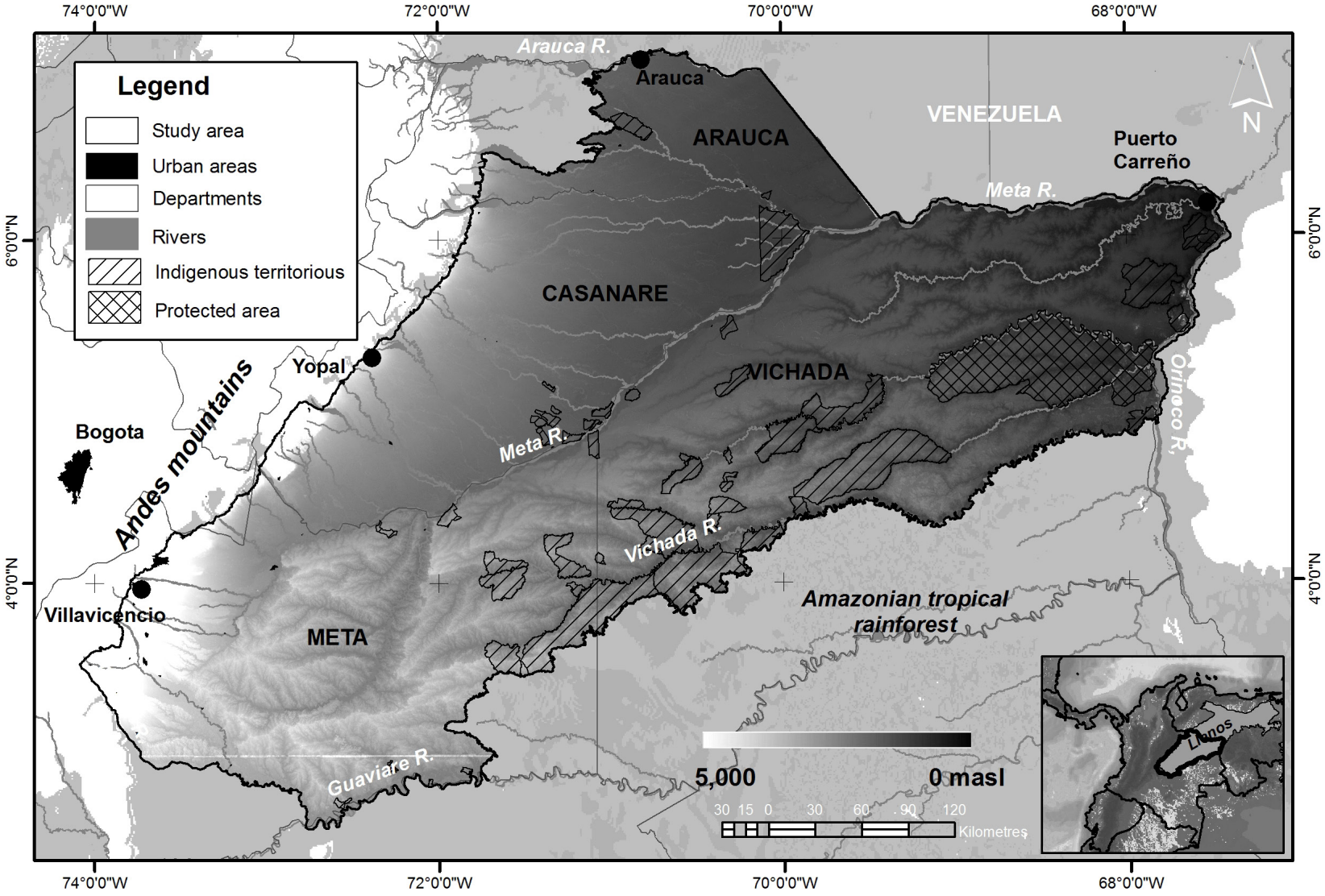

Figure 3.5. *The Legal status of Eastern Colombian Sabanas: urban areas, international boundaries, elevation, protected areas and indigenous territories.*

3.2. Data

3.2.1. Cartographic and thematic information

Different entities provided cartographic, thematic and alphanumeric information, which was analysed and incorporated in this research (Table 3.3). This information was collected, georeferenced and stored in a GEODATA base in ArcGis 9.3.

Table 3.3. Cartographic, thematic and alphanumeric information for ECS.

Topic	Entity	Scale
Ecosystem maps 2000	Instituto Alexander von Humboldt - Instituto Geografico Agustin Codazzi	1:250,000
Bioclimatic map	Wordclim - Global Climate Data	1 km resolution
Climatic stations	IDEAM - Instituto de Hidrología, Meteorología y Estudios Ambientales.	
Geomorphologic map	Paisajes fisiográficos de la Orinoquia - Amazonia (ORAM) Colombia	1:750,000
Digital Elevation Model (DEM)	Shuttle Radar Topography Mission	30 m resolution
Ways and rivers network	Instituto Geografico Agustin Codazzi	1:500,000
Towns and village	Instituto Geografico Agustin Codazzi	1:500,000
Land tenure	Instituto Geografico Agustin Codazzi	1:100,000
National parks areas	Sistema de Parques Nacionales - Colombia	1:100,000
Coca plantations 2000-2006	SIMCI - Sistema Integrado de Monitoreo de Cultivos Ilícitos	1:100,000
Political boundaries	Instituto Geografico Agustin Codazzi	1:100,000
Flora and fauna database	Instituto Alexander von Humboldt Instituto SINCHI	
Population database	Departamento Administrativo de Estadistica - DANE	

3.2.2. Satellite data

3.2.2.1. CBERS data

China and Brazil launched the first China-Brazil Earth Resources Satellite (CBERS-1) in February 2000 putting it into an orbit of 98° inclination to the Equator at a 763 km above Earth. A second satellite (CBERS-2) was launched in

2003 and a third (CBERS-2B) in September 2007 in the same conditions. Thanks to the success of these programs until now, a new satellite launch is planned in 2011 for the CBERS-3 and in 2013 for the CBERS-4. Furthermore the HC camera of the sensor CBERS-2B has been replaced by a Pancromatic Camera of high resolution.

The CBERS satellite is composed by a series of sensors that are divided into a camera of wide angle vision - WFI, a scanning camera of high resolution – CCD, a scanning camera of medium resolution – IRMSS, and a panchromatic camera of high resolution – HRC. The CBERS sensors hold a system to control altitude and in the case of the sensor CBERS-2B it contains a GPS receptor and a star-receptor that allows controlling altitude with increased precision and a system of hydrazine propulsions that corrects pitching of the satellite. The satellites CBERS 3 and 4, obtain improved geometric and radiometric performances through the use of the Camera PanMux – PANMUS, the multispectral camera – MUXCAM, the scanning camera of medium resolution –IRSCAM and the wide angle scanning camera WFICAM. The orbit of these satellites will be the same as the preceding satellites.

The High Resolution Cam - CCD provides images of a swath width of 113 km in sun-synchronical orbit at a 778 km of altitude. The Earth's surface is covered every 26 days at a spatial resolution of 20 m in four spectral bands and one panchromatic band from 0.51 µm to 0.73 µm. This satellite also contains an InfraRed MultiSpectral Scanner (IRMSS) which operates in four spectral bands including thermal infrared (Table 3.4). This provides images of a swath width of 120 km at a spatial resolution of 80 m (160 m in the thermal channel). The panchromatic camera of high resolution – HCR – operates between the visible and part of the near InfraRed (0.5-0.73 µm) producing images of a swath width of 27 km at a resolution of 2.7 m that allows observing the objects on the superficies with more detail. This is only found for the CBERS-2B and five cycles of 26 days are necessary to cover the 113 km which are obtained by the CCD. The local solar time at the crossing of the equator is at 10:30 AM. Table 3.4 describes the

Table 3.4. Spectral and spatial resolution characteristics of CBERS data (http://www.cbers.inpe.br).

CCD Camera			IR Multi-Spectral Scanner		
Band number	Spectral range (microns)	Resolution (m)	Band number	Spectral range (microns)	Resolution (m)
1	Blue (0.42 - 0.52)	20	1	0.5 - 1.10	80
2	Green (0.52 - 0.59)	20	2	1.55 - 1.75	80
3	Red (0.63 - 0.69)	20	3	2.08 - 2.35	80
4	Near infrared (0.77 - 0.89)	20	4	10.40 - 12.50	80
5	Pancromatic (0.51 - 0.73)	20	5		

CBERS sensor in more detail. The objective of this sensor is to obtain information on the Amazon basin with the purpose of identifying forest coverage, agricultural and urban expansion, infrastructural development, geologic and soil formations, fire detection and water dynamics.

3.2.2.2. LANDSAT data

Moderate and high spatial resolution satellite data have been used widely for Earth environmental monitoring. Of these satellites, Landsat has probably been used most for characterizing land cover. The first Landsat was launched on July 23rd, 1972 by the US National Aeronautics and Space Administration (NASA) as a part of the program “Earth Resources Technology Satellites” (ERTS). Posterior, this program was renamed the “Landsat” program. Landsat was placed aboard a Nimbus weather satellite, designed to acquire information of Earth’s resources on a systematically repetitive, multispectral basic and medium resolution. Until now seven satellites have been launched.

Landsat 1,2,3 - Multi Spectral Scanner (MSS) was able to take images of the Earth with a spatial resolution of 80 m and a swath width of 185 km, in four spectral bands distributed into 3 visible and 1 infrared bands (Table 3.5). Only Landsat 3 introduces a new thermal band. This satellite circulates at an altitude of 917 km in the heliosynchronous orbit of the Earth every 103 minutes completing 14 orbits every day to return to the same position after 18 days crossing at the

Table 3.5. Spectral and spatial resolution characteristics of Landsat MSS, TM and ETM+ adapted from Mather (2005).

CCD Camera			IR Multi-Spectral Scanner		
Band number	**Spectral range (microns)**	**Resolution (m)**	**Band number**	**Spectral range (microns)**	**Resolution (m)**
1	Green (0.5 - 0.6)	80	**1**	Blue (0.45 - 0.52)	30
2	Red (0.6 - 0.7)	80	**2**	Green (0.52 - 0.60)	30
3	Near infrared (0.7 - 0.8)	80	**3**	Red (0.63 - 0.69)	30
4	Middle infrared (0.8 - 1.1)	80	**4**	Near infrared (0.75 - 0.90)	30
			5	Middle infrared (1.55 - 1.75)	30
			6	Thermal infrared (10.4 - 12.5)	120, 60
			7	Middle infrared (2.08 - 2.35)	30
			Pan	0.52 - 0.90	15

Equator between 9:30 and 10:30 A.M. The satellite contained two sensors; the first named the Return Beam Videcom (RBV) which was a television camera designed for cartographic applications and the second was a multispectral scanner designed for the spectral analysis of the characteristics of the Earth. This last sensor scans the superficies of the Earth from west to east in an orbit descending from north to south within the sunside orbit of the Earth. The Landsat 1 acquires information since January 6th of 1978, while Landsat 2 and 3 are taking images since February 1982 and March 1983 respectively.

In 1982, Landsat 4 and 5, the Thematic Mapper (TM) sensor was launched and continues to be a success up to today. Compared to Landsat 1,2,3 which was an altitude of 917 km about Earth, Landsat 4 and 5 circulate at an altitude of 705 km, improving its cycle from 18 to 16 days, thanks to the reduced orbital cycle (98.9°). At the Equator the time of image acquirement is approximately 9.45 A.M. local time. These satellites maintained the MSS sensor to guarantee the continuity of previous data, eliminating the RBV camera and incorporating a new sensor named TM (Thematic Mapper). This sensor was designed for thematic cartography that provides information with high spatial, spectral and radiometric resolution. This sensor takes information at a spatial resolution of 30 m in 7 bands from the visible to the medium infrared. It furthermore includes a thermal band with a 120 m resolution and was designed to have an employ time until 1993.

However up to today Landsat 5 keeps functioning and obtaining information of the Earth´s superficies.

The last satellite was launched in April 1999 with a new sensor called ETM+ (Enhanced Thematic Mapper Plus). Landsat 7 was sent to replace the Landsat 6 which never functioned. This satellite has the same bands as the Landsat 5, but the panchromatic band is added which has a 15 m resolution and which covers a spectral range between 0.52 a 0.90 µm and improving the resolution of the thermal band of 120 to 60 meters. The orbit of Landsat 7 is approximately 99 minutes allowing that the satellite circulates the Earth 14 times every day and covering the entire planet in 16 days. The heliosynchronious orbit crosses the Equator between 10 and 10.15 A.M. local time.

3.2.2.3. MODIS data

MODerate Resolution Imaging Spectroradiometer (MODIS) has become one of the best alternatives to detect and map burned areas, because of its spectral (36 bands), spatial (250, 500 m and 1 km) and temporal (daily, 8-days, monthly) resolution characteristics, together with the variety of obtained products. MODIS has converted this sensor into one of the most used product that acquires information of the Earth in a constant and systematic way.

In 1999, the NASA within the framework of the Earth Observing System (EOS) program launched TERRA (EOS-AM); an observation satellite platform which carried on board five research instruments designed to study and monitor the complexities of the Earth and its environmental changes. Advanced Spaceborne Thermal Emission and Reflective Radiometer (ASTER), Multi-angle Imaging SpectroRadiometer (MIRS), Cloud and Earth's Radiant Energy System (CERES), Measurement of Pollution in the Troposphere (MOPITT) and MODIS began to collect information on the land, ocean and atmosphere since February 2000 (http://terra.nasa.gov/about/). In 2002, the Earth Observing System (EOS) program launched AQUA (EOS-PM) with the objective of obtaining information

concerning different aspects of the Earth's water cycle: in the atmosphere, oceans, ice, land and biosphere. Atmospheric Infrared Sounder (AIRS), Advanced Microwave Sounding Unit (AMSU), Humidity Sounder for Brazil (HSB), Advanced Microwave Scanning Radiometer for EOS (AMSR-E) and the Earth's Radiant Energy System (CERES, two) and MODIS began to collect information since September 2002 (http://aqua/nasa.gov).

Both platforms incorporate MODIS sensors. The sensors have the ability to monitor biosphere changes at medium scale obtaining information over land, atmosphere and oceans. Concerning land, MODIS is suitable for net primary productivity, land cover type and change, leaf area index, fraction of photosynthetically active radiation, gridded vegetation indices, fires, burn scars, land surface temperature and emissivity, snow cover, snow albedo and atmospherically corrected surface reflectance.

MODIS presents a robust calibrated system, with high spatial and radiometric capacity that has become the last generation of monitoring system of the last two decades with a moderate resolution (Townshend and Justice 2002; Roy *et al.* 2005). Since its launch, researches have focused on the elaboration of high quality and accurate MODIS products. MODIS has provided information about the Earth's surface in a continuous and periodic form. TERRA platform (EOS-AM) passes in descending orbit from north to south, crossing the equatorial line at 10:30 AM when the cloud cover over land is minimal. The AQUA platform (EOS-PM) passes in an ascending orbit, crossing the equatorial line at 1.30 PM. obtaining maximum information on clouds. MODIS cover a spectral range between 0.405 μm and 14.834 μm. The spatial resolution of band 1 and 2 is 250 m, bands 3 to 7 are of 500 m, while the remaining bands (8-36) are 1 km. MODIS collects a swath of data covering an area of 2330 km across and 10 km along the track. Table 3.6 summarises the general characteristic of the MODIS instrument.

The Earth Observing System Data and Information System (EOSDIS) has the mission of receiving, controlling, processing, archiving and distributing the

Table 3.6. Characteristics of MODIS image (www.modis.gsfc.nasa.gov/).

Launch	TERRA 1998 - Data-collection from February 2000 AQUA 2000 - Data-collection from 2002
Orbit	705 Km sun-synchronous Equatorial crossing at 10:30 AM (TERRA), 1:30 PM (AQUA)
Repeat coverage	Daily, north of - 30° latitude Every 2 day for <-30°latitude
Swath	2,330 km cross-track, 10 km along track
Spectral bands	36 bands between 0.405 and 14.385 μm
Spectral calibration	Band 1-4 2% for reflectance
Radiometric resolution	12 bits
Spatial resolutions	Bands 1-2: 250 m. Bands 3-7: 500 m. Bands 8-36: 1 km
Design period	6 years

information of every spacecraft through the Distributed Active Archives Centers (DAACs). Every platform transfers via “Tracking” and “Data Relay Satellite System” (TDRSS) the acquired information and sends it to ground stations in the EOS Data and Operations System (EDOS part of EOSDIS). The interface between control centres and ground stations for every platform is provided by the EOS Real time Processing System (ERPS). EDOS archives original data (level 0), processes telemetry, conducts calibration radiometric, geometrical and georeferencing processes (level 1 and 2 processing) and produces a cloud mask product. Once this process is completed, this centre sends all information to the appropriate DAACs that process (to level 2, 3 and 4), archive the documents and distribute the data while providing information, services and tools (http://nasadaacs.eos.nasa.gov).

At present, the MODIS team produces over 45 MODIS data sets that are available for scientific studies. They provide new and enhanced tools for monitoring the Earth at a moderate resolution (Justice *et al.* 1998). These products have different levels of processing, that go from level 0 to 4. Level 0 removes telemetry artefacts, places packets in correct time order and duplicates packets. Level 1A calibrates radiometric, geometric coefficients and georeferencing parameters.

Level 1B calibrates radiances from 250 m, 500 m and 1 km bands to sensor unit. Level 2 derives geophysical variables at the same resolution and location as level 1B. Level L2G generates a layer grid that stores all samples for different orbits over a given point, preserving all of the observations obtained in one day. In level 3, the products are spatially-resampled, variables are mapped on average and/or temporally composed to produce a single estimate of a geophysical variable for each grid location; time scale can vary between one day and one year. Level 4 model output results from analysis of lower level data (Justice *et al.* 2002).

Surface reflectance product

MODIS surface-reflectance (MOD09) is one of the MODIS land products that is derived from MODIS low level data L1B and L2. These products identify atmospheric scattering or absorption and estimate spectral reflectance at surface level. The ancillary information, such as aerosol and water vapour, provides the basic information to develop a special algorithm that identifies and corrects gases, aerosols and thin clouds such as cirrus. This algorithm, developed by Tanre *et al.* (1997), is applied to the first 7 MODIS bands. The operational scheme presumes that stoke of aerosol in the atmosphere is constant and Lambertian surface is uniform. A signal that arises at the top of the atmosphere (TOA) is a combination of reflectance from the pixel target and its surrounding pixels weight for a target pixel distance. This effect is known as the 'adjacent effect'. Details about atmospheric correction algorithm are given in Vermote *et al.* (2002).

The accuracy of the MODIS surface reflectance product is evaluated using AVHRR and TM data from selected validation sites. These datasets are used along with information from the Polarization and Directionality of Theatres Reflectances (POLDER) and Sea-viewing (SeaWiFS) instruments. The surface reflectance estimation derives information of Accuracy Quality (AQ) and gives per pixel information on:

i. Integrity of the surface reflectance estimate;

ii. Successful completion of the correction scheme;

iii. Presence of clouds (clear, cloudy, mixed, shadow);

iv. Presence of cirrus clouds (no cirrus, low, average, high);

v. Source of aerosol information: MODIS aerosol, climatology;

vi. Presence of aerosol (low, average, high);

vii. Source of water vapour information: MODIS water vapour, climatology;

viii. Source of ozone information: MODIS ozone, climatology;

ix. Whether the pixel is land or water.

The surface reflectance product is the basic input for the generation of different products such as: Vegetation Indices (VIs), BRDF/albedo and thermal anomaly among others.

Fire MODIS products

At present, MODIS is the main source of data for global fire monitoring (Justice *et al.* 2002; Roy *et al.* 2002b; Roy *et al.* 2005). It allows us to understand better the daily cycles, speed of propagation, radiative source, temperature, location, size of active fires and burn scars (Justice *et al.* 2003; GOFC-GOLD 2004; Roy *et al.* 2005). Diverse products and innovative algorithms have been developed from physical properties of reflectivity (Roy *et al.* 2005; Csiszar *et al.* 2006). The algorithm used to define active fire makes use of the strong emissions of radiation at middle infrared wavelengths (Matson and Dozier 1981; Dozier 1982). Detection is based on the amount of emission or instantaneous radioactive power that is produced in an area by flames which can be detected by the satellite (Dwyer and Pereira 2000; Stropianna *et al.* 2000). With the purpose of detecting the presence of fire, multispectral criteria are applied (Justice *et al.* 2003). Day

and night fire observations are compared to detect changes in temperature so that the difference between the fire pixel and its background becomes apparent (Boles and Verbyla 2000; Justice *et al.* 2002). These algorithms have been applied at a global (Giglio *et al.* 2005) and regional scale by Roy *et al.* (2002b) in South Africa, Northern Eurasia by Csiszar *et al.* (2006), Australia and South America by Roy *et al.* (2005) and at a local scale in southeastern United States by Xie *et al.* (2007). Validation has been done through fieldwork, manual interpretation, aerial photograph, high resolution sensor i.e. Advanced Thermal Spaceborne Emission and Reflection Radiometer (ASTER) (Morisette *et al.* 2005; Csiszar *et al.* 2006) and Landsat, which has shown a high accuracy of the product. Currently MODIS has presented the Thermal Anomalies product (MOD014_Terra and MYD014_Aqua) which contains information on the time and the spatial distribution of active fires (http://modis-fire.umd.edu).

In addition, MODIS has generated an algorithm which by differences in spectral, temporary and structural characteristics defines the areas which have been burned (Roy *et al.* 1999; Roy *et al.* 2002b; Roy *et al.* 2005; Roy and Landmann 2005). This algorithm has been acquired through the Surface Reflectance Product (MOD09_Terra and MYD09_Aqua), using a bidirectional reflectance model (BRDF). This model assumes that reflectance of the surface varies as a function of the angle of the sensor with respect to the sun and the surface (Camacho de Coca *et al.* 2002). The reflectance is detected within a temporary window in a number of fixed days and used to predict the reflectance of the following day. Differences between observed and predicted values are used to determine if any significant change has occurred (Roy *et al.* 2006). Global estimations have been made (Giglio *et al.* 2005) from several studies in southeast Africa (Roy *et al.* 2002b) and North Eurasia (Csiszar *et al.* 2006). MODIS has presented the MCD45 product which contains information on the percentage of burned pixels and is currently in the validation process (http://modis.gsfc.nasa.gov).

3.3. Summary

The ECS formation is a heterogeneous area located in the northeastern part of Colombia. The climate of this region is considered typical tropical wet and dry climate which is classified as 'Aw' according to the Köppen Climate Systems. This wet seasonal tropical climate consists of a single dry season between November and April and a single rainy season between May and October. This ecosystem presents a variety of land-forms within a mainly flat concave landscape, with short and highly inclined slopes and some isolated table-mountains. In addition, this ecosystem comprises of a variety of vegetation types, namely high savannas, flooded savannas, sandy savannas, forest, wetlands, rivers, culture mosaic, along with exotic pastures, palm oil plantations and infrastructure. Since pre-hispanic times local ethnic groups survived on these savannas by fishing, hunting and harvesting activities for subsistence, while cutting and burning the vegetation. In present days, other factors besides farming are causing problems such as expansions of mono-specific African palm and rice plantations, the development of road infrastructure, oil production, sorghum, sugar cane and coca culture.

The objective of the satellite CBERS is to obtain information on the Amazon basin with the purpose of identifying forest coverage, agricultural and urban expansion, infrastructural development, geologic and soil formations, fire detection and water dynamics. The Earth's surface is covered every 26 days at a spatial resolution of 20 m in four spectral bands and one panchromatic band from 0.51 µm to 0.73 µm. Landsat satellite probably has been used most for characterizing land cover. This sensor was designed for thematic cartography that provides information with high spatial, spectral and radiometric resolution, and takes information at a spatial resolution of 30 m in 7 bands from the visible to the medium infrared band. MODerate Resolution Imaging Spectroradiometer (MODIS) has become one of the best alternatives to detect and map burned areas, because of its spectral (36 bands), spatial (250, 500 m and 1 km) and temporal (daily, 8-days, monthly) resolution characteristics, together with the variety of obtained products. MODIS has converted this sensor into one of the most used product that acquires information of the Earth in a constant and systematic way.

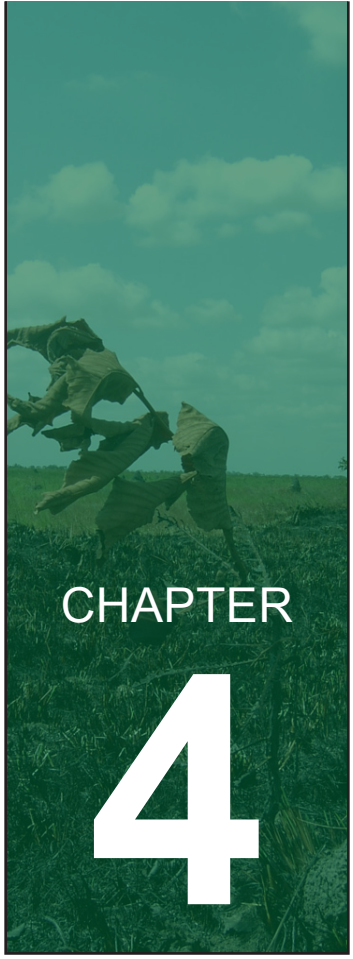

CHAPTER 4

Palm oil (Elaeis guianensis) plantation near Barranca de Upia (Meta, Colombia)

CHAPTER 4

Land use/cover change assessment

The rapid and wide-ranging changes in land cover around the world, has led to the search for methodologies that allow monitoring of change in an efficiently, continuous and low-cost way (Cihlar 2000). Remote sensing technology together with Geographical Information Systems (GIS) have become the most powerful tools for providing, storing, measuring, modelling and analysing spatial data to generate land cover information (Geneletti and Gorte 2003). Land Use/Cover (LUC) combined with Land Use Cover Change (LUCC) assessments is one of the most practical approaches to understand the effects of human activity over ecosystems and potential effects on climate changes, biodiversity loss, land degradation, atmospheric CO_2 concentration, among others (Mas 1999). In this chapter, objective one is developed with the purpose to identify the magnitude of changes due to land use based on land cover maps at scale 1:100,000 for three different periods of time spanning the period between 1988 and 2007.

4.1. Methodology

The methodology to obtain LUC maps is explained in this chapter. This methodology involves preprocessing, processing and validation steps. Furthermore, the direction and magnitude of LUCC is analysed, including a construction of transformation matrices using the 'Markov chain' approach.

Choosing the methodology that is most suitable for the acquirement of LUC maps, can be complex as it depends most of the time on the intrinsic characteristics of the landscape and the local knowledge of the researcher. Nowadays the digital classification of multispectral images is widely used even without previous knowledge which as a consequence causes misclassification and reduced accuracy within the obtained information on land use/cover, and land cover changes (Franklin *et al*. 2000; Zhu *et al*. 2000; Couturier *et al*. 2007). As has been explained in table 2.1, methodologies such as supervised classification, decision trees and artificial neural networks present different advantages and disadvantages; however as has been discussed by authors such as Garcia and Mass (2008), the "best" method of classification depends on the interest of the user to identify specific classes.

Garcia and Mass (2008) present an evaluation of different classifications methods and conclude that the only method that significantly showed improved results is the classification that allows incorporating secondary information and not only the use of the specific algorithm. The implementation of additional data into the spectral information through the use of a priori probabilities is a promising alternative to improve mapping and monitoring land use/cover based on data obtained from remote sensing.

Thus at the moment of choosing the most appropriate methodology for the ECS it was taking in to account the spatial characteristics of the land cover types and therefore the supervised classification was choosing at the best option. This methodology has the advantages of that both objective and quantitative

criteria can be employed, that statistically based algorithms can be used, that secondary information (fieldwork data and previous knowledge of the area) can be implemented and that it is considered consistently and reproducible.

4.1.1. Preprocessing

The first step to obtain LUC maps was the acquisition and georeferencing of images. A set of Landsat and CBERS images from the years 1987-88, 2000-01 and 2007 periods was acquired. Landsat data was downloaded from Maryland University website, (http://glcf.uniacs.umd.edu/) and CBERS data from Institute of Pesquisas Espaciales - INPE website (http://cbers.inpe.br/).

Satellite images were georeferenced using between 15 and 30 ground control points distributed across the each image. The overall accuracy of the transformation expressed as a root mean squared (RMS) error was between 0.4 and 0.7 being a tolerable value according to the scale and precision to which it works. A nearest neighbour algorithm was used to resample the CBERS images from the original 20 m resolution to a 30 m output pixel size. Original Landsat data use WGS84 while CBERS have a 1969 South America project system. Images were rectified based on the oldest Landsat images (1987-1988), using a UTM-Zone 19 projection, with datum WGS-84.

Prior to the interpretation of the LUC classes a modified version of Corine Land Cover legend for Colombia, scale 1:100,000 (IDEAM *et al.* 2008), was adopted. Two categories were considered in this study: 'Natural' and 'Non-natural' categories which were divided into 12 classes. For the 'Non-natural' category, 4 classes were identified: i. Infrastructure; ii. Palm oil plantations; iii. Exotic pastures and iv. Culture mosaic. The 'Natural' category was separated into 9 classes: v. Forest; vi Secondary vegetation; vii. High savannas; viii. Flooded savannas; ix. Sandy savannas; x. Rocky outcrops; xi. Wetlands and xii. Water (Appendix 2). With help of complementary images the burned scars were reclassified to their original vegetation.

4.1.2. Processing

This phase of the satellite imagery analysis, the 'Processing' phase, included a series of steps:

i. Radiometric correction: On each Landsat and CBERS image a radiometric correction was performed according to image metadata from the provider;

ii. Image enhancement: By the use of Principal Components Analysis (PCA), linear contrast stretching and histogram equalization;

iii. Clouds, shadows and non-informative areas were masked and separated using a non-supervised classification algorithm. Categories in these areas were delimited by means of Landsat images 2007;

iv. A water-mask was applied of a 5-over-2 algorithm with the aim to extract and separate water and wetlands from the other categories. This algorithm relates the Middle Infrared (MIR) band with green band allowing the separation of humid areas from other categories. An infrared band (IR) was used in CBERS data, due to absence of the MIR band;

v. A Normalized Difference Vegetation Index (NDVI) was applied to separate vigorous vegetation from other classes. This is calculated by NDVI= (NIR-RED)/(NIR+RED), where NIR corresponds to the near-infrared band and RED is a red band. This index allows the extraction of vigorous vegetation such as forest and plantations;

vi. The LUC map of 2000-2001 was the base to classify the 1987-1988 and 2006-2007 images. A supervised classification using the maximum likelihood algorithm was applied. This classification was achieved extracting different spectral statistical classes through

areas of control called “training areas”. These areas were categorized into the six non-thermal bands of Landsat images and 4 visible and infrared bands of CBERS by Gaussian maximum likelihood algorithm. This algorithm considers the spectral characteristics of a group of pixels and classifies the pixels into the classes of the previous set preliminary legend (Palacios-Sanchez *et al.* 2006);

vii. Post-serial filters were applied to eliminate the “salt and pepper” texture in a classified image. This effect is caused by isolated pixels which generate a grainy appearance in the classified images;

viii. A manual revision was done to correct some errors in the classification as some classes were difficult to separate due to the characteristics of the region. Non-continuous rivers, urban zones, roads and natural gallery forest were digitized manually.

4.1.3. Classification accuracy assessment

The classification assessment of the produced LUC maps was done by two methods:

i. **Field Data Comparison method** by data from 2001 (previous field-check) and field works:

i.1. November - December 2007: Visits to foothill and the north-western areas;

i.2. January - February 2008: Visits to foothill and central-eastern areas (Appendix 3);

i.3. November 2007 and December 2008: Two over-flights to obtain information on the central and southeast part, which are not easy accessible by road.

ii. **Stratified random sampling method**, according to the methodology proposed by Meidinger (2003): For each class (savannas, wetlands, etc.) a set of small, medium and large polygons was selected from a percentile rank. From all three sizes and for each class polygons were selected randomly. Due to the size of the study area, only 2 percent of all polygons were selected making a total of 1,091 polygons distributed in 369 small, 371 medium and 351 large ones. Table 4.1 shows the distribution of the number of polygons for each category. The selected polygons were compared with aerial photography of 2001 and fieldwork. Polygons were labeled with 1 (classified correctly) or 2 (not classified correctly). Information of 1985 could not be validated due to lack of historical information.

Table 4.1. Number of polygons selected per class and size to evaluate the accuracy of LUC maps. See appendix B for datails on the classes.

Classes	Small	Medium	Large
Forest (includes secondary vegetation)	186	186	198
High savannas	61	61	62
Flooded savannas	41	42	17
Sandy savannas	16	15	21
Rocky outcrops	5	6	6
Non-natural (including infrastructure, palm oil plantations, exotic pastures and culture mosaic)	40	41	22
Wetlands	20	20	25
Total	369	371	351

After the application of the above mentioned methods, the accuracy of classified images was evaluated by a Kappa analysis. A Kappa (κ) statistical method is a discrete multivariate way used in accuracy estimation (Congalton and Mead 1983). This method measures the concurrence between two sets of arrangements of a dataset while correcting for possibility agreements between the arrangements (Jenness and Wynne 2007). This concept is based on the construction of the matrix analysis as shown in Table 4.2.

Table 4.2. Kappa matrix analysis: In this matrix, the rows represent the predicted values while the columns represent the observed values.

Observed/predicted	j_1	j_2	$j_{1=k3}$	n_i
i_1	n_{11}	n_{12}	n_{1k}	$n_{1.}$
i_2	n_{21}	n_{22}	n_{2k}	$n_{2.}$
i_k	n_{k1}	n_{k2}	n_{k3}	$n_{k.}$
$n_{.j}$	$n_{.1}$	$n_{.2}$	$n_{.k}$	$n..=n$

Each cell represents the number of sample points that were classified as *i* and observed to be *j*. The diagonal (where $i = j$) represents cases where the predicted value agreed with the observed value.

From the matrix, the κ statistic formula is defined by:

$$\mathbf{K} = \frac{n \sum_{i=1}^{k} n_{ii} - \sum_{i=1}^{k} (n_{i.} n_{.i})}{n^2 - \sum_{i=1}^{k} (n_{i.} n_{.i})} \tag{4.1}$$

Where k is the number of rows in the matrix, n_{ii} is the number of observations in row i and column i respectively and n is the total numbers of observations. **κ** Statistic ranges between 0 and 1, where the value closest to 1 indicates highest concordance.

The Kappa index is accompanied by a set of measures that provides means to calculate numerous additional metrics that reflect the model performance (Table 4.3). Kappa analysis is performed by a confusion matrix analysis, which is based on correct and false observation distributions.

Table 4.3. Construction of confusion matrix.

Observed distribution/predicted	Correct	No correct
Correct	$\sum_{i=1}^{k} n_{ii} = a$	$\sum_{i=1.}^{k} \sum_{j=1.}^{k} n_{ij} = b$
No correct	$\sum_{j=1.}^{k} \sum_{i=1}^{k} n_{ij} = c$	$\sum_{i=1.}^{k} \sum_{i\neq 1.}^{k} \sum_{j=1.}^{k} n_{ij} = d$

(4.2-4.5)

a = number of times a classification agreed with the observed value; b = number of times a point was classified as X when it was observed to not be X. c = number of times a point was not classified as X when it was observed to be X. d = number of times a point was not classified as X when it was not observed to be X.

Overall accuracy (oa) is a simple method to calculate accuracy statistics. This measure is calculated as:

$$oa = \frac{\sum_{i=1}^{k} n_{ii}}{} \tag{4.6}$$

This measure is only one way to calculate accuracy statistics. With the confusion matrix analysis additional metrics can be done. 'Sensitivity' and 'Specificity' are the measurements of accuracy in predicting presence and absence respectively (Fielding and Bell 1997); and 'Omission' and 'Commission' provide the rate to define which sample failed to be classified or was misclassified (Jenness and Wynne 2007). Table 4.4 shows the statistics formula to calculate these measures:

Table 4.4. Sensitivity, specificity, omission and commission formulas.

$\text{Sensitivity} = \frac{a}{(a + c)}$	$\text{Specificity} = \frac{d}{(b + d)}$
$\text{Omission} = \frac{c}{(a + c)}$	$\text{Commission} = \frac{b}{(b + d)}$

(4.7-4.10)

4.1.4. Land Use/Cover Change (LUCC) assessment

The change detection method of "Post-classification comparison" was selected to perform LUCC assessment. Starting with 1987 when the first large crop occupation occurred in Eastern Colombian Savannas (ECS), 13 (1987-2000) and 7 (2000-2007) years periods were set to carry out the multi-temporal analysis. This method allows the comparison on a pixel by pixel basis using a change detection matrix. According to Jensen (2000), Muñoz-Villares and Lopez-Blanco (2008) this method has the benefit of producing detailed "from-to" information and a readily available classification map for the next base year. Additionally, an annual rate of change proposed by Puyravaud (2003) was calculated. This index allows to identify the rate of the change per year of natural vegetation to non-natural vegetation. This index is calculated as:

$$TC_{iht2-1} = \frac{(\ln AT_{iht2} - \ln AT_{iht1}) \cdot 100}{(t_2 - t_1)} \quad (4.11)$$

Where:

$TC_{iht1\text{-}2}$: Annual rate of change (%) of natural cover i, in an area of interest h between two moments of time t_1 (initial time period) and t_2 (final time period);

AT_{iht1} : Total surface (ha) of natural cover i, in an area of interest h, at the t_1;

AT_{iht2} : Total surface (ha) of natural cover i, in an area of interest h at time t_2;

In order to identify the spatial changes between the 1987, 2000 and 2007 maps, a cross-tabulation matrix was produced, showing gains or losses in each class at pixel level. This analysis was done using a Markov chain mathematical model. The Markov chain is a series of values in which the probabilities during a time interval depend on the value of the most recent previous state. This model assumes that land cover change is a stochastic process and different categories are the states of a chain (Weng 2002).

A Markov chain is represented as a symmetrical arrangement table namely “transition matrix” that contains on one axis the categories in the base year and on the other axis, the same categories at the final time period. Each cell of the main diagonal of the matrix represents the probability of each class of land use remaining in the same category, whereas the cells of the rest estimates the category probability to which it can change. This method allows understanding the dynamics of change in LUC at a local or regional scale (Aaviksoo 1995; Lopez *et al.* 2001). This is calculated as:

Where

$$p_{ijt} = \frac{n_{ij}}{\sum_{j=1}^{m} n_j} \quad (4.12)$$

p_{ijt} : The probability of transition of one category in to category *j* during the period

n_{ij} : The number of transitions from category into category *j*

$p_{ijt} = \frac{n_{ij}}{\sum_{j=1}^{m} n_j}$: The number of pixels in category *j* during the period *t*

Six principal LUC classes were identified:

i. Non-natural vegetation (infrastructure, palm oil plantations, exotic pastures and culture mosaics);
ii. Forest;
iii. Secondary vegetation;
iv. High savannas;
v. Sandy savannas;
vi. Flooded savannas and Wetlands.

Rocky outcrops and water bodies were excluded from analysis as no significant changes were observed during any of the analysed years.

4.2. Results

A total of twelve Landsat images and twenty-two CBERS images cover the ECS. All images were obtained for seasonal dry periods between 1987-1988, 2000-2001 and 2004-2007 (Figures 4.1, 4.2, 4.3). CBERS images (resolution 20 m) cover 81% of the ECS, 13% with 80 m resolution an the 5% with no information. In average only 1% of the Landsat and 4% of CBERS images were covered by clouds and shadows. To cover areas without information and areas below clouds and shadows, Landsat images of 2007 and 2008 were used.

Path	Row	Data	% clouds
7	56	26/12/1987	0
	57	11/01/1988	0
	58	11/01/1988	0
6	55	11/01/1988	0
	56	11/01/1987	8
	57	11/01/1987	1
	58	04/01/1988	0
5	55	04/01/1988	0
	56	13/01/1988	0
	57	26/26/1986	0
4	56	12/26/1986	3
	57	12/26/1986	0

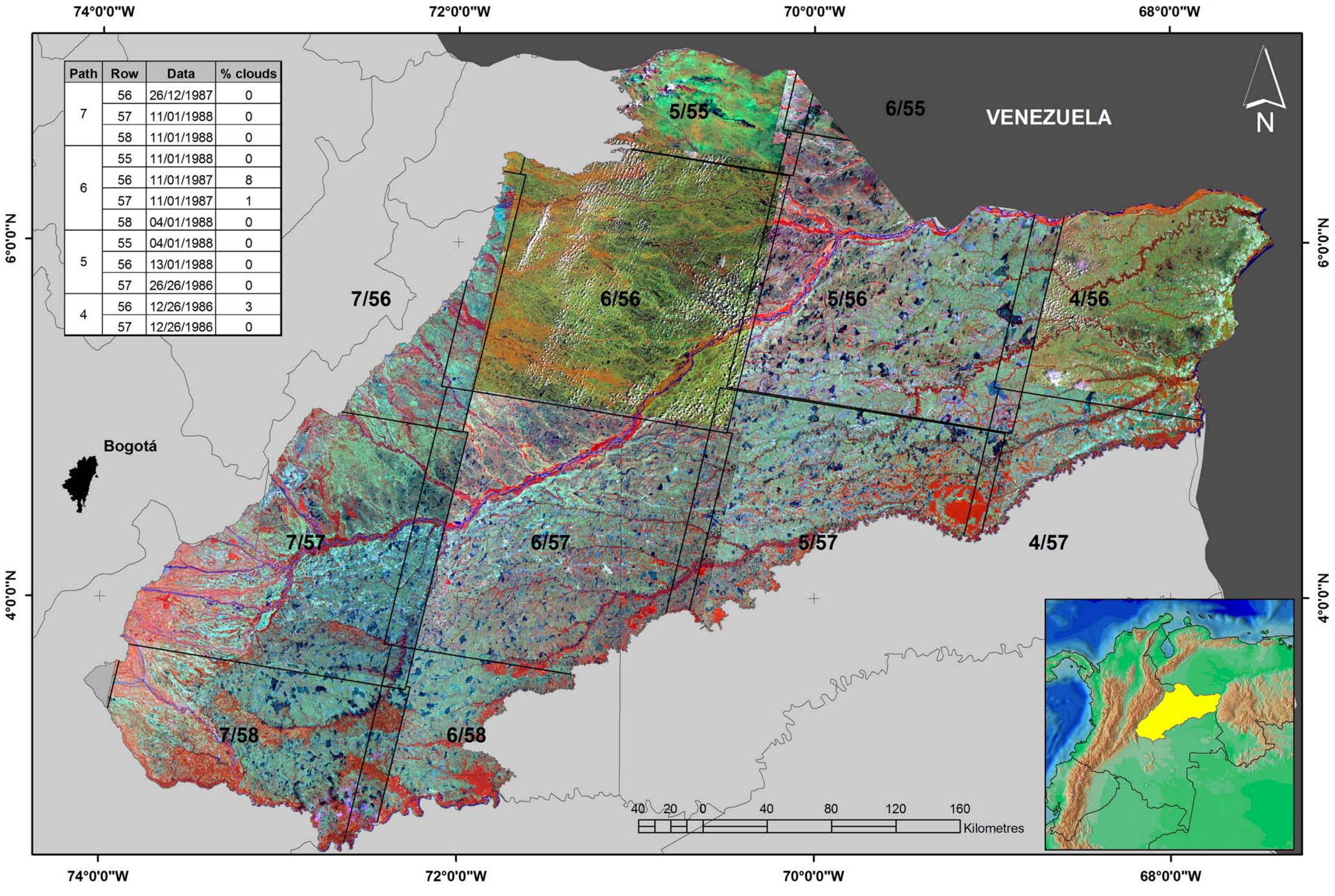

Figure 4.1. *ECS seen through a mosaic of Landsat images from December 1986 to January 1988.*

Path	Row	Data	% clouds
7	56	12/13/2000	0
	57	12/13/2000	0
	58	03/03/2001	0
6	55	01/01/2001	0
	56	2/16/2001	0
	57	2/16/2001	0
	58	03/12/2001	0
5	55	4/22/2001	0
	56	01/08/2001	0
	57	1/22/2001	3
4	56	01/09/2001	0
	57	01/09/2001	0

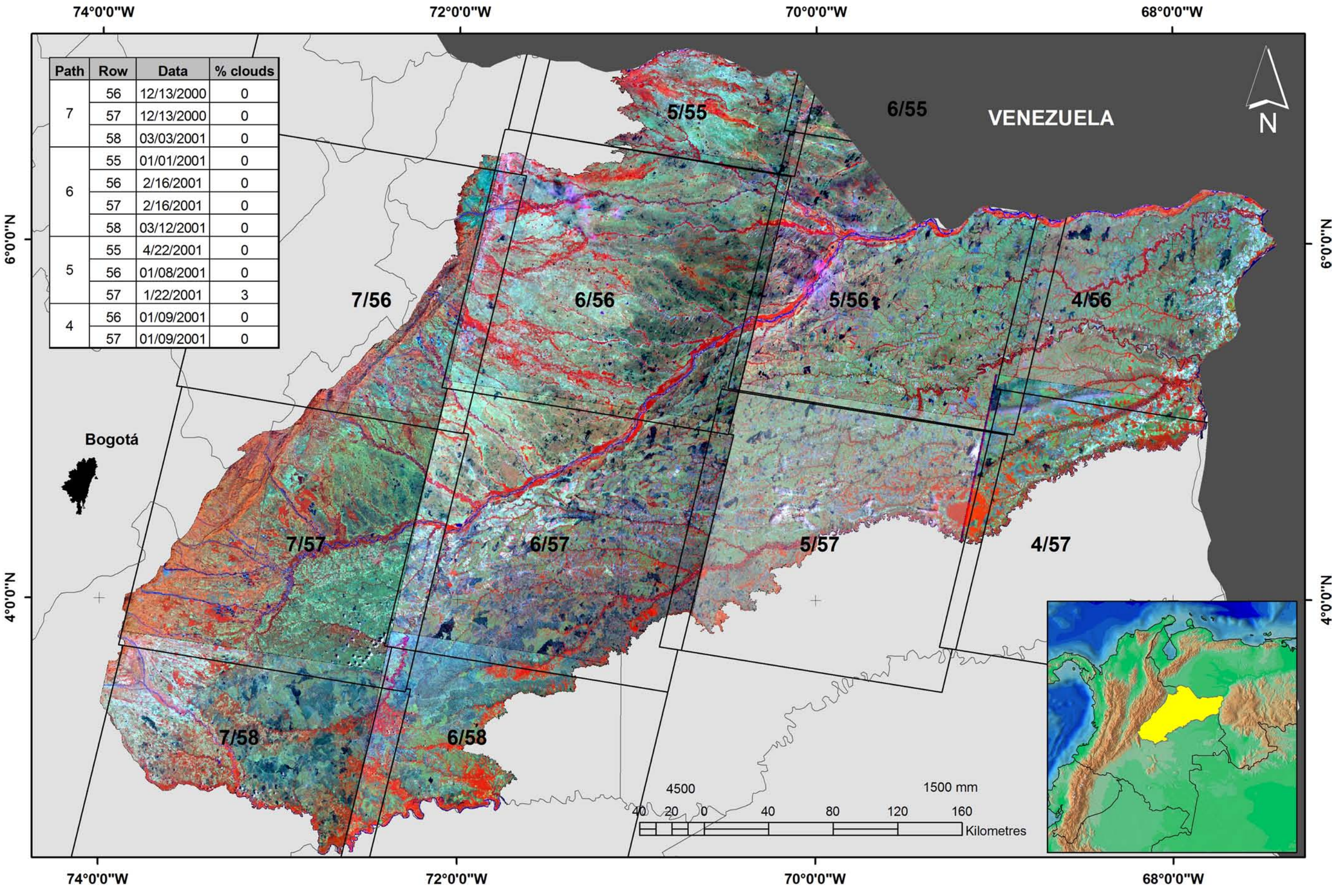

Figure 4.2. *ECS seen through a mosaic of Landsat images from December 2000 to April 2001.*

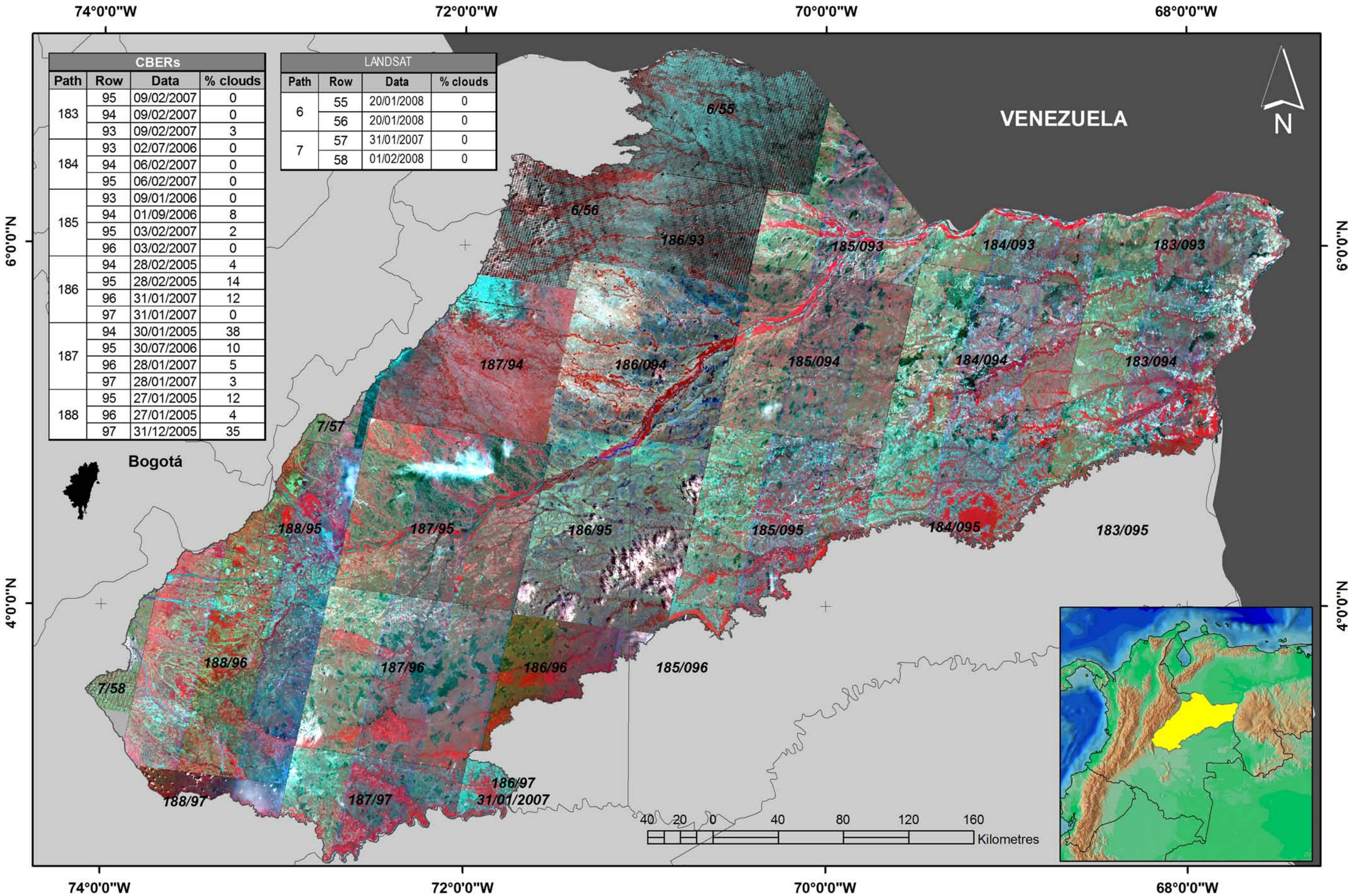

CBERs

Path	Row	Data	% clouds
183	95	09/02/2007	0
	94	09/02/2007	0
	93	09/02/2007	3
184	93	02/07/2006	0
	94	06/02/2007	0
	95	06/02/2007	0
185	93	09/01/2006	0
	94	01/09/2006	8
	95	03/02/2007	2
	96	03/02/2007	0
186	94	28/02/2005	4
	95	28/02/2005	14
	96	31/01/2007	12
	97	31/01/2007	0
187	94	30/01/2005	38
	95	30/07/2006	10
	96	28/01/2007	5
	97	28/01/2007	3
188	95	27/01/2005	12
	96	27/01/2005	4
	97	31/12/2005	35

LANDSAT

Path	Row	Data	% clouds
6	55	20/01/2008	0
	56	20/01/2008	0
7	57	31/01/2007	0
	58	01/02/2008	0

Figure 4.3. *ECS seen through a mosaic of CBERS images from December 2004 to April 2007.*

4.2.1. Spectral profiles of LUC classes

The spectral values for each one of the possible classes are shown in Figure 4.4. In general, for forest, culture mosaic and secondary vegetation the reflectance depends on the structure, humidity and maturity state of vegetation, as well as on the humidity content of the soil. For these classes, the reflectance curve presents high values of radiance in the blue band, decreases in green and shows a minimum value in the red band. This abnormal behaviour is influenced by atmospheric noises that affect the blue band sensibility. After this, the reflectance curve increases steeply into the infrared band showing a high value of around 0.75 μm 10^{-9}. Then a gradual decline is seen to 1.65 μm 10^{-9} after which it declines more rapidly. Culture mosaic and secondary vegetation show an increase in band 5, due to the mixture of vegetation and soil.

In exotic grasslands and savanna classes, the reflectance curve presents high values in the blue band, declining slightly towards the green band and shows a later increment in the red band indicating a lower photosynthetic activity. In the infrared band, the curve decreases showing poorer health of this vegetation. The middle infrared band presents the highest reflectance peak. These classes are principally defined by mixes of soils and low vegetation such as grasses.

In sandy areas, roads and urban areas the reflectance is influenced by the humidity, material and texture of soils and constructions. In general these classes present a low content of humidity, which produces a high reflectance, in visible bands. These classes present a similar reflectance curve between savanna areas and anthropogenic grasslands.

In burned scars (new and old), the reflectance is associated with variation in the composition of soils, charcoal and type of vegetation that it has affected. The curve presents high values in the blue band, diminishing slowly toward the four other bands. Between band 4 and band 5 the values increase after which the values steadily diminish. Clouds present high reflectance values, associated with

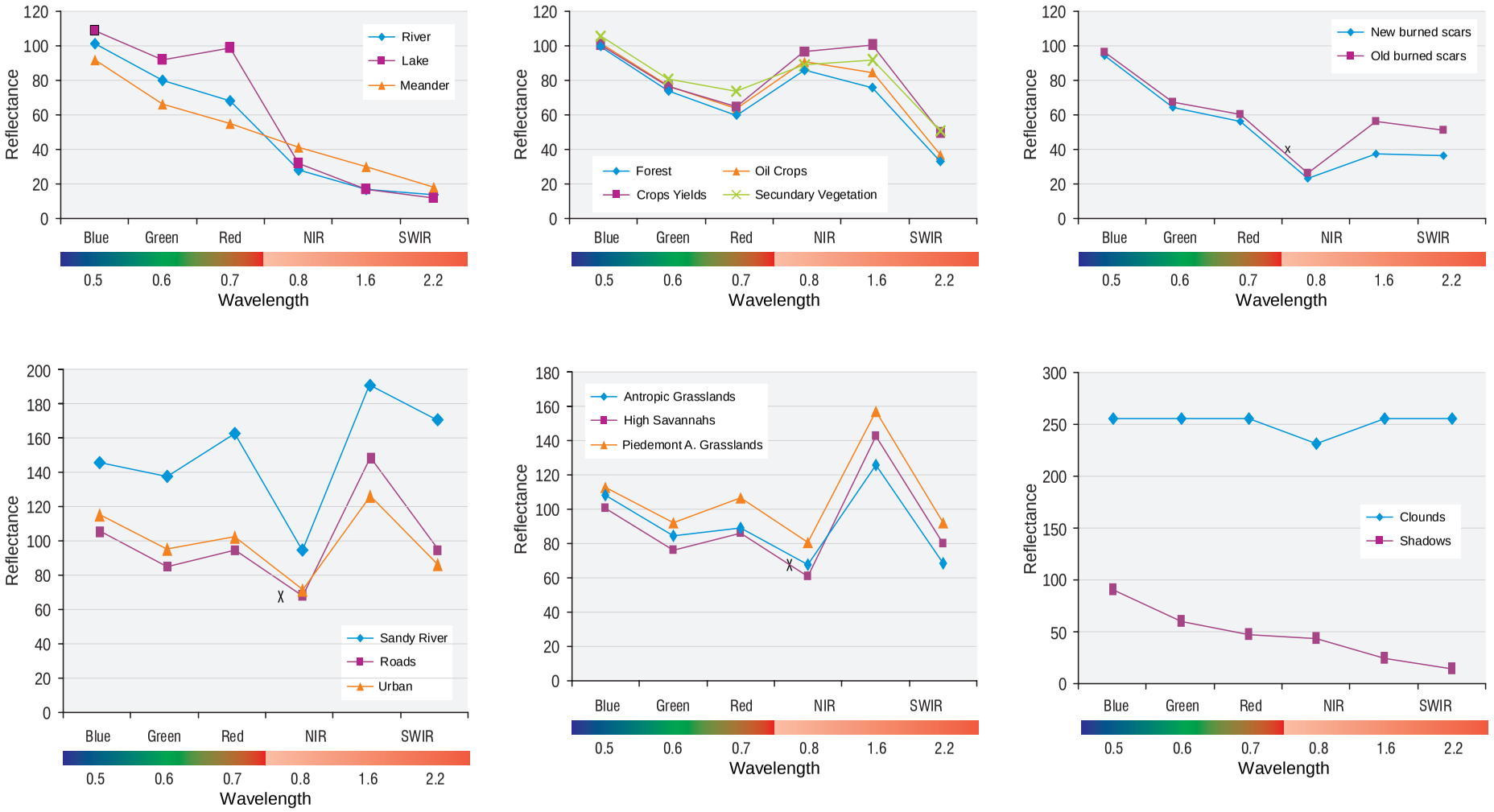

Figure 4.4. *Spectral curves for each of the classes found in the Landsat image 758 of 01-jan-1988 for ECS.*

intrinsic characteristics of the white colour. Shadows present a similar behaviour to water.

4.2.2. Image enhancement process

The enhancement process involves Principal Component Analysis (PCA) and histogram equalization. Using Landsat data of RGB 7-57 of 11-Jan-1988 as an example, a correlation analysis between bands (1, 2, 3, 4, 5 and 7 in case of Landsat) shows that 65,8% of the data variability is defined by the first component (see Table 4.5). Visible and near infrared bands which are highly correlated present low contributions to the variability while the MIR band (band 5) shows the highest contribution 0.83. The second component contributes to 26.7% of the variability that summed up with the first component gives a total of 92%. In this component, band 4 is the one that has the greatest contribution of 0.96. Principal component 3 only contributes to 5.93%, of the variability. In this component the band 5 presents the smallest correlation between bands and contributes with 0.41. Components 4, 5 and 6 show the lowest contribution with only 1.6% of the variability and were therefore removed for this analysis.

Figure 4.5 shows the visual analysis of the PCA for the same image of Table 4.5, pointing out that information from different vegetations types can be obtained by using the first component. The second component gives information related to burned scatter areas and soils, while the third component provides information on water. The other components do not offer additional information.

Moreover, the so-called ‘5-over-2-index’ to construct a Water-mask, allows the extraction of extensive and continuous networks of water bodies and wetlands. This index varies between 0 and 255 and indicates that low values between 0 and 50 coincide with water bodies and values between 51 and 75 correspond to wetlands. The rest of the values corresponds to other categories. Figure 4.6 shows the results for the Landsat image 4-56 of 09-Jan-2001.

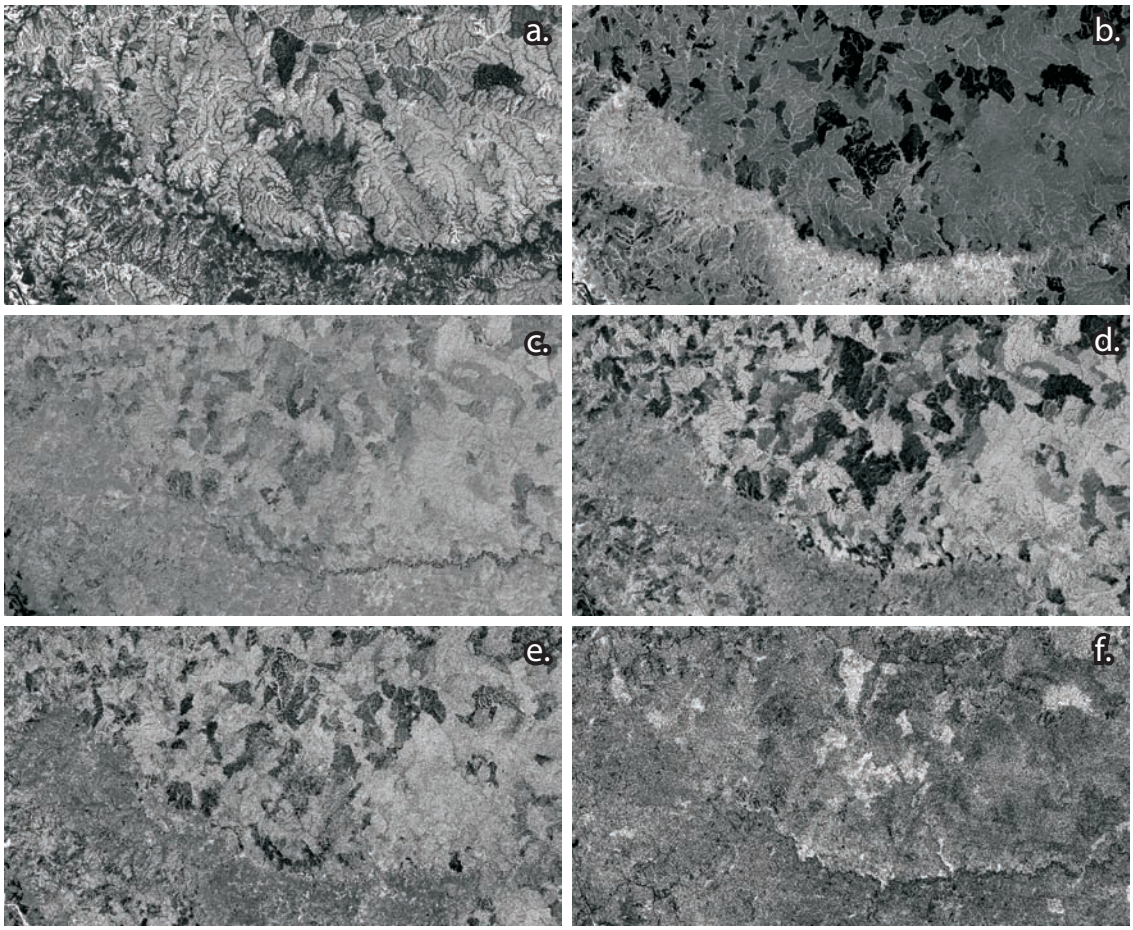

Figure 4.5. *Principal Components Analysis of the Landsat image 7-57 of January 11th 1988 showing the first six components.* ***a)*** *Component 1: 65.8%;* ***b)*** *Component 2: 26.6%;* ***c)*** *Component 3: 5.9%;* ***d)*** *Component 4: 1.1%;* ***e)*** *Component 5: 0.4% and;* ***f)*** *Component 6: 0.1%.*

Table 4.5. Principal Component Analysis for Landsat image 7-57 of 11-Jan-1988. The columns show the six principal components, the rows present each band, the Eigen-value, variance and cumulative variance.

	PCA1	PCA2	PCA3	PCA4	PCA5	PCA6
Band 1	0.21	-0.04	-0.72	-0.16	0.63	-0.14
Band 2	0.14	0.01	-0.34	-0.12	-0.27	0.88
Band 3	0.27	-0.11	-0.40	-0.21	-0.71	-0.44
Band 4	0.03	0.96	-0.15	0.21	-0.08	-0.06
Band 5	0.83	0.12	0.42	-0.32	0.14	0.03
Band 7	0.41	-0.22	-0.08	0.88	-0.02	0.02
Eigen-value	810.52	328.35	73.11	13.69	4.75	0.98
% variance	65.82	26.66	5.94	1.11	0.39	0.08
Cumulative % variance	65.82	92.49	98.42	99.53	99.92	100

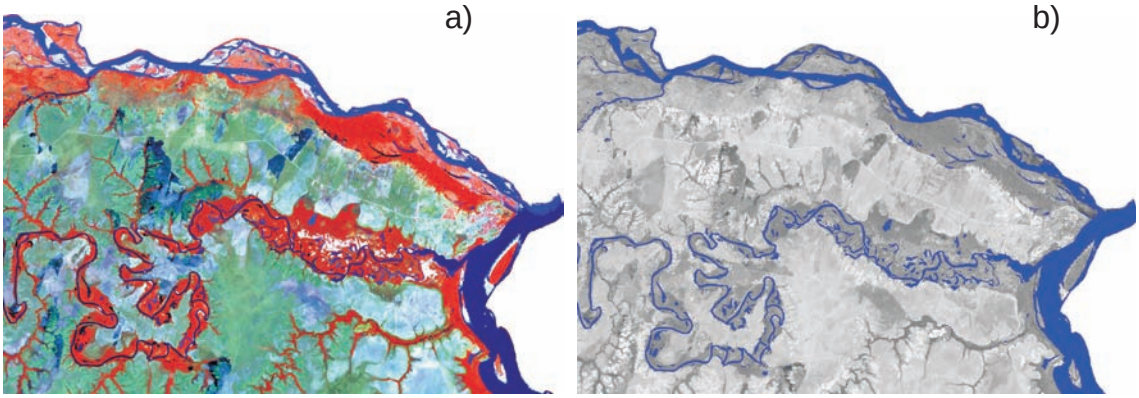

Figure 4.6. *The application of the 5-over-2-index-mask for* ***a)*** *Landsat image of 9-Jan-2001.* ***b)*** *Application of water mask blue areas coinciding with water bodies.*

4.2.3. Normalised Difference Vegetation Index

The Normalized Difference Vegetation Index (NDVI) allows the differentiation of areas where the vegetation presents high vitality, from those where little or none exists, such as burned scatter areas, water, bare soils and clouds. This index varies between 1 and -1 indicating healthy vegetation in high values while low values demonstrate little vegetation. Negative values are present in areas where no vegetation is found. For other classes present in the image, an approximation of the ranges was made (Figure 4.7).

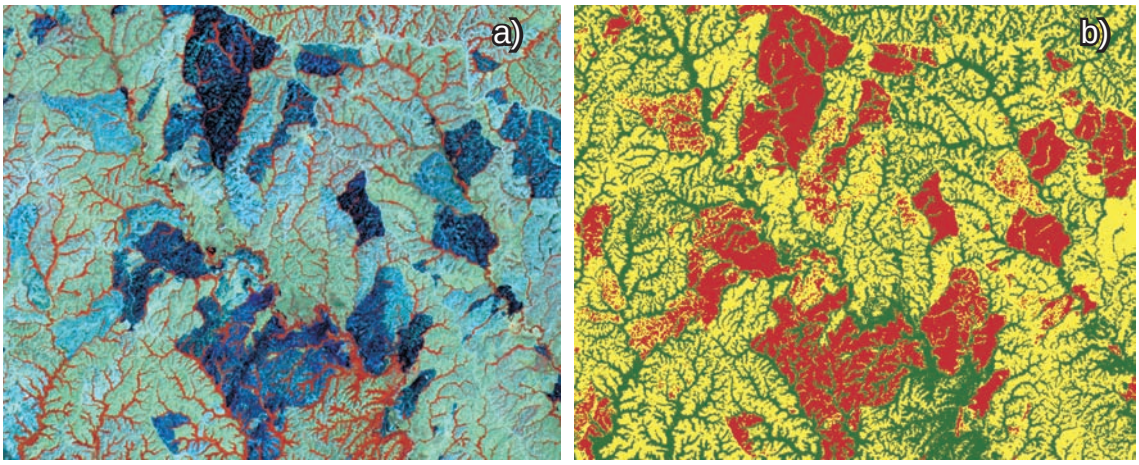

Figure 4.7. *The Normalized Difference Vegetation Index (NDVI) for Landsat image 7-58 of 11-Jan-1987.* ***a)*** *Bright colours indicated high values of NDVI, dark colours low values.* ***b)*** *Green colours show areas with healthy vegetation; orange demonstrates mixed areas of middle high vegetation (such as secondary forest, culture mosaic) with soil; yellow is a mixture between soils and low vegetation (grasslands); and cyan indicates bare soils, burned scatter, urban and water areas.*

4.2.4. Image classification

Before performing the LUC classification, scattergrams were made between the bands to identify and observe the total number of pixels that were in middle range of each of the classes and the independence between the different bands. Figure 4.8 a displays the scattergrams between bands 4 and 5 supporting the separation of savannas and secondary vegetation from the culture fields. The scattergrams between band 3 and 4 presents a better separation of classes (Figure 4.8 b).

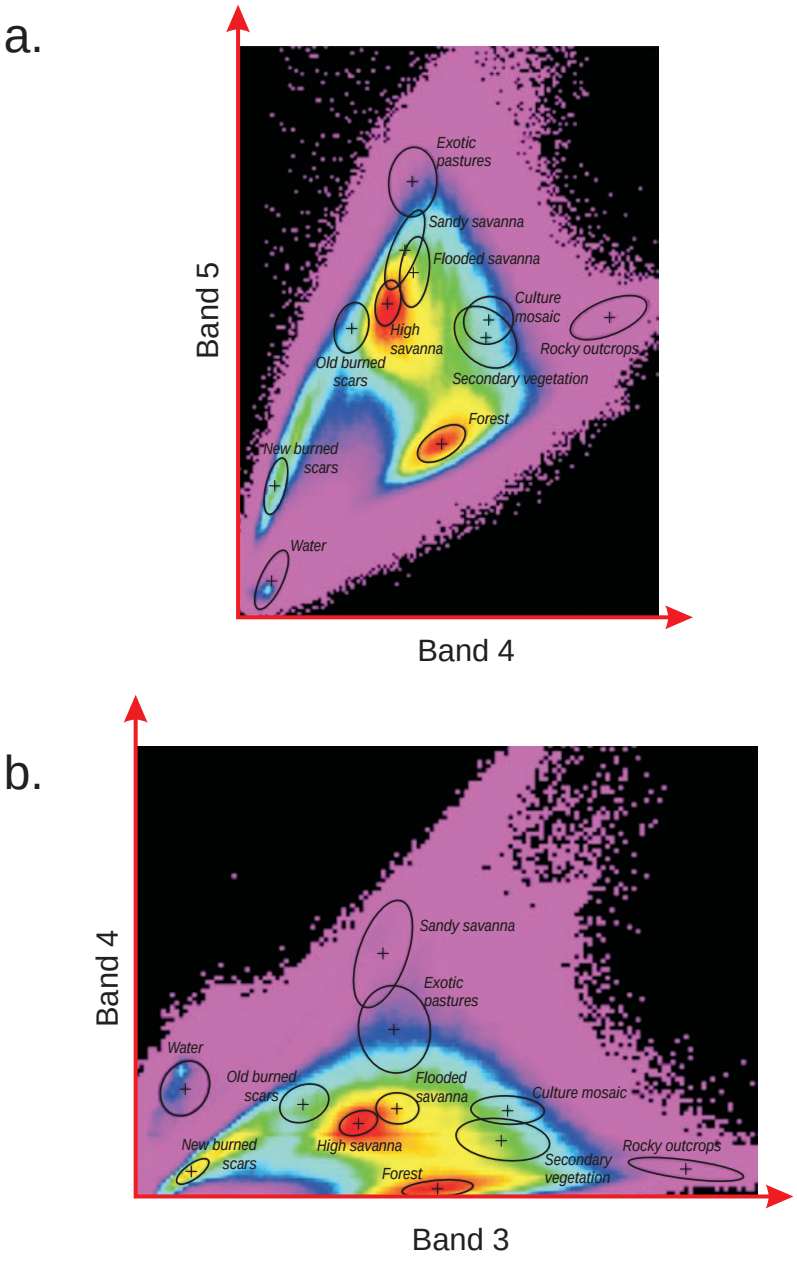

Figure 4.8. *Scattergram between band 4 and 5* ***(a)****, and band 3 and 4* ***(b)****, showing the separation between the different LUC classes.*

After the separation of the classes by scattergrams, the methodology of 'supervised classification' was used in which different types of cover are distinguished visually to define the training areas for the classification process (Figure 4.9). After implementing the water mask, the NDVI indices and the supervised classification, LUC maps were obtained.

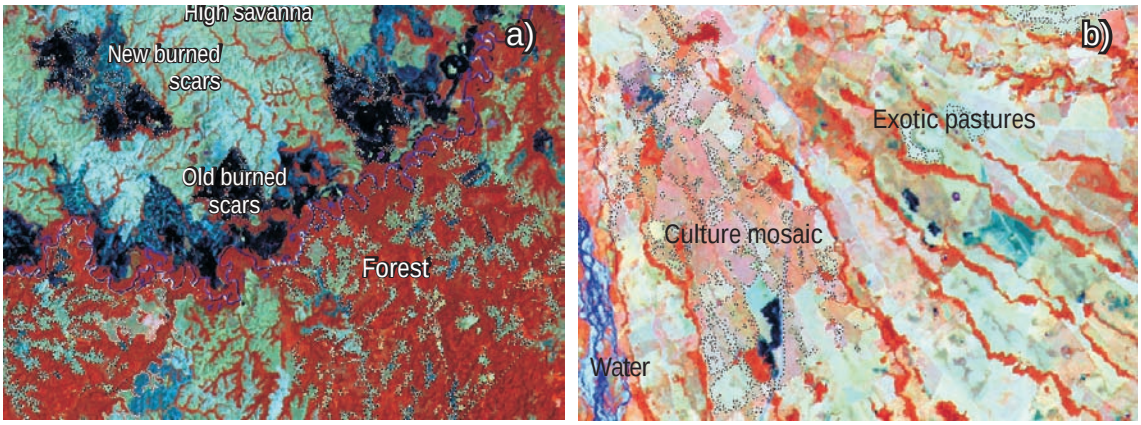

Figure 4.9. *Shows some examples of the training areas for different classes in the Landsat image 7-58 of 11-Jan-1988.* ***a)*** *Burned scars and forest.* ***b)*** *Water, Culture mosaic and Exotic pastures.*

4.2.5. Land use/cover maps

Figures 4.10, 4.11, and 4.12 show the LUC maps for 1987, 2000 and 2007 obtained by Landsat and CBERS image classification.

In general terms, ECS has thirteen cover classes distributed in nine natural and four non-natural classes. For 1987-1988, 92% of the area was covered by natural classes and only eight percent by non-natural classes. 83.7% of natural categories are constituted by high savannas which are the most extensive formation in the study area, occupying 35.6%; followed by flooded savannas (29.3%) and forest (18.8%). The remaining 4.5% corresponds to other minor vegetation formations like sandy savannas, rocky outcrops, wetlands and water. In non-natural categories, exotic pastures have the highest area coverage namely 4.6%, followed by culture mosaic (2.1%), infrastructure (1%) and palm oil plantations with 0.1% (Table 4.6).

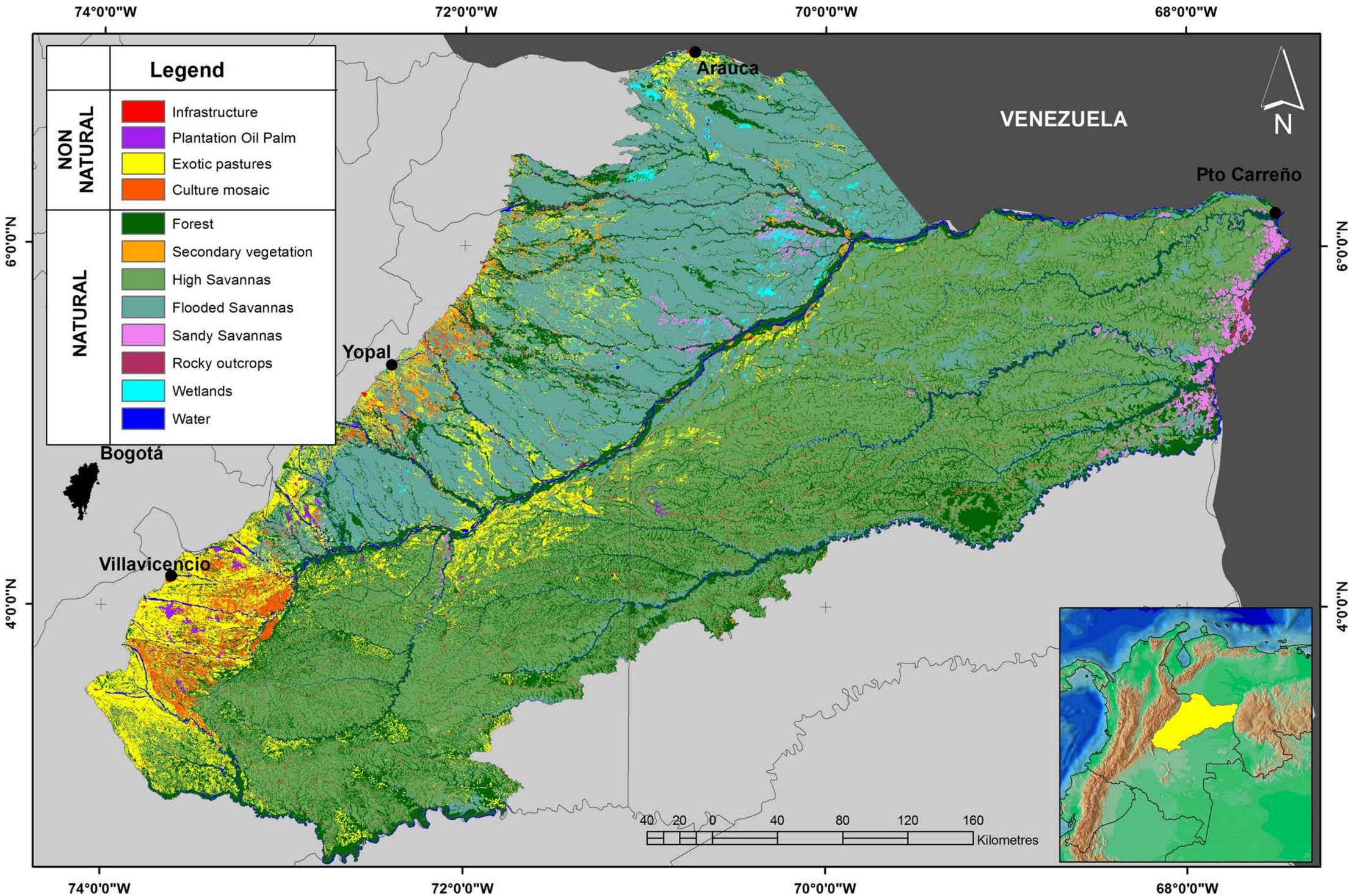

Figure 4.10. *LUC map for 1987-1988 of the ECS derived from supervised and unsupervised classification of Landsat images.*

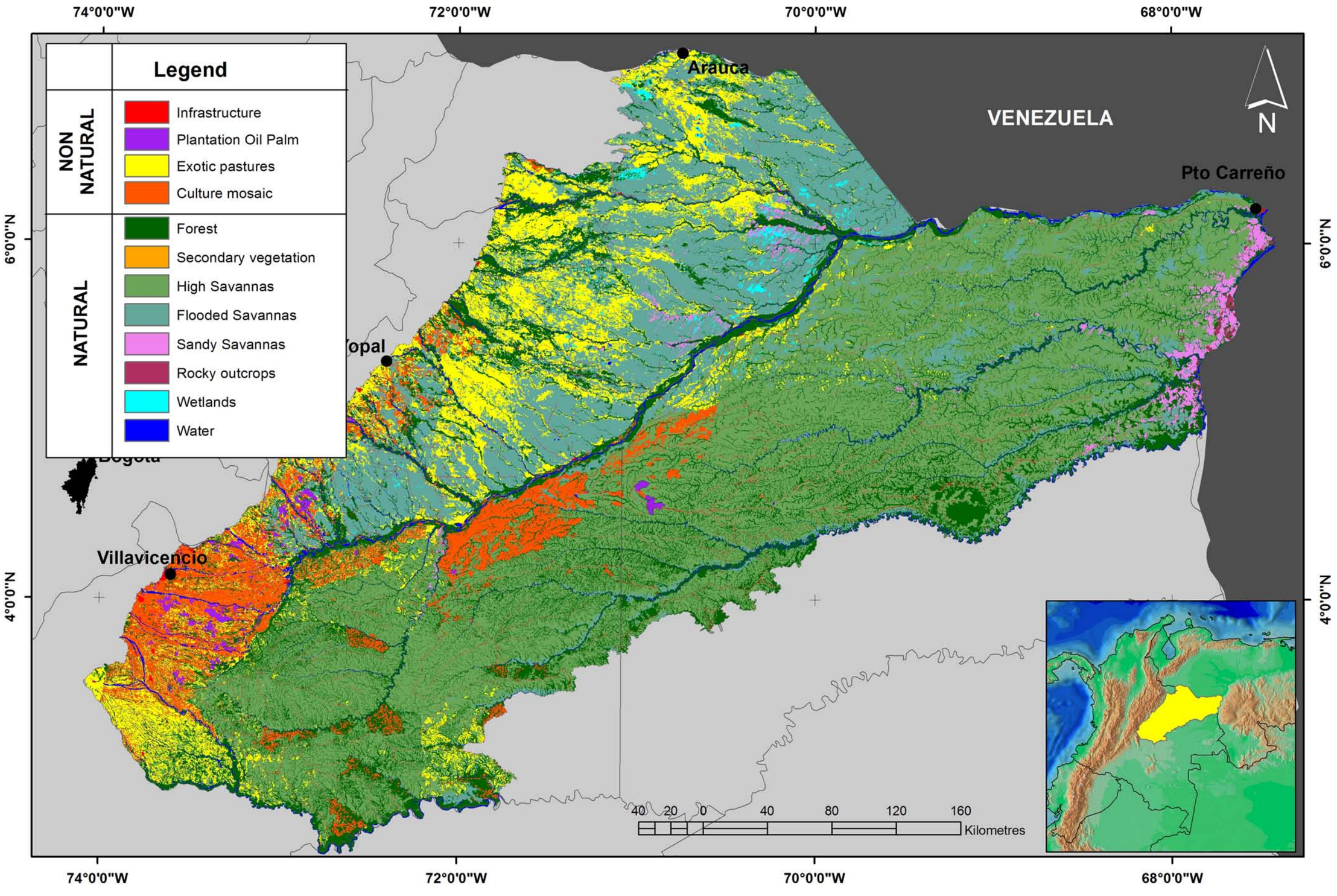

Figure 4.11. *LUC map for 2000-2001 of the ECS derived from supervised and unsupervised classification of Landsat satellite images.*

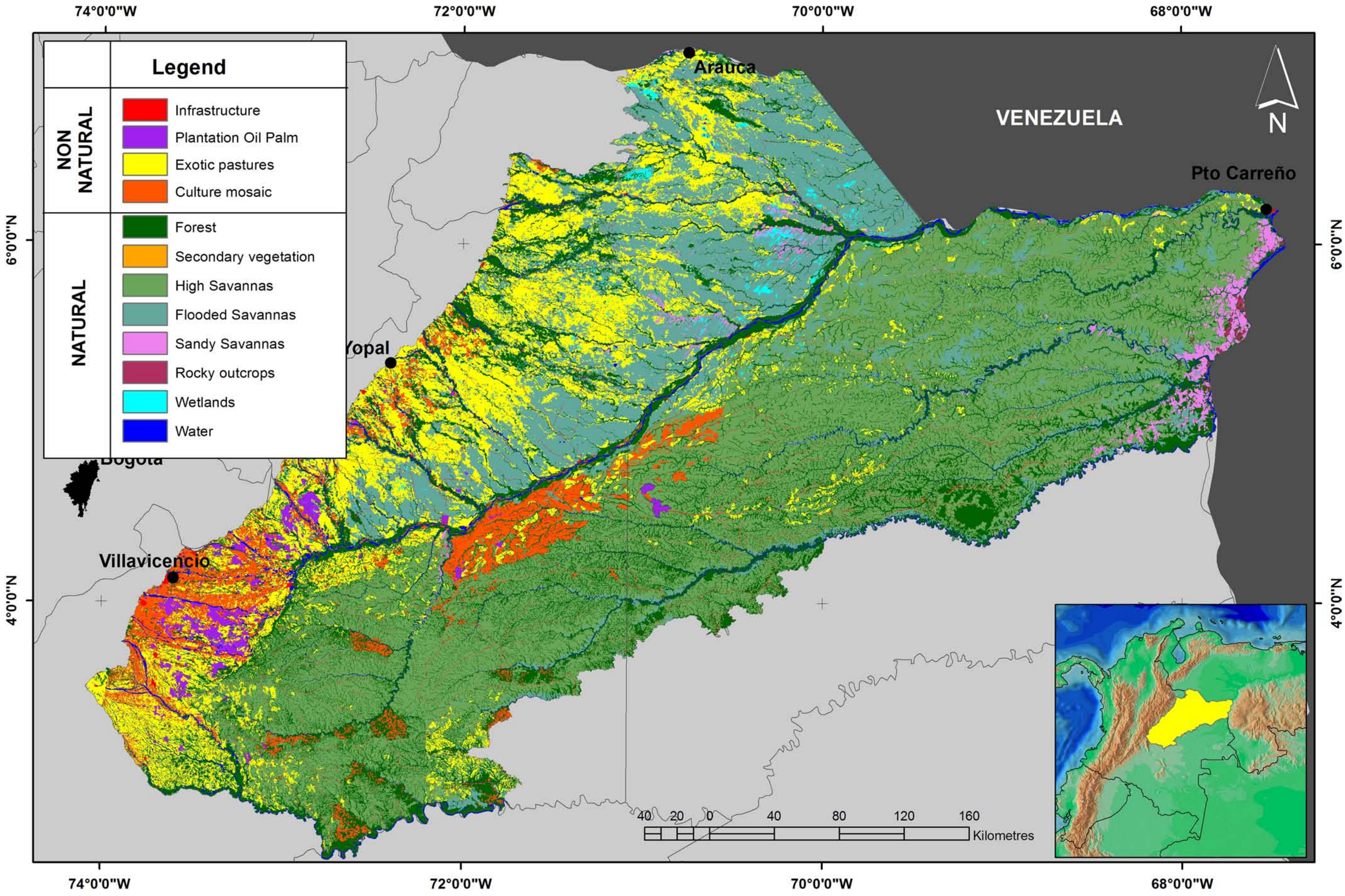

Figure 4.12. *LUC map for 2006-2007 of the ECS derived from supervised and unsupervised classification of CBERS and Landsat satellite data.*

Table 4.6. Area and percentage measurements of LUC for the three periods analysed.

Classes	1987-1988		2000-2001		2006-2007	
	Area (ha)	Area (%)	Area (ha)	Area (%)	Area (ha)	Area (%)
Infrastructure	169,102	1.01	178,424	1.07	190,140	1.14
Plantation palm oil	12,418	0.07	74,828	0.45	163,997	0.98
Exotic pastures	766,819	4.59	2,081,961	12.46	2,615,405	15.66
Culture mosaic	346,727	2.08	749,286	4.49	728,446	4.36
Forest	3,142,437	18.81	3,145,484	18.83	3,126,731	18.72
Secondary vegetation	90,029	0.54	139,752	0.84	139,601	0.84
High savannas	5,940,770	35.56	5,687,751	34.05	5,228,467	31.30
Flooded savannas	4,886,846	29.25	3,521,270	21.08	3,070,314	18.38
Sandy savannas	213,383	1.28	213,373	1.28	198,037	1.19
Rocky outcrops	16,516	0.10	16,516	0.10	16,516	0.10
Wetlands	70,922	0.42	70,471	0.42	70,293	0.42
Water	369,715	2.21	369,715	2.21	369,715	2.00

For the period 2000-2001, 82% of the area is covered by natural classes, while non-natural classes cover eighteen percent. In term of natural classes, this region was predominantly covered by high savannas (34%), flooded savannas (21%) and forest (18.8%). Non-natural formations are constituted by exotic pastures (12.5%), culture mosaic (4.5%) and palm oil plantations (0.45%), which is located mainly towards the west of the ECS. 1.1% of the region is occupied by urban zones and roads (Table 4.6).

For the period 2006-2007, non-natural covers spread along the foothills border and flooded savannas cover 22% of the area. Exotic pastures cover 15.7% of the area, culture mosaic 4.4%, infrastructure 1.1% and plantations 1%. In terms of natural classes high savannas cover 31.3%, flooded savannas 18.4% and forest 18.7% (Table 4.6).

4.2.6. Classification accuracy

For the LUC map of 2000-2001 (which was the reference map for the classification of the images form other years), Kappa analysis showed 83.9%

accuracy, which is an acceptable standard for this type of classification maps (Meidinger 2003). Small polygons were well classified with an 81.2% accuracy and with a confidence interval between 77.7% and 84.6%. Medium polygons showed 87.5% accuracy with confidence interval between 84.7% and 90.3. Finally, large polygons showed 92.3% accuracy with confidence intervals between 89.7% and 94.9% (Table 4.7).

Table 4.7. Kappa index analysis showing a correctly classified, estimated error, confidence interval and Kappa index to evaluate the accuracy of LUC for 2000-2001.

Rank Class polygons	Correctly classified	Estimated error	Confidence interval		Kappa index
			Lower (5%)	Upper (95%)	
Small	81.2	3.5	77.7	84.6	77.6
Medium	87.5	2.8	84.7	90.3	84.2
Large	92.3	2.6	89.7	94.9	89.9

Accuracy estimates for the LUC classes were found between 68.6% and 92.6%. Rocky outcrops showed the highest accuracy compared to wetlands that showed the lowest accuracy. Classification accuracy of High savannas was on average 88.9%, followed by Anthropogenic 85.3%, Flooded savannas 84.7% and Sandy savannas (Table 4.8).

Table 4.8. Classification accuracy of different sizes of polygons samples for each class of LUC maps for 2000.

Classes	Small	Medium	Large
Forest	70.3	85.3	90.1
High savannas	79.1	90.5	97.3
Flooded savannas	77.3	82.9	94.1
Sandy savannas	79.8	81.2	94.3
Rocky outcrops	87.8	90.2	100
Anthropogenic*	80.1	94.3	81.3
Wetlands	65.5	69.6	70.83

** Include plantation palm oil, exotic pastures, culture mosaic and infraestructure*

4.2.7. Land Use/Cover Change (LUCC) 1987-2007

Figure 4.13 shows the LUCC map from 1987 to 2007. The annual rate of change from natural to non-natural during the analysed period of 1987 to 2007 was -0.85%. For the period of time comprising 1987 - 2000, the rate of change was -0.95% which decreased to -0.66% between the years 2000 and 2007.

Comparing the non-natural cover, palm oil plantations show a considerable expansion during these 20 years, with an annual rate of 12.9%. Exotic pastures, culture mosaic and infrastructure have increased by 6.18, 3.7 and 0.6 respectively. For the period between 2000 and 2007 urban zones and roads showed the highest rate of increase namely 0.9, which is nearly twice the rate found between 1987 and 2000. The rate of change for exotic pastures was 7.7 between 1987 and 2000 which decreased to 3.3 during the 2000-2007 period. Culture mosaic showed a negative growth for the period 2000-2007, namely -0.4 which is significantly different to period between 1987 and 2000 where a growth rate of 5.9 was found (Table 4.9).

Table 4.9. Area of change and annual rate of change matrix for each category of LUC, 1987 - 2007.

	Area of Change (ha)			Annual Rate of Change (%)		
Classes	**1987-2000**	**2000-2007**	**1987-2007**	**1987-2000**	**2000-2007**	**1987-2007**
Infrastructure	9,322	11,716	21,038	0.41	0.90	0.58
Plantation palm oil	62,410	89,169	151,579	13.81	11.20	12.90
Exotic pastures	1,315,142	533,444	1,848,586	7.68	3.25	6.13
Culture mosaic	402,559	-20,840	381,719	5.92	-0.40	3.71
Forest	-3,047	-15,706	-18,753	-0.01	-0.07	-0.03
Secondary vegetation	49,723	-151	49,572	3.38	-0.01	2.19
High savannas	-253,019	-459,284	-712,303	-0.33	-1.20	-0.63
Flooded savannas	-1,365,576	-450,956	-1,816,532	-2.52	-1.95	-2.32
Sandy savannas	-10	-15,336	-15,346	0.00	-1.06	-0.37
Rocky outcrops	0	0	0	0.00	0.00	0.00
Wetlands	-451	-178	-629	-0.05	-0.03	-0.04
Water	0	0	0	0.00	0.00	0.00

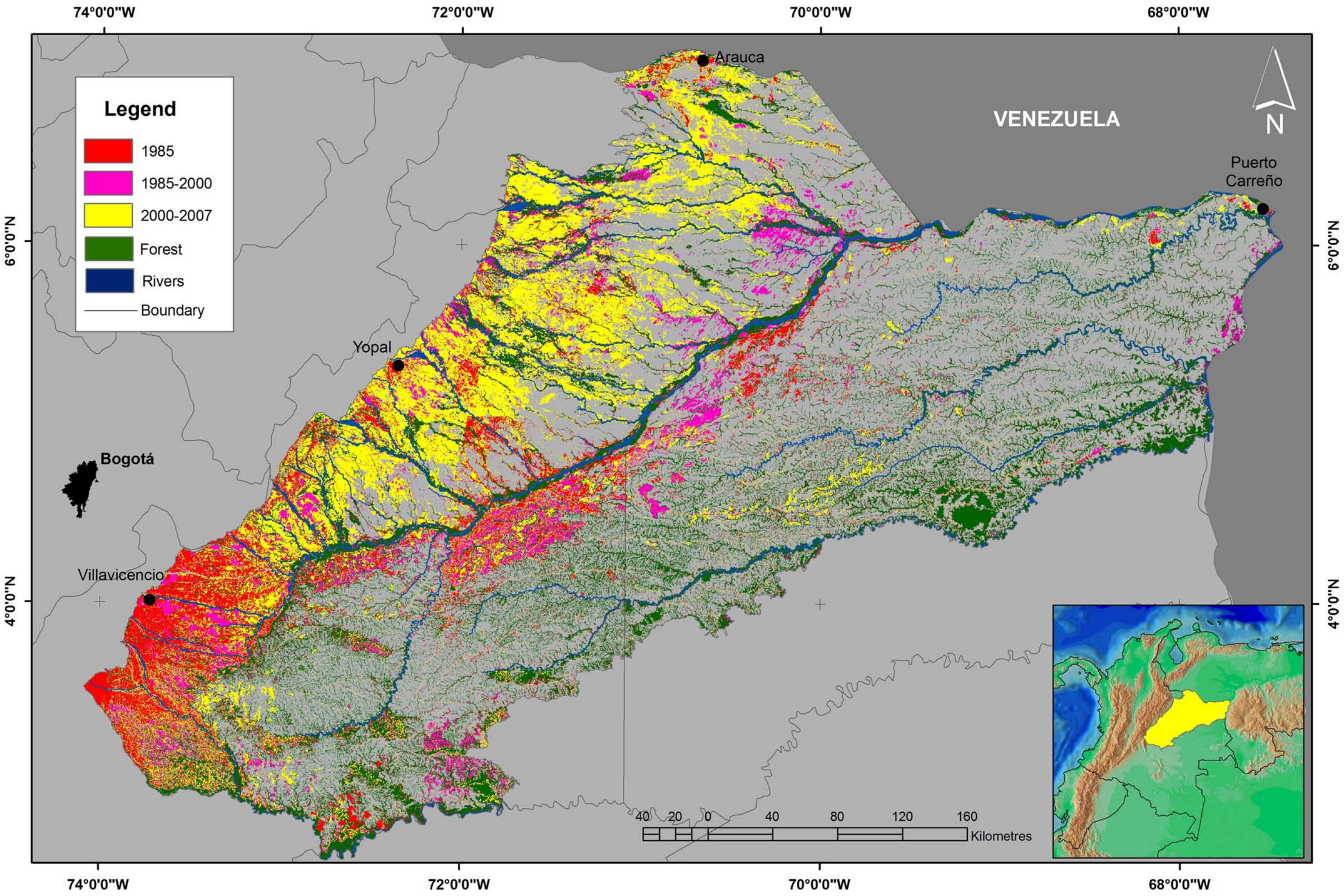

Figure 4.13. *LUCC map for ECS derived from supervised and unsupervised classification of Landsat and CBERS images from 1987 to 2007. Red: transformed area until 1987; orange: transformed area until 2000; yellow: transformed area until 2007.*

For the natural covers, only secondary vegetation showed a positive rate of change 2.2; the rest of the covers showed decreasing rates oscillating between -0.03 for forest and -2.32 for flooded savannas. The annual rate change for high savannas was -0.3 during 1987-2000 and increased to 1.2 during 2000-2007. Flooded savannas showed a rate of -2.5% for 1987-2000 which decreases to -2.0 during 2000-2007. Sandy savannas began to show an increase during the period 2000-2007 by -1.1. On the other hand, forests show rates of -0.01 between 1987 and 2000 which increased to -0.07 during 2000-2007. Finally, Rocky outcrops and Water bodies showed a stable situation through time as no changes were observed at this scale of analysis.

Furthermore, the first-order Markov chains for 1987-2000 and 2000-2007 were calculated. Tables 4.11 and 4.12 showed the transitional probabilities for both periods. During 1987-2000, Forest, Secondary vegetation and Sandy savanna were the most stable categories at 0.99, 0.98 and 0.97 respectively. The most dynamic category was Flooded savannas, with a relatively low stability probability at 0.65, changing principally to anthropogenic areas. High savannas were the second category with the highest change rate with 0.82. Rocky outcrops and water did not show any changes (Table 4.10).

Table 4.10. Expected values of LUC transitional probabilities under Markov hypothesis, 1987-2000.

Classes	Secondary vegetation	Forest	Anthropo-genic*	High savannas	Flooded savannas	Sandy savannas
Secondary vegetation	0.98	0.00	0.02	0.00	0.00	0.00
Forest	0.00	0.99	0.01	0.00	0.00	0.00
Anthropogenic*	0.00	0.00	1.00	0.00	0.00	0.00
High savannas	0.00	0.00	0.17	0.83	0.00	0.00
Flooded savannas	0.00	0.00	0.35	0.00	0.65	0.00
Sandy savannas	0.00	0.00	0.00	0.02	0.01	0.97

** Includes infrastructure, exotic pastures, culture mosaic and palm oil plantations.*

Similar results were found for the period between 2000 and 2007 (Table 4.11). High savannas and Flooded savannas have the highest probability of change by palm oil plantations, [0.27] and [0.14] respectively.

Table 4.11. Expected values of LUC transitional probabilities under Markov hypothesis. 2000-2007.

Classes	Secondary vegetation	Forest	Anthropo-genic*	High savannas	Flooded savannas	Sandy savannas
Secondary vegetation	0.95	0.00	0.05	0.00	0.00	0.00
Forest	0.00	0.98	0.02	0.00	0.00	0.00
Anthropogenic*	0.00	0.00	1.00	0.00	0.00	0.00
High savannas	0.00	0.00	0.15	0.85	0.00	0.01
Flooded savannas	0.00	0.00	0.32	0.00	0.68	0.00
Sandy savannas	0.00	0.00	0.01	0.01	0.01	0.92

** Includes infrastructure, exotic pastures, culture mosaic and palm oil plantations.*

4.3. Discussion

4.3.1. Remote sensing classification

For tropical regions, which are characterized by high spatial landscape complexity, satellite images provide good results for distinguishing LUC and LUCC. In the present study, an interpretation and classification of both Landsat and CBERS images was done to perform the first multi-temporal analysis for this region, during three different periods between 1987 and 2007. The obtained LUC maps show an accuracy of 83 % which is an accepted value according to Meidinger (2003).

In general, a series of straightforward processes have been used for the interpretation of satellite data that include preprocessing, processing and accuracy validation (Cihlar 2000; Lambin *et al.* 2003). During the process of interpretation of satellite image, the ancillary information associated to the taking of the image should be considered, such as platform movement, optical elements, altitude as well as those related to the shape of the Earth like curvature, topography and rotation. Areas where the topography is not flat must apply a more rigorous geometric correction. Thanks to the geographic location and the present topography in the ECS, the geometric correction that was made was minimal (nearest neighbour), not having the necessity to change the digital values of the image.

In the process of mapping LUC in ECS, it became clear that correct land cover classification was difficult due to the landscape's spatial heterogeneity, variable climatic conditions and discontinous satellite image acquisition. To try to avoid some of these problems satellite data of the dry season were classified; a large set of training pixels was incorporated, fieldwork verification was done and ancillary information supported by multi-source reference data including previous cartographic maps and aerial photography was used. In addition the combination between digital and manual interpretation - according to the Corine Land Cover methodology - provided a good method for constructing LUC maps, such as has been shown in the present study. Implementing this method is a suitable way of making use of its advantages and avoiding the limitations of each method separately.

Nevertheless, some difficulties were encountered, trying to separate some classes due to the spectrally mixed and depicted similarity of the CBERS and Landsat imagery. Exotic pastures were most prone to be confused with flooded savannas while high savannas classes caused confusion during classification and resulted in either an over/or underestimation of these classes. This difficulty, mingled with the hydrological regime of these savannas, lead to changes in the pixel reflectance values in the dry and wet seasons.

According to Sarmiento (1990) flooded savanna can present three different type of flooding dynamics: i. Permanently flooding (9 to 12 months); ii. Seasonally flooding (6 to 9 months) and; iii. Occasional flooding (3 to 6 months). In years when the wet season is prolonged even the high savannas could be flooded. To determine the differences between these savannas multi-temporal studies (dry and wet seasons) are required to see how the water availability behaves and how this affects this ecosystem. In this study this problem could be resolved to some extent by application of scattergrams followed by data from fieldwork and aerial photographs.

Furthermore, due to linear patterns of the distribution of gallery forests, which sometimes fail to reach the minimal pixel size of 30 m, separating this class was difficult although the NDVI index showed a good accuracy in extracting this category. Nevertheless to connect adjacent patches of this natural cover it was necessary to use a manual interpretation.

Considering the scale, the approach and the objectives undertaken in this study, the combination of indices, supervised and unsupervised classification, fieldwork and multi-source reference gave an adequate view of the distribution of ecosystems within the landscape, obtaining good results.

4.3.2. Land use-cover change trends

This study found that in the last 20 years in ECS, 22% of this area presents land use changes. The most stable natural classes correspond to rocky outcrops, wetlands and water bodies. Forest and sandy savannas showed minor changes in 1987 and 2000 but have decreased from 2000 to 2007. The most dynamic natural classes were flooded savanna and high savannas changing principally to anthropogenic areas including infrastructure, palm oil plantation, exotic pastures and culture mosaic. These changes were more frequently observed in the southwest region of the ECS near the Andean foothills area. All anthropogenic classes show an increment of area during 1987 to 2007; only the class of culture mosaic showed a minor decrease in area between 2000 and 2007 (around 20,000 ha). The most important transformation is related with the increment of palm oil plantations which shows an astonishing increase of area as the 12,418 ha in 1987 incremented to 163,997 ha in 2007, indicating an annual rate of change of 12.9%.

Up to the 1970s, ECS was of low socio-economic and political interest, and land cover transformation had been relatively slow for this period of time (Etter *et al.* 2006). As a consequence only few scientific studies are available which have tried to understand the dynamic of the present ecosystems (Correa *et al.* 2006).

During the 1980s, the ECS started to receive more attention as it was thought to be a potential area for social and economical development. In this decade several economic processes started to take advantage of these unexplored vast plains of savanna. A development boom in the foothills area of ECS was initiated with the search for petroleum and expansion of agricultural plantations such as rice and palm oil as can be seen in the results of this study. During this period, rice plantations started to dominate the landscape near the foothills of the ECS. However, the high cost of fertilization discouraged the rice plantation continuation in the southwest area of ECS and subsequently an abandonment of these areas occurred (Ocampo 2006). These areas started to be replaced by palm oil cultivations (in 1987 around 12,000 has), while rice started off more towards the north in the more favourable flooded savannas ecosystems (Corzo *et al.* 2009). The palm oil cultivation boom that followed (1987-2000: 13.8) was driven by the international demand for innovative energetic sources such as biodiesel and consumption.

In the last two decades, large areas of flooded (35%) and high savannas (17%) have been converted, mainly into plantations (palm oil and timber) and culture (rice, sorghum, peanut) (IGAC-CORPOICA 2002). In the ECS, this study found that the rate of change was -0.89% during the period 1987 to 2007 which equals 22% of the region. Compared with other Northern savannas in South America this rate of change is relatively low: in Venezuela an annual decrease of 2.3% was reported during the 1980s and 1990s with a transformation of 35% of this ecosystem (San José and Montes 2001). Brazil reports that 50% of the savannas have been lost up to the early 2000, which is equivalent to 70 million ha (Brannstrom *et al.* 2008).

Although the rate of change of ECS is relatively low it must be taken into account that the changes have occurred in a very concentrated zone of the region. Furthermore, due to the lack of any management plan combined with the political and economical instable situation of the country, it is considerably difficult to predict future tendencies. Nevertheless, no doubt arises that it will be

the most affected ecosystem in Colombia. The development boom occurred in a disorganized manner, without any control nor knowledge of the possible impact on the ecological functionality of the region. Future projects in the region include new alternatives for economical development (mineral exploitation, sorghum, sugar cane culture among others), in combination with palm oil expansion, increased petroleum exploitation, infrastructure development and subsequent population growth. Currently occupying 167,000 has, the ECS has 1,2 million ha for the establishment of palm oil cultivations (Corzo *et al.* 2009). Taking into account the many development projects which are planned for the future and the still unexplored potential areas for palm oil cultivations, the ECS are now one of the most threatened ecosystems in Colombia, with high probability of complete loss of its valuable biodiversity.

4.4. Summary

In the ECS, the LUC cover has been analysed for the 1987-2007 period, through the use of Landsat and CBERS high resolution satellite images. This tropical area showed a complex and heterogeneous landscape that can be discriminated thanks to the different spectral pattern responses of the surface objects in a satellite image. Although the use of satellite imagery is limited for depicting detailed information in terms of vegetation complexity (structure and composition), it allows to distinguish general land cover classes whose boundaries can be verified by detailed and intensive field work. Combining these supervised and unsupervised methods is a convenient way of making use of the advantages and avoiding the limitations of each method separately and to increase the classification accuracy which was an accepted value of 83%.

Between 1987 and 2007, the ECS has undergone dramatic changes. These transformations started during the 70s. In 1987, 8% of the area of the ECS had undergone some kind of change increasing to 22% in 2007, with an annual rate of -0.89. The driving forces of land use are basically associated with land

management and land development conducted by government policies. i) During the 1970s the necessity of increasing livestock production caused the change from natural to exotic pastures; ii) During 1980s and 1990s rice cultivations were established in the southwest area and later on in the northwest; iii) By the end of the 1990s plantations were expanded with palm oil cultivations and petroleum exploitation increased.

These transformations have been limited mainly to areas of the foothills where 80% of the population is located. The highest tendency of changes is found in flooded savannas, mainly caused by development of rice culture and petroleum exploitation. The savannas of the high plains towards the east have been identified as a potential area for expansion of palm plantations and sorghum, sugar cane cultures and are thought to be further exploited and affected in the future.

These results offer a detailed analysis and interpretation of LUCC in the study area, which provide a platform to help the scientific community and the decision-makers in identifying the mechanisms of cause-effect, establishing management plans and determining long-term priorities in the conservation of the ECS.

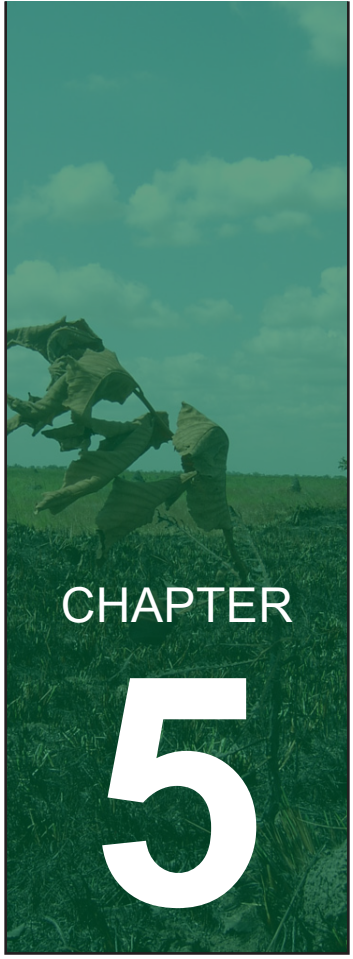

Recently burned scars in high savannas near of Santa Rosalia (Vichada, Colombia)

CHAPTER **5**

Fire Regime

As a part of a natural phenomenon in savannas, fires have to be monitored with the aim to understand the role in the dynamics of this ecosystem. Monitoring fire activity give us the way to determine how it affects ecosystems, contributes to the climate change, biodiversity loss, land degradation, increasing atmospheric CO_2 concentration, among others. Currently, remote sensing provides information from which fire activity data can be extracted efficiently and cheaply in order to monitor changes. In this chapter a regional algorithm is developed to extract burned scars and determine the burned area, frequency and severity, based on a spatial-temporal model for the dry season (2000-2009), using MODIS imagery.

5.1. Methodology

The applied methodology follows the procedures used for fire detection, which has been applied in other geographical areas (Eva and Lambin 2000; Mbon *et al.* 2000; Boschetti *et al.* 2004; Tansey *et al.* 2004a; Chuvieco *et al.* 2005; Laris 2005). A new regional algorithm to detect burned scars in Eastern Colombian Savannas (ECS) is developed and proved, and a set of statistical analysis is implemented with the aim to determine its accuracy and validity. In addition a comparison is presented between different fire global products available with the aim to validate the spatial and temporal results.

According to Chuvieco *et al*. (2005), three different methodologies have been developed for the detection of burned areas: (a) evaluation of new sensors, such as SPOT Vegetation, DMSP OLS and Terra Modis; (b) development or adaptation of methods for burned land discrimination, mainly interferometry, spectral unmixing, logistic regression and change detection analysis, and (c) spectral analysis of burned areas, with the use of algorithms for burned land discrimination. It was decided to apply the method of spectral analysis through an algorithm as this allows the improvement of global mapping of burned areas though the incorporating of regional algorithms (Tansey *et al*. 2004a). It is furthermore, the method that allows straightforward validation with different sensors of different resolutions thanks to the possibility of direct date implementation from the spectral responses of the different remote sensing products. Additionally, different algorithms are required to detect burned area from one ecosystem or climatic zone to another (e.g., boreal forest, tropical forest, grasslands) (Tansey *et al*. 2004), and as such a specific algorithms is developed in this study for the specific local conditions of the ECS.

The suitability of the remotely sensed date for spatial savanna studies depends on the resolution of the images. To create maps of burned areas in savannas, the combined use of high and low resolution images seems more appropriate that using either of the two (Maggi and Stropiana, 2002). The MODIS

algorithms take advantage of the spectral, temporal and structural changes using a change detection approach (Roy *et al*. 2005a). As there were uncertainties concerning the performance of the algorithms in nonvegetated regions the LUC map generated in this study was used as a reference for the different types of cover. These uncertainties were related to deficient observations of outcrop rocks, infrastructure and water bodies in medium resolution images (MODIS), while they can be detected in high resolution images (Landsat and CBERS).

The regional algorithm approach to global mapping will continue to yield several new methods for burned area mapping. The approach has also indicated how algorithms may be improved in the future by combining the best components of several regional algorithms. Intercomparison of products made with different satellite data and/or algorithms provides an indication of gross differences and, possibly, insights into the reasons for the differences (Roy *et al*. 2010).

5.1.1. Satellite data: Acquisition and conversion

The method for the acquisition and conversion of satellite data began with the search of the MODerate Resolution Imaging Spectro-radiometer (MODIS) Surface Reflectance product, at a 500 m spatial resolution in an 8-days period temporal resolution, gridded at a level 3 product (MOD09A1). Based on the spatial, spectral and temporal resolution, the best MODIS product was identified to allow the detection of burned scars at moderate resolution.

A MODIS Surface-Reflectance (MOD09A1) was derived from the MODIS product low level data 1 and 2. An algorithm was applied that identifies gases, aerosols and thin clouds, correcting for noise, scattering and absorption and allows estimation of spectral reflectance at a superficial level. Every pixel of MOD09A1, collection 5 contains the best possible L2G observation during a period of 8 days, which was selected based on high observation coverage, low view angle, the absence of clouds or cloud shadow and aerosol loading. Science data sets of MOD09A1, include information on the reflectance values for Bands

1-7 (Table 5.1), quality assessment, and the day of the year for the pixel along with solar, view and zenith angles (http://edcdaac.usgs.gov/modis/myd09a1v5.asp). Version 5 of MODIS/Terra is in validation phase 1, where its accuracy was estimated using field work in several locations and during a certain period of time (www.modis.com). Despite being in the first validation phase, the MODIS team claimed that this product is suited for scientific research.

Table 5.1. Band description of MODIS/TERRA Surface Reflectance image (MOD09A1), version 5.

Bands	Range nm		Uses
1	620 - 670	Red	Absolute land cover transformation, vegetation chlorophyll
2	841 - 876	NIR	Cloudamount, vegetation land cover transformation
3	459 - 479	Blue	Soil/vegetation differences
4	545 - 564	Green	Green vegetation
5	1230 - 1250	MIR	Leaf/canopy differences
6	1628 - 1652	SWIR	Snow/cloud differences
7	2105 - 2155		Cloud properties, land properties

MODIS09A1 was downloaded from the NASA Earth Observing System Data Gateway - EDG portal (http://wist.echo.nasa.gov/~wist/api/imswelcome/). This virtual platform provides an information search application for the Distributed Active Archive Center - DAACs of Earth Observation Center - EOS. When the required information was identified, the data was requested and made available for download by the MODIS team in FTP format.

Every image of MODis-Surface Reflectance (MOD09A1) includes two data files: hdf - ***H****ierarchical* ***D****ata* ***F****ormat*, which contains image information and xml - *E**x**tensible* ***M****arkup* ***L****anguage*, which contains metadata information. Table 5.2 shows an example of the name structure of these files.

Table 5.2. Example of name structure of a MODIS/TERRA Surface Reflectance image (MOD09A1), version 5.

MOD09A1.A2006337.h10v08.005.2008129102221.hdf	
MOD09A1	Product name (MODIS Terra Surface Reflectance Daily L3 Global 500 m)
A2006337	Acquisition year (2006) and Julian day (337)
h10v08	Tile ID
005	Collection 5
2008129102221:	Production year (2008), Julian day (129), and time (10:22:21)

The MODIS team divided the Earth in tiles of 10° x 10° degrees, covering an area of 1200 x 1200 km by each tile. This cover of the Earth uses the sinusoidal project system, which is defined as:

$$X = (\lambda - \lambda_0)\cos\phi\ ;\ Y = \phi \tag{5.1}$$

Where ϕ is latitude; λ is longitude and λ_0 is a central meridian. This projection allows the division of the Earth in north-south, and east-west at the same map scale. The equatorial parallel scale is uniform and is crossed in straight angles by meridians which allows an unchanged vertical scale along the equator at different longitudes. Due to the Earth curvature, it is necessary to reduce the distortion that is present towards the poles, which applies the interrupt version of a sinusoidal projection. The projection parameters are:

Radius of sphere = 6371007.181000 m
Longitude of C. Meridian = 0.0000000
False Easting = 0.00000 m
False Northing = 0.00000 m
Number of Latitudinal Zones = 21600.0000
Right Justify Columns Flag = 1.00000

To manipulate HDF-EOS (Hierarchical data format - Earth Observing System) it is necessary to transform it to a format which is compatible in GIS. For this purpose the MODIS team developed a MODIS Reprojection Tool -MRT. This

tool is designed to resample mosaics and change projections of MODIS satellite data. Detailed information is available in the user manual (http://edcdaac.usgs.gov/landdaac/tools/modis/info/MRT_Users_Manual.pdf).

For this study, the first step was to load a continuous image of the h10 and h11 tiles scenes. The metadata information was verified, with the purpose of extracting information concerning the project system, the image dimensions, bands numbers, vertices point (latitude/longitude), pixel dimensions and data classes. Subsequently, bands 1-7 were selected from which a subset image was created using the four vertices coordinates of the study area, that correspond to latitude between 7°00' and 2°00' N and -74°00' to -67°30' E longitude. Next, a resampling transformation with cubic convolution method was applied and the UTM - Zone 19, with datum WGS-84 was selected. Every band was stored as an independent file and a new name data with extension GEOTIFF was give.

These GEOTIFF files were processed by ERDAS-Image software, to merge the bands with the 'layer stack tools'. Finally, with the shape of the study area the image was cut or 'subset' to obtain the exact area of interest.

5.1.2. Preprocessing

Figure 5.1 shows the methodology for the preprocessing steps. This process began with the elaboration of a mask to eliminate covers which are not susceptible to fire, due to the absence of any vegetation formation (Figure 5.1a). Water bodies, rocky outcrops, infrastructure and bare areas such as sandy rivers were included in this mask cover. These areas were extracted from the LUC maps obtained from the Landsat and CBERS image interpretation (Figure 5.1b, c, d), as described previously in Chapter 4. This process was done with the subset tool of ERDAS-Image software. Subsequent, some images presented clouds and shadow contamination which can be observed in the 8 days composition and are necessary to remove. Different methodologies are being proposed for the MODIS product by using unsupervised classification or algorithms that combine

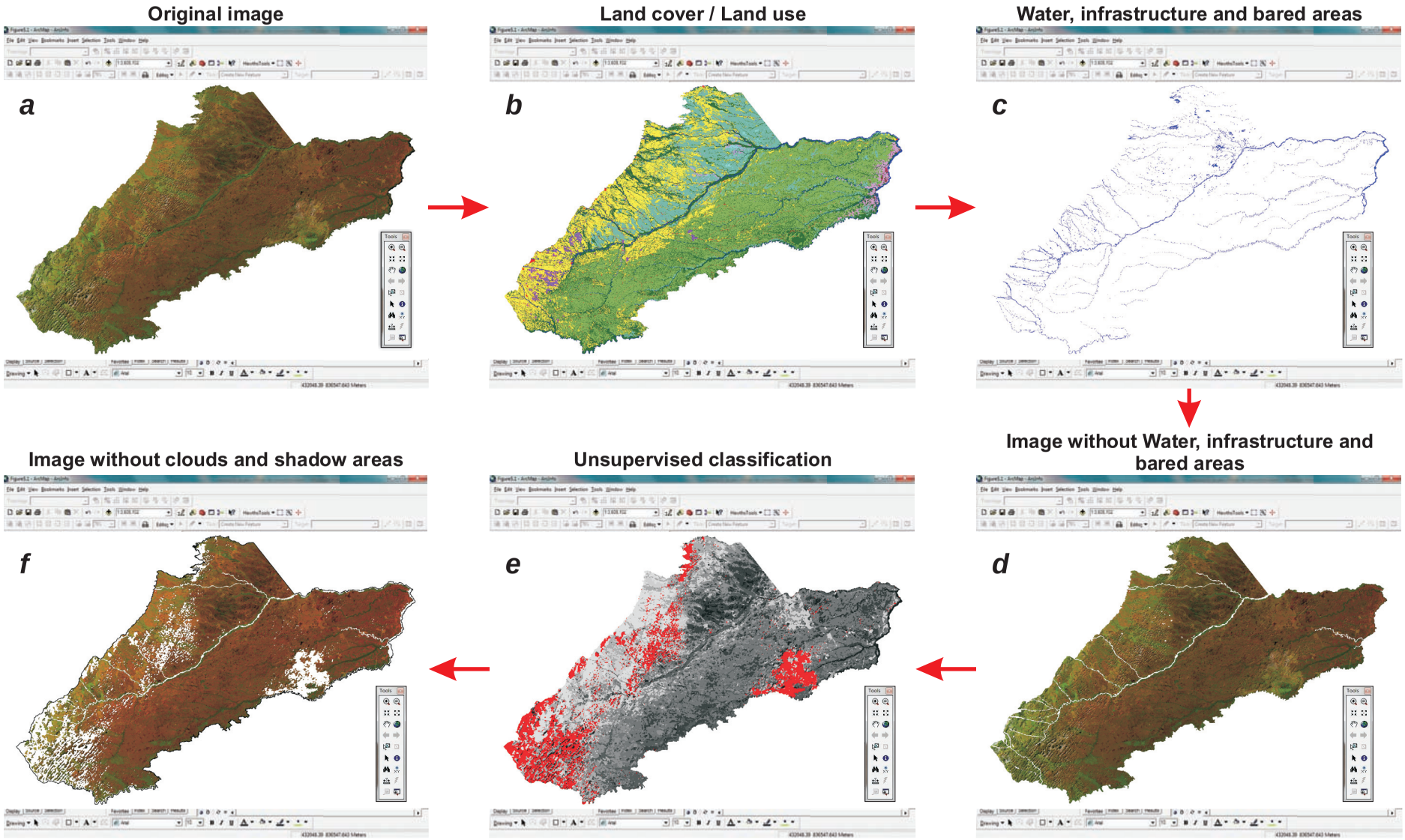

Figure 5.1. *Flowchart preprocessing steps for eliminate unburned, clouds and shadows areas of MODIS/TERRA. Surface Reflectance images (MOD09A1), version 5.*

techniques of visible and infrared spectrum with the purpose of differentiating clouds by their physical and radioactive properties (Chuvieco *et al.* 2004).

In this case, an unsupervised classification was used (Figure 5.1e). Every image was classified individually and the contaminated areas were extracted. With the aim to determine the percentage of clouds and shadows for each image, the total number of pixels was calculated that included clouds and shadows. Subsequently, all images were overlapped and the percentage of clouds and shadows was calculated for all periods and for Julian day of different years.

5.1.3. Savanna Fire Index Development

The SFI development started with the assessment of the accuracy of different vegetation indices for burned land mapping from MODIS data. Several authors have shown higher accuracies in the near-infrared and short wave infrared (NIR–SWIR) spectral domain for burned land discrimination such (Pereira 1999, Trigg and Flasse 2001) which are used by the Mid-InfraREd Bi Spectral Index MIRBI, (Trigg and Flasser, 2001) Burned Area Index BAI (Martin *et al*. 1999) and Normalized Burn Radio NBR (Hunt and Rock 1989). The Normalized Difference Vegetation Index which uses the red–near infrared band has also been applied in burn land mapping (Rouse *et al*. 1974) and therefore included in the assessment to define its accuracy.

The four mentioned indices have been validated at global and regional scales, in diverse vegetations formations and for different sensors (Chuvieco *et al*. 2005; Gómez and Martín 2008). Burned Area Index – BAI was developed by Martin *et al*. (1999) with the objective of separating burned and unburned areas in AVHRR images. The Normalized Burned Ratio - NBR (Hunt and Rock 1989) was developed to detect water content in vegetation, but Key and Benson (2002) applied it to evaluate burned areas. NDVI was developed by Rouse *et al*. (1974) with the purpose of detecting vegetation vigour and is currently applied

to extract burned areas. MIRBI is used to detect burned areas in savannas and other grasslands areas (Trigg and Flasser 2001) (Table 5.3).

Table 5.3. Vegetation and burned index evaluated in this study to detect burned scars. BAI: Burned Area Index; NBR: Normalized Burn Radio; NDVI: Normalized Difference Vegetation Index; MIRBI: Mid-InfraRed Bi-spectral Index.

BAI	NBR	NDVI	MIRBI
$\frac{1}{(\rho_{Cswir}-\rho_{swir})^2+(\rho_{Cnir}-\rho_{nir})^2}$	$\frac{\rho_{swir}-\rho_{nir}}{\rho_{nir}+\rho_{swir}}$	$\frac{\rho_{nir}-\rho_{r}}{\rho_{nir}+\rho_{r}}$	$10\rho_{SWIR}-9.8\rho_{LNIR}+2.0$

ρ_{Cnir} = near-infrared reference reflectance;
ρ_{nir} = near-infrared pixel reflectance;
ρ_{Cswir} = shortwave - infrared reference reflectance;
ρ_{swir} = shortwave - infrared pixel reflectance;
ρ_{Cnir} = 0.08
ρ_{Cswir} = 0.20.

(5.2-5.5)

To do the burned scars assessment, Modis Surface Reflectance product (MOD09) from the ECS in the dry season between 2000 and 2009 images were used. They correspond to an 8 day composition, 500 m of special resolution and 7 band spectral resolutions.

With the help of the obtained land use/cover maps of the ECS, pixels were selected from the MODIS images based on each of the LUC classes and the values of each band per class was extracted into a database. To these values the NDVI, BAI, MIRBI and NBI indices were applied and the results were compared for each of the different classes. Next, representative pixels from the burned areas were extracted from the MODIS images to which the same indices were applied. Based on this information the threshold was defined that allows the separation between burned areas and other LUC classes. After that the indices and the corresponding threshold values were applied to the Landsat images 4_56_2001_01_09 and MODIS image 2001_01_09 which resulted in burned area maps. As a result of this procedure it was observed through a visual revision that the NDVI and NBI indices presented high confusion mainly between burned areas and sandy savannas while the MIRBI overestimated the total of burned area. Therefore it was necessary to develop a new regional index that allows incorporating other bands to be able to separate recently burned areas from the other classes.

Through a trail – and - error process other bands were incorporated to assess the differences in precision to detect burned areas, using as principal bands the Near Infrared and Middle Infrared (NI-MIR) from images with a 8-days period difference. The time elapsed after the fire extinction is important for burned land discrimination, since the main spectral characteristics of burned areas change over short post-fire periods, from ash and charcoal during the first days/ weeks to vegetation reduction in the following months (Pereira *et al*. 1999). Given the temporality of fire events it was observed that some indices are too sensible in the detection of burned areas: old burned scars (older than 8 days) are detected by some indices several times causing an overestimation of burned areas for the analysed period. Equally some applied indices show a spectral response in which the areas of sandy, flooded savannas and burned scars are classified into the same category (ie. NDVI). Finally by incorporating the blue band, an increased accuracy was obtained in the separation of classes and a new index named Savanna Fire Index (SFI) was created.

To provide a high contrast between burned and unburned areas the SFI takes the sum of NIR and MIR bands. When a fire occurs, the leaf structure is modified which in turn is translated in changes of reflectance value of energy in the electromagnetic spectrum due to the vegetation pigmentation decline. Therefore, after a fire event, the charcoal deposited over the ground has very low reflectance in the visible and infrared portions of the electromagnetic spectrum (Eva and Lambin 1998; Chuvieco *et al*. 2005; Laris 2005). Making use of these changes, the NIR and MIR bands provide the necessary high contrast between burned and unburned areas. This contrast is maximized when the results are divided by the blue band, which increases the spectral distance between burned areas and other class covers (in particular those that have a potential of confusion, like sandy and flooded savannas):

$$SFI = \frac{\rho_{nir} + \rho_{mir}}{\rho_{blue}} \tag{5.6}$$

Where ρ_{nir} = Near-infrared pixel reflectance

ρ_{mir} = Middle-infrared pixel reflectance

ρ_{blue} = Blue-infrared pixel reflectance

5.1.4. Fire index comparative analysis

To evaluate the discrimination ability of these indices, a comparative analysis was done in which a methodology was adapted from Gomez and Martin, (2008). Initially, a set of MODIS and Landsat data of approximately the same date was chosen. Almost one thousand pixels were taken randomly from the Landsat data frame. Pixels over burned areas were extracted, taking Landsat data as a reference. Not-burned areas (Savannas, sandy savannas, culture mosaic and exotic pastures, forest and outcrops rocks), were excluded from the land cover map developed in this project (see chapter 4). Pixels containing confusion like clouds and shadow edges were eliminated. To discriminate between burned and unburned areas a threshold for each index was applied using a simple technique: Threshold determinations were based on the calculated mean (μ) and standard deviation (σ) of each MODIS data after the applied index. For all indices a mean threshold was obtained and revised. The threshold was adjusted for each index, according to the best maximum value of separation between burned and unburned areas. With the result of this analysis, the best algorithms to detect burned scars were chosen and applied to all MODIS data.

5.1.5. Burned area mapping validation

With the purpose of evaluating the over-estimation and under-estimation of the results, a comparison was made between the burned classification pixels obtained from every index applied in MODIS data and visual and automated mapping techniques for Landsat and CBERS data. To extract burned scars from Landsat and CBERS initially a supervised classification was applied, using the 4,5,3 band combination allowing the discrimination of 12 spectral classes including clouds and cloud-shadows for each image. Unburned areas were compared and

classified according to the LUC map developed in this project (chapter 4), while burned areas were classified in old and new burn scars. Next, a map of old and new burned areas was generated removing all pixels that were identified in a different category. A 3x3 filter was applied to remove the “salt and pepper” effect of automatic classification. After that, a visual classification was done to separate old and new burned areas, taking the darkest clusters as recent burn scars. Finally a new map of new burned areas was generated. A similar methodology was apply in savannas of Australia by Yates and Russell-Smith (2002).

All these products were spatially compared to a hexagonal tessellation of 5 x 5 km. The total burned scars area inside of every grid cell was divided by the overall of the grid cell area to obtain the percentage of burned scars in every cell. The accuracy of classified images was evaluated by a Kappa (κ) statistical method (see chapter 4).

5.1.6. Area, frequency and severity

To be able to quantify the fire dynamics in the dry season for all burned areas the area, the frequency and severity was defined for 8-days, monthly and yearly periods. A monthly and annual period analysis area was calculated at polygon level with map overlapping. Area was calculated as:

$$TBA_t = \sum_{j=1}^{n} a_j \tag{5.7}$$

Where

TBA = Total burned area in ha during time period t;

a = Burned surface (ha) fragment j during time period t;

n = Number of burned fragments j during time period t;

t = Time period (8-days, monthly, annual or the entire period of time).

Frequency was calculated at a pixel level, using a map overlapping grid per year and for the period of interest using:

$$BF_t = \sum_{t=i}^{j} BP_t / TP_t \quad (5.8)$$

Where

BF_t = Burned frequency in pixels during time period *t*;

BP = Burned pixels in period *t* between the time *i* and *j*;

TP = Total pixels in period *t* between the time *i* and *j*;

t = Time period (yearly, whole period)

Currently, the concept of severity has been widely discussed by various authors and new terminologies are being developed (Chuvieco *et al.* 2006; Key and Benson 2006; Lentile *et al.* 2006; Keeley 2009). Within all these approximations, the term 'burn severity' is used to avoid confusion with the direct impact of the combustion process which is related to the fire severity and its subsequent effects after extinguished (Chuvieco *et al.* 2007). In this case it is used referring to the loss of organic matter in or on the soil surface after burning without including ecosystem responses (Key and Benson 2006; Keeley 2009). The persistence of a burn scar in the same pixel detected by the threshold set, is calculated by the number of the consecutive period (every 8 days) until the scar is not detected anymore, multiplied by the total area of the scar where the pixel is located and related to the total area burned. Severity index formula was calculated as:

$$SI_t = \frac{BF_t * a_{jt}}{TBA_t} * 100 \quad (5.9)$$

Where

SI_t = Severity index in ha during period t;

BF = Burned persistence in pixel during period t;

a = Burned surface (ha) fragment j in a time

TBA = Total burned area in ha during period *t;*

t = Period time (total period of interest)

The results were categorised in five classes using a percentile statistic method: *very high, high, medium, low* and *very low* severity. Analysis was done for the entire period of time, 2000-2009.

5.1.7. Comparison between burned scars and active fires products

Three multi-annual burned area products (SFI, L3JRC, MOD045) and one multi-annual active fire product (MOD014) were generated and across the ECS compared for a period burning season across the ECS. The methodology consisted of a comparison of the burned area (L3JRC, MOD045) and active fires (MOD014) with burned scars obtained from the surface reflectance (MOD09A1) product. Figure 5.2 describes this process which was adapted from Roy *et al.* (2008). This process began with the search of MODerate-Resolution Imaging Spectro-radiometer (MODIS) - Burned Area product (MOD045) and active fires (MOD09A2 and MYD014A2). The MOD045 product has a 500 m spatial resolution, monthly temporal resolution and gridded level 3. A MOD045A1 was derived of the MODIS product low level data 1 and 2. Science Data Sets of MOD045 include the approximate Julian day of burning, confidence of detection, and other ancillary information. Collection 4 of MODIS/Terra is a ***provisional*** version, which is available for evaluation purposes. Furthermore, MODIS active fires (MOD14A2 and MYD14A2) are level 3 fire products, provided on a grid of 1 km containing the fire pixels detected in each grid cell at the time of satellite overpass over each daily period. The 8-days composite is the highest value of the individual level 2 pixel classes that falls into each 1 km grid cell over the entire 8-days period.

Burned areas and active fires information was downloaded from: https://wist.echo.nasa.gov/~wist/api/imswelcome/. The same process of acquisition and conversion was applied for the surface reflectance products (see Section 5.1).

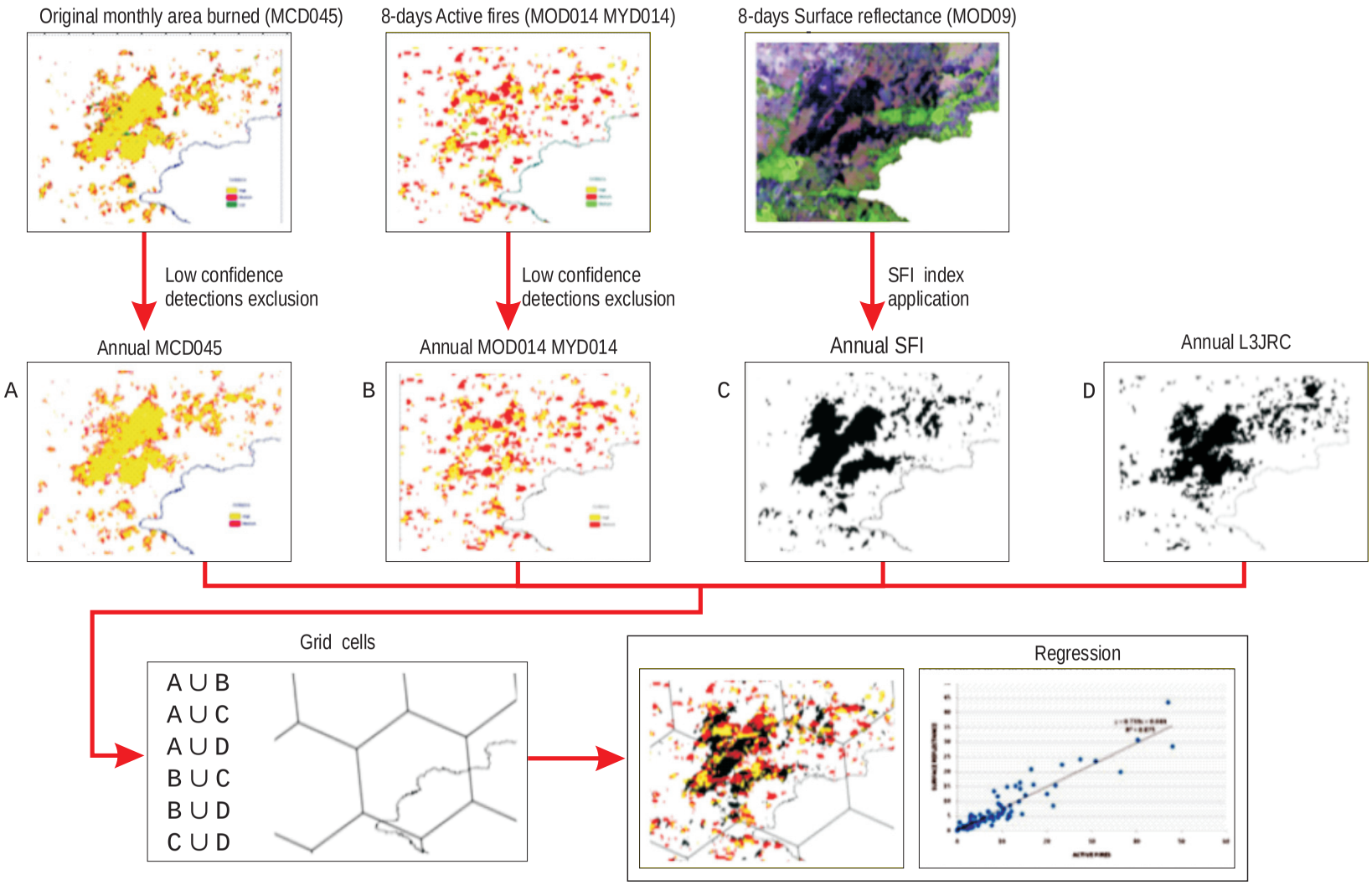

Figure 5.2. *Flowchart to compare MOD014, MOD045, L3JRC and SFI fire products derived from specific algorithms developed for extract burned areas and active fires using MODIS and SPOT-VEGETATION data.*

L3JRC annual product was generated from 1 km SPOT Vegetation data. Each grid cell contains burned or unburned information which is based on the difference in reflectance from the near infrared band between consecutive days. The burned pixel is flagged, when the index value is lower than the mean minus two times the standard deviation. Every pixel includes information on the Julian day of burning starting on the 1 April of every year. Possible commission errors generated by algorithms are corrected using land cover GLC2300 vegetation map, where non-burned surfaces are eliminated (Tansey *et al.* 2008).

Moreover, for the monthly MOD045 product (collection 5, 500 m resolution), two procedures were developed: i. Pixels with high and medium detection confidence were selected, excluding low confidence in order to reduce potential commission errors and; ii. Pixels from the overlap period between consecutive months were eliminated, to avoid double count of burned scars.

For the 8-days MODIS active fires product (1 km resolution) an intermediate product was generated, keeping original pixel information (confidence, clouds, water and non-classification). After that, extraction of pixels of high and medium detection confidence was done, in order to reduce commission errors. Finally, a 500 m resampling was applied and the monthly product generated.

With L3JRC, Julian days that correspond to the dry season were extracted and a new annual product was generated. With the 8-days MOD09A1, surface reflectance product (collection V at 500 m resolution) a monthly and annual product was produced after applying SFI index to extract burned scars.

To verify accuracy, all these products were spatial-temporal compared with respect to a hexagonal tessellation of 25 x 25 km and resampled to a 500 m resolution. The total burned scars area or active fires inside each grid cell were divided by the overall of the grid cell area to obtain the percentage of burned scars in every cell. Scatter plots were calculated between active fires and the burned scars products as well as between burned scars products. For each scatter plot

a lineal regression analysis was performed. In addition, confusion matrices were generated for every year, to obtain the percentage of correct classified pixels, and omission and commission errors of all global products with respect to the SFI regional index.

5.2. Results

A total of 175 MODIS surface reflectance (MOD09A1) images were obtained for seasonal dry periods between 2000 and 2009. Of the area, 3.2% is covered with unburned area surfaces such as water bodies, sandy beaches and infrastructure (roads and urban areas). Table 5.4 shows the percentages of clouds and cloud shadows of the different Julian days and years. Yellow indicates the maximum percentage of clouds and shadows coverage during that specific Julian period. Images containing more that 50% of clouds and shadows (red) were eliminated for analysis. On average, 11% of the study area was covered with clouds and shadows during the nine analysed years. The year 2002 was the year with the highest average of cloud and shadow coverage, namely 17.3%, followed by 2003 (16.4%) and 2000 (14.7%). In terms of Julian days between 81 and 105 (March 14 - April 14) the average cloud cover was between 21.4% and 32.1%, followed by the period between 329 and 337 (November 17 - December 2), periods which coincide with the beginning and end of the humid season. Between 345 and 73 (December 3 - March 13) the cloud average was between 0.8 and 16.6%, showing the lowest cover of clouds and shadows during the 33 Julian day period. Maximum percentages indicated 90% cloud coverage for 2000-97, 2002-73 and 2002-81 images, and 71% for 2007-89. Percentages ranged from a 40 to 50% for 2005-105(49.8%); 2003-329 (49.8%) and 2006-25 (44.8%) images. The rest presented a cover between 0 and 40%.

Figure 5.3 shows an example of cover percentage. MOD09A1_2001009 showed a 0% of clouds cover; MOD09A1_2008089 2.1%; MOD09A1_2006353 12.4% and MOD09A1_2070089 a 71%. MODIS images that presented more

Table 5.4. Percentages of clouds and cloud-shadows in every Surface Reflectance MODIS/TERRA (MOD09A1) data.

Julian Day	% Clouds and Shadows										
	2000	2001	2002	2003	2004	2005	2006	2007	2008	2009	Mean
1	0.00	0.57	0.10	0.00	14.86	3.43	2.00	0.00	0.00	7.52	2.85
9	0.00	0.00	0.10	1.00	0.10	4.04	1.00	2.93	10.31	7.67	2.72
17	0.00	0.57	0.20	0.00	1.40	0.00	2.73	11.32	0.00	1.84	1.81
25	0.00	0.57	24.84	3.22	0.10	0.00	44.78	0.00	0.00	0.00	7.35
33	0.00	0.57	4.20	13.91	0.00	19.61	1.00	0.00	0.20	0.00	3.95
41	0.00	0.57	0.10	0.00	0.00	2.66	1.00	0.00	2.56	1.95	0.88
49	0.00	0.00	0.10	1.00	18.44	0.10	3.03	0.00	10.15	0.00	3.28
57	21.60	0.00	7.04	4.03	2.74	10.94	12.32	0.00	1.00	0.00	5.97
65	3.69	1.00	0.10	3.23	0.10	0.00	5.02	0.00	0.00	1.22	1.44
73	0.56	4.09	90.00	23.95	0.00	1.00	3.76	14.97	11.08	13,63	16.60
81	70.23	3.21	90.00	32.11	25.49	1.00	26.40	33.67	10.95	28.19	32.13
89	25.90	2.91	35.09	17.92	17.51	19.72	0.00	71.00	2.09		21.35
97	90.00	9.47	20.36	43.65	6.68	51.52	2.98	4.40	16.26		27.26
105	15.82	0.56	36.96	35.05	27.71	49.80	31.49	46.44	10.39		28.25
329	20.04	15.99	19.69	44.06	4.30	0.20	17.00	0.10	22.35		15.97
337	29.80	26.25	0.00	21.37	16.86	11.67	14.19	1.00	1.20		13.59
345	0.31	36.19	0.00	28.77	2.92	1.00	2.43	9.30	0.00		8.99
353	0.57	28.94	0.10	28.23	3.91	8.56	12.24	30.24	9.85		13.63
361	0.57	0.10	0.00	9.50	0.00	0.00	2.20	0.00	0.00		1.37
Mean	14.69	6.92	17.31	16.37	7.53	9.75	9.77	11.86	5.70	4.84	11.02
Max	90.00	36.19	90.00	44.06	27.71	51.52	44.78	71.00	22.35	28.19	32.13
Min	0.00	0.00	0.00	0.00	0.00	0.00	0.00	0.00	0.00	0.00	0.88

Red: Maximum values of more than 50% of clouds and shadow coverage (Eliminated for analysis)

than 40% of clouds were treated by replacing the clouded areas with MODIS-Aqua image from the same day.

5.2.1. Processing

A total of 167 images were processed. Three MODIS images were tested to assess the accuracy of five indices for burned land mapping (01-01-2001, 09-01-2001, 13-03-2001, 25-01-2001, 09-01-2006, 01-25-2007, 02-02-2007 and 10-

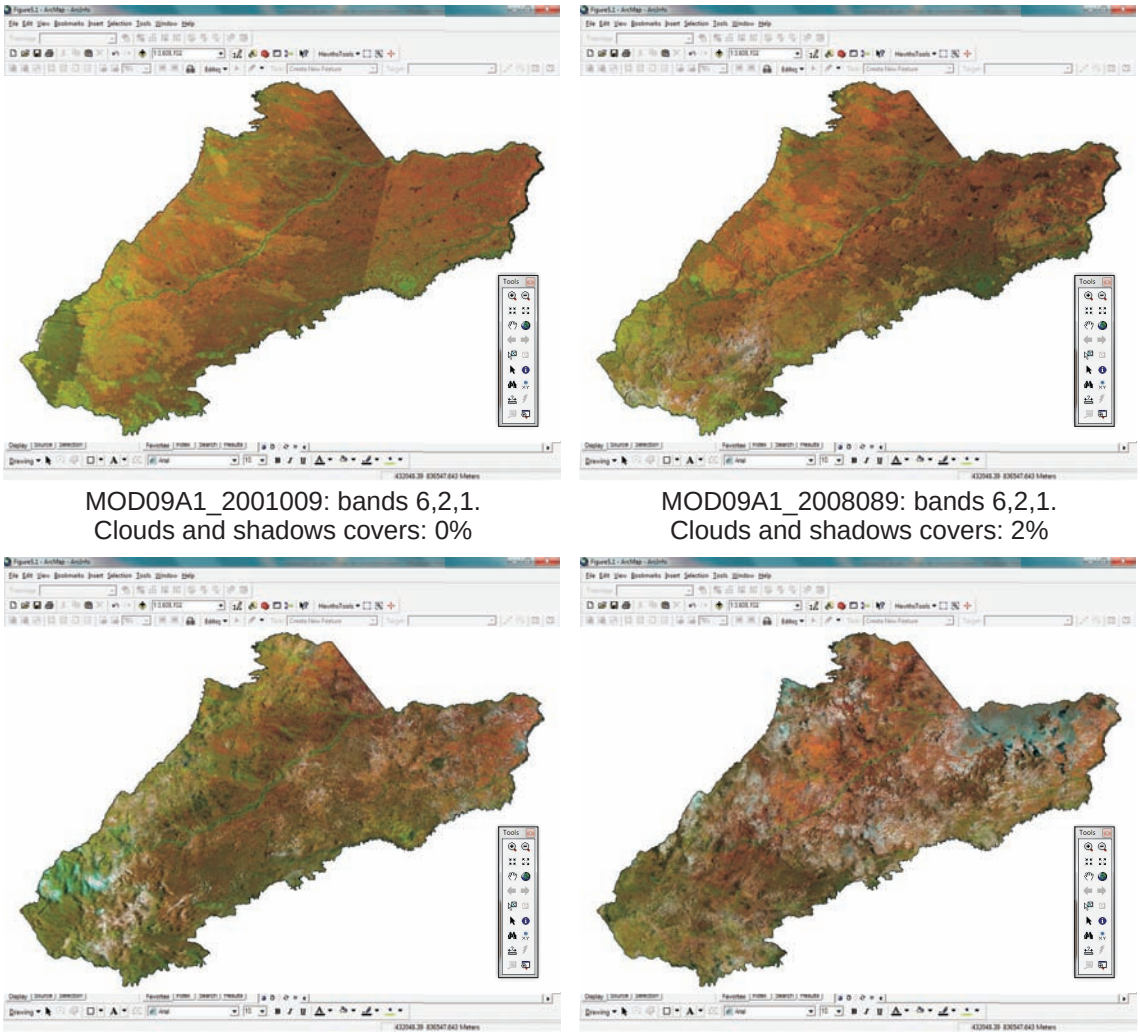

MOD09A1_2001009: bands 6,2,1.
Clouds and shadows covers: 0%

MOD09A1_2008089: bands 6,2,1.
Clouds and shadows covers: 2%

MOD09A1_2006353: bands 6,2,1.
Clouds and shadows covers: 10%

MOD09A1_2007089: bands 6,2,1.
Clouds and shadows covers: 65%

Figure 5.3. *Examples of different percentage cover of clouds and shadows in different MODIS/TERRA Surface Reflectance (MOD09A1) data.*

02-2007). They correspond to the Landsat data (456_2001-01-01, 456_2001-01-09, 457_2001-03-14, 556_2001-01-08 and 557_2001-02-01) and CBERS data (09-01-2006, 25-01-2007, 02-02-2007 and 10-02-2007) images that were taken the same date. Figure 5.4 shows a grey display of MIRBI, SFI, BAI, NBR and NDVI (left) and burned scar definition with different thresholds for index (right). MIRBI, SFI and BAI showed similar patterns for burned scars areas being MIRBI the index with high contrast. On the contrary, NBR and NDVI show high contrasts between forest and other categories, being higher in NBR. The later and NDVI show a high confusion between mainly burned scars areas and sandy savannas in the east area of the ECS.

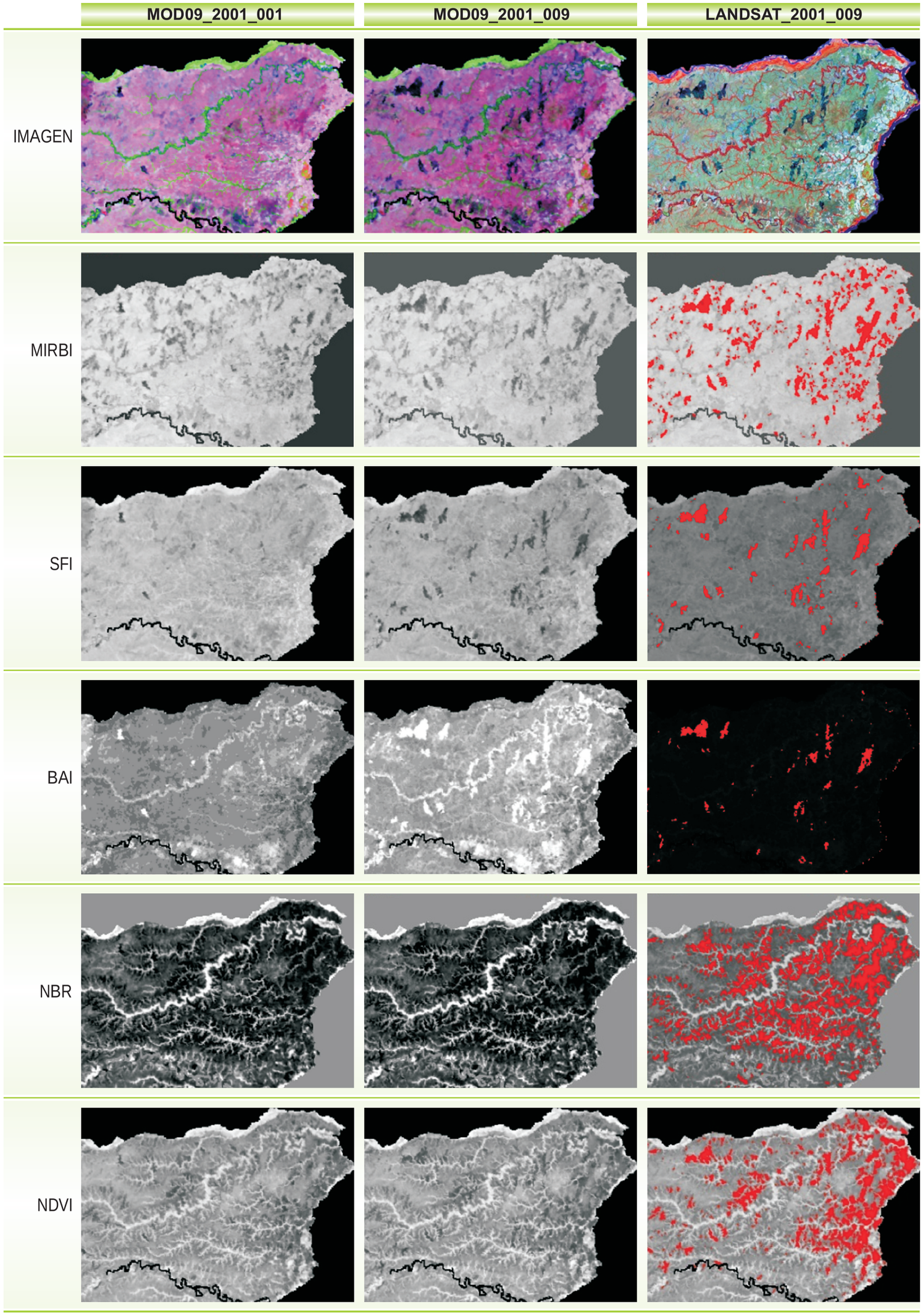

Figure 5.4. *MODIS/TERRA Surface Reflectance (MOD09A1) data tested of five indices (MIRBI, SIF, BAI, NBR and NDVI) for burned land mapping. Left images correspond MODIS 2001001; centre images correspond MODIS 2001009 and right images correspond burned scar definition with different thresholds for index.*

Table 5.5 show the omission and commission error, using mean values as a threshold, for the five analysed indices. Around 50% of the identified burned scars were detected by MIRBI, SFI and BAI; this value ascends to 60% in NBR and decreases to 21% in NDVI, leaving an overall omission of 50% in MIRBI, SFI and BAI, 40% in NBR and 79% in NDVI. In terms of commission, SFI and BAI do not introduce commission errors and MIRBI presents a low outcome in only one category. NBR has the highest value of success in burned areas, but in turn it also presents the highest value of categories confusion. The highest value of commission was produced by the NDVI index.

Table 5.5. Omission and commission error matrix, using mean values as a threshold for the five analysed indices (MIRBI, SFI, BAI, NBR and NDVI).

	Category	Mean				
		MIRBI	SFI	BAI	NBR	NVDI
Commission error	Burned Scar (true)	51.2	47.8	50.7	60.4	20.5
	Forest	0.0	0.0	0.0	0.0	0.0
	Savannas	0.3	0.0	0.0	18.2	0.0
	Sandy savannas	0.0	0.0	0.0	19.1	1.0
	Outcrops rocks	0.0	0.0	0.0	0.0	0.0
	Total commission	1			30	50

Starting with this fairly restrictive threshold, a series of less restrictive thresholds was applied afterwards. Adding and subtracting successive fractions of standard deviation value to the mean value resulted in a percentage similar to all indices, presenting a 90% of success rate (Table 5.6). However, with the NBR and NDVI index, the commission percentage remained very high despite continuous adjustments while the percentage of confusion among classes was minor. By MIRBI and NDVI, all pixels were defined as burned if their index value fell within the range $\mu+\delta/3$, for SFI $\mu+3/\delta$; BAI: $\mu+3\delta$ and NBR $\mu-2\delta$. All indices showed confusion between savannas and sandy savannas, with major differences among them. NBR and NDVI showed commissions errors between 10 and 21%, MIRBI 7.8% and BAI and SFI only 1%. Also, all indices presented confusion with outcrops rocks and SFI index showed some with forest category. MIRBI, SFI and BAI (in order of magnitude) showed highest values.

Table 5.6. Omission and commission error matrix, using different values as a threshold for the five analysed indices. By MIRBI and NDVI all pixels were defined as burned if their index value fell within the range $\mu + \delta/3$, for SFI $\mu+3/\delta$; BAI: $\mu+3\delta$ and NBR $\mu-2\delta$.

	Category	Mean				
		MIRBI	SFI	BAI	NBR	NVDI
Commission error	Burned Scar (true)	93.2	92.1	91.5	59.3	54.0
	Forest	0.0	0.1	0.0	0.0	0.0
	Savannas	7.8	0.3	0.8	17.4	10.0
	Sandy savannas	9.5	0.7	0.3	25.1	21.0
	Outcrops Rocks	0.0	0.0	0.0	0.0	0.0

In general terms, NBR and NDVI report the highest percentage of confusion between categories while MIRBI, SFI and BAI showed the lowest values. SFI and BAI index demonstrated higher success in defining burned areas and MIRBI showed medium outcome. In conclusion, it was shown that the SFI performed as the best index to extract burned areas, given the specific regional characteristics of the savannas.

5.2.2. Burned maps accuracy

The results of the accuracy comparison are shown in figure 5.5. Four Landsat images acquired in 2001 (456_01-09-2001, 457_14-03-2001, 556_08-01-2001 and 557_01-02-2001) and six CBERS images (183093 and 183094_09-02-2007, 185093 and 185094_01-09-2006, 185095 03-02-2007 and 187096_31-01-2007) were compared with the SFI product. In terms of temporal analysis, for images taken the same day, there is a generally high correspondence between fine and medium scale areas as shapes and areas for large and medium scars coincide. This correspondence diminishes when the images have been taken on different days (for example CBERS 183093_184094_09-02-2007 versus MODIS Surface Reflectance, 11-02-2007) where the sizes and shapes of the scars change. For small areas (<10 ha), the correspondence is medium, due to the course resolution of these data.

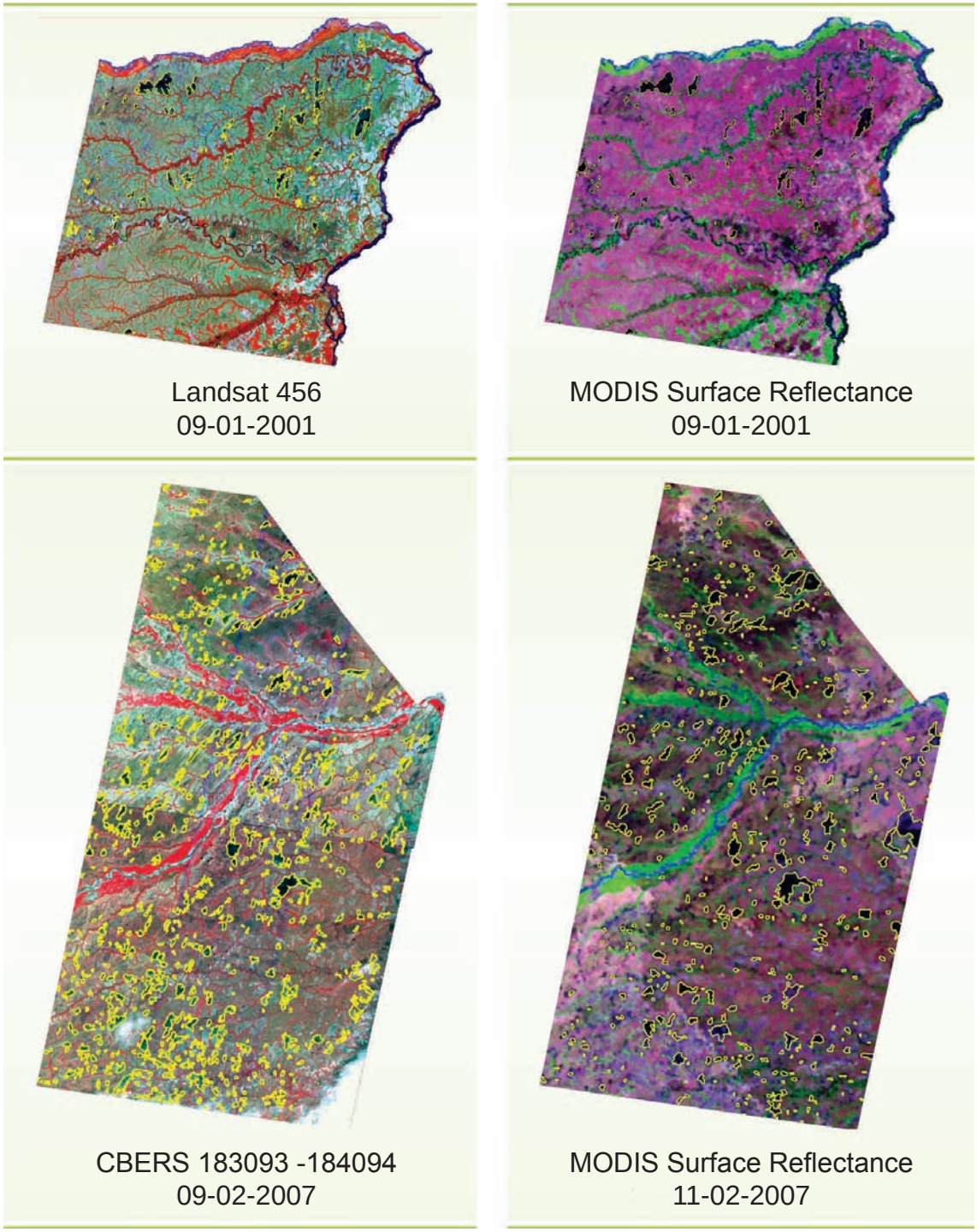

Figure 5.5. *Comparison between fine resolution data (Landsat 457_09-01_2001 and CBERS 183093_184094_09-02-2007) versus SFI product obtained from coarse resolution data (MODIS_09-01-2001 and 11-02-2007).*

In terms of spatial analysis, Landsat and CBERS show approximately the same burned area in comparison to MODIS data. High discrepancy was found between Landsat 557_02-02-2001 and MODIS_25-01-2001 (Table 5.7), due to difference of date. These differences are mainly found for small scar areas and mixes of burned and unburned areas that can be detected or distinguished by high resolution sensor.

Table 5.7. Percentage of burned area between Landsat and CBERS data versus MODIS Surface Reflectance (MOD09A1) data.

Landat	Modis	Area Burned (% Landsat)	Area Burned (%) MODIS
456_09-01-2001	09-01-2001	2.91	2.97
457_14-03-2001	13-03-2001	0.016	0.015
556_08-01-2001	01-01-2001	0.026	0.022
557_01-02-2001	25-01-2001	0.036	0.021
CBERS	**Modis**	**Area Burned (% Landsat)**	**Area Burned (%) MODIS**
183093_09-02-2007	10-02-2007	0.1	0.09
183094_09-02-2007	10-02-2007	0.1	0.09
185093_09-01-2006	09-01-2006	0.85	0.7
185094_09-01-2006	09-01-2006	0.85	0.7
185095_03-02-2007	02-02-2007	0.41	0.3
187096_31-01-2007	25-01-2007	0.17	0.11

The linear correlation between Landsat and CBERS products with MODIS data is highest, obtaining $R^2 = 0.86$ for Landsat and $R^2 = 0.875$ for CBERS. Kappa coefficients reached a value of 0.85 with Landsat data and 0.83 with CBERS data. In areas larger than 1,000 ha this value reached a value of 0.88, while it showed a decreased value for areas of less than 1,000 ha. This indicates good spatial assessment of burns, at least for medium to large sized fires (Figure. 5.6).

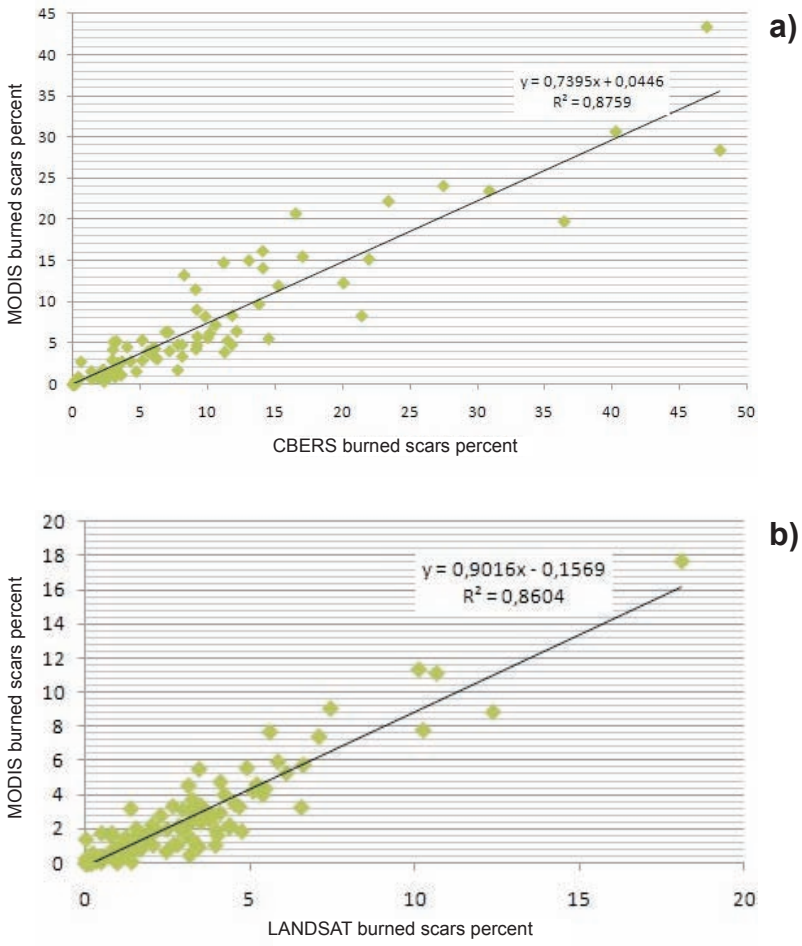

Figure 5.6. *Linear correlation of burned areas between fine and coarse resolution data.* ***a)*** *CBERS versus MODIS;* ***b)*** *Landsat versus MODIS*

5.2.3. Burned scars

5.2.3.1. Burned scars area

The overall burned areas in a dry period between 2000 and 2009 was obtained by applying the SFI index (Figure 5.7). Over 8.5 million ha were burned, which is equivalent to 50% of the ECS. In terms of cover, savannas formations were the most affected by fire activity. 55% of fires occurs in high savanna, and 22% in flooded savannas. Only 12% occurs in forest; 8% in transformed areas and between 0.5 and 1.5% occurs in sandy savannas and outcrops rocks formations. The results show that a small percentage (0.5%) of fires are located in infrastructure and water which is an error attributed to scale problems.

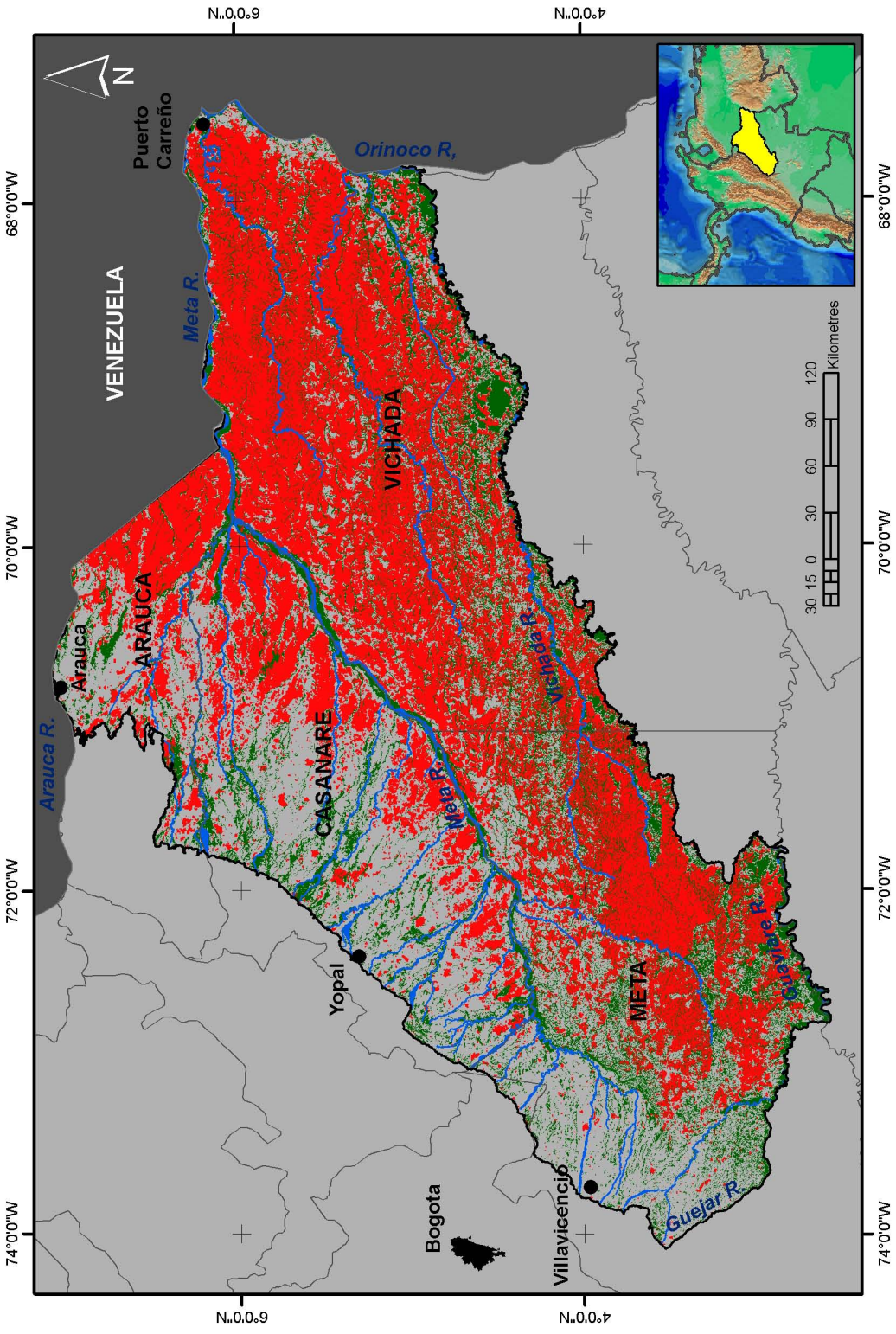

Figure 5.7. *Total burned areas during the dry period of 2000-2009 in ECS, derived from MODIS Surface Reflectance (MOD09A1) using SFI index.*

Annual burning patterns exhibit high variability. Figure 5.8 shows the total burned area for every year for ECS. The annual average of burned scars areas for the entire ECS is 2.95 +/- 0.5 million ha which corresponds to 18.2% of the area. During the dry season of 2000-2001, 3.3 million ha were identified as burned scars. This value decreased in 2001-2002 to 2.9 million ha. In 2002-2003, 3.6 million ha had fire activity reaching the maximum value of burned scars during the entire analysed period. Next, a slight decrease of burned area occurs in 2003-2004. This tendency continues until 2004-2005 where a strong diminishment can be seen which results to be the period of lowest fire activity between 2000 and 2009. After that, a sudden increase of burned area takes place in 2005-2006 and remains relatively constant until 2007-2008. Finally in 2008-2009 the total burned area decreases to around 900,000 ha.

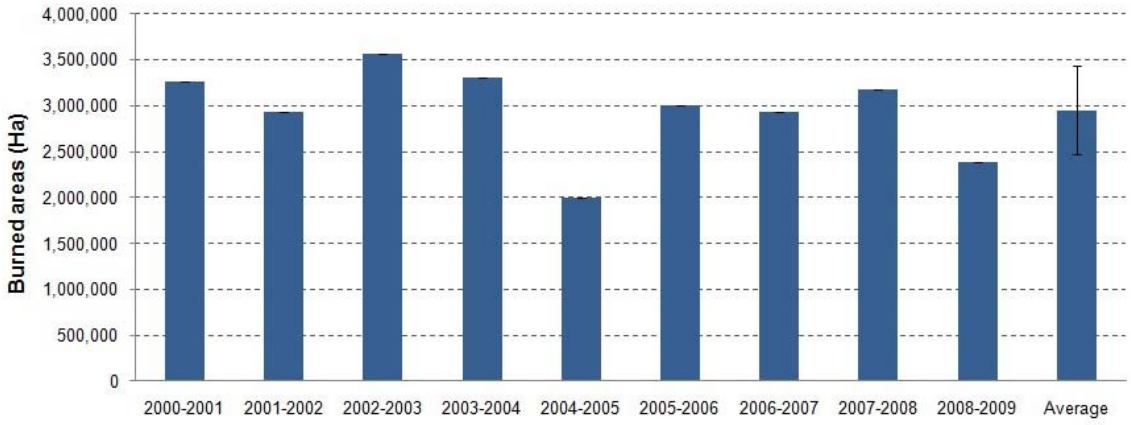

Figure 5.8. *Total and average burned area 2000-2009 in ECS, derived from MODIS Surface Reflectance (MOD09A1) using SFI index.*

Figure 5.9 shows a map of burned areas for each year between 2000 and 2009. In general, the west part located closer to the mountain range and savannas with high replacement by the introduction of exotic pastures, culture mosaic and palm oil plantations, presents a lower fire density. In contrast, the northeast and southwest part of the study area shows high recurrence of fires. An average, 85% of the burned scars took place in savannas formations, like the high, flooded and sandy savannas.

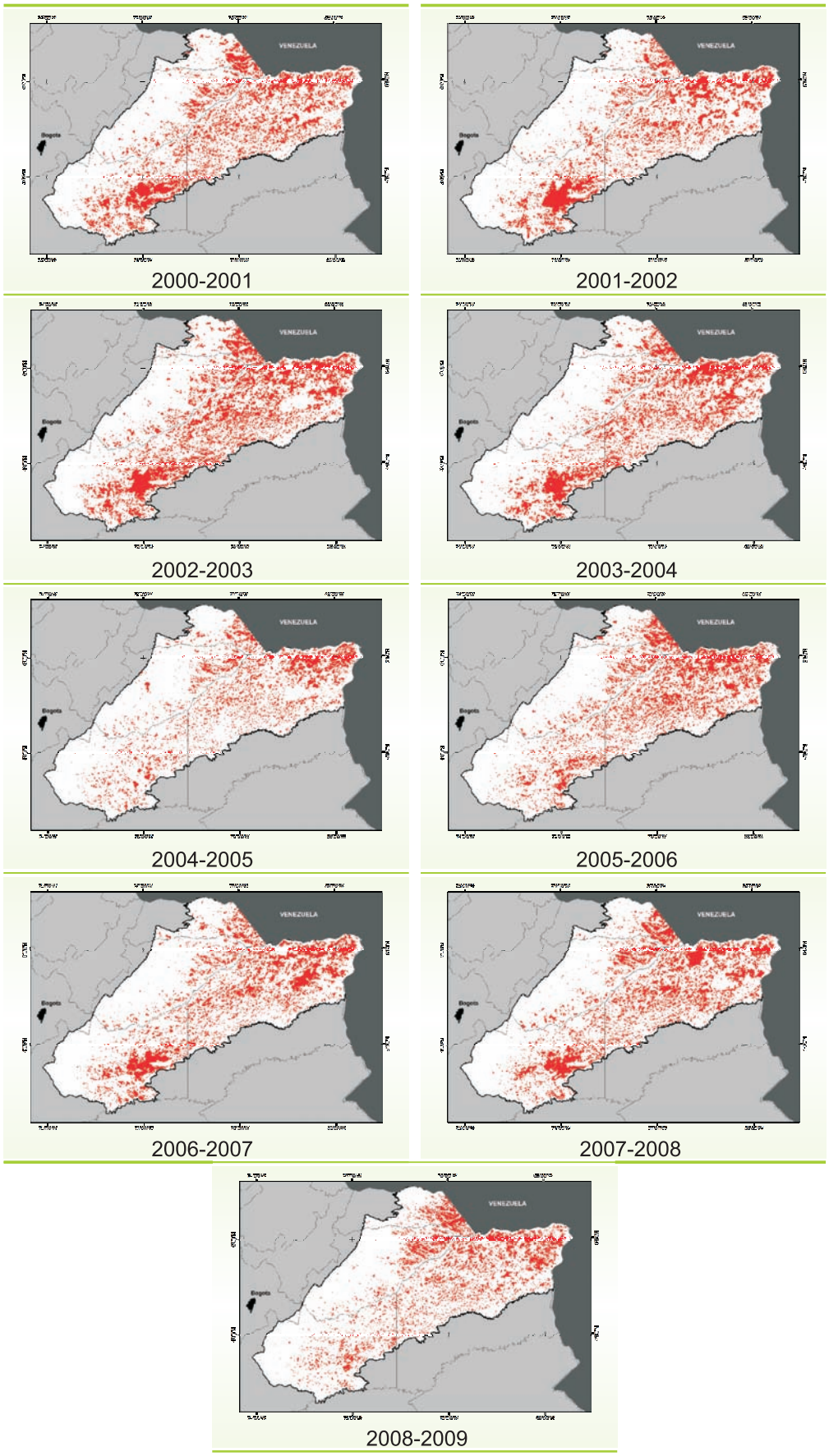

Figure 5.9. *Burned scar detection maps for each year between 2000 and 2009, derived from MODIS Surface Reflectance (MOD09A1) using SFI index.*

Furthermore, an important characteristic of fires and their impact concerns the spatial patterns of scars and the variability of their metrics. The mean size of burned scars is 556 ha with a variation coefficient of 180 ha. The largest area detected was 474,347 ha during 2001-2002 and the smallest area detectable at this level of resolution was 20 ha. Fire activity in 2008-2009 displayed a different behaviour with respect to the other analysed periods. During the mentioned period the number of polygons doubles, but the average size of every patch decreases abruptly; the maximum burned area of any polygon was 30,824 ha which is under the annual average (Table 5.8).

Table 5.8. Polygons number, maximum area (ha), means size (ha) and deviation of burned areas between 2000-2009, derived from MODIS Surface Reflectance (MOD09A1) using SFI index.

Year	Polygons	Maximum	Average	Deviations
2000-2001	5,976	416,069	546.74	6,624.83
2001-2002	5,006	474,347	586.52	7,804.09
2002-2003	4,819	418,682	804.57	7,559.03
2003-2004	4,633	377,031	711.81	8,297.88
2004-2005	5,510	178,133	361.53	3,221.81
2005-2006	5,750	275,238	524.11	4,502.25
2006-2007	4,598	328,785	637.95	6,557.98
2007-2008	5,079	295,370	624.75	5,679.97
2008-2009	11,200	30,824	205.37	596.39
Average	5,841	310,498	555.93	5,649.36
Deviation	2,067	137,689	180.38	2,495.59

Fire activity in the ECS is highly concentrated in the dry season that span the months of December through March (329-105 Julian days) following a seasonal cycle. The fire activity began at the second week of November (329 Julian day) and gradually increased until reaching a clear peak at the end of February and first week of March (57 Julian day) (Figure 5.10). After that, activity progressively decreases until reaching the lowest value at the middle of April (105 Julian day). The average of burned scars per month is 869,967 ha, with 237 to 1,200 polygons, and means size of 417 ha. The biggest scars are observed between 19-02-2002 and 21-03-2002 covering 269,741 ha, which correspond to 10% of the total burned area during that specific period.

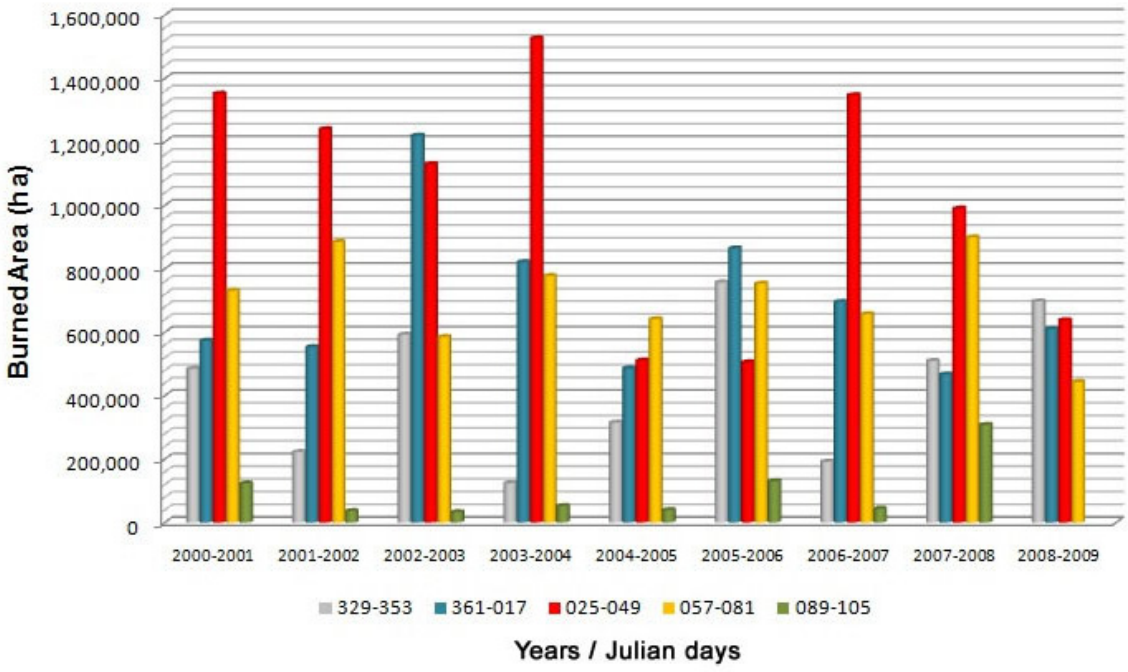

Figure 5.10. *Size average of burned areas per period of Julian days betwen 2000-2009.*

An 8-days analysis shows similarities to the monthly patterns. In average, 320,000 ha are burned every 8-days during the dry season. High fire activity took places between 9 and 65 Julian days, while between 81 and 105 the activity is low (Figure 5.11). The highest fire activity could be seen between 58 and 65 Julian days, followed by Julian days between 25 and 33. The lowest activity occurred at the end of the dry season between 97 to 105 Julian days. The maximum fire activity was observed from 3 to 10 of February 2004 where 1,270,023 ha was burned. Between 27-02-2002 and 07-03-2002 the largest area was burned forming a burn scar of 269,741 ha.

On average 49% of the burned scars has a size between 40 and 100 ha; 30% between 101 and 300, 11% between 300 and 700 ha, 5% between 700-1,400 ha, 2% between 1,400 and 2,500 ha and 1.6% greater than 2,501 ha (Figure 5.12). In terms of burned area, polygons with more than 2,500 ha represent more than 40% of the total burned area, while polygons of less than 300 ha correspond to 21.8% of the burned area. Burned scars between 301 and 2,500 embody the remaining 39.2%.

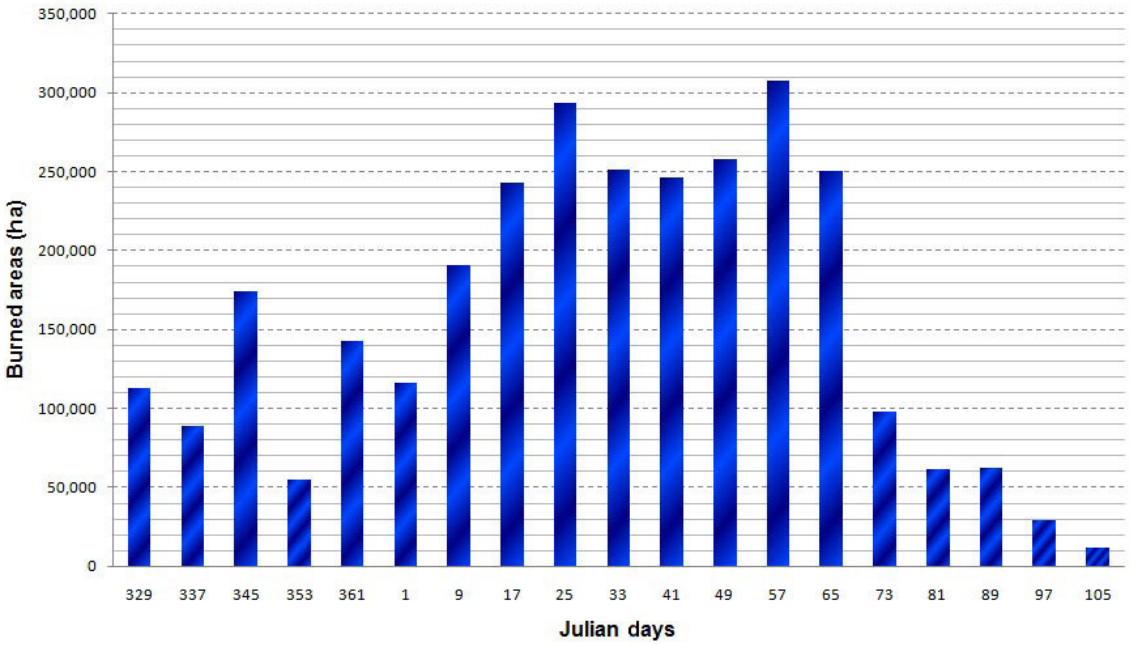

Figure 5.11. *Size average of burned areas per 8-days period of Julian days in the ECS between 2000-2009, derived from MODIS Surface Reflectance (MOD09A1) using SFI index.*

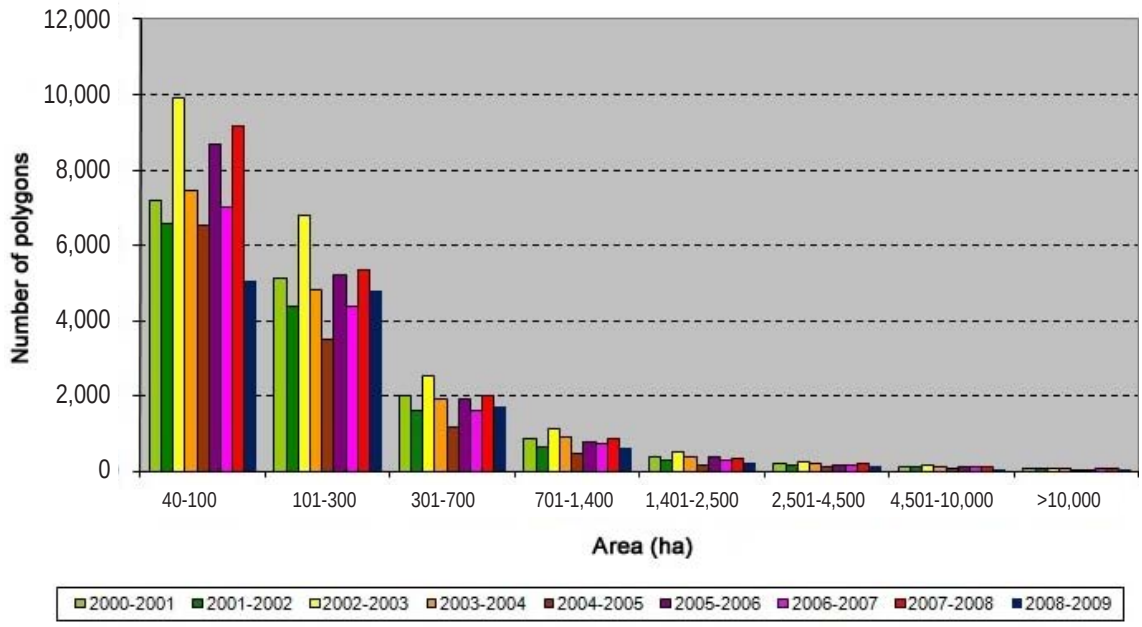

Figure 5.12. *Number of polygons per average burned area size between 2000-2009.*

5.2.3.2. Burned Frequency

The recurrence of fire in the ECS is shown in Figure 5.13. Some 3.7 million ha (33.5%) of savannas were never burned. 29% of the total burned area has only burned once; 19% twice, 15% three times, 12% four times, 10% five times,

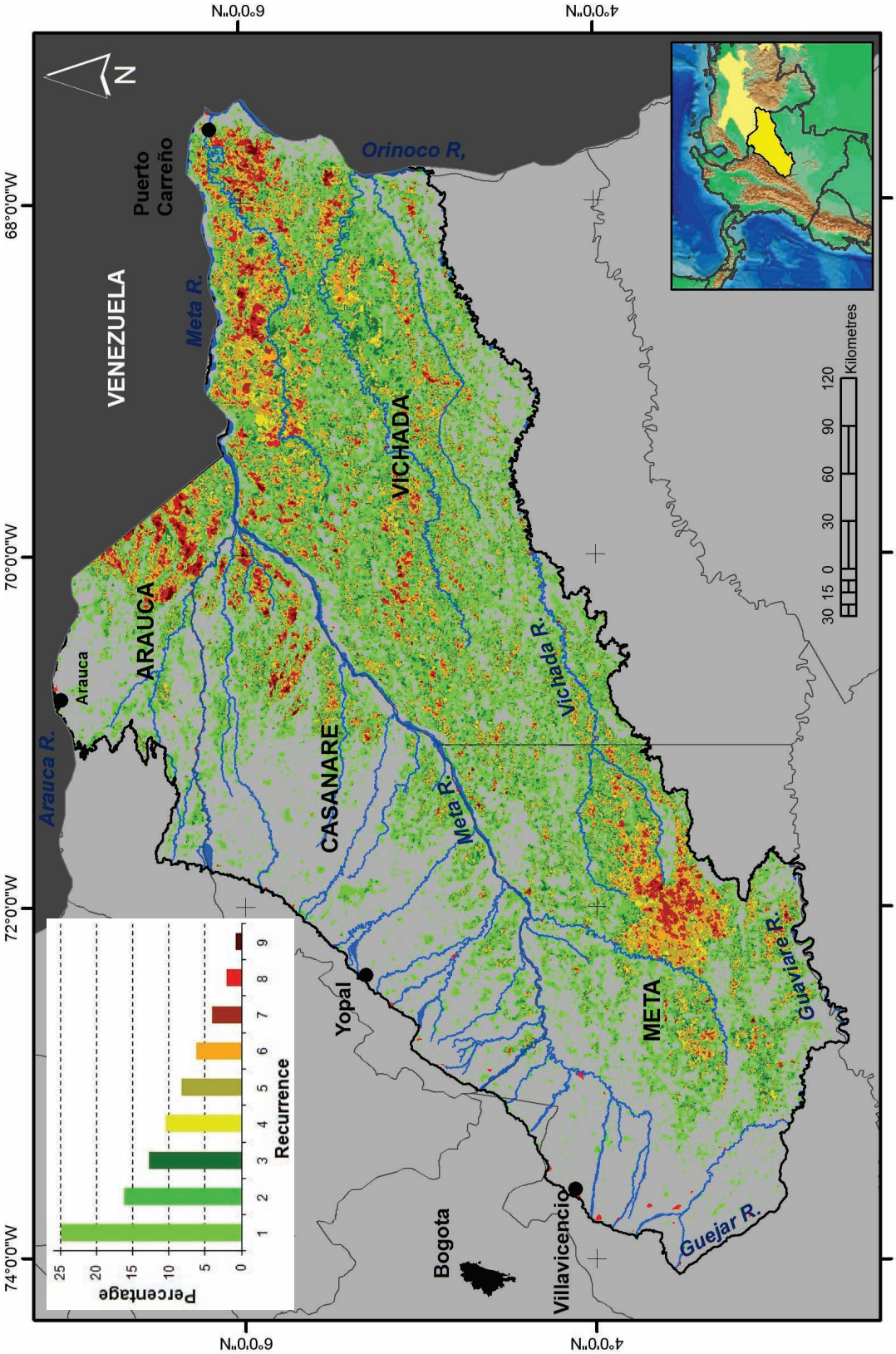

Figure 5.13. *Burned map recurrence between 2000 and 2009 derived from SFI Index applied in MODIS Surface Reflectance (MOD09A1) data.*

and 15% between 6 and 9 times. The areas of high recurrence correspond to the high savannas located in the northeastern sector along the Meta and Bita rivers in Vichada department, the southwestern sector, near to the Manacacias river in Meta department and the northern sector along the Arauca and Casanare rivers in Arauca department. Some isolated areas of flood savannas around dunes savannas in Casanare department, present high recurrence of fires while other areas closer to the mountain range and savannas with high replacement by pastures and plantations show much lower fire recurrence.

5.2.3.3. Burned Severity

Figure 5.14 shows the severity of the burned areas during the studied period. 1.5% of the areas show a very high severity, 4.1% high, 10.9% medium, 21.7% low and 61.8% very low. The greatest burn severity is found in the southwestern areas located in the headwaters of the Manacacias river; the northeastern interfluves of the Bita and Meta rivers and southwestern area between Casanare and Arauca interfluves. In contrast, the southeastern region and foothills present low to medium severity, where fires have a short duration, small size and low frequency.

5.2.4. Burned scars indices versus active fires and burned scars maps

Figure 5.15 shows a comparison between the four analysed products for the period 2003-2004. The red colour symbolizes the burned areas while white areas represent unburned areas. It can be observed that SFI and L3RJC burned area products showed similar patterns, in contrast to the MODIS product that presented a total absence of burned areas in the entire southwest and central part and only small burned areas in the north-eastern part, except during the years 2000-01, 2003-04 and 2006-07. With respect to active fires patterns, the MOD014 product shows a spread pattern throughout the ECS during the analysed years.

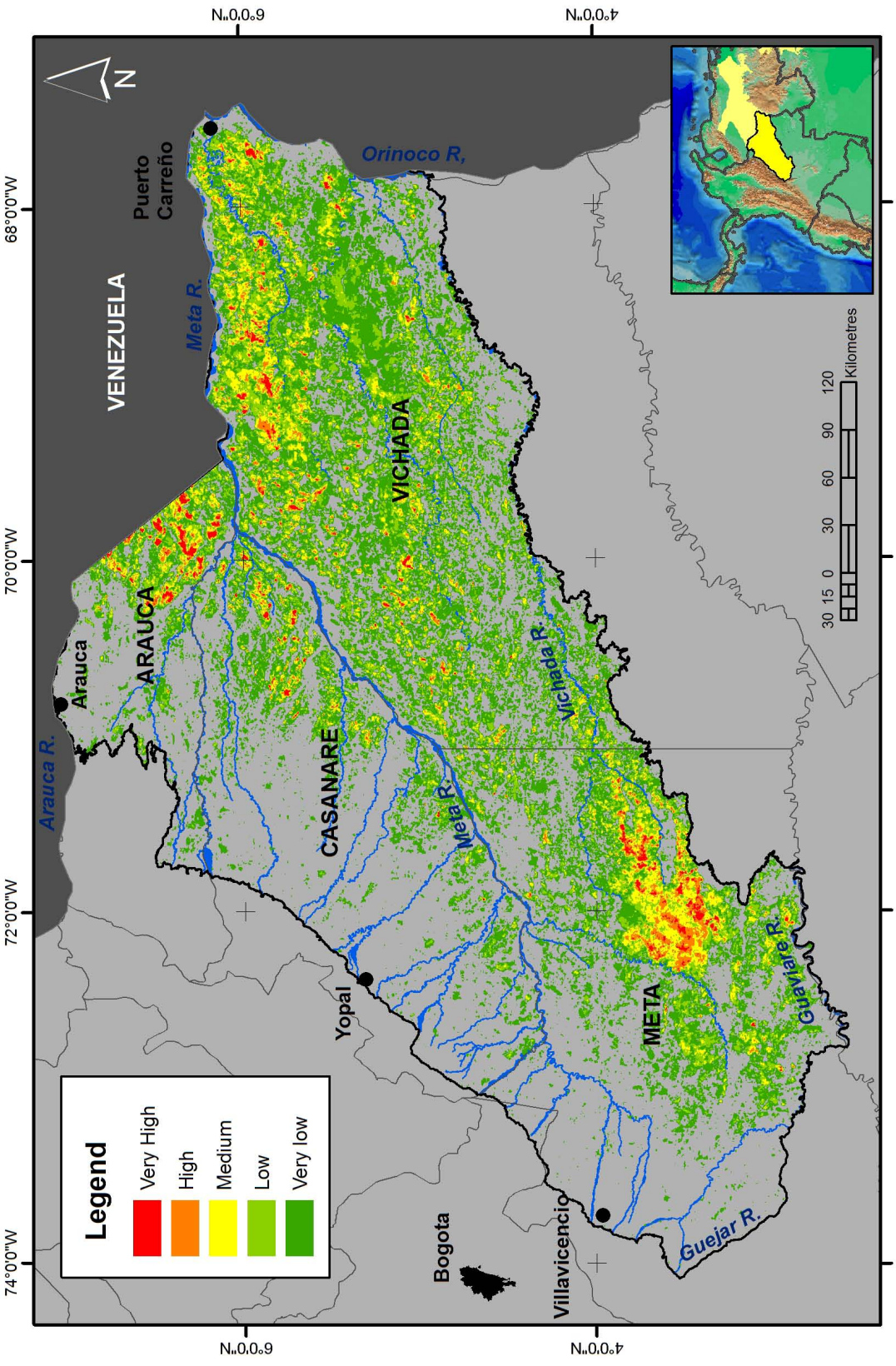

Figure 5.14. *Burned severity map between 2000 and 2009 derived from SFI Index applied to MODIS Surface Reflectance (MOD09A1) data.*

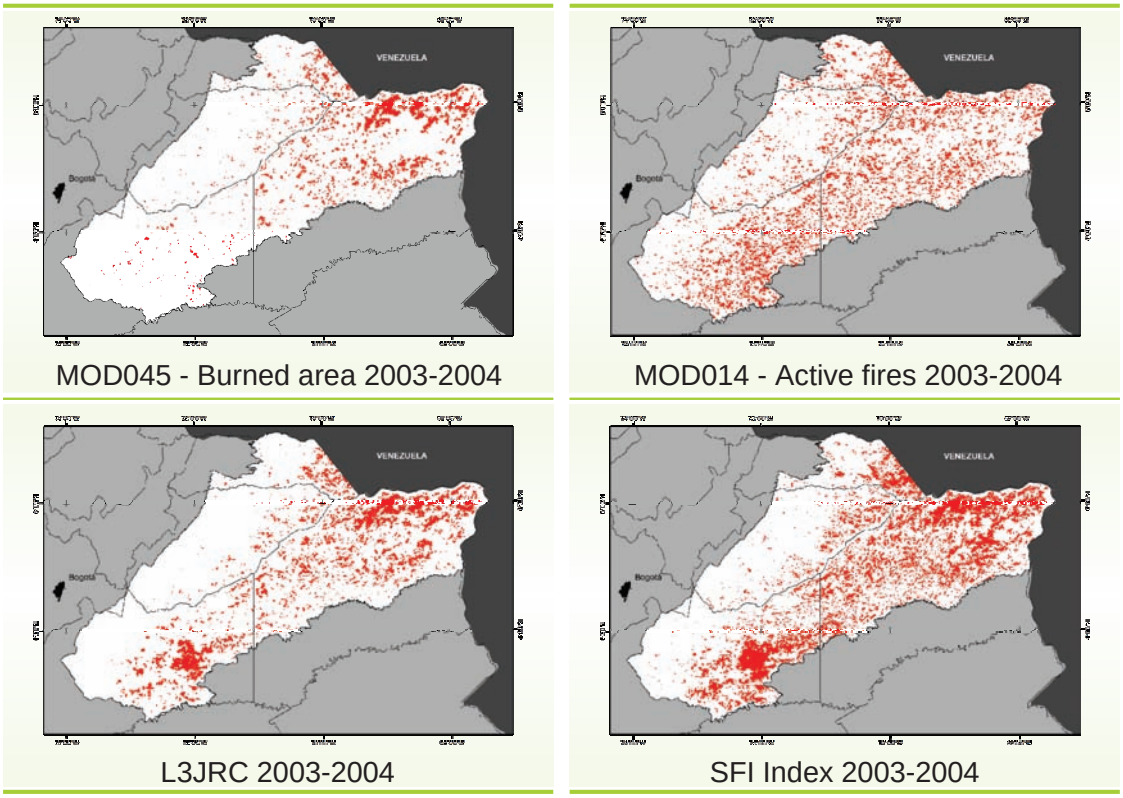

Figure 5.15. *Burned observed area comparison between MOD045, MOD014, L3JRC and SFI for the period 2003-2004. Red colour symbolizes the burned areas while white areas represent unburned areas.*

Figure 5.16 shows the total burned area for the four index results. The temporal analysis shows similar tendencies for different years between these indices but there exist significant differences in spatial terms and total area affected. The total burned area detected by MOD045 product is only 5% of the total area detected by the SFI index, except for the periods of 2000-2001, 2003-2004 and 2006-2007 where the average arises to 35%. L3JRC and MOD045 reach an average of 35% and MOD014 an average of 8%.

Table 5.9 summarises the spatial analysis using Pearson's correlation coefficients between the four products. Figure 5.17 shows the comparison between the four fire products. SFI product shows a weak correlation with MOD burned area product (R^2=0.29); moderate with MOD014 active fires (R^2=0.45) and moderately strong with L3RJC (R^2=0.74). L3RJC shows a moderate correlation with MOD burned areas (R^2=0.45) and performs weak with active fires (R^2=0.36). MOD014 active fires and MOD045 burned areas product shows the weakest correlation of all (R^2=0.28).

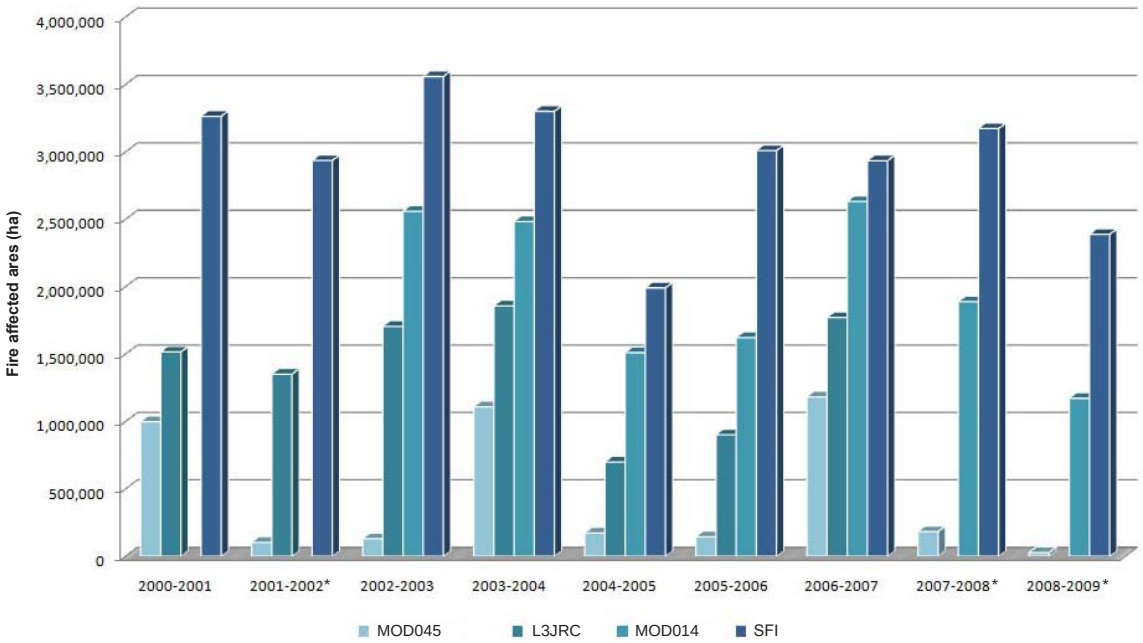

Figure 5.16. *Total burned area for MOD045, MOD014, L3JRC and SFI for the period between 2000 and 2009.*
** During the period of 2000-2002 no information was available of MOD014 and in 2007 to 2009 this was the case for L3JRC*

Table 5.9. Spatial analysis matrix using Pearson's correlation coefficients for comparing SFI, L3RJC, MOD045 and MOD014 products.

	SFI	L3RJC	MOD045	MOD014
SFI	1	0.742	0.292	0.454
L3RJC	0.742	1	0.455	0.361
MOD045	0.292	0.455	1	0.282
MOD014	0.454	0.361	0.282	1

Tables 5.10-5.12 summarize the accuracy of SFI, compared to L3JRC, MOD045 and MOD014 products. The percentages of the areas reported as burned by SFI and by the other indices are shown in the second and third columns. The fourth column shows the percentages correctly classified values. The fifth and sixth columns shows the commission and omission errors.

On average SFI reported twice as much area burned than L3RJC (table 5.10), and nearly three times for period of 2005-2006. The percentage correctly classified values in 2002-2003 is 77.3% and 89.1% in 2004-2005. The commission errors are low for the entire analysed period while all omission errors are greater than 0.5%.

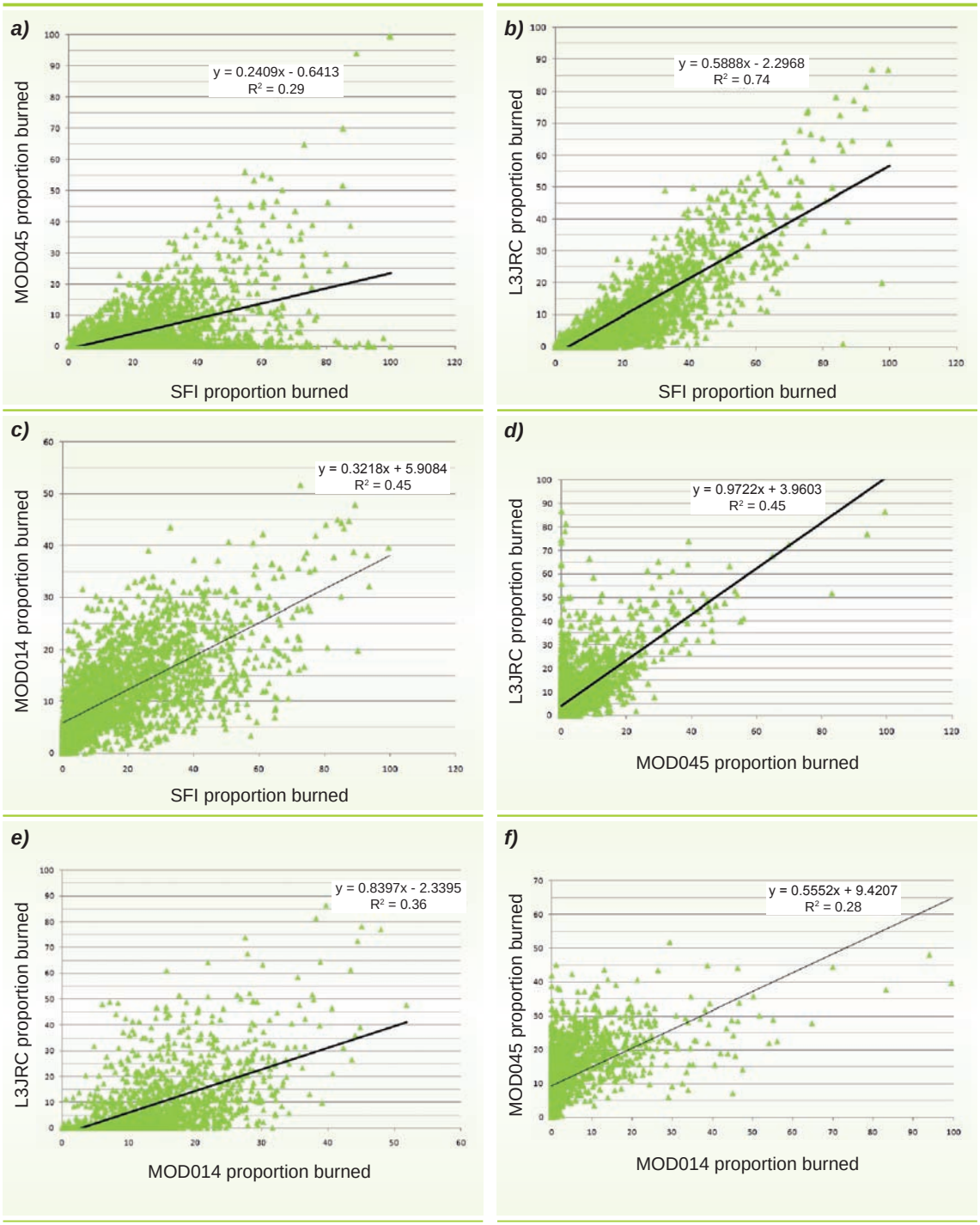

Figure 5.17. *Scatter plots: Comparison between the four fire products.*

Table 5.10. Commission and omission error validation between SIF and L3JRC product.

Period	SIF (%)	L3JRC (%)	Correct (%)	Commission Error	Omission Error
2000-2001	19.13	8.88	80.87	0.071	0.817
2001-2002	17.56	7.89	82.44	0.065	0.837
2002-2003	22.65	10.00	77.35	0.091	0.856
2003-2004	19.30	10.85	84.36	0.045	0.624
2004-2005	11.63	4.09	89.10	0.019	0.793
2005-2006	17.65	5.26	84.16	0.021	0.800
2006-2007	17.16	10.35	85.89	0.044	0.604

Otherwise, MOD045 detected less burned area in comparison to SFI (Table 5.11). The percentages correctly classified values are between 74.7% and 88.8%. Commission errors are low for the entire analysed period while omission errors are greater than 0.7%.

Table 5.11. Commission and omission error validation between SIF and MOD045 product.

Period	SIF (%)	MOD045 (%)	Correct (%)	Commission Error	Omission Error
2000-2001	19.13	5.84	83.84	0.037	0.700
2001-2002	17.56	0.61	82.73	0.002	0.975
2002-2003	22.65	8.91	81.40	0.023	0.741
2003-2004	19.30	6.50	82.64	0.028	0.782
2004-2005	11.63	1.00	88.80	0.003	0.939
2005-2006	17.65	0.85	82.73	0.003	0.965
2006-2007	17.16	6.94	85.01	0.029	0.735
2007-2008	18.57	1.08	74.70	0.003	0.968
2008-2009	13.46	0.16	86.54	0.001	0.996

Finally, MOD014 reported a smaller percentage of area burned with respect to the SFI product (Table 5.12). The percentages correctly classified values are between 78.7% and 84.6%. Commission errors for all of the periods are very low while omission errors are greater than 0.6%.

Table 5.12. Commission and omission error validation between SIF and MOD014 product.

Period	SIF (%)	MOD014 (%)	Correct (%)	Commission Error	Omission Error
2002-2003	22.65	69.50	76.56	0.101	0.688
2003-2004	19.30	72.28	78.33	0.104	0.686
2004-2005	11.63	82.06	84.58	0.100	0.715
2005-2006	17.65	76.41	79.95	0.072	0.799
2006-2007	17.16	73.09	78.72	0.136	0.634
2007-2008	18.57	74.95	79.59	0.080	0.750
2008-2009	13.46	81.86	84.01	0.054	0.840

5.3. Discussion

5.3.1. Remote sensing approach

Different methodologies to determine fire activity have been developed and applied according to spatial, spectral and temporal characteristics of the sensors. A wide range of global fire products are available and many of them have been validated in the field or by using independent reference data (Roy and Boschetti 2009). Results of these validations show large discrepancies in area estimates and temporal occurrence of fire activity and have been discussed by several studies conducted at a regional scale (Li *et al.* 2001; Zhang *et al.* 2003). Generally, these methodologies use algorithms which are designed to be applied at a global scale and only in a few cases at regional scales. As a consequence, these algorithms do not take into account the intrinsic characteristics of the landscape like atmospheric conditions, type of vegetation, land use and geographical distribution, heterogeneity and combustion rates by type of fuel (Lobada and Csiszar 2007).

This is where the different authors identify the necessity to build algorithms according to the characteristics of the region, that allow to estimate the fire activity by removing the possible commission and omission errors (Csiszar *et al.* 2003). At a global scale, algorithms use thresholds, that identify potential burned pixels, but occasionally these thresholds do not reach a reasonable compromise

between commission and omission errors at regional scales (Xie *et al.* 2007). This study presents an innovative regional index for fire activity detection for the ECS. The Savanna Fire Index (SFI) benefits from the difference in reflectance value in each band (mainly in infrared bands) after a fire event. Algorithms that use infrared bands give better results in the extraction of burned areas than those that only use NIR or the visible band (Smith *et al.* 2007).

Currently, a series of algorithms identifies fires in savanna ecosystems. Nevertheless, the majority of them have not been applied to savannas in South America. Using the MIRBI index in savannas of South Africa, Smith *et al.* (2007) found a high differentiation of burned areas and low level of confusion with other classes, in comparison to NBR, CSIT and SAVIT index. Martin *et al.* (2006), using BAIM index in Mediterranean vegetation formation, found high precision for extracting big and medium burned areas in comparison with BAI and NBR indices. Xie *et al.* (2007) discuss the sensitivity limitations of NDVI index related to atmospheric conditions and soil data and its tendency to saturate at closed vegetation canopies. In this study, SFI provides a high level of precision for large and medium sized burned areas and an intermediate level for small areas, nevertheless higher than MIRBI, BAI, NBR and NDVI indices. In addition, SFI was approved as it presented the smallest error rate in confusion of burned areas with other land cover, followed by the BAI and MIRBI index.

The particular conditions of the savanna ecosystems, as soil humidity, heterogeneity, fragmented landscape and vegetation phenology, cause analysis problems with MODIS images. They present a challenge to calculate a representative index and to establish a unique threshold for burned area mapping (Laris 2005; Lobada and Csiszar 2007). MIRBI, BAI, SFI, NBR and NDVI were applied and evaluated for a set of 8-days MODIS product. Finally, SFI has shown to be the best applied index to avoid confusion between sandy and flooded savannas with burned areas, in comparison to the NBR and NDVI indices.

5.3.2. Accuracy validation

Accuracy is an essential and critical step to validate the quality of any product generated from a remote sensor (Li *et al.* 2001). Usually, accuracy validation is performed using independent data derived from high resolution satellite data which are compared with the product of approximately the same date of acquisition (Roy and Boschetti 2009). Although coarse-resolution burned area products underestimate the amount of burned area, high-resolution sensors give the means to determine the importance of this discrepancy (Laris 2005). In this study, using Landsat and CBERS images, the Kappa value had a value of 0.85 and 0.83 respectively. The precision of the large and medium areas has a high value, which compensates the omission errors that increase due to the fact that MODIS cannot accurately distinguish and map smaller areas. Discrepancy was caused mainly due to difference in date of image taking and intrinsic problems with coarse resolution that do not detect small burned areas.

The commission and omission errors resulting from this validation process can be attributed to several problems related to the input data (Laris 2005; Lobada and Csiszar 2007). First of all, the temporal differences between the sensors. Landsat and CBERS: Images frequently differ in date that the image was taken with respect to MODIS products (i.e. CBERS 183093_184094_09-02-2007 versus MODIS Surface Reflectance, 11-02-2007). Some scars were not identified by the algorithm due to the occurrence of many fires at the beginning of the 8-days period in the MODIS composition, while the high resolution images could be taken at the end of the 8-days of composition. In savanna vegetation, burned areas recover very quickly and become less pronounced during the following days, making it more difficult for the threshold to identify burned area (Laris 2005). In addition, with Landsat and CBERS it is unusual to find a series of dataset with similar temporal frequency.

Secondly, the spatial differences between MODIS (500 m), Landsat (30 m) and CBERS (20 m) images is discussed by Laris (2005). Identifying burned

areas in medium and low resolution images becomes ambiguous as it often occurs in a fraction of a pixel area, intermixed with an unburned background, consequently decreasing the capacity to detect burned areas. In this study, due to these differences, the validation was done only by comparing the perimeters of the fire scars taking into account that fires often burn only in a fraction of a pixel area.

Thirdly, atmospheric contamination of the MODIS data possibly cause: i. Omission errors as burned areas under clouds and shadow areas can not be identified; ii. Commission errors due to the fact that some pixels are classified as burned by having similar reflectance values which in reality are 'edge noise' after cloud and shadow eliminations (Lobada and Csiszar 2007). The final problem occurs during the classification process when the thresholds are defined and implemented. In this study some mistakes were eliminated by visual inspection. Nevertheless, this solution is extremely time consuming. Lobada and Csiszar (2007) discuss the means to eliminate this error but they consider that it is only feasible for small areas.

5.3.3. Area, frequency and severity

Global studies confirm that savanna ecosystems are the most continuously affected ecosystem in terms of area, frequency and severity of fire (Chuvieco *et al.* 2008; Tansey *et al.* 2008). It is in this ecosystem, where the fire activity is an essential factor for its preservation, as their species have developed adaptations that respond positively to fire events and facility propagation (Myers 2006). In Colombia, savannas are concentrated in the ECS, covering 15% of the national territory. According to Van der Werf *et al.* (2003) and Tansey *et al.* (2004a) the burned areas of the ECS contribute 3 to 6% of the total burned ecosystems and 4% of the total of burned areas in South America. Chuvieco *et al.* (2008) using 32 day composition MODIS dates calculated that for Colombia a total of 1.2% of the territory burns annually, which alone is less than half of the 3.11 million ha of the ECS.

In this study, fire activity in the ECS produces a seasonal mosaic of patches of burned and unburned vegetation, which is consistent with other studies from other savannas in the world (Laris 2002). Equally the occurrence of fires has a consistent strong spatial pattern during the analysed period, where some areas show high frequency of burning while other shows a low frequency. As Chuvieco *et al.* (2008) described, in contrast to other tropical areas with high frequency of fires, the ECS is characterized by low accessibility, little use, low population density and is dominated by land cover of grasses and gallery forests, where fires are predominantly of high frequency, short duration and high spatial variability. In the ECS, the species have evolved in response to the fire characteristics of frequency, severity and seasonality. According to Van der Werft *et al.* (2003), in the tropics and subtropics, on average 8 to 10 years are needed for a fire event to return to the same place, while in the sandy savannas in the North of Brazil the average is 4 years (Barbosa and Fearnside 2005). For ECS it is only two years.

The size area, duration and severity of the fire depend on its behaviour, which in turn depends on the type and properties of fuel (mixture of vegetation, chemical properties, load), topography (aspect, slope), and climatic conditions (rainfall, temperature, wind) at the moment of the fire (Dwyer *et al.* 2000; Chuvieco *et al.* 2006). Van der Werft *et al.* (2003) showed that in tropical and subtropical savannas (with less than 5% of trees) the burned size area is on average 5,000 ha, which is approximately seven times the average burned patch size found in this study. The inter-annual average burned patch size was very constant with exception of the years 2004-2005 and 2008-2009 where low numbers of burned scars were observed.

Several studies have shown that the severity of the fires changes during the dry season. At the beginning of the dry period, events are superficial, small and of low severity, leaving more fragmented patches in the landscape, while as the dry season progresses the fires are more severe, continuous and of longer duration (Louppe *et al.* 1995; Russell-Smith *et al.* 1997; Laris 2005). In this study it was found that at the beginning of the dry season burned areas are small and

their scars are of short duration. They become much bigger and scars persist longer as the dry season progresses. They diminish in size again by the end of the dry period, which is in accordance to the results found in a study by Laris (2005) in the African savannas. Most of the medium and large burned scars during the dry period which are of long duration, show an irregular form, influenced by the variations in speed and direction of the wind, while small burned scars are generally of short duration and present an elliptic form.

Although it is well known that fire can exert strong control on stand structure, composition, and dynamics in savannas and woodlands, the relationship between fire severity and stand structure has been characterized in few of the world's savanna ecosystems. It is known that with increase in fire frequency, seedling densities, overstory density and basal area decline, while mortality rates in burned areas increase. However, in these ecosystems, grasses typically rejuvenate quickly, indicating low burn severity although fires typically consume large portions of aboveground biomass (Peterson *et al*, 2001).

Nevertheless severe burns have long-lasting ecological effects because they alter belowground processes (hydrologic, biogeochemical, microbial), which are essential to the health and sustainability of aboveground systems (Neary *et al*. 1999). Long-term ecological changes can potentially result from severe fires that remove aboveground overstory vegetation, even if impacts to belowground processes are minimal. Post-fire weather conditions can also influence severity, in particular when looking at vegetation change through time in relation to severity (Key 2005).

Burn severity assessments are one of the most critical measures in fire activity. However, they implicate very costly and long hours of fieldwork to have sufficient information on the variability of this effect (Chuvieco *et al.* 2006). Remote sensing provides an alternative method to assess these phenomena, thanks to the scars fires leave after an event. Soils and vegetation show changes in spectral reflectance after a fire event due to the presence of charcoal. Indices

have been developed that allow estimations of the spectral reflectance changes detected by satellite sensors (Van Wagtendonk *et al.* 2004). As these indices compare pixels before and after a fire event occurs, a new index is presented in this study which follows that approach.

5.3.4. Burned scars products

There is a general concern that science has not too been able to estimate and monitor fire activity due to the lack of knowledge on its spatial and temporal distribution (Dwyer and Pereira 2000; Boschetti *et al.* 2004). In the last decade, the generation of new products that allow the detection and quantification of fires has been progressing thanks to advances in remote sensing. At present, these products have been developed in such way to obtain information about fire activity and nowadays a wide range of products, derived mainly from remote sensors of low resolution, are available (Boschetti *et al.* 2004).

Simultaneously, with the generation of new products, an arduous work has been undertaken to compare the quality of the products. At continental scale Roy and Boschetti (2009) validated three products using sensor of high resolution, namely MODIS-Burned fires, L3JRC and GlobCarbon applied to South Africa. Boschetti *et al.* (2004) compared the data of burned areas and active fires derived from ATSR (Along Track Scanning Radiometer), and burned areas obtained from SPOT Vegetation for the year 2000. Lately, burned areas maps produced with high resolution sensors have been used to validate active fires products, but they do not provide a real validation due to the lack of temporal resolution under areas of clouds and shadows.

Several studies have shown high discrepancies in terms of areal estimation, fire activity date and localization confirming the urgent necessity to validate these products (Li *et al.* 2001; Korontzi *et al.* 2004; Roy and Boschetti 2009). These discrepancies were detected mainly at a regional scale when active fires and burned areas products acquired from different sensors were compared (Li *et al.*

2001). According to Boschetti (2004) and Roy and Boschetti (2009) without a validation process of these products, research will be continued with a high degree of uncertainty. In this study, comparisons between SFI burned products and the Active Fires product confirm these high discrepancies discussed by the different authors. The main inconsistency is in terms of localization: The active fire product shows areas of fire activity that are not perceived by the SFI burned product as some events do not leave scars. Even when this product is compared with high resolution data, the existence of some fire events could not be shown. Robinson (1991), Eva and Lambin (1998) and Roy and Boschetti (2009) discuss in more detail this discrepancy and argument that the lack of correspondence between the indices does not indicate superior or inferior performance but spectral, spatial and temporal differences of the sensors and the threshold definition.

In general, the validation of burned products for direct mapping does not require data provided by independent satellites as the effects on the land surface persist in time and can be observed days, weeks (savanna ecosystems), even years after the event (forest). As a consequence, images like Landsat can be used for validation.

5.4. Summary

Burned maps of the ECS have been analysed for a period between 2000 and 2009, through MODIS medium resolution satellite images. The new SFI algorithm which was developed and proved to be suitable for the ECS showed a strong potential for regional specific burned area mapping and creation of a long-term record of fire effect on these savannas. This tropical area showed a complex and heterogeneous burned pattern, displaying a high variability in terms of area, frequency and severity. Between 2000 and 2009 the ECS contributed with 25% to the overall burned areas of the continent. Fire in this region affects an annual average of 2.75 million ha which represent globally a significant 3-6% of herbaceous vegetation.

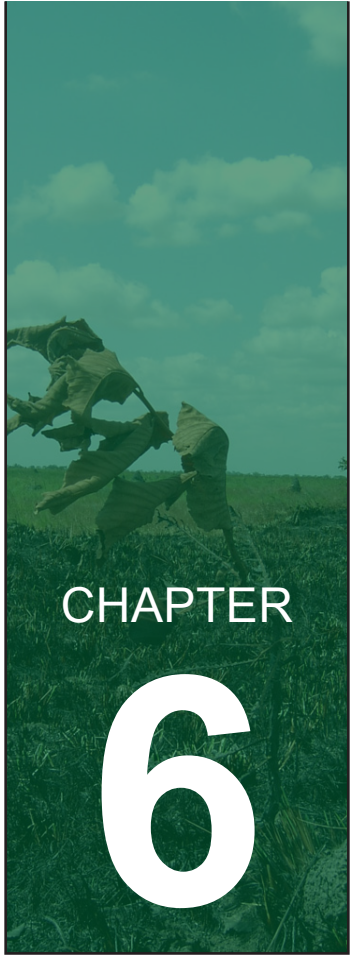

Flooded savannas, wetlands, meanders and burned scars near of La Hermosa (Casanare, Colombia)

CHAPTER 6

Modelling fire regime

In the llanos region, fire is a normal event that occurs every year in the dry season (Sarmiento 1984). To determine where and why fire takes place, natural and non-natural aspects that influence the location of this phenomenon have been analysed. According to Stolle *et al.* (2003) and Finney (1998) topographic, climatic and anthropogenic aspects explain the majority of fire. This chapter addresses the third object of this study, in which an analysis of how aspects like land use/cover (LUC), precipitation, temperature, topography, land form (LFor), Digital Elevation Model (DEM) and slope influence the probability that a fire event occurs in a given location.

6.1. Methodology

Patterns are the outcome of processes that have acted over time and space. Consequently patters are indicators of the processes that have shaped them, and the spatial patterns indicate the presence of the spatial processes. Thus as a simple rule of thumb for model development if there is a least one spatial pattern observed at the range of scales relevant to the question being studied one should consider developing a spatial model (Meyer *et al*. 2010). Descriptive approaches such as conceptual and statistical models and applications of remote sensing and GIS contribute to spatial savanna modelling by formalizing and quantifying spatial relationships (Meyer *et al*. 2010). Remote sensing is frequently used in combination with other descriptive techniques such as GIS and spatial statistics. The GIS captures spatial date in layer that can be superimposed and related to each other (Wiegand *et al*. 2000b). Spatial statistics cover a broad spectral of techniques ranging from neighbourhood analysis to spatial point pattern methods. In the case of this study an autocorrelation method is used with the aim to obtain a predictive model of fire occurrence. First of all Principal Component Analysis (PCA) method is used followed by factor analysis and Logistic Regression. The main idea of PCA is to form, a new variable (or several variables but as few as possible), the so-called “component”, from a set of existing variables, that contain as much variability of the original data as possible. This is a method of data reduction; the number of variables is reduced in order to handle data more easily (Flantua *et al*. 2007). Once spatial models have been thoroughly analysed and have provided an improved insight into the ecosystem dynamics it may well be possible to simplify the model and to remove the spatial components (Adler and Mosquera, 20000; Wiegand *et al*. 2004a). The importance of the component is determined by the relative size of its variance - high variance means higher importance of that variable. With PCA we try to explain as much variance of the original data as possible by forming new synthetic variables. In factor analysis we try to find some dimensions, traits, that cannot be measured directly, but affect certain variables that can be measured.

The functionality of Logistic Regression is to measure the impact of multiple variables at the same time, determining the importance and evaluating the effect of such interaction. This statistical approach has been used in numerous studies to relate a dependent variable with independents variables (Stolle *et al*. 2003).

To determinate the likelihood of fire occurrence as a function of predisposing conditions, a statistical analysis was undertaken using logistic regression approximation. This model is a part of a conjunction of models called Generalized Linear Model (GLM), which are used to predict the probability of occurrence of an event (independent variable) as a function of a series of dependent variables (Hosmer and Lemishow 1989). The functionality of these models is to measure the impact of multiple variables at the same time, determining the importance and evaluating the effect of such interaction (Flantua *et al.* 2007). The aim of this model is to find the best fitting variables that allow an accurate prediction of the distribution of the fire activity in the Eastern Colombian Savannas (ECS). To describe the relationships between these variables, three principal components are used: i. A dichotomous dependent response variable (0, 1) which gives the possible result as presence or absence of a specific event; ii. A set of parameters and explanatory variables (predictor variables) and; iii. the function that establishes the links between dependent and independent variables. As a result of this analysis a formula is produced that predicts the probability of occurrence of an event (in this case fire) based on the independent variables which have the following expression.

$$\log it(P_i) = \log_e\left(\frac{P_i}{1-P_i}\right) = \alpha + \beta_1 X_1 + \beta_2 X_2 + \beta_3 X_3 + \beta_4 X_4 + \beta_5 X_5 \quad (6.1)$$

Log*it* : Logistic regression;

P_i: Probability that a fire occurs;

$1-P_i$: Probability that a fire does not occur;

α : Intercept constant;

X_i^T : Matrix independent variables or dummy variables;

β_n : Slope parameters associated with independent variables;

P_i : The probability of the fire occurrence is expressed as:

$$P_i = \frac{\exp(\propto + \beta_1 X_1 + \beta_2 X_2 + \cdots + \beta_n X_n)}{1 + \exp(\propto + \beta_1 X_1 + \beta_2 X_2 + \cdots + \beta_n X_n)} \quad (6.2)$$

The P_i is the ratio of the probability that fire will occur, divided by the probability that fire will not occur. The threshold value indicates the condition of the binomial response (i.e. fire), while everything below this value equals the other condition of the variable (i.e. not fire). The threshold (default 0.5) was defined according to the different models.

To measure the model's goodness of fit a ROC curve (Receiver Operating Characteristic) is used which indicates a perfect fit when this value equals 1. A value of 0.5 indicates a random fit. ROC values between 0.7 and 0.9 should be considered as a good fit (Swets 1995).

Data of the dependent variable, "fire occurrence", were extracted from the 2000-2001 database of fires from this study (Chapter 5).

The independent variables were collected from different sources and were reclassified as:

i. **LUC** dataset was derived from Landsat data 2000-2001 (see chapter 4). The dataset was aggregated in seven classes: ***a)*** high savannas; ***b)*** flooded savannas; ***c)*** sandy savannas; ***d)*** forest; ***e)*** anthropogenic areas (exotic pastures, culture mosaic and palm oil plantations); ***f)*** rocky outcrops and; ***g)*** wetlands. Water and infrastructure were omitted, since fires occurrence can only be explained in areas with vegetation;

ii. **Bioclimatic** variables derived from the monthly temperature and rainfall value which represent annual trends. The dataset was collected from WORLDCLIM database (http://www.worldclim.org/) which include 19 variables at resolution of 1 km. In this case only the 9 variables were selected whish are considered representative for the dry season (December to March):

B1 = Annual temperature
B2 = Minimum Temperature of Driest Quarter (December to March)*
B5 = Maximum Temperature of Warmest Month of the year
B9 = Mean Temperature of Driest Quarter (December to March)
B10 = Mean Temperature of Warmest Quarter (December to March)
B12 = Mean Precipitation of Driest Quarter (December to March)
B14 = Precipitation of Driest Month of the year (December to March)
B17 = Precipitation of Driest Quarter (December to March)
B18 = Mean Precipitation of Driest Quarter (December to March)*

** Bio 2 and Bio 18 were calculated from the monthly information.*

iii. **Evapotranspiration**: This variable was derived from the monthly precipitation and temperature Worldclim data at resolution of 1 km, using a Thornthwaite climate classification;

iv. **Digital Elevation Model (DEM)**: Dataset was extracted from Shuttle Radar Topography Mission -SRTM- 30 m resolution;

v. **Slope**: Describes the terrain grade inclination and was derived from Digital Elevation Model (DEM) at resolution of 30 m;

v. **LFor**: Land form categorical variable were derived from Romero *et al.* (2004) at resolution of 240 m (see chapter 2).

All maps were spatially linked and resampled to a pixel size of 150 m with the aim to homogenize the different scales of the datasets. Around ten thousand random points for data extraction were created which is equivalent to approximately 10% of the area. For every point, the underlying data of the variable layers was extracted into a DBF-format.

One of the most difficult tasks in multivariate analysis is the definition of independent variables that affect a dependent variable (Ayalew and Yamagishi 2005). In general, the more independent the variables included, the more complete the model. Nevertheless, to include an independent variable, some requirements have to be satisfied such as: Certain degree of affinity with the dependent variable; to be represented throughout the study area, present spatial variation, to be measurable in space and not correlated highly with others variables. Before applying the logistic regression in PCCord and IDRISI software several statistical tests like correlation matrices were done with the objective to avoid multicollinearity and/or irrelevant variables. The variables with high correlation (Pearson > 0.65) were excluded for presenting high correlation with the selected variables. A total of four categories and 14 variables were included. To apply the logistic model, the selected variables for the model were introduced in IDRISI.

During the process of selecting the most effective model the logistic regression is tested eliminating each variable individually to measure its relevance in the model and to avoid reduction of the model's accuracy. Using a combination of different variables, five models were tested and evaluated. An equation was produced and implemented into the GIS, with the different data layers as input for the calculation. Next, the predictive capacity of each model was evaluated using a fire frequency map, which allowed the comparison of fire occurrence for each category of the models providing an approximation of the model's accuracy. Furthermore, a false positive and false negative prediction error estimation was extracted. A false positive means that the model predicted presence while fire was absence. A false negative is the prediction of absence when fire activity is present.

Finally, a 'sensitivity' index was defined as the proportion of correctly predicted occurrences; 'specificity' as the proportion of correctly predicted absences and overall accuracy was defined as the percentage of correctly predicted in the entire area of interest (Fielding and Bell 1997).

6.2. Results

6.2.1. LUC and LFor versus fires

In terms of land covers, savannas formations were the most affected by fire activity. On average, 60 ± 2.8% of fires occur in high plain savannas, and 25 ± 2.3% in aeolian overflow plain savannas. Only, a 9.6 ± 0.6% occurs in forest; 3.2 ± 2% in transformed areas and finally 3.2 ± 0.1% and 0.1 ± 0.01% occurs in sandy savannas and outcrops rocks respectively. Results show a low percentage (1.1%) of fires in wetlands and water bodies which is attributed to differences in resolution between MODIS and Landsat and CBERS data (Figure 6.1).

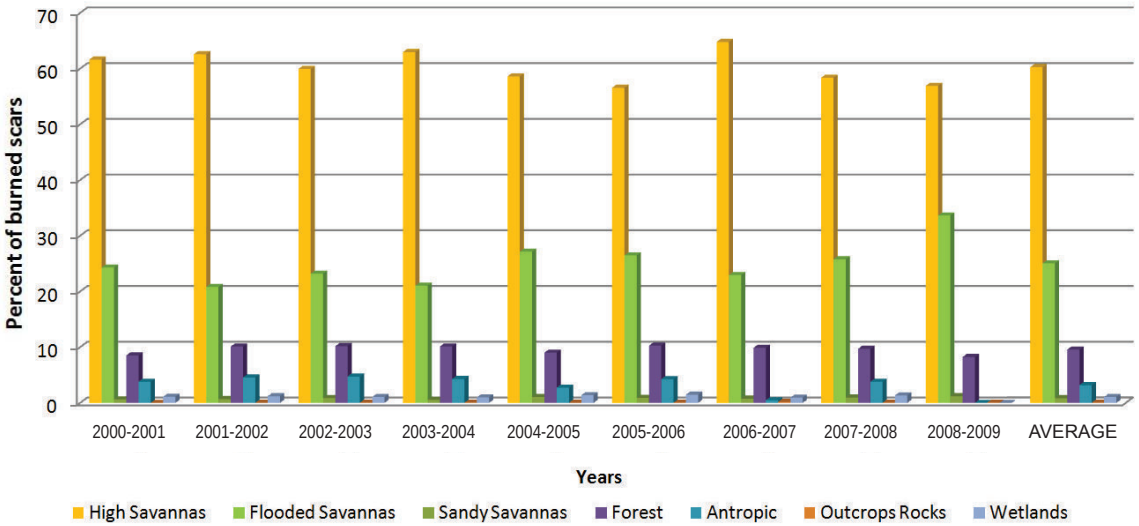

Figure 6.1. *Fire presence percentages and average for different land cover types for the period between 2000 and 2009.*

With respect to LFor, the most frequent events take place over the structural high plains formation (SHP) with 62.1 ± 4.2%. Followed by the alluvial plain with aeolian influence (AOPAI) with in average of 15.9 ± 2.9%; depositional high plain (DHP) with 9.0 ± 1.1%; Guiana Kraton shield (CGS) with 7.9 ± 1.9% and the rest of LFor with only 5% of the fires events (Figure 6.2).

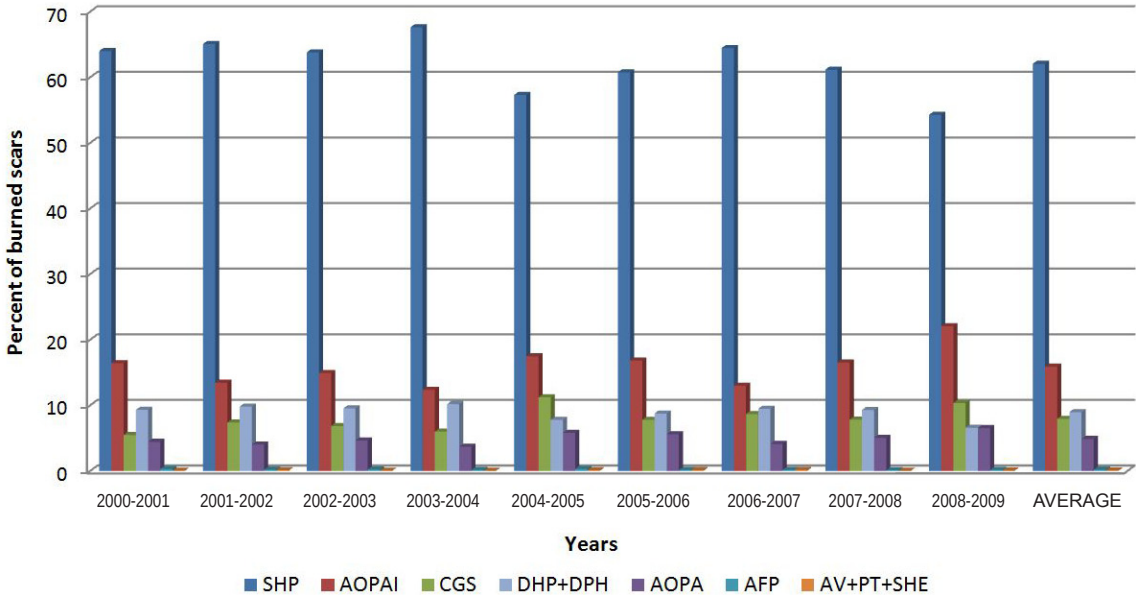

Figure 6.2. *Fire presence percentages and average for different types of LandForm for the period between 2000 and 2009.* ***DHP****: Depositional High Plains;* ***SHP****: Structural High Plains;* ***GKS****: Guiana Kraton Shield;* ***SHE****: Structural and Erosional Hills;* ***AFP****: Alluvial and Fluvial Piedmont;* ***TP****: Tectonic Piedmont;* ***AOPA****: Alluvial Overflow Plain of Andean rivers;* ***AOPAI****: Alluvial Overflow Plain with Aeolian Influence);* ***AV****: Alluvial Valley.*

6.2.2. Climate variables versus fires

Figure 6.3 shows the fire presence percentages by different ranges of precipitation for the period between 2000 and 2009. In average 44.2 ± 2.6% of fire activity is situated over areas where the precipitation oscillates between 40 and 60 mm, followed by 31.1 ± 3.9% with precipitation between 0 and 40 mm; 7.8± 1.7% with precipitation between 60 to 80 mm which are located within the boundaries of the Amazon rain forest region. Only 7.7 ± 1.6% occurs where precipitation is between 80 and 100 mm and 0.4 ± 0.2% in areas with precipitation above of 100 mm, which corresponds to the southwestern and foothill areas.

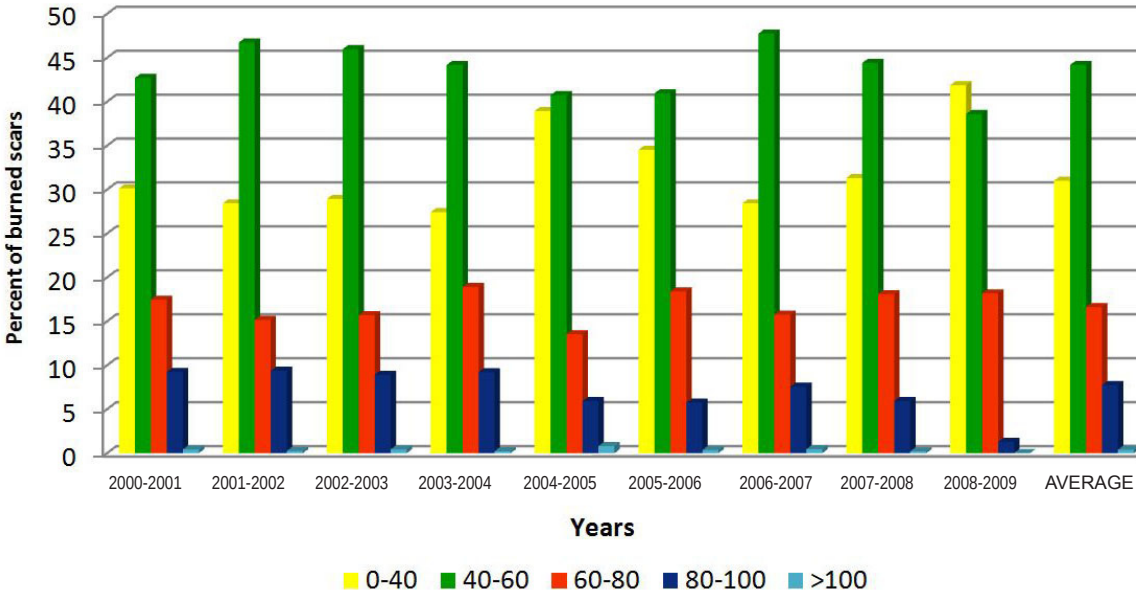

Figure 6.3. *Fire presence percentages and average for different ranges of precipitation by a period between 2000 and 2009.*

In terms of temperature, regardless of the fact that temperature is relatively uniform in the ECS, the majority (42 ± 3.5%) of fire events occur in areas with temperatures between 27.5 and 28 °C. In the temperature range between 28 and 28.5 °C, a 24.6 ±1.6% of the events occurs, followed by temperatures between 28.5 and 29 °C where 16 ± 1.8% of the events are found. Only 3% of fire events occur in areas with temperature between 24 and 27.5 °C (Figure 6.4).

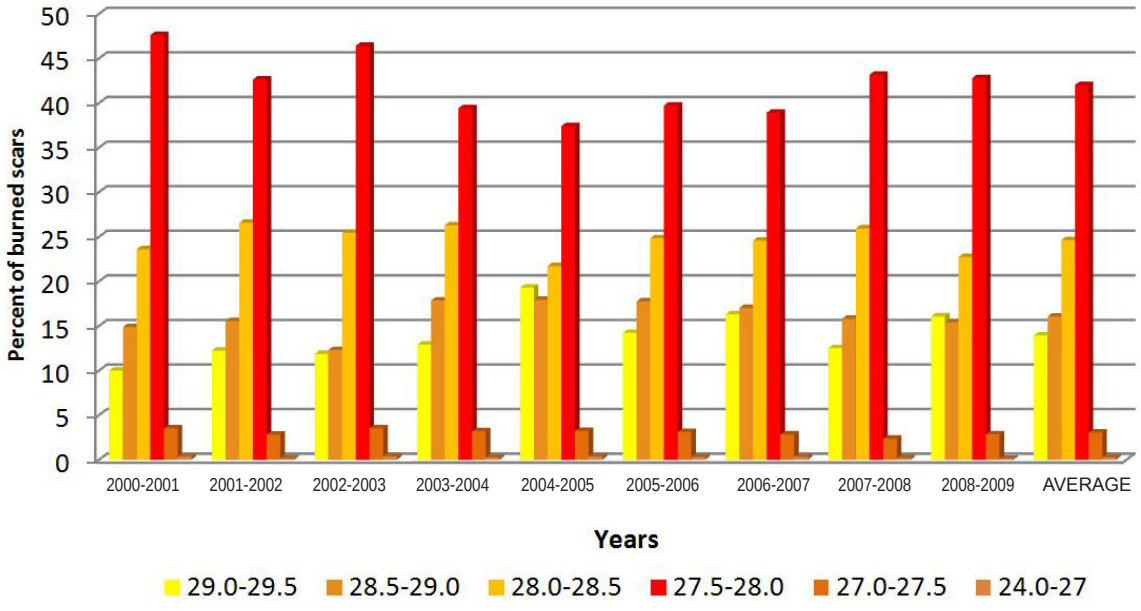

Figure 6.4. *Fire presence percentages and average for different ranges of temperature for the period between 2000 and 2009.*

6.2.3. Topography versus fires

In the ECS, the prevalence of the topography is flat with slopes between 0 to 20%. In areas totally flat (slopes around zero) 47.8 ± 3.6% of burned scars are present, following by slopes between 0.1-1 % which yield 30.1 ± 1% of the scars; and 14.5 ± 1.5% of fires events occur on slopes between 1 to 3%. Only 1.3% of burned areas occur on slopes greater than 3% (Figure 6.5).

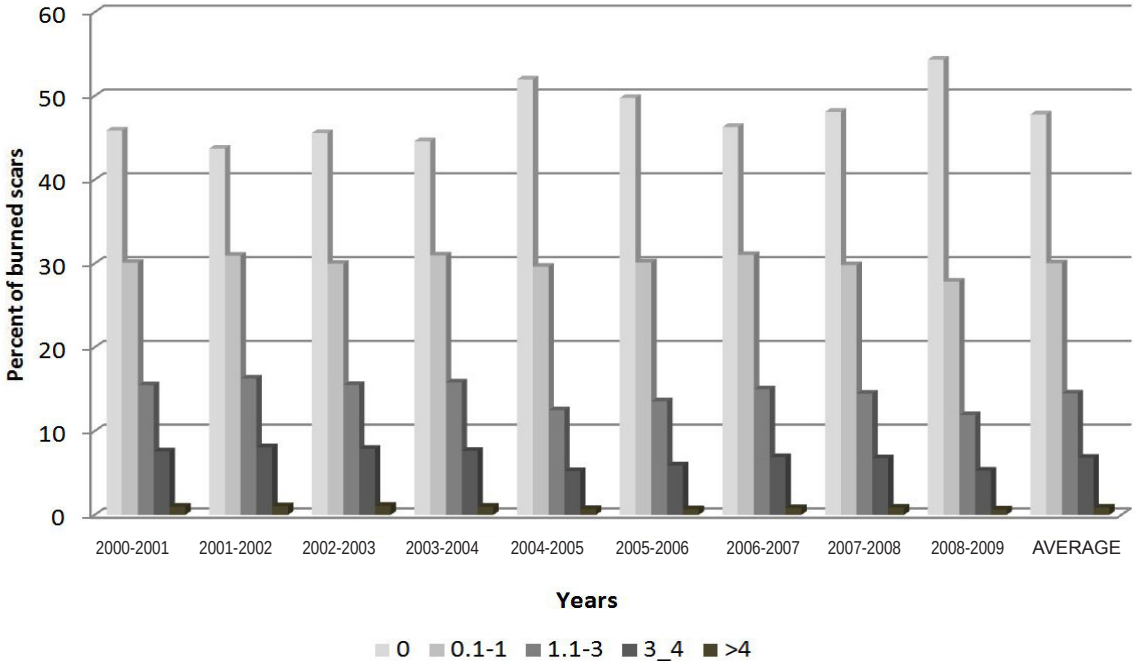

Figure 6.5. *Fire presence percentages and average for different ranges of slope for the period between 2000 and 2009.*

In terms of elevation, 44 ± 3.1% of the fires scars are found in elevations between 100 to 150 masl. 25.8 ± 4% of these scars are found between 1 and 100 masl and only 12% occurs in elevations higher than 200 m These tendencies are constant during the different periods (Figure 6.6).

6.2.4. PCA and logistic regression

Table 6.1 shows the matrix results of the correlation analysis for the considered variables. This analysis shows that a first group is formed by a strong association between all of the temperature variables: mean temperature of driest

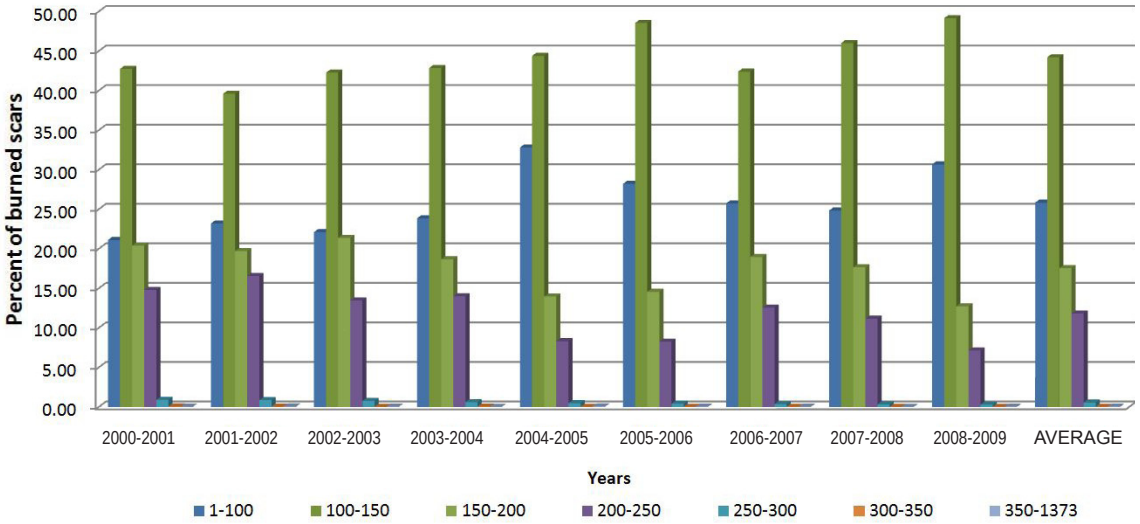

Figure 6.6. *Fire presence percentages and average for different ranges of elevation for the period between 2000 and 2009.*

quarter (B9), minimum temperature of driest quarter (B2), mean temperature of warmest quarter (B10), annual mean temperature (B1) and maximum temperature of warmest month (B5). In addition, precipitation variables like precipitation of driest month (B14), precipitation of driest quarter (B17), annual precipitation (B12), mean precipitation of warmest quarter (B18), evapo-transpiration (EVAPO) show a strong correlation in a second group. The rest of the variables show a weak correlation between them and are not included in a specific variable group.

Figure 6.7 shows the correlation analysis graph, based on the association values between the different variables. In this graph, each blue line indicates one of the analysed variables; the longer the line the stronger it's the influence over the distribution of the red points which represent the fire events. In addition, the more the lines are grouped together, more correlation exists between these variables. In Tile C, it can be seen that all temperature variables are highly correlated between them with values between 0.67 and 0.99 (Table 6.1). Furthermore these variables show a high tendency towards the first axis which indicates that temperature is the major influence over the fire events. The same behaviour is seen between precipitation variables (Tile A) with correlation values between 0.75 and 0.96 (Table 6.1). As this precipitation group inclines towards Axis 2 it is considered as the second most important variable group that influences the fire events. The

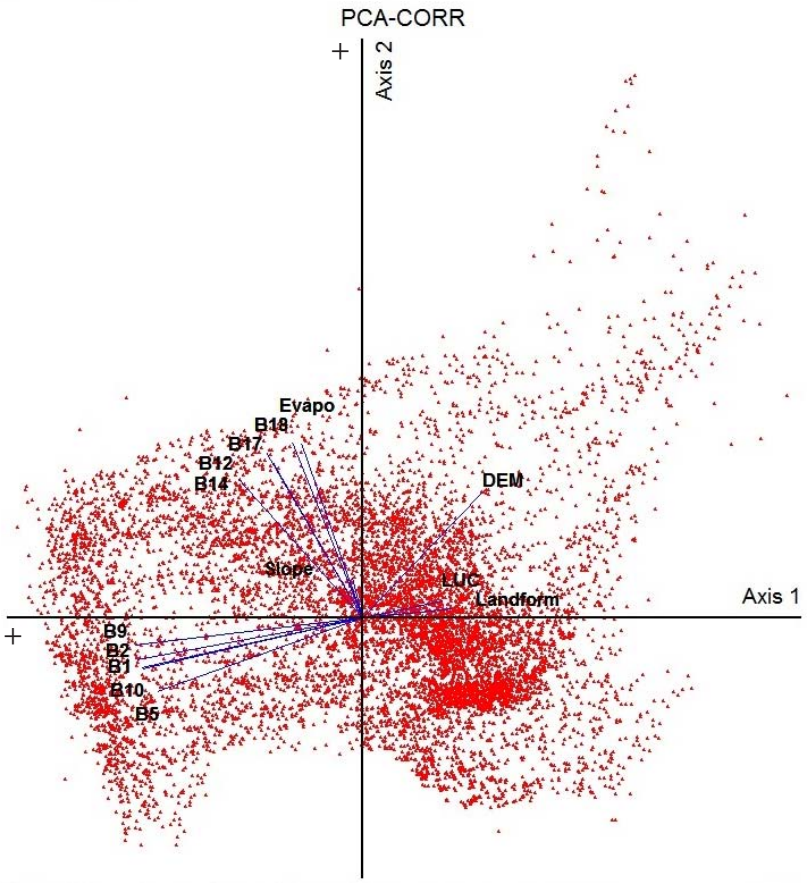

Figure 6.7. *Principal components analysis, Axis 1: Component 1; Axis 2: Component 2 for a fourteen variables. Red points indicates fire presence; blue lines variables.*

Table 6.1. Correlation analysis between different climatic, topographic, LUC and LFor variables. Yellow boxes indicates a high correlation between variables (Pearson >= 0.65).

VAR	CLIMATE										TOPOGRAPHY		LUC	LFor
	B1	B2	B5	B9	B10	B12	B14	B17	B18	EVAPO	DEM	Slope		
B1	1													
B2	0.99	1												
B5	0.97	0.67	1											
B9	0.98	0.69	0.98	1										
B10	0.99	0.69	0.99	0.99	1									
B12	0.18	0.07	0.13	0.22	0.17	1								
B14	0.09	0.06	0.01	0.12	0.07	0.75	1							
B17	0.06	0.02	0.02	0.10	0.05	0.85	0.92	1						
B18	0.03	0.01	0.10	0.01	0.04	0.86	0.88	0.97	1					
EVAPO	0.01	0.08	0.04	0.07	0.01	0.88	0.82	0.91	0.96	1				
DEM	0.32	0.36	0.32	0.28	0.31	0.50	0.39	0.52	0.57	0.58	1			
Slope	0.20	0.05	0.20	0.20	0.20	0.12	0.14	0.16	0.18	0.16	0.16	1		
LUC	0.13	0.17	0.15	0.13	0.14	0.02	0.05	0.04	0.06	0.05	0.25	0.16	1	
LFor	0.17	0.24	0.21	0.19	0.20	0.00	0.04	0.01	0.02	0.03	0.31	0.00	0.31	1

evapo-transpiration variable also in Tile A is higher correlated to precipitation than temperature. DEM, slope, LUC and LFor variables show a low correlation between them and the climatic variables.

Based on the high correlation between the variables within each group, there is no need to include each of the separate variables within the logistic regression. Therefore the variable B2 (Minimum temperature of driest quarter) was selected to represent the temperature factor, while B18 (Mean precipitation of driest quarter) was selected for precipitation. These variables were selected due to the highest tendency towards their corresponding axes. Although the climate variables are identified as the most important variables, the disperse distribution of the points in the graph, indicate that other variables play an additional important role in the occurrence of fires. Nevertheless, a concentration of fire events can be seen in Tile B and D which represents the zone where temperature ranges between 27.5°C and 28.5°C (Figure 6.4) and precipitation ranges between 0 and 60 mm (Figure 6.3). DEM, slope, LUC and LFor were considered as other relevant variables and therefore also included in the logistic regression.

Table 6.2 shows the matrix results of the factor analysis. Four components were extracted, which together explain 90.4%. The first component corresponds to the temperature variable explaining 40.4% of the total variance; the second component was precipitation and DEM which together explain 33.7% of the

Table 6.2. Principal component analysis between six variables: climate, topography, LUC and LFor. Yellow boxes indicates a high value of the factor in each component (Pearson >= 0.65).

Factor	1	2	3	4
B2	-0.96	-0.23	0.11	-0.01
B18	-0.30	0.94	-0.01	0.04
DEM	0.51	0.68	-0.09	-0.01
LUC	0.34	0.09	0.79	-0.07
LAND FORM	0.38	0.05	0.78	0.05
SLOPE	-0.05	0.21	-0.01	-0.97

total variance. Third component includes Land Use/Cover and Geomorphology that explains the 9.3% of the total variance and finally the fourth and smallest component represented by 'slope' explaining by itself 6.9% of the total variance.

Based on the results of the factor analysis, five models were built with the aim to define the best predictive model to determine fire occurrence. Figures 6.8 to 6.12 show the fire probability predicted by each of the models.

Model 1: Climatic variables: Component 1 and 2 explain 74.1% of the total variance found in the data base indicating a strong influence of the temperature and precipitation gradient. A first model includes only these two categories of variables obtaining the following logistic regression formula:

LR = -20.4475 - 0.01 × B18 + 0.07 × B2; with a ROC = 0.62 with a threshold = 0.21; true positive = 99.9%; false positive = 16.1%; sensitivity = 0.43; specificity = 0.44; overall accuracy 0.44 (Figure 6.8).

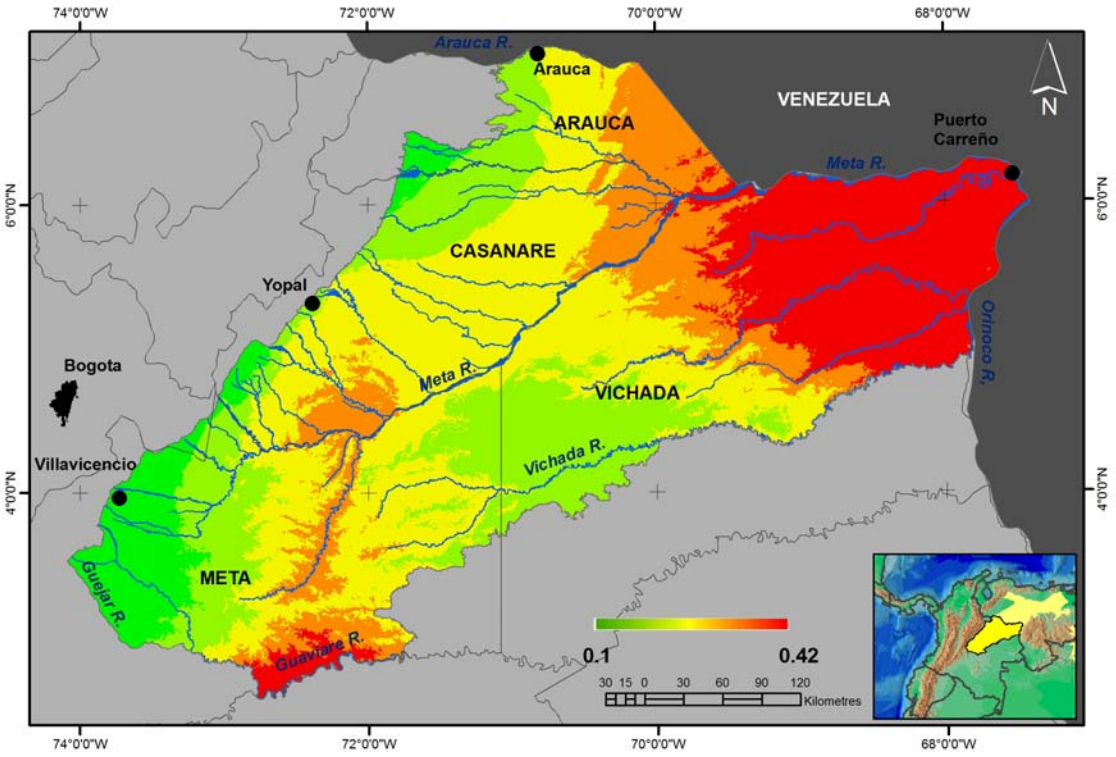

Figure 6.8. *Map of predicted fire probability by Model 1 using mean precipitation and min. temperature, which explain 74.1% of the total variance of the factor analysis. Green indicates lower probability; yellow medium and red higher probability.*

Model 2: Climatic, topography (DEM) and LFor variables: Component 1 and 2 explain 74.1% of the total variance found in the data base indicating a strong influence of the precipitation and temperature gradient. Nevertheless, DEM was a part of Component 2 with a medium influence and Component 3 includes a strong influence of the LFor variable which together with LUC explained 9.3% of the total variance. To determine which of the last mentioned variables influences most fire presence (between LFor and LUC), Model 2 only included LFor while Model 3 only included LUC along with the climatic variables. The logistic regression formula for Model 2 was:

LR = -14.0740 - 0.016976 × B2 + 0.051191 × B18 + 0.000428 × DEM - 0.453947 × LFor with a ROC = 0.69 and threshold = 0.25; true Positive = 99.9%; false Positive = 15.4%; sensitivity = 0.77; specificity = 0.68; overall accuracy = 0.71 (Figure 6.9).

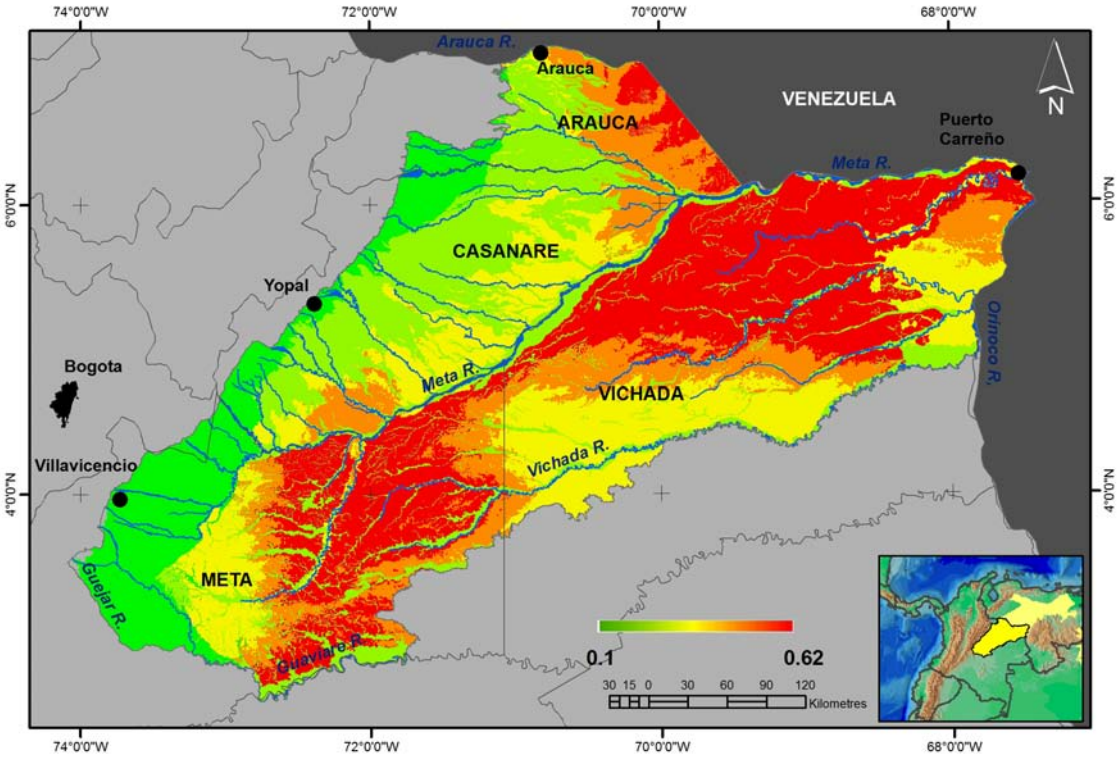

Figure 6.9. *Map of predicted fire probability by Model 2, using mean precipitation and min temperature, digital elevation model and LFor variables, explaining 83% of the total variance of the factor analysis. Green indicates lower probability; yellow medium and red higher probability.*

Model 3: Climatic, topography (DEM) and LUC variables: Similar to Model 2 but LFor was substituted by LUC. The logistic regression formula was:

LR = -10.5320 - 0.015699 × B18 + 0.039840 × B2 + 0.001071 × DEM - 0.720210 × LUC with ROC = 0.76 and threshold = 0.31; true Positive = 99.9%; false Positive = 14%; sensitivity = 0.78; specificity = 0.79; overall accuracy = 0.78 (Figure 6.10).

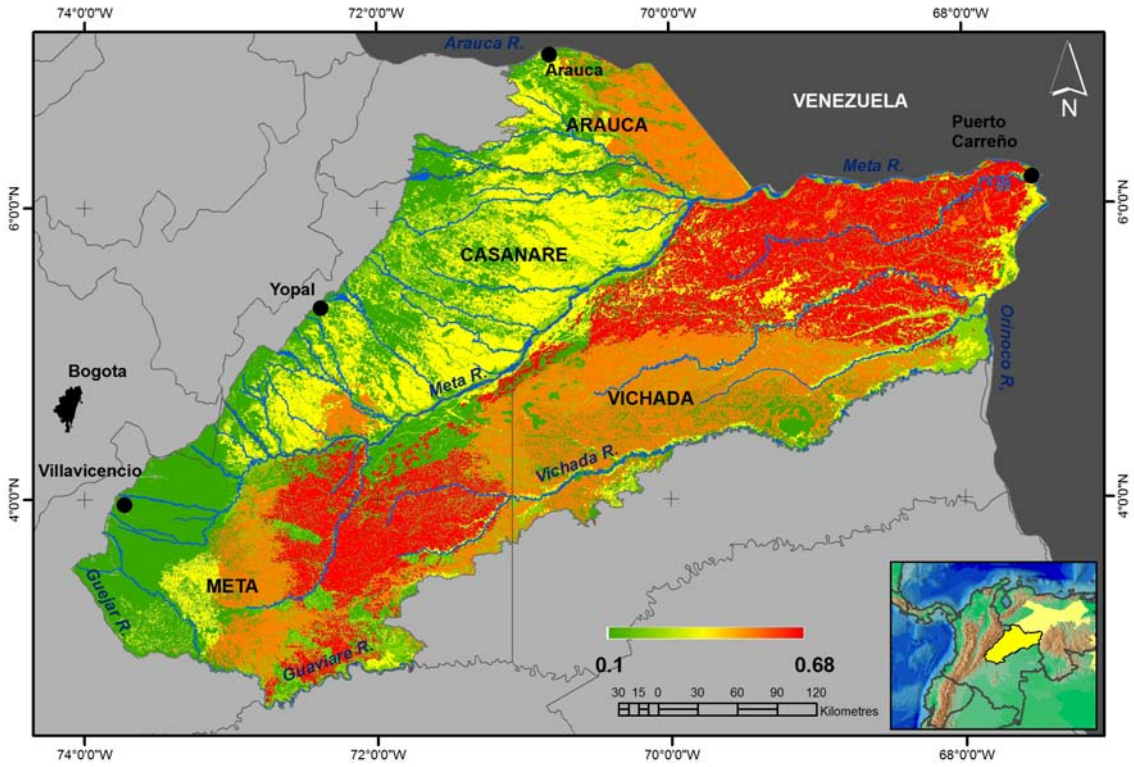

Figure 6.10. *Map of predicted fire probability by Model 3, using mean precipitation and min, temperature, DEM and LUC variables which explain 83% of the total variance of the factor analysis. Green indicates lower probability; yellow medium and red higher probability.*

Model 4: Climatic, topography (DEM), LFor and land cover/use (LUC) variables: In this model all the above mentioned variables were included. The logistic regression formula was:

LR = -9.1252 - 0.019831 × B18 + 0.036506 × B2 - 0.587848 × LUC + 0.001211 × DEM - 0.257442 × LFor with a ROC = 0.77 and threshold = 0.33; true Positive = 99.9%; false Positive = 13.6%; sensitivity = 0.73; specificity = 0.80; overall accuracy = 0.76 (Figure 6.11).

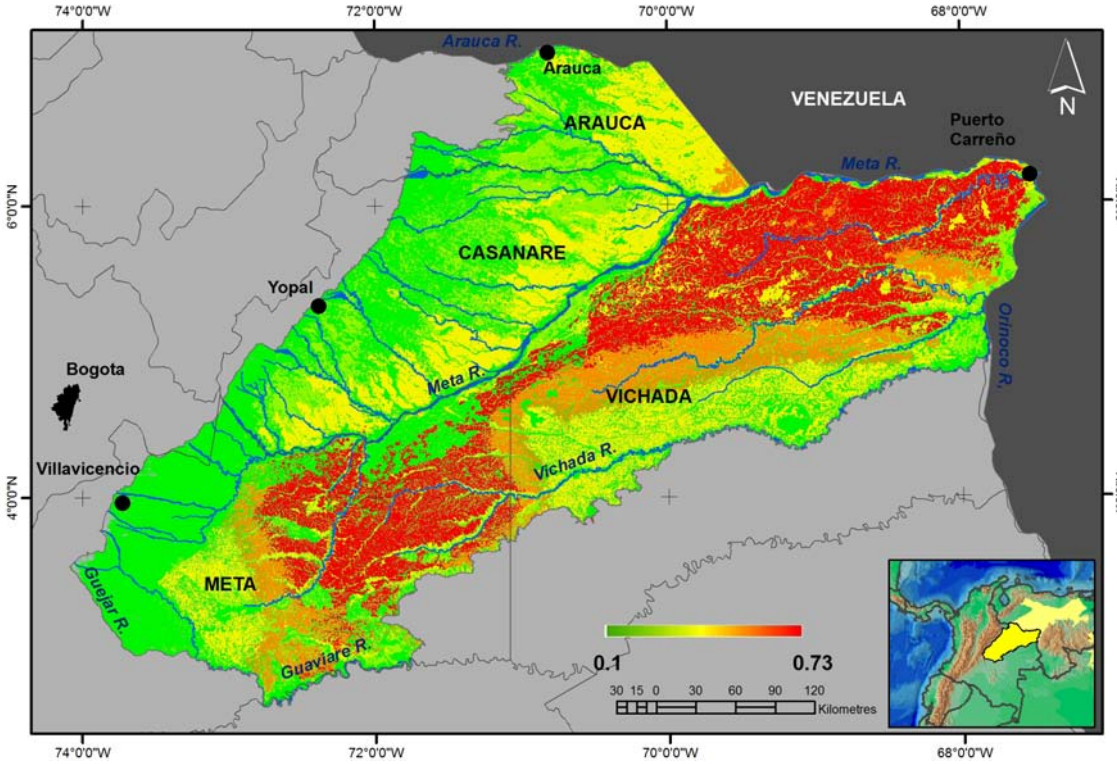

Figure 6.11. *Map of predicted fire probability by Model 4, using mean precipitation, min temperature, DEM, LUC and LFor which explain 83% of the total variance of the factor analysis. Green indicates lower probability; yellow medium and red higher probability.*

Model 5: Climatic, topography (DEM and Slope), LFor and land use/cover (LUC) variables: The fourth component within the PCA explained only 6.9 of the total variable, but was still considered important enough to include because it is constituted by only one variable: slope. The logistic regression formula was:

LR = -9.2429 - 0.018365 × B18 + 0.036839 × B2 - 0.590152 × LUC - 0.097025 × slope + 0.001667 × DEM - 0.267677 × LFor, with a ROC = 0.78 and threshold = 0.34; true Positive = 99.9%; false Positive = 13.4%; sensitivity = 0.77; specificity = 0.79; overall accuracy = 0.78 (Figure 6.12).

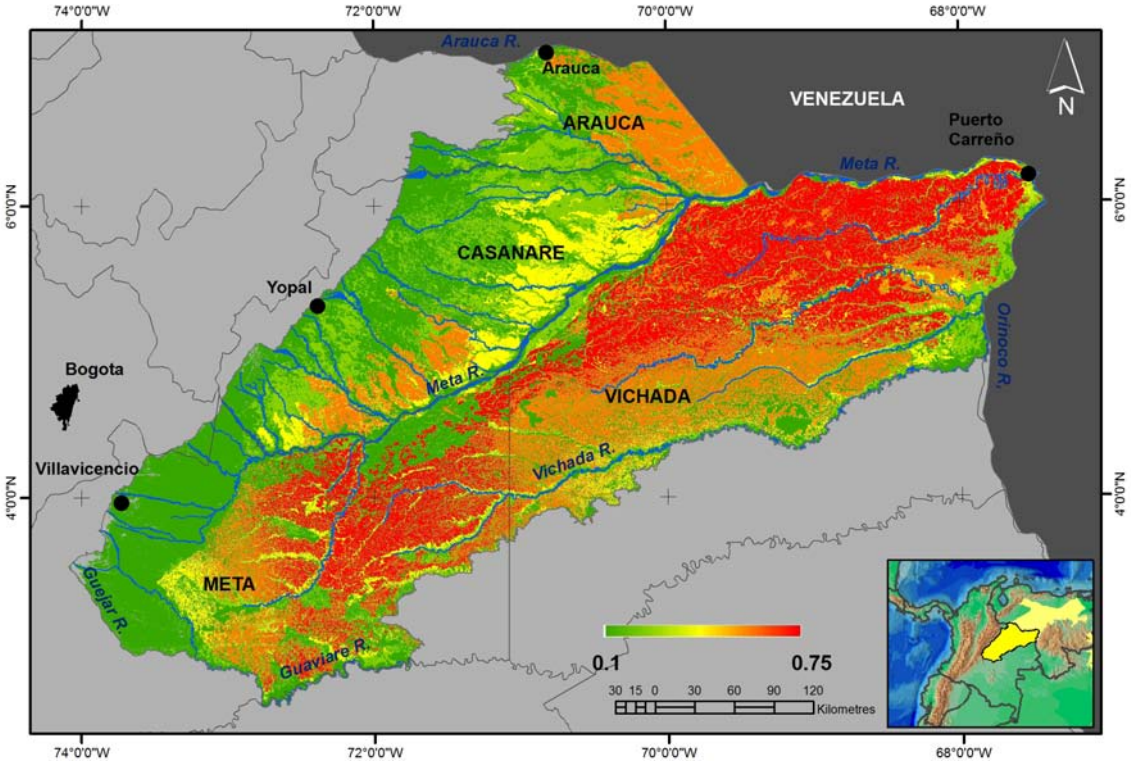

Figure 6.12. *Map of predicted fire probability by Model 5, Fire probability using mean precipitation, min temperature, DEM, slope, LUC and LFor. Green indicate lower probability, yellow medium and red higher probability.*

6.3. Discussion

Logistic analysis shows the role of the significant variables in the natural predisposing conditions for fire occurrence such as LFor, temperature, precipitation and slope. Although this analysis does not have detailed information on the quality and quantity of combustion material present in each land use/cover classes, it contributes to a first approximation of how the variables analysed may be influencing the fire behaviour.

According to the results found at a regional level, it is shown that in the ECS, the fire variation is not only influenced by climatic fluctuations but also depend on the elevation, LFor differences such as soil composition and the type of land cover that constitute the principal source of combustion and available biomass to be burned. The generated models confirm this tendency. Although Model 1 has a high correct prediction of presence due to threshold equal 0.21, it shows very low values in the ROC, sensitivity, specificity and overall accuracy.

As model 1 is only composed of climatic variables it shows that for a fire event to occur these variables are not the exclusive dominant factors. By including other variables the models show better predictive values in which Model five present the highest accuracy of correct predictions. Based on the statistical analysis it is stated that the ROC between 0.77 and 0.78 is an acceptable value for this model of fire distribution prediction (Flantua *et al.* 2007).

With respect to climatic factors, the wet season constitutes one of the most important period previous to the fire season. It is during this period that the production of above-ground biomass is high due to the elevated atmospheric humidity facilitating plant growth and reproduction. By the end of this period (Middle of November) the accumulated biomass forms in the principal source of combustion for fire. Nevertheless, the relatively high humidity inhibits the beginning of the fire season. As a result the fire events during the first weeks of December are patchy, of short duration and small area. As the dry season advances, the precipitation decreases and the relative humidity drops, causing woody elements and grasses to dry while fire events become more extensive, frequent and severe. In February and March the rainfall starts to increase again in a small percentage but still in an insufficient quantity to diminish fire activity. As the end of the dry season approaches, the availability of biomass becomes reduced while being consumed by fires. At the beginning of April the fire frequency, severity and area have decreased substantially. Finally, although the spatial and temporal variation of temperature in the ECS seems minimal (1.5°C) both the PCA and Logistic regression indicate temperature as an important variable in the fire prediction. In the PCA temperature forms in the most important climate component which explains 40% of the present variance. The first mode by logistic regression based en only two variables (B2 and B18) already predicted 44% of fire occurrence.

Land cover is one of the other vital factors for fire to occur: in High savannas, the vegetation reaches up to 2 to 3 m and presents a high quantity of wood material during the dry season. Although Flooded savannas are inundated during most of the year, isolated dry patches remain after the dry season, providing

the conditions for small fire events. Due to the presence of rocky outcrops and wetlands combined with a patchy distribution of low biomass, Sandy savannas rarely present large areas of fires. Finally, in exotic pastures and culture mosaic, the fires events are isolated and small.

In the case of LFor, it can be concluded that the fire events do not occur at random but are related to soil composition, LFor structure and historical geology. For example in Structural High Plain (SHP) LFor where 62% of the fire events occur, the soils are generally of clay loam to silty loam and moderately deep to deep. These fertile soils provide the necessary conditions for vigorous vegetation to grew which naturally supply the fuel for fire events to occur. In Alluvial Overflow plains with Aeolian influence (AOPAI) LFor, where only 15% of the fire events occur, the soils are sandy loam to sandy, sandy loam to silty and deep to very deep. These soils in general sustain low biomass vegetation due to the low fertility and there for fewer fire events occur.

Finally, the slope plays an important role as the angle can influence and stimulate the velocity and spread of fire events (Zárate 2004). Although in the ECS the slope is not very pronounced, the small hills are important in the distribution of the vegetation formations, such as gallery forest and wetlands, which are related with depressions and flat and narrow areas in the landscape close to water bodies. These formations form a natural barrier to the spread of fire, and as such define the form and area of the burned scar and give the particular microclimatic conditions which act as a limiting factor to fire presence.

For the prediction of fire occurrence, it is important to integrate the ensemble of the above mentioned factors. Each of the variables plays an important role but do not exclude or dominate as a single factor. It is the combination of different factors that determine the distribution and behaviour of fire. The particular conditions of the ECS are translated into different fire regimes in terms of area, density, frequency and severity.

The inclusion of characteristics that act at a local scale such as biomass, microclimate, vegetation composition, soil structure, and human influence among others, will improve the predictive capacity of the model. Using paleoecological techniques Gillson (2004) found the patterns of vegetation change differed among micro, local, and landscape spatial scales, with the most rapid changes at the micro scale. For the aims of this study the developed models at a larger scale have contributed significantly to an improved comprehension of fire dynamics in ECS, taking into account the lack of knowledge on the ecosystems diversity of the savannas of Northern South America.

6.4. Summary

Climatic, DEM, slope, LUC and LFor variables have been included in predictive models as possible factors that determine the presence of fire events in ECS. A total of 5 models were developed in which different variables were combined to assess the predictive accuracy of each of the models. It was shown that the model represented by only climate variables (model 1) could only predict fire occurrence at an overall accuracy of 0.44. As more variables were included in the predictive model such as DEM and LFor the overall accuracy increased to 0.71 (model 2). When LFor was substituted by LUC the overall accuracy increased to 0.78 (model 3). In model 4 the combination of climatic, DEM, LUC and LFor variables resulted in an overall accuracy decrease to 0.76. Finally, when slope was included together with all other variables, the model showed an overall accuracy of 0.78 (model 5). Although similar overall accuracy values of the five models, model number 5 shows furthermore the highest ROC value (0.78) and therefore was selected as the best fitting model for the prediction of the fire event in the ECS. These results show that the climatic variables are not the only factors that determine the occurrence of fire. Factors associated with topography, LUC and LFor play an additional significant role in the fire activity in the ECS.

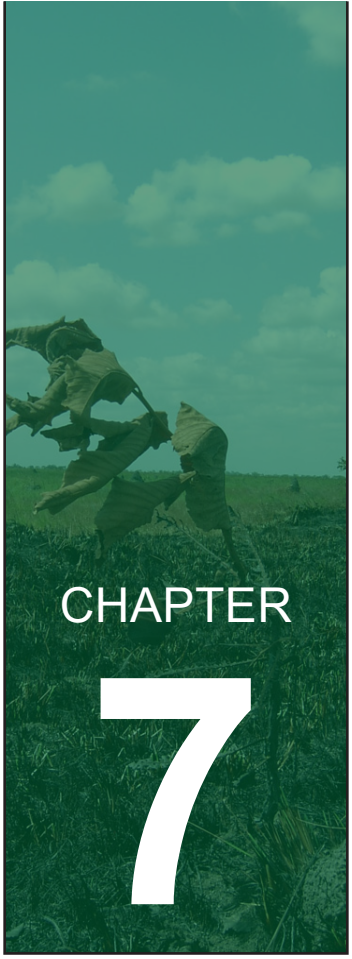

CHAPTER 7

Gallery forest and wetlands near of Villavicencio (Meta, Colombia)

CHAPTER **7**

Conclusion

This chapter aims to bring the various results of the study together and to provide answers to the research questions. Each section of this chapter, discusses a specific objective of this study based on the results in comparison with existing literature. Finally the main findings of this study are concluded and followed by recommendations for future research.

Objective 1: To identify the spatial patterns of regional land use/ cover changes (LUCC) in the Eastern Colombian Savannas during the last three decades (1980-2007) based on satellite imagery analysis and fieldwork.

Based on high resolution images (Landsat and CBERS data) for a period between 1985 to 2007, LUC maps, were produced and compared to obtain information on LUCC. The analyses of the images showed that the Eastern Colombian Savannas (ECS) is not a homogeneous and continuous vegetation formation as is often considered in the literature, such as large scale vegetation map of the world (Bartholome and Belward 2005). This study shows a mosaic of

different types of savannas, gallery forest, wetlands, rocky outcrops and a variety of land uses that form the characteristic savanna landscape. Although the ECS were of low governmental interest and economic and political interference up to the 70s, since the 80s dramatic changes occurred in the region. This study found that in 1987, 8% of the area of the ECS experienced some kind of change. This value increased to 22% in 2007, with an annual rate of loss of natural land cover of 0.89%. Compared with other savannas in northern South America the rate of change in the ECS is relatively low: in Venezuela an annual decrease of 2.3% was reported during the 80s and 90s with a transformation of 35% of this ecosystem (San José and Montes 2001). Brazil reports that 50% of the savannas have been lost up to the early 2000 (Brannstrom *et al.* 2008). Although the rate of change of the ECS is relatively low it must be taken into account that the changes have occurred in a very concentrated area in the southwest part of the ECS near the Andean foothills.

The most stable natural classes correspond to rocky outcrops, wetlands and water bodies. Forest and sandy savannas showed minor changes during 1987 and 2000 but have decreased in area from 2000 to 2007. The most dynamic natural classes were Flooded savanna and High savannas changing principally to anthropogenic areas including infrastructure, palm oil plantation, exotic pastures and culture mosaic. All anthropogenic classes show an increment of area during 1987 to 2007; only the class of culture mosaic showed a minor decrease in area between 2000 and 2007 (around 20,000 ha). The most important transformation is related with the increment of oil palm plantation which shows an large increase of area from 12,418 ha in 1987 to 163,997 ha in 2007, indicating an annual rate of change of 12.9%.

The driving forces behind the land use changes are basically associated with land management and development conducted by government policies: i. During the 80s and 90s rice cultivations was established in the southwest area and later on in the northwest; ii. By the end of the 90s palm oil plantations expanded and petroleum exploitation and coca cultures increased, converting into a palm

oil, petroleum and mining boom in the last years (Becerra *et al.* 2009). Changes mainly occurred in flooded and high savannas which were primarily replaced by palm oil plantations and petroleum infrastructure.

Objective two: Develop a regional algorithm to extract burned scars and determine the burned area, frequency and severity, based on a spatial-temporal model over a period of 10 years (2000-2009).

In Chapter 5 the development of an innovative regional algorithm to detect burned scars was described. The Savanna Fire Index (SFI) benefits from the difference in reflectance value in each band (mainly in infrared bands) after a fire event. When compared to other burned indices the SFI presents a high level of precision for detecting large and medium sized burned areas and an intermediate level for small areas. This algorithm shows some limitations related to the detection of small burned scars, which are often confused with flooded areas. Nevertheless its precision is shown to be higher than other related indices such as MIRBI, BAI, NBR and NDVI. For this reason, SFI was applied to analyse the MODIS data images for the period between 2000 and 2009.

Fire activity in the ECS is shown to produce a seasonal mosaic of patches of burned and unburned vegetation, which is consistent with other studies from other savannas in the world (Laris 2002). Equally the occurrence of fires has a consistent strong spatial pattern during the analysed period, where some areas show high frequency of burning while other shows a low frequency. In contrast to other tropical areas with high frequency of fires (Chuvieco *et al.* 2008), the fires in the ECS are predominantly of high density, short duration and high spatial variability. The flora has evolved in response to the fire characteristics as frequency, severity and seasonality. According to Van der Werf *et al.* (2003), in the tropics and subtropics, on average of 8 to 10 years are needed for a fire event to return to the same place, while in the Sandy savannas in the North of Brazil the average is 4 years (Barbosa and Fearnside 2005). For the ECS it is only two years.

The size area, duration and severity of the fire depend on its behaviour, which in turn depends on the type and properties of fuel (mixture of vegetation, chemical properties, load), topography (aspect, slope) and climatic conditions (rainfall, temperature, wind) at the moment of the fire (Dwyer *et al.* 2000; Chuvieco *et al.* 2006). Van der Werf *et al.* (2003) showed that in tropical and subtropical savannas (with less than 5% of trees) the burned size area is in average 5,000 ha, which is approximately seven times the average burned patch size found in this study. The inter-annual average burned patches size was very constant with exception of the years 2004-2005 and 2008-2009 where small burned scars were observed.

It was furthermore found that at the beginning of the dry season burned areas are small and their scars are of short duration. They become much bigger and scars persist longer as the dry season progresses. They diminish in size again by the end of the dry period, which is in accordance whit the results found in a study by Laris (2005) in the African savannas. Most of the medium and large burned scars during the dry period which are of long duration show an irregular form, influenced by the variations in speed and direction of the wind, while small burned scars are generally of short duration and present an elliptic form. These findings are in whit to other fire studies in savannas (Louppe *et al.* 1995; Russell-Smith *et al.* 1997; Laris 2005). In addition, the results indicate that the burned areas of the ECS contribute between 3% and 6% of the globally burned herbaceous vegetation area, and about 4% of the annually burned area in South America which coincides with the information Van der Werf *et al.* (2003) and Tansey *et al.* (2004) presented.

Objective three: Analyse and discuss the role of LUC, climate and topography on the fire regime using spatial and statistical methods.

The role of the ecological factors that form the savannas landscape and determine the ecological fire dynamics has been discussed by numerous authors for different savannas of the world such as Roraima savannas of the Brazilian

Amazon (Barbosa and Fearnside 2005); Southern Africa (Archibald *et al.* 2010); and in the Australian savannas (Bradstock 2010). Likewise Finney (1998), Shvidenko & Nilson (2000), Hudak *et al.* (2004), Barbosa & Fearnside (2005), Pennington *et al.* (2006) and Bradstock (2010) stated that these factors are related to: i. The climatic seasonality, responsible for providing the meteorological conditions of temperature and precipitation and determines the quantity of water that is deposited over the soil during the year; ii. The geomorphological processes and in particular its geological history and the composition of the soils that condition the flooding and distribution of the species; iii. The fire activity during the dry season which is the factor that shapes the landscape and regulates the savanna and; iv. The LUCC which are related to the presence of humans who have replaced the natural vegetation by the introduction of exotic grasses, infrastructure development and agricultural frontier expansion.

In chapter 6 the relationship between fire occurrence and environmental factors was analysed and discussed. Using two statistical methods, namely PCA and logistic regression, five predictive models were developed in which the importance of different environmental factors such as climate, topography, LFor and LUC on the occurrence of fire were investigated. It was found that although climate plays the most important role in the fire activity, it is not the only factor that determines this activity. It was shown that the model represented by only climate variables (model 1) could only predict fire occurrence at an overall accuracy of 0.44 (at the scale between 0 and 1). As more variables were included in the predictive model such as DEM and LFor the overall accuracy increased to 0.71 (model 2). When LFor was substituted by LUC the overall accuracy increased to 0.78 (model 3). In model 4 the combination of climatic, DEM, LUC and LFor variables resulted in an overall accuracy decrease to 0.76. Finally, when slope was included together with all other variables, the model showed an overall accuracy of 0.78 (model 5). Although similar overall accuracy values of the five models, model number 5 shows furthermore the highest ROC value (0.78) and was therefore selected as the best fitting model for the prediction of fire events in the ECS.

According to the results, fire activity in the ECS shows a high degree of spatial variability related to the different environmental factors. It can be argued that this variability is based on the presence of the different vegetation formations. For flooded savannas, fire activity is marked by the fluvial regime to which it is submitted during most part of the year. For this type of savanna, the proximity to the Andean mountains and its extreme alteration in topography from the flat to convex planes, means that during the rainy season the rivers that originate in the mountains burst their banks, flooding these savannas during periods of 3 to 8 months. Thus during the period of flooding, the activity of fires and the intensive use of agriculture and livestock is practically impossible. By the end of the rainy season a retreat in the flooded areas commences, leaving the elevated areas free of flooding which are made use of by humans to induce the first burnings to renew the grasses and establish areas for their livestock. By the end of November, the period of fires starts which is characterized by burnings of small size, low frequency and severity. As the dry season advances (December to March) the activity of fire increases (frequency goes up) and the size of burning scars expands.

The fire activity is controlled by the presence of Sandy savannas in its near surroundings which are located on the elevated topographical formations called ‘dunes’ and the higher representations of wetlands. These savannas are typically configured by a mosaic of burned areas, Flooded savannas and wetlands. During the dry season a system of livestock ranching is implemented which begins by the reallocation of the livestock from the elevated areas that the flooding did not reach to the areas formerly flooded incorporating a rotation system of burnings, regeneration and ranching use to be able to raise and maintain the livestock. Once the area has been burned and recovered, the livestock starts to consume new pastures. As the dry season progresses, new areas are being burned and the livestock steadily advances entering other areas that have recovered.

High savannas are subject to extensive periods of rain from April to November, that are waterlogged due to high water table from their soil, leading

to high biomass production and growth of woody elements that become potential fuel for occurrence of fires. In late November and middle-April, begins the period of the fires which initially occur in patches of low area and severity. As the season progresses, the fires become more widespread, frequent and intense which form the shape and area of fires, reaching areas between 500,000 and 600,000 ha. Compared to other types of savannas in the ECS, the largest burned event in the high savannas is nearly seven times larger than the Sandy savanna. For these savannas it is also found that in periods of severe drought, fire reaches gallery forest areas, which become a natural barrier that control the area and expansion of fire activity. These riparian strips form microclimates that dampen the severity of the fire due to the increased humidity in these forest strips (Venehlaas *et al*. 2005). At the beginning of the dry season, the fire impact on gallery forests and isolated trees is low, in contrast with the end of the dry season where fires can cause major damage. This behaviour is similar to dry savannas in Southern Africa (Archibald *et al.* 2010).

With respect to the forest formations the burning events have been associated mainly to two causes: i. Prolonged duration of the dry season: the gallery forests that are found on the high plains are affected by the activity of fire mainly at the end of the dry season, due to the large disposition of dry material that accumulates during the entire season and the low conditions of humidity, converting itself in combustion for large fires that originate from the savannas and ii. Human action for hunting and cleaning and expansion of savanna areas to establish cultures and livestock areas. The forests of the ECS are being submitted to processes of selective extraction for personal and in some cases commercial purposes.

From the ecological point of view, the fire in the savannas is a process absolutely essential to the ecosystem and should not be altered beyond its “normal range”. When removed, savannas are transformed into forest and shrub and loss of habitats and species occur (Bond *et al.* 2004).

Objective four: To discuss the impact of land use/cover change and fire regime in savannas on a regional and global scale.

Regional differences are highly relevant because savannas vary much depending on the proportions of grass and shrub/tree components as a response to soil, climate and management (Eiten, 1971). Delmas *et al*. (1995) and Barbosa and Fearnside (2005a) have shown the complexity of the burning processes in savanna fires, with fire density and severity influenced by physical controls (combustion), biological characteristics (biomass quantity and quality), environmental factors (topography and climate) and management practices. With global warming some of these factors will change due to the expected temperature increases and longer droughts in this biome. Hoffmann *et al*. (2002) conclude that there is an apparent positive feedback between rising carbon emissions, global warming and fires, which could increase fire frequency by 40% in the near future.

The complex heterogeneity of savannas makes it difficult to develop a general method for all applications in different savanna regions in the world. Fine resolution, spatially explicit data on land-use/cover changes are required to define the impact of landscape fragmentation on biodiversity, composition, structure and functionality of ecosystems. However the methodological approach of this study is considered suitable for several regional savannas founds in Brazil, Bolivia, Paraguay, Venezuela and Guiana, due to similarity in structure, composition and environmental conditions. A valuable and interesting comparison would be also possible with savannas of South Africa and Australia (Archibald *et al*. 2009). The incorporating of this regional study on spectral analysis, LUC, LUCC, algorithm development, product validation and comparison allows the improvement of global mapping of LUC and burned maps.

Moreover regional information generated systematically over a long period of time on land cover changes and fire regime contributes greatly to improving

estimations of carbon emission by savanna fires (Etter, *et al*. 2010). The major impact of land use changes along the expanding agricultural fronts on climate is through carbon emissions from deforestation in forests and changing fire patterns, cattle densities, and vegetation biomass in savannas. Although forests have been considered to be the key land cover component of the terrestrial carbon cycle (Ramankutty *et al*. 2007; Houghton, 2005), the importance of savannas is being increasingly recognized as growing human impacts transform this ecosystem (Grace, 2004).

The intercomparison of different satellite data and algorithms provides an indication of gross differences and insights into the reasons for the differences. This approach gives the tools to obtain products suitable to compare with independent reference data and finally give information to help users decide if and perhaps how to use a product and, combined with product quality assessment, to identify needed improvements in satellite data and products (Roy *et al*. 2010).

7.1. Future work

Several aspects which have not been considered within this study have given the basis for a series of questions that are proposed for future studies:

i. How can we determine if the fires are anthropogenic or natural? Although during this study an analysis was done on the presence/ absence of fire events during a very short period of time, it is not sufficient to determine its origin;

ii. Which micro-climatic factors of composition, structure and others can explain in more detail the regime of fire?;

iii. Which factors determine that some areas present high frequency of burnings and others do not have a single event during a decade?;

iv. How to define the differences in composition, structure and biomass of the vegetation formation between the areas frequently and rarely/ never burned?;

v. Is it possible to determine management strategies for fire according to the different types of savannas?. Which strategies would be the best concerning the different land-cover characteristics?;

vi. What is the role of the hydrological regime in the dynamics of the ECS?. The regime of inundation is one of the determinant factors in this ecosystem and especially in the flooded savannas;

vii. What is the process of degradation of the land in the ECS?. The climatic variation, the change of land-use and the increase of the population could affect the actual characteristics of the soil (content of organic material, humidity and chemistry).

This study promotes the first understanding of the processes of transformation in the land-use and the fire regime in the ECS, from the point of view of remote sensing. Using this knowledge provides a detailed view to understand the dynamics of this important ecosystem in Colombia. Although the obtained results accomplished adequately the stated objectives, it is considered important to compare the results and developed index to other similar ecosystems in South America such as the Cerrado in Brazil, the savannas of Bolivia and Venezuela and savanna regions in Africa and Australia. As technology in remote sensing advances, it is important to continue investigation, development and improvement of new indices and techniques that allow a continuous monitoring of changes of LUC and the ecological factors that form this valuable ecosystem.

Temperature and precipitation data average to 34 climatic station and climatic graphs of monthly rainfall and temperature average acquired from IDEAM between 1938 and 2007.

CODE	STATION	Lat. N	Long.W	Alt.	YEARS	January	February	March	April	May	June	July	August	September	October	November	December	Prom
3519503	AGUAZUL	5.1800	-72.5500	380	1974/2006	27.6	27.8	27.7	26.5	25.9	25.2	25.1	25.5	25.9	26.3	26.7	27.2	26.4
3705501	APTO ARAUCA	26.400	-70.7300	128	1951/2007	27.4	28.4	28.9	27.8	26.6	25.9	25.7	26.1	26.6	26.9	27.0	27.1	27.1
3801503	APTO PTO CARREÑO	6.1800	-67.4800	50	1972/2007	29.3	30.4	30.8	29.4	27.7	26.7	26.4	26.8	27.3	27.9	28.3	28.7	28.3
3503502	APTO VANGUARDIA	4.1700	-73.6200	423	1941/2007	27.4	27.5	26.7	25.7	25.4	24.6	24.6	25.1	25.6	25.9	26.1	26.6	25.9
3521501	APTO YOPAL	5.3200	-72.3800	325	1974/2006	26.7	27.3	26.9	25.7	25.2	24.5	24.2	24.9	25.6	25.6	25.6	25.9	25.7
3203502	BALSORALA	2.5000	-73.9300	372	1983/2007	28.0	28.4	28.2	26.5	25.7	25.0	24.9	25.1	25.8	26.1	26.5	27.0	26.2
3501505	BARBASCAL	3.7000	-73.4000	250	1992/2207	26.3	26.4	26.0	25.4	24.9	24.1	23.7	24.1	24.7	25.1	25.5	25.9	25.3
3503501	BASE AEREA APIAY	4.0800	-73.5700	400	1972/2007	26.6	27.4	26.5	26.1	25.4	24.7	24.5	25.1	25.6	26.0	26.1	26.2	25.9
3504502	LA CABANAHDA	4.2700	-73.2700	305	1979/2007	26.7	27.0	26.6	25.6	25.2	24.6	24.2	24.9	25.3	25.5	25.6	26.0	25.7
3303501	CARIMAGUA	4.5800	-71.3700	200	1972/2006	27.0	27.8	27.8	26.5	25.5	24.8	24.6	25.0	25.5	26.0	26.4	26.5	26.2
3207506	LA COOPERATIVA	3.3700	-73.7000	280	1986/2005	25.8	25.8	25.8	25.4	25.2	24.7	24.6	24.8	25.3	25.4	25.5	25.7	25.3
3305501	CUMARIBO	4.4000	-69.8500	125	1991/2007	27.2	27.6	27.3	26.4	25.7	25.2	24.9	25.2	25.9	26.1	26.4	26.8	26.3
3401501	LAS GAVIOTAS	4.5500	-70.9300	171	1967/2007	27.3	27.4	27.3	26.5	26.2	25.6	25.4	25.7	26.6	26.7	26.7	27.0	26.8
3510505	GUAICARAMO	4.4000	-72.9500	190	1993/2007	26.5	26.8	26.4	25.7	25.3	24.8	24.5	24.8	25.5	25.4	25.6	25.8	25.6
3207504	LA HOLANDA	3.5200	-73.7200	360	1981/2007	27.3	27.5	27.1	25.7	24.9	24.5	24.2	24.8	25.3	25.7	26.0	26.5	25.9
3509511	HUERTA LA GRANDE	4.6500	-72.9200	255	1995/2007	24.4	24.8	24.1	23.4	23.0	22.5	22.1	22.8	23.3	23.4	23.3	23.6	23.4
3206501	LEJANIAS	3.5300	-74.0200	680	1989/2007	26.9	27.4	27.0	25.7	25.2	24.4	24.2	24.9	25.4	25.6	25.8	26.1	25.7
3502502	LA LIBERTAD	4.0700	-73.4700	336	1968/2007	26.7	26.5	26.4	25.6	25.3	24.6	24.2	24.7	25.3	25.5	25.9	26.2	25.6
3203501	LA MACARENA	2.1800	-73.8000	350	1967/2007	28.1	28.3	28.3	27.1	26.2	25.4	25.2	25.7	26.1	26.4	26.6	27.0	26.7
3512501	HDAL MARGARITAS	4.3500	-72.1700	150	1976/2007	25.2	25.5	25.1	24.5	24.1	23.5	23.1	23.5	24.3	24.4	24.5	24.8	24.5
3207505	MESETAS	3.3500	-74.0300	620	1983/2007	27.4	28.1	28.2	26.9	26.1	25.6	25.4	25.8	26.4	26.7	27.0	26.9	26.8
3522502	MODULOS	4.8700	-71.4000	130	1978/2007	27.9	28.4	28.8	27.2	26.2	25.5	25.3	25.8	26.4	26.8	26.9	27.2	26.9
3601501	PAZ DEARIPORO	5.8800	-71.8800	342	1996/2006	27.2	28.1	27.7	26.3	25.4	24.8	24.5	24.9	25.4	25.8	26.1	26.3	26.1
3207508	PTO LLERAS	3.2800	-73.3800	245	1991/2007	26.2	26.6	26.4	25.8	25.5	25.0	24.6	25.1	25.6	25.9	25.8	26.2	25.8
3704501	SARAVENA	6.9500	-71.8800	148	1976/2006	25.4	26.1	26.2	25.9	25.6	24.7	24.8	25.0	25.4	25.7	25.7	25.4	25.5
3523502	TAMARA	5.8300	-72.1700	1200	1996/2006	22.4	21.9	22.3	21.8	21.2	20.9	20.0	20.7	20.6	22.0	22.2	22.3	21.8
3602501	TAME	6.4500	-71.7700	350	1987/2006	26.1	26.4	26.8	26.3	26.0	25.5	25.2	25.4	25.7	26.0	26.0	26.2	26.0
3403502	EL TAPON	5.1200	-69.1500	315	1973/2003	27.8	28.4	28.0	26.8	25.9	25.3	25.0	25.3	25.8	26.2	26.6	27.0	26.6
3519502	TAURAMENA	5.0200	-72.7500	460	1974/2005	26.0	26.5	26.3	25.3	25.1	24.7	24.4	24.7	25.1	25.4	25.5	25.7	25.3
3523503	TRINIDAD	5.4200	-71.6500	265	1996/2006	27.1	27.6	28.0	26.6	26.0	25.6	25.5	25.9	26.5	26.1	26.7	26.8	26.5
3403501	TUPARROBOCASTO	5.3500	-67.8700	250	1972/2006	28.7	29.0	29.0	27.9	26.8	26.1	26.0	26.3	26.8	27.1	27.4	27.8	27.3
3503507	UNILLANOS	4.1200	-73.6300	340	1983/2007	26.4	26.5	26.2	25.4	24.9	24.2	24.1	24.6	25.1	25.4	25.5	25.7	25.3
3207503	VISTA HERMOSA	3.0300	-73.7300	325	1969/2007	27.0	27.4	27.2	26.2	25.6	24.9	24.7	25.2	25.7	25.9	26.1	26.4	26.0

Annual evolution of water balance (Thornwaite) - Aguazul

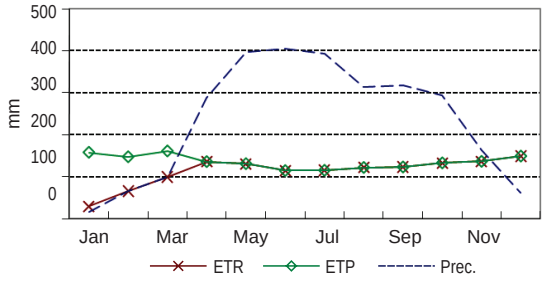

Annual evolution of water balance (Thornwaite) - Arauca

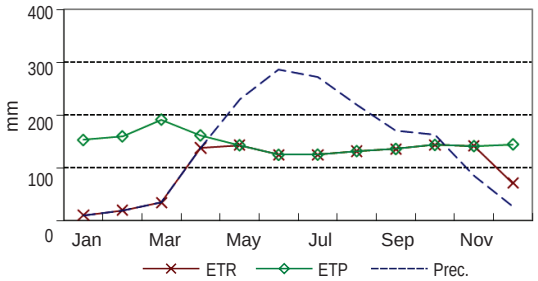

Annual evolution of water balance (Thornwaite) - Pto Carreño

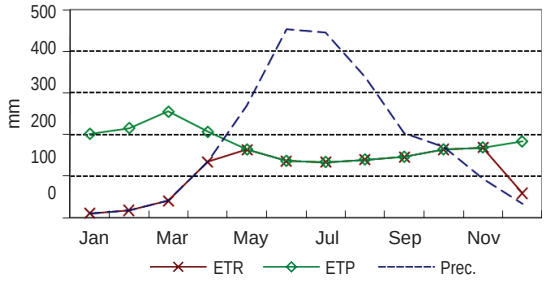

Annual evolution of water balance (Thornwaite) - Yopal

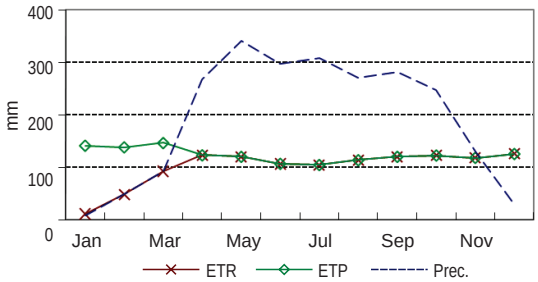

Annual evolution of water balance (Thornwaite) - Balsorala

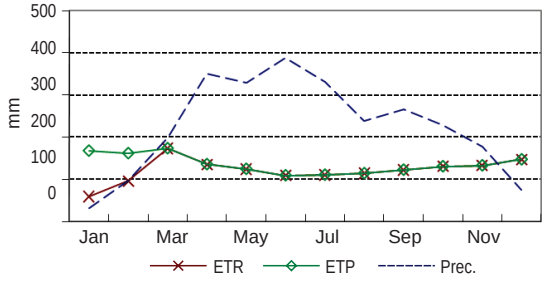

Annual evolution of water balance (Thornwaite) - Barbascal

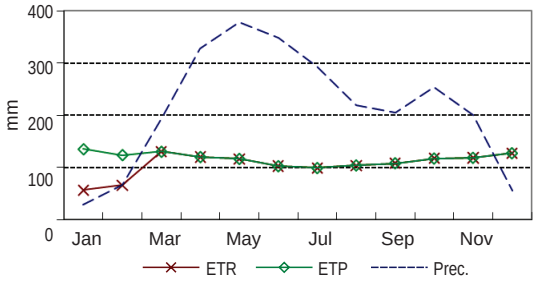

Annual evolution of water balance (Thornwaite) - Apiay

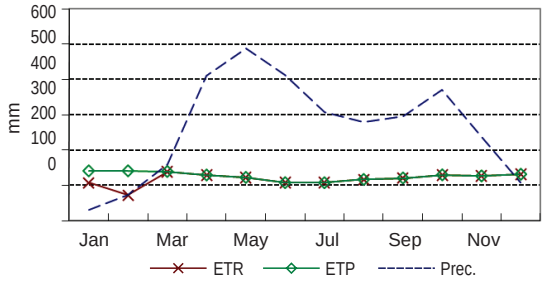

Annual evolution of water balance (Thornwaite) - La Cabanahda

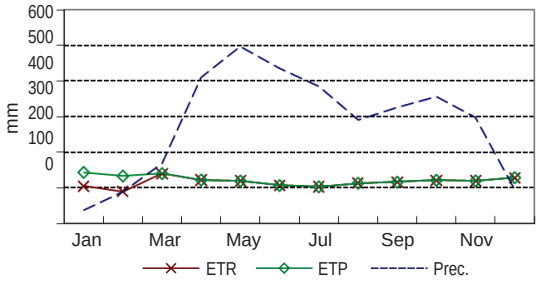

Annual evolution of water balance (Thornwaite) - Carimagua

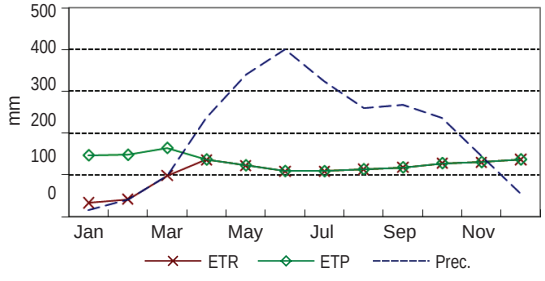

Annual evolution of water balance (Thornwaite) - La Cooperativa

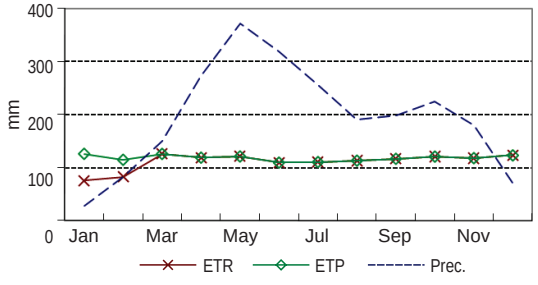

Annual evolution of water balance (Thornwaite) - Cumaribo

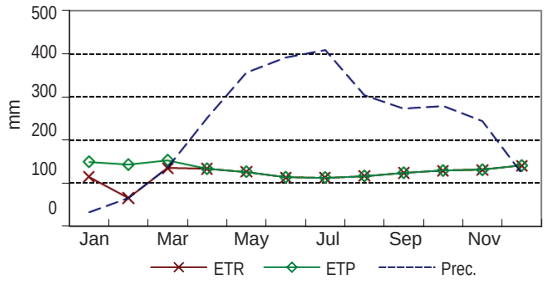

Annual evolution of water balance (Thornwaite) - Las Gaviotas

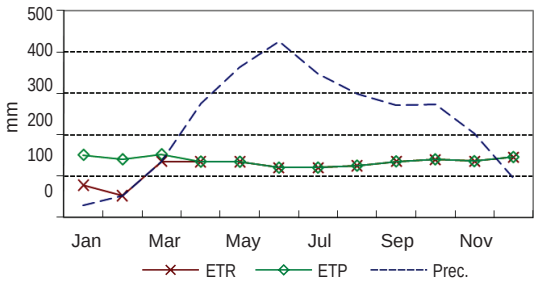

Annual evolution of water balance (Thornwaite) - Guicaramo

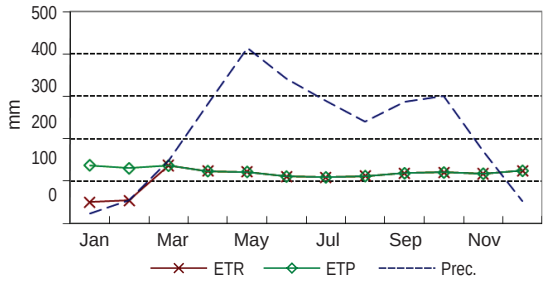

Annual evolution of water balance (Thornwaite) - La Holanda

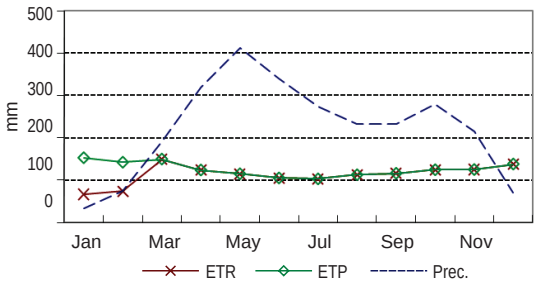

Annual evolution of water balance (Thornwaite) - Huerta La Grande

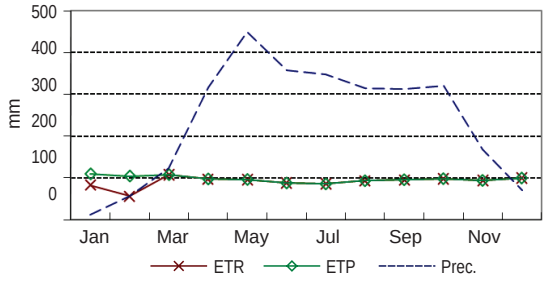

Annual evolution of water balance (Thornwaite) - Lejanias

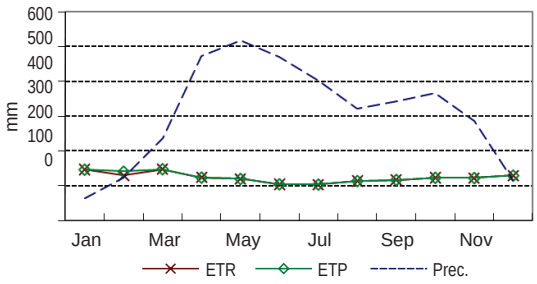

Annual evolution of water balance (Thornwaite) - La Libertad

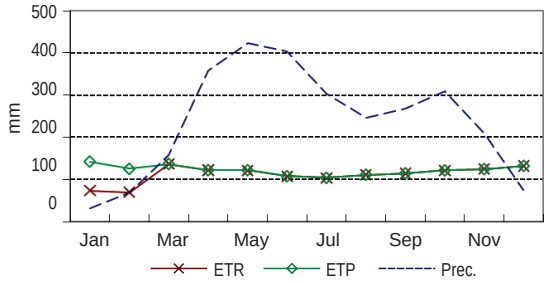

Annual evolution of water balance (Thornwaite) - La Macarena

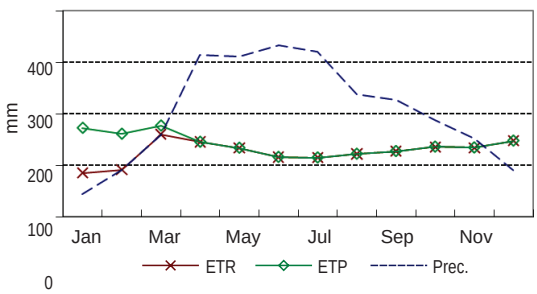

Annual evolution of water balance (Thornwaite) - Margaritas

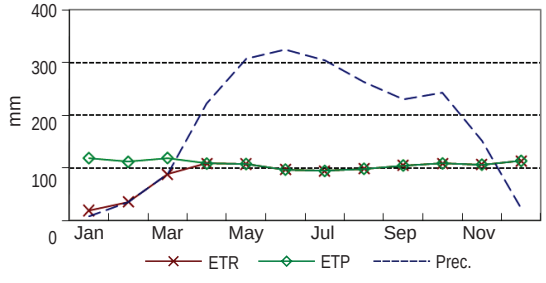

Annual evolution of water balance (Thornwaite) - Mesetas

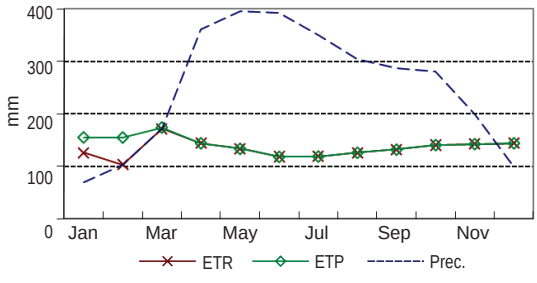

Annual evolution of water balance (Thornwaite) - Modulos

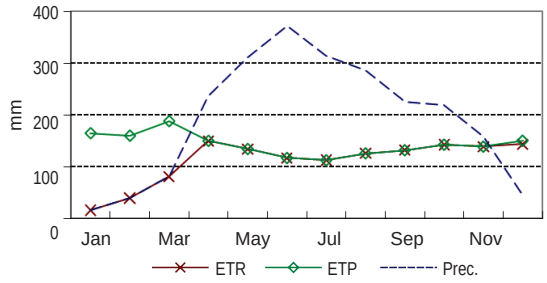

Annual evolution of water balance (Thornwaite) - Paz de Ariporo

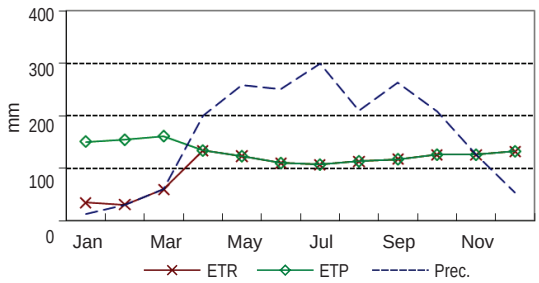

Annual evolution of water balance (Thornwaite) - Pto Lleras

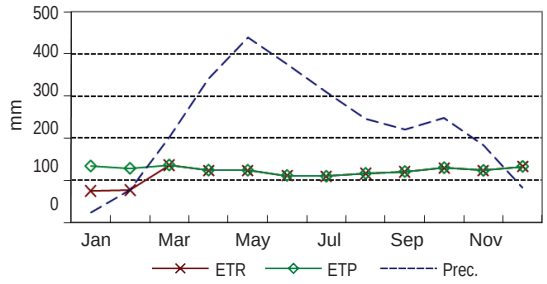

Annual evolution of water balance (Thornwaite) - Saravena

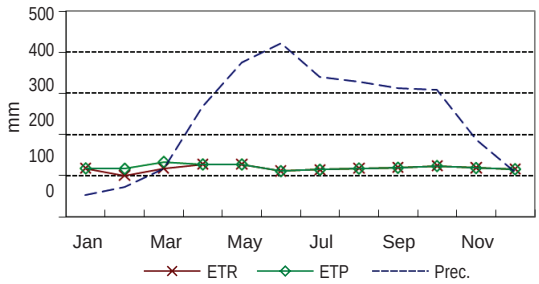

Annual evolution of water balance (Thornwaite) - Tamara

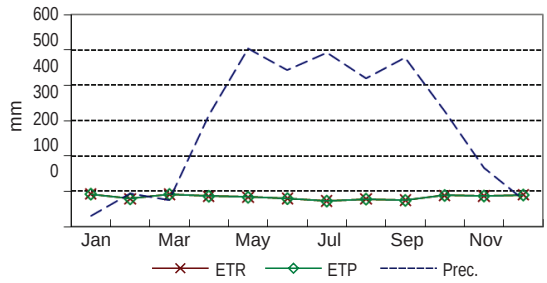

Annual evolution of water balance (Thornwaite) - Tame

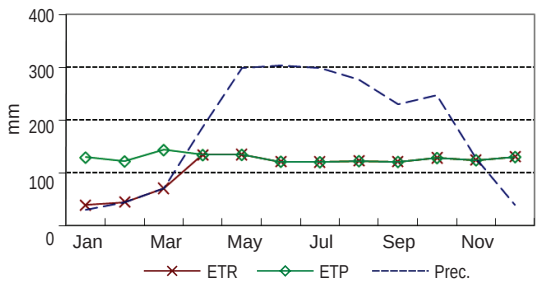

Annual evolution of water balance (Thornwaite) - El Tapon

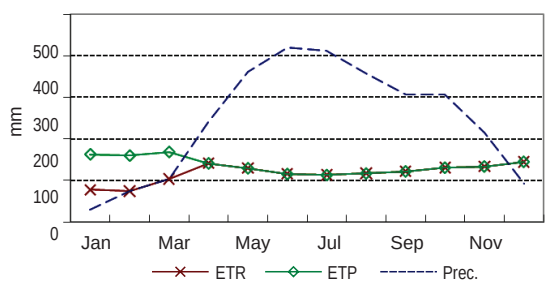

Annual evolution of water balance (Thornwaite) - Tauramena

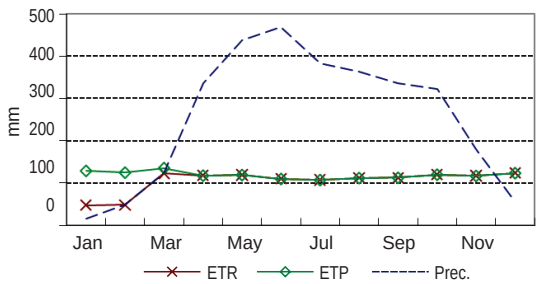

Annual evolution of water balance (Thornwaite) - Trinidad

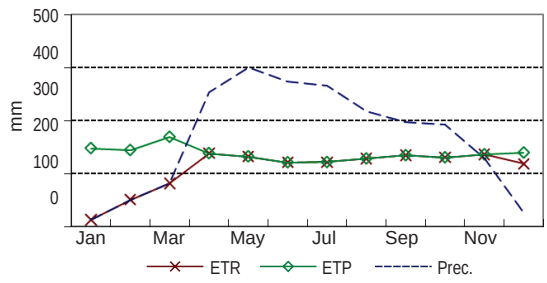

Annual evolution of water balance (Thornwaite) - Tuparrobocasto

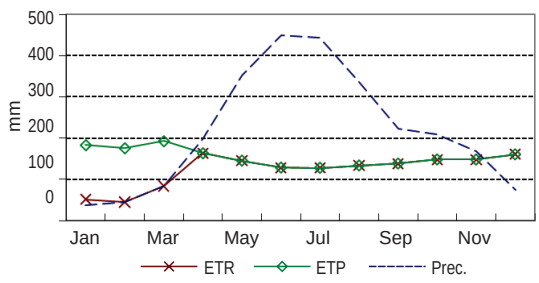

Annual evolution of water balance (Thornwaite) - Unillanos

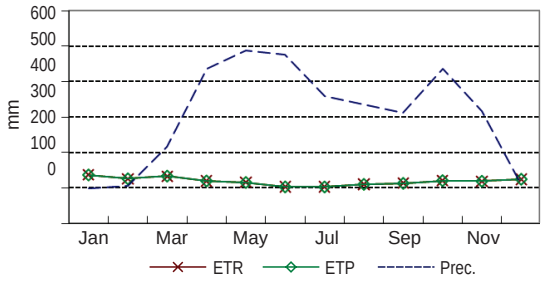

Annual evolution of water balance (Thornwaite) - Vanguardia

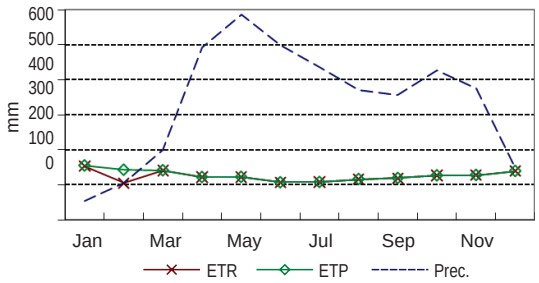

Annual evolution of water balance (Thornwaite) - Vista Hermosa

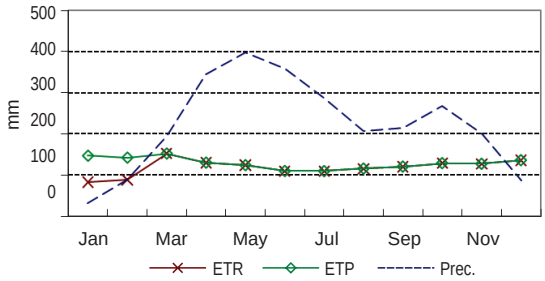

Land Use/Cover (LUC) legend description using Landsat and photography patterns

CATEGORY	DESCRIPTION	LANDSAT IMAGE	PHOTOGRAPHY
Infrastructure	Cities, towns, areas covered by road infrastructure such as roads, highways, bridges and airports. These surfaces incorporate all of these areas through a process of urbanization and land-use change to commercial, industrial and recreational services.	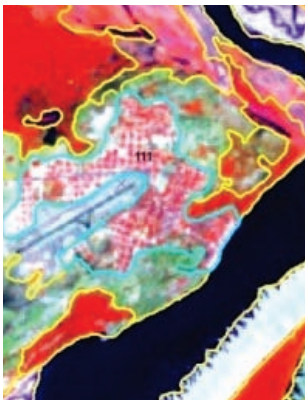	
Palm oil plantations	Coverage dominatedby oil palm (Elaeis guineensis), per*ennial stem solit*ary pinnate leaves belonging to the family Arecaceae, which can reach heights of up to 12 meters. Cultivation takes place preferentially on flat to slightly hilly terrain, situated on land below 500 m.	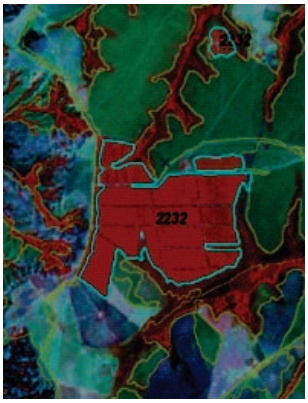	
Exotic pastures	This coverage includes land occupied by introduced grasses (Poaceae), the production oriented management practices (cleaning, liming and/or fertilizer, etc.) and a certain level of technology used to prevent the presence or development of other types of land cover and assigned as grazing for a period of two years or more.	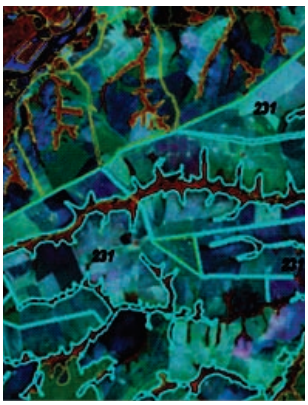	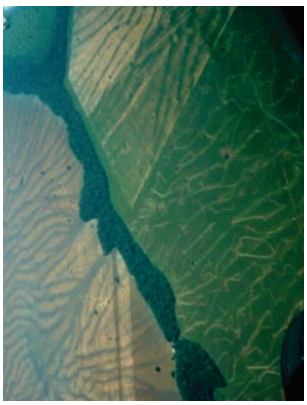
Culture Mosaic	Units that include two kinds of agriculture (pastures and crops) arranged in an intricate pattern of geometric mosaics that makes it difficult to separate them in individual geometric arrangements. This cover is related to artificial management practices and local land tenure as crops and pastures, where the plot size is very small (less than 25 ha)	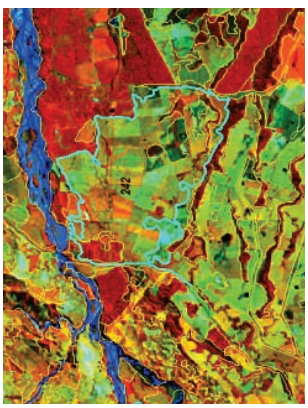	

CATEGORY	DESCRIPTION	LANDSAT IMAGE	PHOTOGRAPHY
Forest	Plant community dominated by elements typically trees, which form a closed crown (canopy) of more or less continuous coverage. Tree cover represents over 70% of the total area with height above the 15 meters. This category also includes gallery forest which forms narrow strips of forest networks dominated by trees associated with palms and scrubs elements, located around permanent or temporary flooded banks of rivers and creeks.		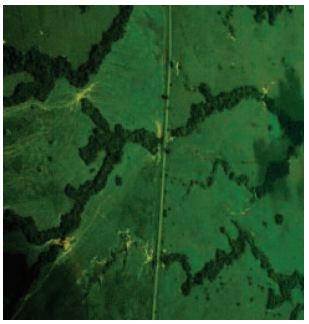
High savanna	Plant community dominated by herbaceous elements typically developed naturally, which form a dense cover (>70% occupancy). This cover is developed in areas which are not subject to periodically flooding and may or not have trees and/or scattered shrubs elements.	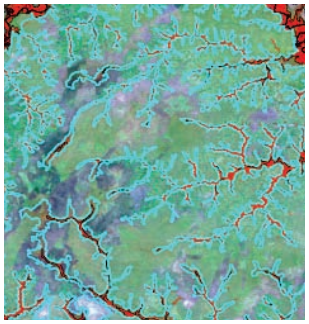	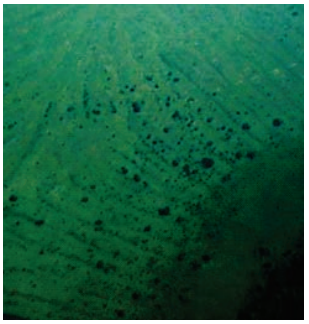
Flooded savanna	Plant community dominated by herbaceous elements typically developed naturally, which forms a dense cover (> 70% occupancy). This covers develops in areas subject to periodically flooding, and may or not have tree and/or scattered shrubs elements.	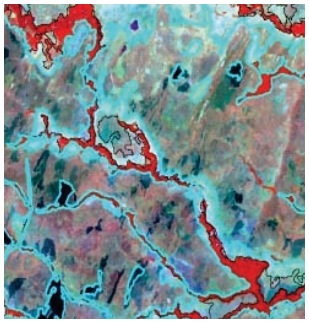	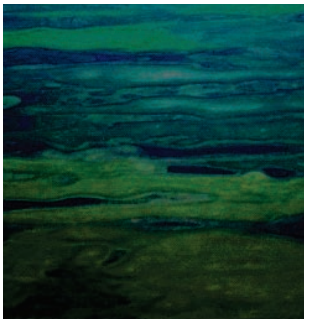
Sandy savanna	Plant community dominated by open herbaceous vegetation with coverage between 30% and 70%. No presence of tree. Developed on areas of sandy soils that do not retain moisture	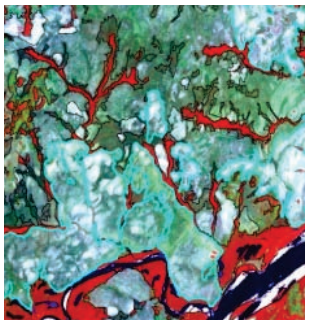	
Rocky outcrops	Areas where the ground surface consists of layers of exposed rocks, without development of vegetation, usually arranged in steep slopes, forming steep cliffs, rocks and bare areas associated with volcanic activity or glacier.	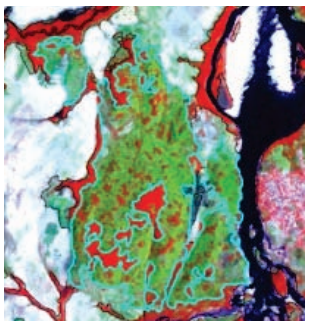	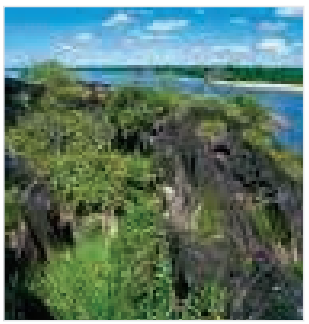

CATEGORY	DESCRIPTION	LANDSAT IMAGE	PHOTOGRAPHY
Secondary vegetation	Area covered by natural forests where there is human intervention and forest recovery. This category is seen as patches of a variety of forms that are distributed irregular in the matrix of forest.		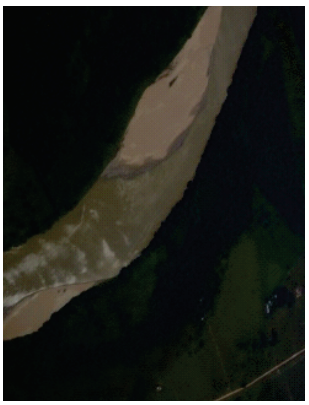
Burned areas	Areas affected by recent fires, for which charcoal materials are still present. These areas are found in semi-natural areas, such as forests, crops, savannas and shrubs.	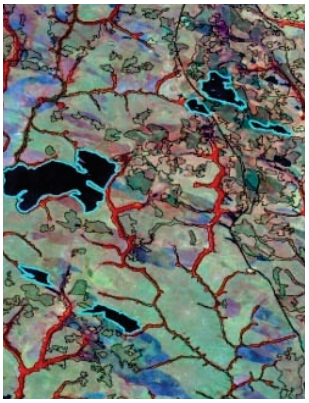	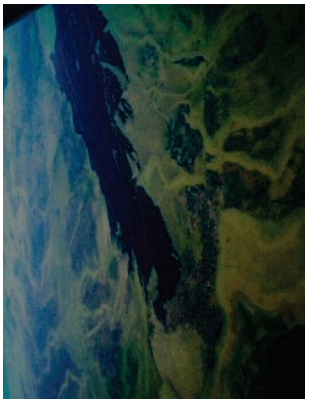
Wetland	Lowlands, usually flooded during most of the year such as flood plains, ancient valleys and natural depressions where the water table remains on a stable level or rises during season.	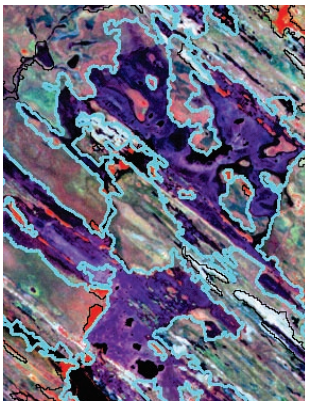	
Water	Natural strems of water flowing continuously and water surface reservoirs, open or closed, fresh or brackish, which may or may not be connected with a river. The flood plains are formed from bodies called marshes, which are associated with areas of major overflowing rivers overflowing. Swamps may contain sandy and muddy islets, irregularly shaped elongated and fragmented.	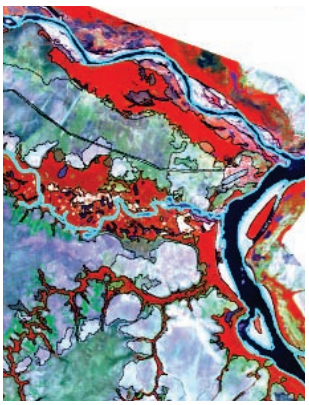	

APPENDIX C

Photography register obtain in different visits in the Eastern Colombian Savannas (Romero-Ruiz, M. 2006, 2007 and 2008)

Cumaral town, near Meta river (Meta, Colombia)

Palm oil plantations in Castilla La Nueva (Meta, Colombia)

Forestal plantation, near Villanueva (Casanare, Colombia)

Manacacias river mouth (Puerto Gaitan, Meta, Colombia)

Flooded savannas and wetlands in Paz de Ariporo (Casanare, Colombia)

High flat savannas in Primavera (Vichada, Colombia)

Morichal forest over Pauto river (Casanare, Colombia)

Foothills forest, near Restrepo (Meta, Colombia)

Indigenous reservation near Santa Rosalia (Vichada, Colombia)

Andropogum bicornis (Rabo de Zorro) in High savannas (Meta, Colombia)

Smoke plume near to Puerto Gaitan (Meta, Colombia)

Fire activity in High savannas near Santa Rosalia (Vichada, Colombia)

Fire smoke in High savannas

Aerial view of smoke plume in High savannas of Puerto Gaitan, Meta

Burned scars in High savanna near or Puerto Gaitan (Meta, Colombia)

Old and recently burned scars in High savannas of Puerto Gaitan

Old burned scard in High savanna of Puerto Gaitan

Aerial view of old and recently burned scars in High savannas

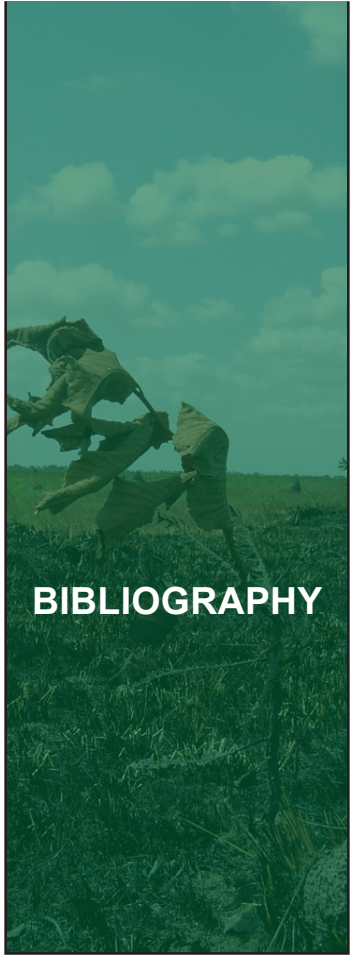

BIBLIOGRAPHY

Plume smoke in high savannas near of Carimagua (Meta, Colombia)

Bibliography

Aaviksoo, K. (1995). “Simulating vegetation dynamics and land-use in a mire landscape using a Markov model.” *Landscape and Urban Planning* **31**: 129-142.

Adler, F.R. and J. Mosquera. 2000. Is space necessary? Interference competition and limits to biodiversity. *Ecology* **81**: 3226-3232.

Andreae, M. O. (1992). Biomass burning: its history, use and distribution and its impact on environmental quality and global climate. In: *Global Biomass Burning, Atmospheric, Climatic, and Biospheric Implications*. J. Levine. Cambridge, MA, MIT press**:** 3-21.

Archibald, S., D.P. Roy, B. W. Van Wilgen, and R.J. Scholes. (2009). What Limits Fire?: An examination of drivers of burnt area in sub-equatorial Africa. *Global Change Biology* **15**: 613-630.

Arino, O. and J. M. Melinotte (1995). *Firex Index Atlas Earth Observation Quartely ESA/ESRIN*. Frascati, Italy, Project & Engineering Department, Earth Observation Division. **50**.

Arino, O., I. Piccolini, E. Kasinshke, F. Siegert, E. Chuvieco and P. Martin (2001). Methods of mapping surfaces burned in vegetation fires. In: *Global and regional vegetation fire monitoring from space, planning a coordinated international effort*. J. G. Ahern, J. G. Goldhammer and C. O. Justice. The Hague, SPB Academic Publishing.

Armenteras, D., M. Romero and G. Galindo (2005). “Vegetation fire in the savannas of the Llanos Orientales of Colombia.” *Word Resources Review* **17**: 628-640.

Ayalew, L. and H. Yamagishi (2005). “The application of GIS-baed logistic regression for landslide susceptibility mapping in the Kakuda-Yahiko Mountains, Central Japan.” *Geomorphology* **65**: 15-31.

Ayarza, M., E. Amézquita, I. Rao, E. Barrios., M. Rondon., Y. Rubiano and M. Quintero. (2007). Advances in improving agricultural profitability and overcoming land degradation in savanna and hillside agroecosystems of tropical America. In Advances in Integrated Soil Fertility Management in Sub-Saharan Africa: Challenges and Opportunities, ed. A. Bationo. New York: Springer.

Bachmann, A. and B. Allgoewer (2001). "A consistent wildland fire risk terminology is needed." In: *Fire Management Today (Washington Forest Service USDA)* **61(4)**: 28-33. Available at: htpp://www.fs.fed.us/fire/planning/fmt/fmt-pdfs/fmt61-24.pdf.

Bannanari, A., D. Morin, F. Bonn and A. R. Huete (1995). "A review of vegetation indices." *Remote Sensing of Environment* **13**: 95-120.

Baptiste, G. (2006). Utilizar. In: *Plan de Acción en Biodiversidad de la Cuenca del Orinoco, Colombia 2005-2015*. H. Correa, S. L. Ruiz and L. M. Arevalo (ed). Bogotá, Instituto de Investigaciones en Recursos Biológicos Alexander von Humboldt.

Barbosa, P. M., J. M. Gregoire and J. M. Pereira (1999). "An algorithm for extracting burned areas from time series of AVHRR GAC data applied at a continental scale." *Remote Sensing of Environment* **69**: 253-263.

Barbosa, R. I. and P. M. Fearnside (2005). "Above-ground biomass and the fate of carbon after burning in the savannas of Roraima, Brazilian Amazonia." *Forest Ecology and Management* **216(1-3)**: 295-316.

Barbosa, R. I. and P. M. Fearnside (2005). "Fire frequency and area burned in the Roraima savannas of Brazilian Amazonia." *Forest Ecology and Management* **204(2-3)**: 371-384.

Bartholome, E. and A. S. Belward (2005). "GLC2000: a new approach to global land cover mapping from Earth observation data." International Journal of Remote Sensing **26**: 1959-1977.

Bauer, T. and K. Steinnocker (2001). "Pre-parcel land use classification in urban areas applying a rule-based techniques." *GeoBIT* **6**: 24-27.

Beard, J. S. (1955). "The classification of tropical American vegetation-types." *Ecology* **36**: 89-100.

Biddulph, J. and M. Kellman (1988). "Fuels and fire at savannas-gallery forest boundaries in southeastern Venezuela." *Journal of Tropical Ecology* **14**: 445-461.

Bilbao B. and Medina E. (1990). Nitrogen-use efficiency for growth in a cultivated African grass and a native South American pasture grass. *J. Biogeography* **17**: 421-425.

Blaschke, T. and J. Strobl (2001). "What's wrong with pixels?: Some recent developments interfacing remote sensing and GIS." *GeoBIT* **6**: 12-17.

Blydenstein, J. (1967). "Tropical savannas vegetation of the Llanos of Colombia." *Ecology* **48**: 1-15.

Boles, S. H. and D. L. Verbyla (2000). "Comparison of three AVHRR based fire detection algorithms for interior Alaska." *Remote Sensing of Environment* **72**: 1-16.

Bond, W. J., F. I. Woodward and G. F. Midgley (2004). "The global distribution of ecosystems in a world without fire." *New Phytologist* **165**: 525-538.

Bond W.J. and J.E. Keeley. 2005. Fire as a global 'herbivore'the ecology and evolution of flammable ecosystems. *Trends in Ecology and Evolution* **20**: 387-394.

Boschetti, L. and D.P. Roy. (2008). Defining a fire year for reporting and analysis of global interannual fire variability. *Journal of Geophysical Research* **113**: G03020.

Boschetti, L., H. Eva, P. A. Brivio and J. M. Gregoire (2004). "Lessons to be learned from the comparison of three satellite derived biomass burning product." *Geophysical Research Letters* **31**: 1-4.

Bowman, D. M., J. Balch, P. Artaxo, W. J. Bond, J. Carlson, M. Cochrane, C. D´Antonio, R. DeFries, J. Doyle, S. Harrison, F. Johnston, J. Keeley, M. Krawchuk, C. Kull, B. Martson, M. Moritz, I. C. Prentice, C. I. Roos, A. C. Scott, T. W. Swetman, G. Van der Werf and S. Pyne (2009). "Fire in the Earth Systems." *Science* **324**: 481-484.

Bowman, D. M., Y. Zang, A. Walsh and R. J. Williams (2003). "Experimental comparison of four remote sensing techniques to map tropical savanna fire scar using Landsat TM imagery." *International Journal of Wildland Fire* **12**: 341-348.

Bradstock, R. A. (2010). "A biogeographic model of fire regimes in Australia: current and future implications." Global Ecology and Biogeography **19**(2): 145-158.

Brannstrom, C., W. Jepson, A. M. Filippi, D. Redo, Z. Xu and S. Ganesh (2008). "Land change in the Brazilian Savanna (Cerrado), 1986-2002: Comparative analysis and implications for land-use policy." *Land Use Policy* **25(4)**: 579-595.

Bucini, G. and E. F. Lambin (2002). "Fire impact on vegetation in Central Africa. A remote sensing based statistical analysis." *Applied Geography* **22**: 27-48.

Bush, M. B., M. R. Silman, C. McMichael and S. Saatchi (2008). "Fire, climate change and biodiversity in Amazonia: a Late-Holocene perspective." *Philosophical Transaction of The Royal Society* **363**: 1795-1802.

Camacho de Coca, F., G.-H. F., M. Giabert and J. Melia (2002). *La Anisotropía de la BRDF: Una nueva signatura de las cubiertas vegetales*. Valencia, Departament de Termodinámica. Facultat de Física, Universitat de Valencia.

Carmona-Moreno C., A. Belward ., J.P. Malingreau., A. Hartley., M. Garcia-Alegre., M. L. Antonous., K. Iyz., V. Buchshtaber and V. Pivivarov (2005). Characterizing interannual variations in global fire calendar using data from Earth observin satellites. *Global Change Biology* **11**: 1537-1555.

Chacón, E. M. (2007). Ecological and spatial modelling: Mapping ecosystems, landscape changes and plant species distribution in Llanos del Orinoco Venezuela. In: *School for Production Ecology and Resource Conservation (PE&RC)*. Wageningen, Wageningen University. **PhD:** 217.

Chavez, M. E. and M. Santamaria (2006). *Informe nacional sobre el estado de avance en el conocimiento y la información de la biodiversidad (1998-2004)*. Bogotá, Colombia.

Chavez, P. S. and A. Y. Kwarteng (1989). "Extracting spectral contrast in Landsat Thematic Mapper image data using selective principal components analysis." *Photogrammetric Engineering and Remote Sensing* **3**: 339-348.

Chuvieco, E., A. De Santis, D. Riaño and K. Halligan (2007). "Simulation approaches for burn severity estimation using remotely sensed images." *Fire Ecology Special Issue* **3(1)**: 129-150.

Chuvieco, E., L. Giglio and C. Justice (2008). "Global characterization of fire activity: toward defining fire regimes from Earth observation data." *Global Change Biology* **14(7)**: 1488-1502.

Chuvieco, E. and P. Martin (1994). "A simple method for fire growth monitoring using AVHRR channel 3 data." *International Journal of Remote Sensing* **15**: 3141-3146.

Chuvieco, E. and P. Martin (2002). "Assessment of difference spectral indices in the red-near-infrared spectral domain for burned land discrimination." *International Journal of Remote Sensing* **23(23)**: 5103-5110.

Chuvieco, E., S. Opaso, H. Del Valle, W. Sione, J. Anaya, F. Gonzalez, C. Loope G Di Bella, M. Nicolas, A. Setter, I. Csiszar, L. Manzo, F. Morelli, P. Acevedo and A. Bastarrika (2004). Cartografía global de áreas quemadas en América Latina: experiencias del proyecto AQL 2004. *XII Simposio internacional en percepción remota y sistemas de información geográfica*. Cartagena, Septiembre 2006.

Chuvieco, E., D. Riaño, F. M. Danson and M. P. Martin (2006). "Use of a radiative transfer model to simulate the post-fire spectral response to burn severity." *Journal of Geophysical Research* **111**: 1-15.

Chuvieco, E., F. J. Salas, I. Aguado, D. Cocero and D. Riaño (2001). "Estimación del estado hídrico de la vegetación a partir de sensores de alta y baja resolución." *GeoFocus* **1**: 1-16.

Chuvieco, E., G. Ventura, M. P. Martin and I. Gomez (2005). "Assessment of multitemporal compositing techniques of MODis and AVHRR images for burned land mapping." *Remote Sensing of Environment* **94**: 450-462.

Chuvieco, E. S., W. Opazo, H. Sione, J. del Valle, C. Anaya, I. di Bella, L. Cruz, G. Manzo, N. Lopez, F. Mari, F. Gonzalez-Alonso, A. Morelli, I. Setzer, J. Csiszar, A. Kanpendegi, Bastarrika and R. Libonati (2008). "Global Burned-Land estimation in Latin America using MODis composite data." *Ecological Applications* **18(1)**: 64-79.

Cihlar, J. (2000). "Land cover mapping of large areas from satellites: status and research priorities." *International Journal of Remote Sensing* **21(6-7)**: 1093-1114.

Civco, D. (1993). "Artificial neural networks for land-cover classification and mapping." *International Journal of Geographical Information Systems* **7(2)**: 173-186.

Cochrane, T. T., L. G. Sanchez, L. G. de Acevedo, J. A. Porras and C. L. Garver (1985). Land in Tropical America, A guide to climatic, landscape and soils for agronomists. In: *Amazonia, the Andean Piedmont, Central Brazil and Orinoco*. Cali, Colombia, EMBRAPA-CIAT**:** 144.

Congalton, R. G. and R. A. Mead (1983). "A quantitative method to test for consistency and correctness in photointerpretation." *Photogrammetric, Engineering and Remote Sensing* **49**: 69-74.

Coppin, P., I. Jonckheere, K. Nackaerts, B. Muys and E. F. Lambin (2004). "Digital change detection methods in ecosystem monitoring: A review." *International Journal of Remote Sensing* **25**: 1565-1596.

Correa, H., S. L. Ruiz and L. M. Arevalo (2006). *Plan de Acción en Biodiversidad de la Cuenca del Orinoco, Colombia 2005-2015. Propuesta Técnica.* Bogotá, Instituto de Investigaciones en Recursos Biológicos Alexander von Humboldt.

Corzo, G., C. Sarmiento and K. Arcila-Burgos (2009). *Avances en el análisis del componente ecológico en el marco de la construcción del mapa de aptitudes de áreas para el cultivo de palma de aceite en Colombia, programa de apoyo al Sina II*. Instituto de Hidrología, Metereología y Estudios Ambientales**:** 1-87.

Coutinho, L. M. (1990). Fire in the ecology of the Brazilian cerrado. In: *Fire in the Tropical Biota — Ecosystem Processes and Global Challenges*. J. G. Goldammer. Berlin, Springer-Verlag**:** 82-105.

Couturier, S., J. F. Mas, E. López, G. Cuevas, A. Vega and V. Tapia (2007). "Accuracy assessment of land cover maps in sub tropical countries: a sampling design for the Mexican National Forest Inventory". *Online Journal of Earth Sciences* **1**: 127-135.

Critchley, W. R. S., C. P. Reij and S. P. Turner (1992). *Soil and water conservation in Sub-Sahara Africa*. Amsterdam, Centre for Development Cooperation Services Free 110.

Crutzen, P. J. and M. O. Andreae (1990). "Biomass burning in the tropics: Impact on atmospheric chemistry and biogeochemical cycles." *Science* **250**: 1669-1678.

Crutzen P. J., Heidt L.E., Krasnec J.P. *et al*. (1979) Biomass burning as a source of atmospheric gases CO, H2, N2O, NO, CH3Cl and COS. *Nature* **282**: 253–256.

Csiszar, I., A. Adbdelgadir, Z. Li, J. Jin, R. Fraser and W. M. Hao (2003). "Interannual changes of active fire detectability in North America from long term records of the advanced very high resolution radiometer." *Journal of Geophysical Research* **108(2)**: 4075-4085.

Csiszar, I., J. Morisette and L. Giglio (2006). "Validation of active fire detection from moderate resolution satellite sensors: the MODis example in Northern Eurasia." *IEEE Transactions on Geoscience and Remote Sensing* **44(7)**: 1757-1764.

Dedios, N. (2007). "Management and conservation of dry forest ecosystems, ecological Park Kurt-Beer." *Lyona a Journal of Ecology and Application* **9(12)**: 21-27.

Delmas, R., J. P. Lacaux, and D. Brocard. 1995. Determination of biomass burning emission factors: Methods and results. *Environmental Monitoring and Assessment* **38**: 181–204.

Diaz, P. H. J. (1999). *Estudio de la composición y estructura de las comunidades de macrófitas acuáticas asociadas a dos sistemas lénticos en el municipio de Paz de Ariporo, departamemento de Casanare*. Bogotá, D.C., Instituto de Ciencias Naturales, Universidad Nacional de Colombia.

Dozier, J. (1982). "A method for satellite identification of surface temperature fields of sub-pixel resolution." *Remote Sensing of Environment* **11**: 221-229.

Dwyer, E. and J. M. Pereira (2000). "Global spatial and temporal distribution of vegetation fire as determined from satellite observations." *International Journal of Remote Sensing* **21 (6-7)**: 1289-1302.

Dwyer, E., J. M. C. Pereira, J.-M. Gregoire and C. C. DaCamara (2000). "Characterization of the spatio-temporal patterns of global fire activity using satellite imagery for the period April 1992 to March 1993." *Journal of Biogeography* **27(1)**: 57-69.

Ehlers, M., M. A. Jadkowski, R. R. Howard and D. E. Brostuen (1990). "Application of SPOT data for regional growth analysis and local planing." *Photogrammetric Engineering and Remote Sensing* **56**: 175-180.

Eiten G (1971) The Cerrado vegetation of Brazil. *Botanical Review* **38**: 201–341.

Emery, W., J. Brown and Z. P. Nowak (1989). "AVHRR image navigation: summary and review." *Photogrammetric Engineering and Remote Sensing* **55**: 1175–1183.

Etter A (1985) A Landscape Ecological Approach for Grazing *Development: A Case in the Colombian Llanos Orientales*, pp. 187, Department of Land and Rural Surveys. ITC, Enschede, The Netherlands.

Etter A (1998a) Ecosistemas de Sabanas. In: *Informe Nacional sobre el Estado de la Biodiversidad Colombia 1997* (eds Chaves ME, Arango N), pp. 76–95. IAvH y PNUD, Bogota.

Etter, A., C. McAlpine, D. Pullar and H. Possingham (2006). "Modeling the conversion of Colombian lowland ecosystems since 1940: drivers, patterns and rates." *Journal of Environmental Management* **79**: 74-87.

Etter, A., A. Sarmiento, and M. Romero (2010). Lan d use changes (1970-2020) and carbon emission in the Colombia Llanos. In M. J. Hill and N. P. Hannan (Ed). *Ecosystem function in savannas. Measurament and modeling at landscape to global scales*. CRC Press.

Eva, H. and S. Flasse (1996). "Contextual and multiple-threshold algorithms for regional active fire detection with AVHRR data." *Remote Sensing Reviews* **14**: 333-351.

Eva, H. and E. F. Lambin (1998). "Remote sensing of biomass burning in tropical regions: Sampling issues and multisensor approach." *Remote Sensing of Environment* **65**: 292-315.

Eva, H. and E. F. Lambin (2000). "Fires and land cover change in the tropics: A remote sensing analysis at the landscape scales." *Journal of Biogeography* **27**: 765-776.

Evas, H. and E. F. Lambin (1998). "Remote sensing of biomass burning in tropical regions: Sampling issues and multisensor approach." *Remote Sensing of Environment* **65**: 295-315.

FAO (1966). *Reconocimiento edafológico de los Llanos Orientales de Colombia. La Vegetación Natural y la Ganadería en los Llanos Orientales*. Roma.

Farinas, R. (2008). Agricultural activities, management and conservation of natural resources of Central and South American savannas. *IX simposion Nacional Cerrado, II Simposio Internacional Savanas Tropicais*, Brasilia, D.F., Embrapa.

Fernandez, A., P. Illera and J. L. Casanava (1997). "Automatic mapping of surfaces affected by forest fire in Spain using AVHRR NDVI composite image data." *Remote Sensing of Environment* **60**: 153-162.

Fielding, A. H. and J. F. Bell (1997). "A review of methods for the assessment of prediction errors in conservation presence/absence models." *Environment Conservation* **24**: 38-49.

Fielding, H. and J. F. Bell (1997). "A review of methods for the assessment of prediction errors in conservation presence/absence models." *Environment Conservation* **24**: 38-49.

Finney, M. (1998). FARSITE: *Fire Area Simulator-model development and evaluation.* Ogden, Department of Agriculture, Forest Service, Rocky Mountain Research Station**:** 47.

Flantua, S., J. Van Boxel, H. Hooghiemstra and J. Van Smaalen (2007). "Application of GIS and logistic regression to fossil pollen data in modelling present and past spatial distribution of the Colombian savanna." *Climate dynamic* **29**: 697-712.

Flenningan, M. D., K. A. Logan, B. D. Amiro, W. R. Skinner and B. J. Stocks (2005). "Future area burned in Canada." *Climatic Change* **72 (1-2)**: 1-16.

Foley, J. A., R. DeFries, G. P. Asner, C. Barford, G. Bonan, S. R. Carpenter, F. S. Chapin, M. T. Coe, G. C. Daily, H. K. Gibbs, J. H. Helkowski, T. Holloway, E. A. Howard, C. J. Kucharik, C. Monfreda, J. A. Patz, I. C. Prentice, N. Ramankutty and P. K. Snyder (2005). "Global consequences of land use." *Science* **309**(5734): 570-574.

Franca, J. R., J. M. Brustet and J. Fontan (1995). "Multispectral remote sensing of biomass burning in West Africa." *Journal of Atmospheric Chemistry* **21**: 81-110.

Franklin, J., C. E. Woodcock and R. Warbington (2000), "Multi-attribute vegetation maps of forest services lands in California supporting resource management decisions", *Photogrammetric Engineering and Remote Sensing* **66**: 1209-1217.

Fraser, R. H., R. J. Hall, R. Landry, T. Lynham, D. Raymond and B. Lee (2004). "Validation and calibration of Canada wide coarse resolution satellite burned areas maps." *Photogrammetric Engineering and Remote Sensing* **70**: 451-460.

Frost, P.G.H. 1999. Fire in southern African woodlands: Origins, impacts, effects, and control. In *Proceedings of an FAO meeting on public policies affecting forest fire*. FAO Forestry Paper, 138.

Furley, P. (1999). "The nature and diversity of neotropical savanna vegetation with particular reference to the Brazilian cerrados." *Global Ecology and Biogeography* **8**: 223-241.

Galanter M, Levy HII, Carmichael GR (2000) Impacts of biomass burning on tropospheric CO, NOx and O3. *Journal of Geophysical Research* **105**: 6633–6653.

Garcia, T & HJ. Mass, 2008. Comparacion de metodologias para el mapeo de de la cobertura y uso del suelo en el sureste de Mexico. *Investigaciones Geograficas, Boletín del Instituto de Geografia, UNAM* **67**: 7-19.

Geneletti, D. and B. G. H. Gorte (2003). "A method for object-oriented land cover classification combining Landsat data and aerial photographs." *International Journal of Remote Sensing* **24**: 1273-1286.

Giglio, L. and C. O. Justice (2003). "Effect of wavelength selection on characterization of fire size and temperature." *International Journal of Remote Sensing* **24(17)**: 3515-3520.

Giglio, L., I. Csiszar and C.O. Justice. (2006). Global distribution and seasonality of active fires as observed with the Terra and Aqua Moderate Resolution

Imaging Spectroradiometer (MODIS) sensors. *Journal of Geophysical Research* **111**: G02016, doi: 10.1029/2005JG000142.

Giglio, L., G. R. Van der Werf, J. Randensro, G. Collatz and P. Kasibhatla (2005). "Global estimation of burnt areas using MODis active fire observations." *Atmosphere Chemistry Physic Discuss.* **5**: 11091-11141.

Gill, A.M. 1975. Fire and the Australian flora: A review. *Australian Forestry* **38**: 4–25.

GOFC-GOLD. (2004). "Fire Monitoring and Mapping Implementation Team." Available at: http://gofc-fire.umd.edu.index.asp.

Goldammer, J. G. (1993). "Wildfire management in forests and other vegetation: a global perspectvie." *Disaster Management* **5**: 3-10.

Goldewijk, K. and N. Ramankutty (2003). "Land cover change over the last three centuries due to human activities: The availability of new global data set." *Geojornal* **61**: 335-344.

Gomez, I. and I. Martín (2008). "Estudio comparativo de índices espectrales para la cartografía de áreas quemadas con imágenes MODis." *Revista de Teledetección de la Asociación Española de Teledetección* **29**: 15-24.

Grace, J. 2004. Understanding and managing the global carbon cycle. *Journal of Ecology* **92**: 189–202.

Grace, J., J. S. Jose, P. Meir, H. S. Miranda and R. A. Montes (2006). "Productivity and carbon fluxes of tropical savannas." *Journal of Biogeography* **33(3)**: 387-400.

Gregoire, J. M., K. Tansey and S. J.M. (2003). "The GBA2000 initiative: Developing a global burned area database from SPOT-VEGETATION imagery." *International Journal of Remote Sensing* **24**: 1369-1376.

Guillson, L. and K. J. Willis. 2004. As Earth's testimonies tell': wilderness conservation in a changing world. *Ecology Letters* **7**: 990–998.

Hall, D. O. and J. M. O. Scurlock (1991). "Climate change and productivity of natural grasslands." *Annals of Botanic* **67**(supp1): 49-55.

Hansen, M. C., R. DeFries, J. R. Townshend, R. Sohlberg, C. Deimiceli and M. Carroll (2002). "Towards an operational MODis continuous field of percent tree cover algorithm: examples using AVHRR and MODis data." *Remote Sensing of Environment* **83**: 303-319.

Hoelzmann, J., M. Schultz, G. Brasseur and C. Granier (2004). "Global wildland fire emission model (GWEM), evaluating the use of global area burnt satellite data." *Journal of Geophysical Research* **109**: 1-18.

Hoffmann, W. A., W. Schroeder, and R. B. Jackson. (2002). Positive feedbacks of fire, climate, and vegetation and the conversion of tropical savanna. *Geophysical Research Letters* **29**: 2052–2055.

Hoffmann, W. A. and M. Haridasan. (2008). The invasive grass, Melinis minutiflora, inhibits tree regeneration in a Neotropical savanna. *Austral Ecology* **33**: 29–36.

Hosmer, D. W. and S. Lemishow (1989). *Applied logistic regression*. Wiley, New York.

Hough, J. L. (1993). "Why burn the bush? Social approaches to bush fire management in West Africa National Park." *Biological Conservation* **65**: 23-28.

Houghton, R. A. 2005. Aboveground forest biomass and the global carbon balance. *Global Change Biology* **11**: 945–958.

Huber, O., D. De Stephano and G. Aymard (2006). Flora and vegetation of the venezuelan llanos: A Review. In: *Neotropical Savannas and Seasonally Dry Forest*. T. Pennington, G. Lewis and J. Ratter. Edinburg, Taylor & Francis. **1:** 96- 118.

Hudak, A., D. Fairbanks and B. Brockett (2004). "Trends in fire patterns in a southern African savanna under alternative land use practices." *Agriculture, Ecosystems and Environment* **101**: 307-325.

Hunt, E. R. and B. N. Rock (1989). "Detection of change in leaf water content using near and middle-infrared reflectance." *Remote Sensing of Environment* **30**: 43-54.

Huntley, B.J. and B.H. Walker. (1982). Ecology of tropical savannas. 669 pp.

Hutchinson, M. F. (1995). "Interpolating mean rainfall using thin plate smoothing splines." *International Journal of Geographical Information Systems* **9**: 385-403.

IDEAM (2004). Informe Anual sobre el Estado del Medio Ambiente y los Recursos Renovables en Colombia. Bogota, Colombia.

IDEAM, IGAC and CORMAGDALENA (2008). *Mapa de cobertura de la tierra de la cuenca Magdalena-Cauca: Metodología CORINE Land Cover adaptada para Colombia a escala 1:100.000*. Bogotá, D.C., Instituto de Hidrología, Meteorología y Estudios Ambientales, Instituto Geográfico Agustín Codazzi y Corporación Autónoma Regional del río Grande de la Magdalena.

IGAC-CORPOICA (2002). *Zonificación de los conflictos de uso de la tierra en Colombia.* Bogotá.

IGAC (1979). *Proyecto radargramético del Amazonas: La Amazonía colombiana y sus recursos* Bogotá, IGAC-CIAF, Mindefensa.

IGAC (1983a). *Estudio general de suelos de la comisaria del Vichada*. Bogotá, Colombia, Instituto Geografico Agustin Codazzi, Subdireccion de Agrología.

IGAC, I. G. A. C. (1999). *Paisajes fisiográficos de Orinoquia-Amazonia (ORAM)*. Bogotá.

IPCC (2007). Cambio Climático 2007: Mitigación del cambio climático. In: *Contribucion del grupo de trabajo III al cuarto informe de evaluación del IPCC*. Cambrige, Cambrige University Press.

Jenness, J. and J. J. Wynne. (2007). "Cohen's kappa and classification table metric 2.1. An arcView3x extension for accuracy assessment of spatially-explicit models." Available at: http://www.jennessent.com/arcview/kappa_stats.htm.

Jensen, J. R. (2000). *Remote sensing of the environment: An Earth resource perspectives*. Upper Saddle River, Prentice-Hall.

Jones, S. H. (1997). *Vegetation fire in mainland southeast Asia: spatio-temporal of AVHRR 1 km data for the 1992/03 dry season*. Luxembourg, European Commission. **EUR 17282**.

Justice, C. O., L. Giglio, S. Korontzi, J. Owens, J. Morisette and D. Roy (2002). "The MODis fire products." *Remote Sensing of Environment* **83**: 244-262.

Justice, C. O., R. Smith, M. Gill and I. Csiszar (2003). "A review of current space-based fire monitoring in Australia and the GOFC/GOLD program for international coordination." *International Journal of Wildland Fire* **12**: 247-258.

Justice, C. O., E. Vermote, J. R. Townshend, R. DeFries, D. P. Roy, D. K. Hall, V. V. Salomonson, J. L. Privette, A. H. Strahler, W. Lucht, R. B. Myneni,

Y. Knyazikhin, S. W. Running, R. Nemani, Z. Wan, A. R. Huete, W. Wan Leeuwen, R. E. Wolfe, L. Giglio, J. P. Muller, P. Lewis and J. Barnsley (1998). "The MODerate resolution imaging spectroradiometer (MODis): Land remote sensing for global change research." *IEEE. Transactions of Geoscience and Remote Sensing* **36**: 1228-1249.

Justice., C. O., L. Giglio, S. Korontzi, J. Owens, J. T. Morisette, D. P. Roy, J. Descloitres, S. Alleaume, F. Petitcolin and Y. Kaufman (2002). "The MODis fire products." *Remote Sensing of Environment* **83**: 244-262.

Kartikeyan, B., A. Sarkar and K. Maumder (1998). "A segmentation approach to classification of remote sensing imagery." *International Journal of Remote Sensing* **19**: 1695-1709.

Kasischke, E. S. (1996). Fire, Climate change and carbon cycling in Alaskan boreal forests. *Biomass Burning and Global Change 2*. C.O. Justice. Cambridge, MA-MIT Press**:** 827-833.

Kasischke, E. S. and N. H. Frech (1995). "Locating and estimating the areal extent of wildfired in Alaskan boreal forest using multiple-season AVHRR NDVI composite data." *Remote Sensing of Environment* **51**: 263-275.

Keeley, J. (2009). "Fire intensity, fire severity and burn severity: a brief review and suggestged usage." *International Journal of Wildland Fire* **18**: 116-126.

Kendall, J. D., C. O. Justice, P. R. Dowty, C. D. Elvidge and J. G. Goldemmer (1997). Remote sensing of fires in southern Africa during the SAFARI 1992 campaign. *Fire in southern african savannas, ecological and atmospheric pesperctives.* B. Van Wilgen, M. O. Andreae, J. G. Goldammer and J. Lindsay. Johannesburg, Wittwaterrand Press.

Key C.H. (2005) Remote sensing sensitivity to fire severity and fire recovery. In '*Proceedings of the 5th international workshop on remote sensing and GIS applications to forest fire management: Fire effects assessment*'. (Eds J. De la Riva, F. Perez-Cabello, E. Chuvieco) pp. 29–39. (Universidad de Zaragoza: Spain)

Key, C. H. and N. C. Benson (2002). Landscape assessment in fire effects monitoring (FireMon) and inventory protocol: Integration of standardized field data collection techniques and sampling design with remote sensing to assess fire effects. In: *NPS-USGS National Burn Severity Mapping Project.*

Key, C. H. and N. C. Benson (2006). Landscape assessment: Sampling and analysis methods. In: *Usda, Forestal Service. Rocky Mountain Research Station General Technical Report RMSRS-GTR-164-CD. (Ogden, UT)*. Available at: www.fire.org/medcia/la.final.pdf. **30 March, 2006**.

Koffi, B., J. M. Gregoire and H. Eva (1996). Satellite monitoring of vegetation fires on a multi-annual basis at continental scale in Africa. In: *Biomass, Burning and Global Change* J. E. Levine. Cambridge, MA:MIT Press. **1:** 225-235.

Korontzi, S., D. P. Roy, C. O. Justice and D. E. Ward (2004). "Modelling and sensibility analysis of fire emission in southern Africa during SAFARI 2000." *Remote Sensing of Environment* **92**: 255-275.

Koufman, Y. J., C. O. Justice, L. P. Flynn, J. D. Kendall, E. M. Prins, L. Giglio, D. E. Ward, W. P. Menzell and A. W. Setzer (1998). "Potential global fire monitoring from EOS-MODis." *Journal of Geophysical Research* **103**: 332-315.

Lambin, E. F., H. Geist and E. Leper (2003). "Dynamics of land-use and land-cover change in tropical regions." *Annual Revision Enviromental Resources* **28**: 205-241.

Laris, P. (2002). "Burning the seasonal mosaic. Preventitive burning strategies in the wooded savanna of sourthern Mali." *Human Ecology* **30**: 155-186.

Laris, P. (2005). "Spatiotemporal problems with detecting and mapping mosaic fires regimes with coarse-resolution satellite data in savanna environments." *Remote Sensing of Environment* **99**: 412-424.

Lea, R. (2005). *A comparison of forest change detection methods and implications for forest management*. Missouri, Columbia, University of Missouri.

Lentile, L. B., Z. A. Holden, A. M. S. Smith, M. J. Falkowski, A. Hudak, P. Morgan, S. A. Lewis, P. E. Gessler and N. C. Benson (2006). "Remote sensing techniques to assess active fire characteristics and post-fire effects." *International Journal of Wildland Fire* **15**: 319-345.

Levine, J. S. (1992). Introduction: global biomass burning: atmospheric climatic, and biospheric implications. In: *Global Biomass Burning, Atmospheric, Climatic and Biospheric Impications*. J. E. Levine. Cambrigde MA, MIT Press.

Laris, P. (2005). "Spatiotemporal problems with detecting and mapping mosaic fires regime with coarse-resolution satellite data in savannas environment." *Remote Sensing of Environment* **99**: 412-424.

Li, Z., Y. Kaufman, J. Ichoku, R. Fraser, R. Trishehenko and L. Giglio (2001). A review of AVHRR based active fire detection algorithms. Principles limitations and recommendations. In: *Global and regional vegetation fire monitoring from space. Planning a coordinated international efforts*. F. J. Ahern, J. G. Goldaammer and C. O. Justice. The Hague, SPB Academic Publisching**:** 199-226.

Lillesand, T.M. and R.W. Kiefer. 1994. Remote sensing and image interpretation. John Wiley and Sons, USA.

Lobada, T. V. and I. Csiszar (2007). "Reconstruction of fire spread within wildland fire events in Northern Eurasia from the MODis active fire product." *Global and Planetary Change* **56(3-4)** 258-273.

Lopez, D., R. M. Hernandez and M. Brossard (2005). "Historia del uso reciente de tierras de la sabana de América del Sur. Estudio de caso en sabanas del Orinoco." *Interciencia* **30**: 10.

Lopez, E., G. Bocco, M. Mendoza and E. Duhau (2001). "Predicting land-cover and land-use change in the urban fringe: A case in Morelia city, Mexico." *Landscape and Urban Planning* **55**: 271-285.

Louppe, D., N. Oattara and A. Coulibaly (1995). "The effects of brush fire on vegetation: The Aubreville fire plots after 60 years." *Commonwealth Forestry Review* **74**: 288-291.

Lozano, F., S. Suarez-Seoane and E. de Luis (2005). "Vegetation dynamics after fire opportunities of the combined used of fire detection and ecological indices. A study case in west Spain."

MA, M. E. A. (2005). *Ecosystems and Human well-being*. Washington, D.C., Island Press.

Maggi, M. and D. Stroppiana (2002). "Advantages and drawbacks of NOAA-AVHBRR and SPOT-VGT for burnt area mapping in a tropical savanna ecosystem." *Canadian Journal of Forest Reserarch* **28**: 231-245.

Magnussen, S. (1997). “Calibrating photo-interpreted forest cover types and relative species compositions to their ground expectations.” *Canadian Journal of Forest Research* **27**: 491-500.

Malagon, D. (2003). “Ensayo sobre tipología de suelos Colombianos - Énfasis en génesis y aspectos ambientales.” *Revista Colombiana de la Academia de Ciencias Naturales* **104**: 319-342.

Maldonado-Ocampo, J. A. and J. S. Usma (2006). Estado del conocimiento sobre peces dulceacuícolas en Colombia. In: *Informe nacional sobre el avance en el conocimiento e información sobre biodiversidad 1998-2004*. M. E. Chavez and M. Santamaria. Bogotá.

Malingreau, J. P. and J. M. Gregoire (1996). Developing a global vegetation fire monitoring system for global change studies: a framework. In: *Biomass Burning and Global Change*. L. J.S. Cambrige, MIT Press.

Malingreau, J. P., N. Laponte and J. M. Gregoire (1990). “Exceptional fire event in the tropics: Southern Guinea, January 1987.” *International Journal of Remote Sensing* **11**: 2121-2123.

Martin, M. P., I. Gomez and E. Chuvieco (2006). “Performance of a burned-area index (BAIM) for mapping mediterranean burned scars from MODis data.” In: *Proceeding of the 5th International Workshop of Remote Sensing and GIS applications to Forest Fire Management: Fire Effects Assessment*: 193-198.

Martin, P., P. Ceccato, S. Flasse and I. Downey (1999). Fire detection and fire growth monitoring using satellite data. In: *Remote sensing of large wildfires in the European mediterranean basin*. E. Chuvieco. Berlin, Heidelberg: Springer-Varlag**:** 212.

Mas, J. F. (1999). “Monitoring land-cover changes: a comparison of change detection techniques.” *International Journal of Remote Sensing* **20(1)**: 139-152.

Mather, P. (2005). *Computer processing of remotely-sensed images. An introduction.* Cambridge, John Wiley and Sons, Ltda.

Matson, M. and J. Dozier (1981). “Identification of subresolution high temperature sources using a thermal IR sensor.” *Photogrammetric Engineering and Remote Sensing* **47**: 1311-1318.

Mbon, C., K. Goita and G. Benie (2004). “Spectral indices and fire behaviour simulation for FIRE risk assessment in savannas ecosystems “ *Remote Sensing of Environment* **91**: 1-13.

Mbon, C., T. T. Nielsen and K. Rusmusser (2000). “Savanna fires in east-central Senegal: Distribution, patterns, resource management and perceptions.” *Human Ecology* **28(4)**: 561-583.

McNaughton, J., O. E. Sala and M. Oesterheld (1993). Comparative ecology of African and South American arid to sub-humid ecosystems. In: *Biological relationships between Africa and South America*. P. Goldblatt. New Haven, C.T. USA, Yale University Press.

McNish, T. (2007). *Las aves de los Llanos de la Orinoquía*. Bogotá.

Meidinger, D. (2003). *Protocol for Accuracy Assessment of Ecosystem Maps*. Research Branch, BC MOF. Ministry of Forests, Victoria, B.C.

Menault, J. C., L. Abbadie and P. M. Vitousek (1993). Nutrient and organic matter dynamics in tropical ecosistems. In: *Fire in the environment: the ecological,*

atmospheric and climatic importance of vegetation fires. P. J. Crutzen and J. G. Goldemmer. Chichester. **3:** 215-231.

Meneaut, J. C., L. Abbadie, F. Lavenu, P. Laudjani and A. Podaire (1992). Biomass burnig in west African savannas. In: *Global Biomass Burning Atmospheric, Climatic and Biospheric Implications*. J. E. Levine. Cambridge, MA:MIT Press**:** 133-142.

Meyer, K. M., K. Wiegand and D. Ward. (2010) Spatial Explicit Modeling of Savanna Processes. In M.J. Hill and N. P. Hannan (ed). *Ecosystem function in savannas. Measurament and modeling at landscape to global scales*. CRC Press.

Miranda, E., E. De Setter and A. M. Takeda (1994). *Monitoreamiento orbital das queimadas no Brasil*. Campinas, SP Brasil, Embrapa - NMA.

Mistry, J. and A. Berardi. (2005). Assessing Fire Potential in a Brazilian Savanna Nature Reserve1. *Biotropica* **37**, 439–451.

Moody, A. and C. Woodcock (1996). "Calibration based models for correction of area estimates derived from coarse resolution land cover data." *Remote Sensing of Environment* **58**: 225-241.

Morisette, J., L. Giglio, I. Csiszar and C. O. Justice (2005). "Validation of the MODis active fire product over southern Africa with Aster data." *International Journal of Remote Sensing* **26(19)**: 4239-4264.

Mouillot, F., A. Narasimha, Y. Balkanski, J. Lamarque and C. B. Field (2006). "Global carbon emissions from biomass burning in the 20th century." *Geophysical Research Letters* **33**: L01801.

Muchoney, D. and B. Haack (1994). "Change detection for monitoring forest defoliation." *Photogrammetric, Engineering and Remote Sensing* **60(10)**: 1243-1251.

Muñoz-Villares, L. E. and J. Lopez-Blanco (2008). "Land use/cover changes using Landsat TM/ETM images in a tropical and biodiverse mountainous area of central-eastern Mexico." *International Journal of Remote Sensing* **29(1)**: 71-93.

Myers, R. I. (2006). *Living with fire-sustaining ecosystems & liverlihoods through integrated fire management*. Tallahassee, Florida, USA, The Nature Conservancy.

Neary D.G., Klopatek C.C., DeBano L.F., Ffolliott P.F. (1999) Fire effects on belowground sustainability: a review and synthesis. *Forest Ecology and Management* **122**: 51–71. doi:10.1016/S0378-1127(99)00032-8.

Nepstad D., S. Schwartzman., B. Bamberger., M. Santilli., d. Ray., P. Schlesinger., P. Lefebvre., A. Alencar., E. Prinz., G. Fiske and A. Rolla. (2006). Inhibition of Amazon deforestation and fire by parks and indigenous lands. *Conservation Biology* **20**: 65–73.

Nishihama, M., R. E. Wolfe, D. Solomon, F. Patt, J. Blanchette, A. Fleig and E. Masouka (1997). *MODis Level 1A Earth location: Algorithm theoretical basin Document*. Greenbelt, MD, Laboratory for Terrestrial Physics, NASA.

Ocampo, A. (2006). Biodiversidad y actividades productivas. In: *Plan de acción en biodiversidad para la Orinoquía*. H. Correa. Bogotá.

Olson, D. M., E. Dinestein, E. Wikramanayare, N. D. Burgess, G. V. Powell, E. C. Underwood, J. A. D'Amico, I. Itoua, H. Strand, M. J, C. Wettengel, P. Hedao and K. Kassem (2001). "Terrestrial ecoregions of the world: A new map of live on Earth." *BioScience* **51**: 933-938.

Palacios-Sanchez, L., F. Paz-Pellat, J. Oropeza-Mota, M. Figueroa-Sandoval, C. Martinez-Menes, C. Ortiz-Solorio and A. Exebio-Garcia (2006). "Generis object clasificator on ETM+ imagens." *Red de Revistas Científicas de América Latina y el Caribe, España y Portugal.*: 613-626.

Pennington, T., G. Lewis and J. Ratter (2006). *Neotropical Savannas and Seassonally Dry Forest*. Edinburg, Taylor & Francis.

Pereira, J. M. (1999). "A comparative evaluation of NOAA/AVHRR vegetation indices for fire scar detection and mapping in the Mediterranean type region." *IEEE Transactions on Geoscience and Remote Sensing* **37**: 217-226.

Pereira, J. M. (2003). "Remote sensing of burned areas in tropical savannas." *International Journal of Wildland Fire* **12**: 259-270.

Peterson, David W., and Peter B. Reich. (2001). Prescribed fire in oak savanna: Fire frequency effects on stand structure and dynamics. *Ecological Applications* **11**:914–927.

Phua, M. H., S. Tsuyuki, J. S. Lee and H. Sasakawa (2007). "Detection of burned peat swamp forest in a heterogeneous tropical landscape: A case stude of the Klias Peninsula, Sabah Malasi." *Landscape and Urban Planning* **82**: 103-116.

Pielke, R. A., G. Marland, R. Betts, T. Chase, J. Eastman, J. O. Niles, D. D. S. Niyogi and S. Running (2002). "The influence of land use change and landscape dynamics on the climate system: relevance to climate change policy beyond the radiative effect of greenhouse gases." *Philosophical Transactions of the Royal Society of London A* **360**: 1705-1719.

Puyravaud, J. P. (2003). "Standardizing the calculation of the annual rate of deforestation." *Forest Ecology and Management* **177**: 593-596.

Ramankutty, N., H. K. Gibbs, F. Achard, R. Defries, J. A. Foley, and R. A. Houghton. (2007). Challenges to estimating carbon emissions from tropical deforestation. *Global Change Biology* **13**: 51–66.

Rangel., O., H. Sanchez, P. Lowy, P. Aguilar and A. Castle (1995). Región Orinoquía. In: *Colombia Diversidad Biótica.* O. Rangel. Bogotá, Colombia, Instituto de Ciencias Naturales. Universidad Nacional de Colombia. **1:** 239-254.

Raupach, M., G. Marland, P. Ciais, C. Le Quere, J. Canadell, G. Klapper and C. Field (2007). "Global and regional drivers of accelerating CO_2 emissions." *The National Academy of Sciences of the USA* **104(24)**: 10288-10293.

Razafimpanilo, H., R. Frouin, S. F. Lacobellis and R. C. Semmorville (1995). "Methodology for estimating burned area from AVHRR reflectance data." *Remote Sensing of Environment* **54**: 273-289.

Rippstein, G., G. Escobar and F. Motta (2001). *Agroecología y biodiversidad de la sabana en los llanos orientales de Colombia.* Centro de agricultura tropical - CIAT.

Robinson, J. M. (1991). Problems in global fire evaluation - Is remote sensing the solution?. In: *Global, Biomass Burning*. J. E. Levine. Cambridge, MA:MIT Press.

Rogan, J., J. Frankin and D. Robers (2002). "A comparison of methods for monitoring multitemporal vegetation changes using Thematic Mapper Imagery." *Remote Sensing of Environment* **80**: 143-156.

Rogan, J., J. Miller, D. Stow, J. Franklin, L. Levine and C. Fischer (2003). "Land cover change monitoring with classification trees using Landsat TM and ancillary data." *Photogrammetric, Engineering and Remote Sensing* **69**: 793-804.

Romero-Ruiz, M., A. Etter, A. Sarmiento and K. Tansey (2010). "Spatial an temporal variability of fires in relation to ecosystems, land tenure and rainfall in savannas of Northern South America." *Global Change Biology* **16(7)**:2013-2023.

Romero, M., J. A. Maldonado-Ocampo, J. D. Bogotá-Gregory, J. S. Usma, A. M. Umaña-Villaveces, J. I. Murillo, S. Restrepo-Calle, M. Alvarez, M. T. Palacios-Lozano, M. S. Valbuena, M.S.L., A.D. J. and E. Payan (2009). *Informe sobre el estado de la biodiversidad en Colombia 2007-2008: piedemonte orinoquense, sabanas y bosques asociados al norte del río Guaviare*. Instituto de Investigaciones en Recursos Biologicos "Alexander von Humboldt".

Romero, M. E. (1993). "Achagua". In: *Geografía Humana de Colombia. Región de la Orinoquía* **III**(1).

Romero, M., G. Galindo, J. Otero and D. Armenteras (2004). *Ecosistemas de la cuenca del Orinoco colombiano*. Instituto de Investigaciones en Recursos Biológicos "Alexander von Humboldt" - Instituto Geográfico Agustín Codazzi - IGAC.

Rothermel, R. C. (1991). *Predicting behaviour and size of crown fires in the northern rocky mountains*. USDA For. Serv. Gen. Tech. Rep. INT-438.

Rouse, J. W., R. H. Haas, D. W. Deering and J. A. Schell (1974). Monitoring the vernal advancement and retrogradation (Green wave effect) of natural vegetation. *Final Report RSC 1978-4.* Texas A & M University, Remote Sensing Center, College Station, Texas.

Roy, D.P., Boschetti, L. and L. Giglio. 2010 Remote sensing of global savanna fire occurrence, extent, and properties. In M. J. Hill and N. P. Hannan (Ed). *Ecosystem function in savannas. 'Measurament and modeling at landscape to global scales'*. CRC Press.

Roy, D., L. Giglio, J. Kendall and C. O. Justice (1999). "Multitemporal active fire based burn scar detection algorithm." *International Journal of Remote Sensing* **20**: 1031-1038.

Roy, D., J. Jin, P. E. Lewis and C. O. Justice (2005). "Prototyping a global algorithms for systematic fire-affected area mapping using MODis time series data." *Remote Sensing of Environment* **97(2)**: 137-162.

Roy, D. and T. Landmann (2005). "Characterizing the surface heterogeneity of fire effects using multi-temporal reflective wavelengths data." *International Journal of Remote Sensing* **26**: 4197-4218.

Roy, D., P. E. Lewis and C. O. Justice (2002b). "Burned area mapping using multi-temporal moderate spatial resolution data - a bidirectional reflectance model based expectation approach." *Remote Sensing of Environment* **83**: 263-286.

Roy, D., S. N. Trigg, R. Bhima, B. H. Brockett, O. Dube, P. Frost, N. Govender, T. Landmann, J. Le Roux, T. Lepono, J. Macuacua, C. Mbow, K. Mhwandangara, B. Mosepele, O. Mutanga, G. Neo-Mahupelaeng, M. Norman and S. Virgilo (2006). "The utility of satellite fire product accuracy information-perspectives and recommendations from the southern Africa

fire network." *IEEE Transactions on Geoscience and Remote Sensing* **44**: 1928-1930.

Roy, D. P. (2003). SAFARI 2000 July and September MODis 500 m burned area products for Southern Africa. In: *SAFARO 2000 CD-ROM series*. N. J. Greenbelt, MD. USA, National Aeronautics and Space Administration, Goddard Space Flight Center.

Roy, D. P. and L. Boschetti (2009). "Southern Africa validation of the MODis, L3JRC, and GlobCarbon Burned-Area Products." *IEEE Transactions of Geoscience and Remote Sensing* **47(4)**: 1032-1044.

Rudas, G. (2003). Propuesta de un sistema de indicadors del seguimiento del convenio sobre la biodiversidad biológica en la cuenca del Orinoco: Marco conceptual y metodológico. Bogotá, Instituto de Investigaciones en Recursos Biológicos Alexander von Humboldt - Fondo Mundial para la Naturaleza - WWF.

Russell-Smith, J., P. G. Ryan and R. Duieu (1997). "A Landsat MSS derived fire history of Kakadu National Park monsoonal northern Australia 1980-94. Seasonal extend, frequency and patchiness." *Journal of Applied Ecology* **34**: 748-766.

Russell-Smith, J., P. J. Whitehead, R. J. Williams and M. D. Flanningan (2003). "Fire and savanna landscape in northern Australia. Regional lessons and global challenger." *International Journal of Wildland Fire* **12**.

Sabins, F. (1997). *Remote Sensing: Principles and Interpretation.* New York, W.H. Freeman and Co.

San José, J. J. and R. A. Montes (2001). "Management effects on carbon stocks and fluxes across the Orinoco savannas." *Forest, Ecology and Management* **150**: 293-311.

Sanchez, L. (2005). *Caracterización de los grupos humanos rurales de la cuenca hidrográfica del Orinoco en Colombia.* Bogotá, Instituto de Investigaciones en Recursos Biologicos Alexander von Humboldt.

Sarmiento, G. (1984). *Ecology of neotropical savannas*. Boston, Harvard University Press.

Sarmiento, G. (1990). Ecología comparada de ecosistemas de sabanas en America del Sur. In: *Las sabannas americanas. Aspecto de su biogeografía y utilización*. G. Sarmiento. Merida, Centro de Investigaciones Ecológicas de los Andes Tropicales.

Scanlan, J. C. (2002). "Some aspects of tree=grass dynamic in Queensland's grazing lands." *Rengeland Journal* **24(1)**: 56-82.

Shvidenko, A. Z. and S. Nilsson (2000). Extent, distribution and ecological role of fire in Russian forest. In: *Fire climate change and carbon cycling in the boreal forest, series ecological studies*. E. Kasiscke and B. Stricks. New York, Springer.

Sigh, A. (1989). "Digital change detection techniques using remotely sensed data." *International Journal of Remote Sensing* **10**: 989-1003.

Silva, J. M. and J. M. Pereira (2005). "Comparison of burned area estimated derived from SPOT-VEGETATION and Landsat ETM+ data in Africa: Influence of spatial patterns and vegetation type." *Remote Sensing of Environment* **96**: 188-201.

Smith, A., N. Drake, M. Wooster, A. Hadak, Z. Holden and C. Gibbons (2007). "Production of Landsat ETM+ reference imagery of burned areas within

Southern African Savannahs: Comparison of methods and application to MODis." *International Journal of Remote Sensing* **28(12)**: 2753-2775.

Solbrig, O. T., E. Medina and J. Silva (1996). *Biodiversity and Savanna Ecosystem Processes: A Global Perspective*. Berlin, John Wiley & Sons Ltd.

Speranza, F. C. and H. R. Zerda (2005). *Potencialidad de los índices de vegetación para la discriminación de coberturas forestales*. In: Actas del III Congreso Forestal Argentino y Latinoamericano, Corrientes, Argentina C.D. 6-9 de septiembre de 2005.

Stolle, F., K. Chomitz, E. F. Lambin and T. P. Tomich (2003). "Land use and vegetation fires in Jambi Province, Sumatra, Indonesia." *Forest Ecology and Management* **179**: 277-292.

Stow, D. (1995). Monitoring ecosystem response to global change: multitemporal remote sensing analyses. In: *Anticipated effects of a changing global environment in Mediterranean type ecosystems.* J. Moreno and W. Oechel. New York, Springer-Verlag**:** 254-286.

Stow, D., D. Collins and D. McKinsey (1990). "Land use change detection based on multi-date imagery from different satellite sensor systems." *Geocarto International* **5**: 1-12.

Stropianna, D., S. Pinnock and J. M. Gregoire (2000). "The Global Fire Product: dialy fire occurrence form Abril 1992 to December 1993 derived from NOAA AVHRR data." *International Journal of Remote Sensing* **21**: 1279-1288.

Swets, J. A. (1995). *Signal detection theory and ROC analysis in psychology and diagnostics: Collected papers*. Mahwah, New Jersey, Lawrence Erlbaum.

Tanre, D., Y. Kaufman, M. Herman and S. Mattoo (1997). "Remote sensing of aerosol properties over oceans from EOS-MODis." *Journal of Geophysical Research* **102**: 16971-16988.

Tansey, K., J.-M. Grégoire, P. Defourny, R. Leigh, J.-F. Pekel, E. van Bogaert and E. Bartholomé (2008). "A new, global, multi-annual (2000-2007) burnt area product at 1 km resolution." *Geophysical Research Letters* **35**: L01401.

Tansey, K., J. M. Gregoire, E. Binaghi, L. Boschetti, P. A. Brivio, D. Ershov, S. Flasse, R. Fraser, D. Graetz, M. Maggi, P. Peduzzi, J. M. Pereira, J. F. Silva, A. Sousa and D. Stroppiana (2004a). "A global inventory of burned areas at 1 km resolution for the year 2000 derived from SPOT VEGETATION data." *Climatic Change* **67(2)**: 345-377.

Townshend, J. R. and C. O. Justice (2002). "Towards operational monitoring of terrestrial systems by moderate-resolution remote sensing." *Remote Sensing of Environment* **83**: 351-359.

Trigg, S. N. and S. Flasser (2001). "An evaluation of different bi-spectral spaces for discriminating burned shrub-savannah." *International Journal of Remote Sensing* **22**: 2651-2647.

USDA (1995). *Weather information management system user's guide U.S.* Washington, D.C., Deparment of Agriculture, Forest Service, Fire and Aviation Management.

Van der Werf, G. R., J. T. Randerson, G. J. Collatz and L. Giglio (2003). "Carbon emissions from fires in tropical and subtropical ecosystems." *Global Change Biology* **9(4)**: 547-562.

van Wagner, C. E. (1997). The development and structure of the Canadian forest fire weather index system. In: *Forestry Technical Report FTR 35*. Chalk

River, Ontario, Canadian Forest Service, Petewawa National Forestry Institute.

Van Wagtendonk, J. W., R. R. Root and C. H. Key (2004). "Comparison of AVIRIS and Landsat ETM+ detection capabilities for burn severity." *Remote Sensing of Environment* **92(3)**: 397-408.

Veneklaas, E., A. Fajardo, S. Obregon and J. Lozano (2005). "Gallery forest types and their environmental correlates in a Colombian savanna landscape." *Ecography* **28**: 236-252.

Vermote, E., N. Z. El Saleous and C. O. Justice (2002). "Atmospheric correction of MODis data in the visible to middle infrared: first results." *Remote Sensing of Environment* **83**: 97-111.

Villota, H. (1992). "Geomorfología aplicada a levantamentos edafológicos y zonificación física de las tierras." *Instituto Geografico Agustin Codazzi*: 258.

Vogelmann, J. E. and B. M. Rock (1988). "Assessing forest damage in high-elevation coniferous forest in Vermont and New Hampshire using Thematic Mapper data." *Remote Sensing of Environment* **24**: 227-246.

Wang, W., J. Qu, X. Hao, Y. Liu and W. Sommer (2006). "An improved algorithm for small and cool fire detection using MODis data: A preliminary study in the southeastern United Stated." *Remote Sensing of Environment* **108**: 163-170.

Wassmann, R. and P. L. G. Vlek. 2004. Mitigating greenhouse gas emissions from tropical agriculture: Scope and research priorities. *Environment, Development and Sustainability* **6**: 1–9.

Weng, Q. (2001). "A remote sensing-GIS evaluation of urban expansion and its impact on surface temperature in the Zhujiang Delta, China." *International Journal of Remote Sensing* **22(10)**: 1999-2014.

Weng, Q. (2002). "Land use change analysis in the Zhujiang Delta of China using satellite remote sensing, GIS and stochastic modelling." *Journal of Environmental Management* **64**: 273-284.

Wiegand , K.,, F. Jeltsche, and D. Ward. 2000b. Do spatial effects play a role in the spatial distribution of desert-dwelling Acacia raddiana? *Journal of Vegetation Science* **11**: 473-484.

Wiegand, K., F. Jeltsche, and D. Ward. 2004a. Minimum recruitment frequency in plants with episodic recruitment. *Oecologia* **141**:363-372.

Willhauck, G. (2000). "Comparison of object oriented classification techniques and standard image analysis for the use of change detection between spot multispectral satellite images and aerial photos." In: *Proceedings of the XIX ISPRS congress on comparison of object oriented classification techniques and standard image analysis for the use of change detection between spot multispectral satellite images and aerial photos*: 1-8.

Williams, D.L., S. Goward, and T. Arvidson. (2006). Landsat: yesterday, today, and tomorrow. *Photogrammetric Engineering and Remote Sensing* **72**: 1171-1178

Williams, D., Cook., A. M. Gill., P.H.R. Moore (2009). Fire regime, fire intensity and tree survival in a tropical savanna in northern Australia. *Australian Journal of Ecology* **24(1)**: 50-59.

Wooster, M. J. and Y. H. Zhang (2004). “Boreal forest fire burn less intensely in Russia that in North America.” *Geophysical Research Letters* **31(20)**: L20505.

WWF (1978). *Diagnóstico y definición de prioridades para la conservación y manejo de la biodiversidad en la Orinoquía colombiana.* Cali, World Wildlife Foundation.

Xie, Y., J. J. Qu, X. Xiong, X. Hao, N. Che and W. Sommer (2007). “Smoke plume detection in the eastern United States using MODis.” *International Journal of Remote Sensing* **20(10)**:2367-23774.

Xiuwan, C. (2002). Using remote sensing and GIS to analyse land cover change and its impacts on regional sustainable development. *International Journal Remote Sensing* **23(1)**: 107-124.

Yates, C. and J. Russell-Smith (2002). *An assessment of the accuracy of DOLA’s northern Australia NOAA-AVHRR fire affected area (FAA) map products.* Camberra, Deparment of the Environment and Heritage.

Zárate, L. (2004). Estudio de las careacterísticas físicas y geométricas de la llama en los incendios forestales. *Departamento de Ingeniería Química*. Cataluña, Universidad Politécnica de Cataluña.

Zhang, Y. H., M. J. Wooster, O. Tutubalina and G. L. W. Perry (2003). “Monthly burned area and forest fire carbon emission estimates for the Russian Federation from SPOT VGT.” *Remote Sensing of Environment* **87**: 1-15.

Zhu, Z. L., L. M. Yang, S. V. Stehman and R. L. Czaplewski (2000), “Accuracy assessment for the U.S. Geological Survey Regional Land-Cover Mapping Program: New York and New Jersey Region”. *Photogrammetric Engineering and Remote Sensing* **66**: 1425–1435.